COASTAL FRONTIERS

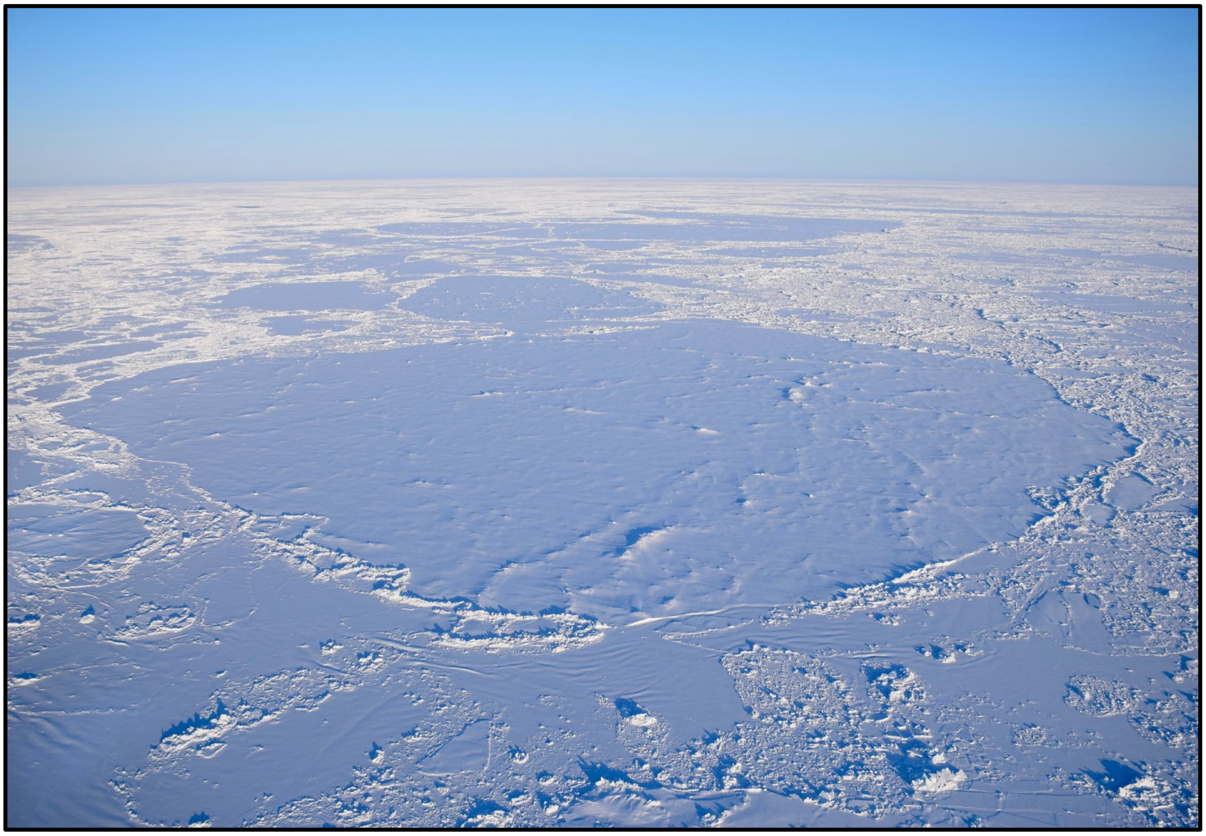

Multi-Year Ice Floe off Point Barrow (February 24, 2020)

2019-20 FREEZE-UP STUDY OF ARCTIC SEA ICE IN THE ALASKAN BEAUFORT AND CHUKCHI SEAS

BSEE

Coastal Frontiers Corporation
882A Patriot Drive
Moorpark, CA 93021-3544
(818) 341-8133

Vaudrey & Associates, Inc.
1685 El Caserio Court
San Luis Obispo, CA 93401
(805) 544-9399

CFC-1070

2019-20 FREEZE-UP STUDY OF ARCTIC SEA ICE IN THE ALASKAN BEAUFORT AND CHUKCHI SEAS

FINAL REPORT

Prepared for:

U.S. Department of the Interior, Bureau of Safety and Environmental Enforcement
Washington, D.C.

Prepared by:

Coastal Frontiers Corporation
Moorpark, California

Vaudrey & Associates, Inc.
San Luis Obispo, California

November 2020

Funding was provided by the U.S. Department of the Interior, Bureau of Safety and Environmental Enforcement (BSEE), Office of Offshore Regulatory Programs, Washington, DC under Contract Number ***140E0119C001.*** *The opinions, findings, conclusions, and recommendations expressed in this report are those of the authors and they do not necessarily represent the views or policies of BSEE.*

EXECUTIVE SUMMARY

This report describes an investigation of the ice conditions that prevailed in the Alaskan Beaufort and Chukchi Seas during the 2019-20 freeze-up season. The study was performed for the U.S. Department of the Interior, Bureau of Safety and Environmental Enforcement (BSEE), by Coastal Frontiers Corporation and Vaudrey & Associates, Inc.

The 2019-20 study was the ninth in a series of recent freeze-up investigations that began in 2009-10 and continued through 2016-17 on an annual basis. It was designed to address five specific objectives:

1. Describe the ice conditions that evolve during the freeze-up season, including the development of the landfast ice zone and early shear zone;
2. Locate and map features of potential importance for offshore exploration and production activities, including ice movement lines, substantial leads and polynyas, first-year ridges and rubble fields, and multi-year ice floes;
3. Locate, map, and characterize ice pile-ups on natural shorelines and man-made structures;
4. Correlate significant changes in the ice canopy with the corresponding meteorological conditions;
5. Using the data acquired from 2009-10 through 2016-17 and in 2020, characterize present-day freeze-up processes and compare them with those in the 1980s.

The study was conducted using publicly available data, proprietary data, and aerial reconnaissance missions. The acquisition of open-source meteorological data, ice charts, drift buoy data, and satellite imagery began in September 2019 and continued through February 2020. These data were supplemented with 20 high-resolution, proprietary RADARSAT-2 images purchased from MDA Geospatial Services Inc., for the period from mid-October 2019 through late February 2020.

Four aerial reconnaissance missions were conducted in late February 2020 to supplement the remotely sensed data obtained from the sources enumerated above. The flights, consisting of two in the Beaufort Sea and two in the Chukchi, were used to document the conditions that prevailed at the end of the freeze-up season.

The principal study findings are summarized below:

Entire Study Area

1. ***Air Temperatures:*** The air temperatures during the 2019-20 winter season were warm by historical standards, but unexceptional compared to those in the recent past. Specifically, the temperatures at Utqiagvik Airport were the sixth warmest in past 50 winters, but also the sixth warmest in the 11 winters from 2009-11 through 2019-20. Those at Deadhorse Airport were the ninth warmest in this 11-winter period.

2. ***First-Year Ice Growth:*** The computed thickness of undeformed first-year ice at the end of the 2019-20 winter season was 162 cm in the Alaskan Beaufort Sea and 148 cm in the Chukchi Sea, based on accumulations of 7,143 and 6,122 FDD at Deadhorse and Utqiagvik Airports, respectively. The thickness in the Beaufort was the third highest in the past 11 winters, while that in the Chukchi was tied with that in 2014-15 as the sixth highest. The highest values in recent years, 176 cm in the Beaufort and 167 cm in the Chukchi, occurred in 2011-12.

Beaufort Sea

1. ***Late Summer:*** The ice cover in the Alaskan Beaufort Sea diminished rapidly in July and early August, reflecting the prevalence of warm air temperatures and clear skies. Subsequently, from mid-August through mid-September, the rate of loss slowed. The minimum ice extent, which occurred on September 18th, tied those in 2007 and 2016 as the second lowest since the acquisition of satellite-based data began in 1979.

2. ***Timing of Freeze-Up:*** Freeze-up began in mid-October with the formation of ice along the coast between Admiralty Bay and Point Brownlow. Nearshore freeze-up occurred on November 11th, followed by complete freeze-up on November 24th. During the nine years covered by recent freeze-up studies (2009-11 through 2016-17 and 2019-20), the average date for the occurrence of nearshore freeze-up was October 28th with a standard deviation of nine days. The average date for the occurrence of complete freeze-up was November 10th with a standard deviation of ten days.

3. ***Duration of Freeze-Up:*** The duration of freeze-up was 41 days, consisting of 28 days from first ice to nearshore freeze-up and an additional 13 days from nearshore freeze-up to complete freeze-up. During the nine years covered by recent freeze-up studies, the duration averaged 37 days with a standard deviation of 11 days.

4. ***Wind Regime:*** Based on the daily average wind directions recorded at Deadhorse Airport, westerlies predominated in each of the five months from October through February. The frequencies of occurrence ranged from 55% in December to 79% in February. Over the entire five-month study period, westerlies outnumbered easterlies by a margin of 64% to 36%. The average monthly speeds were tightly clustered and

relatively low by historical standards, with values of 11 kt (6 m/s) recorded in October, November, and December, and 9 kt (5 m/s) in January and February.

5. ***Storm Events:*** Storm events with daily average wind speeds exceeding 15 kt (8 m/s) occurred on only nine occasions encompassing 18 days. Four of the events were easterlies, while five were westerlies. The numbers of easterly storms (4), easterly storm days (9), total storms (9), and total storm days (18) all represented historical minima relative to 2009-10 through 2016-17. Storm duration was low, averaging 2.3 days/event for easterlies and 1.8 days/event for westerlies.

6. ***Landfast Ice:*** Landfast ice began to develop in early November, with growth occurring first in the western portion of the study area and subsequently in the eastern portion. The ice continued to expand offshore through the first half of December, but the advance stalled during the second half of the month. Substantial expansion followed in January, causing the landfast ice edge to reach one of its customary anchor points, Weller Bank, by mid-month and a second, Stamukhi Shoal, by early February. A reversal occurred at the end of February when a brief westerly storm caused the ice edge to retreat by distances up to 20 nm (37 km). Although the ice remained grounded on Weller Bank, it was displaced from Stamukhi Shoal - a development that underscored the absence of a well-developed, firmly-grounded shear zone during the 2019-20 freeze-up season.

7. ***Ice Pile-Ups:*** Thirty-two ice pile-ups formed in the central portion of the Alaskan Beaufort Sea during the 2019-20 freeze-up season. Two were located on the Endicott Project's Endeavor Island, two on Northstar Production Island, one on the Oooguruk Offshore Drillsite (ODS), one on the Spy Island Drillsite (SID), and 26 on natural barrier islands and shoals. The dimensions of the pile-ups were unexceptional by historical standards, with heights ranging from 1 to 7 m above sea level, encroachment distances from negligible to 20 m onto the subaerial beach, and lengths from 50 m to 2 km alongshore. The thicknesses of the ice blocks comprising the piles ranged from 20 to 50 cm.

8. ***Multi-Year Ice:*** Multi-year ice began to drift west into the Alaskan Beaufort Sea study area during the second week in October. In the absence of a well-developed first-year ice canopy, the multi-year floes advanced rapidly to the west in November. Some of the ice at the southern boundary was incorporated into the landfast ice zone in late November and early December, and remained there through the end of the freeze-up study period in February. The concentrations typically were less than 10%. Farther offshore, where the multi-year floes tended to be larger, the concentrations ranged from less than 10% to 50% in December, less than 10% to 60% in January, and less than 10% to 70% in February. The only region lacking multi-year ice for an extended period of time was a tongue of first-year ice that developed between the U.S.-Canadian border and Harrison

Bay in mid-December and persisted through February just offshore of the landfast ice zone.

Chukchi Sea

1. ***Timing of Freeze-Up:*** Ice began to form in Kasegaluk Lagoon, the Kuk River Inlet, and Peard Bay in mid-October, but freeze-up proceeded slowly in the weeks that followed. Complete coverage of these semi-enclosed basins did not take place until the last week in November. Although ice appeared in the exposed waters adjacent to the coast during the first week in November, it failed to coalesce into a near-continuous strip spanning the entire length of the study area until the end of the month. Farther offshore, first-year pack ice began to stream west past Point Barrow during the second week of November but stalled in response to periods of westerly winds. As a result, most of the Chukchi Sea remained ice-free at the end of November. A strong predominance of easterly winds in December delayed the attainment of complete ice cover adjacent to the coast until December 26th. On that date, nearshore freeze-up and complete freeze-up occurred simultaneously. During the nine years covered by recent freeze-up studies (2009-11 through 2016-17 and 2019-20), the average date for the occurrence of nearshore freeze-up was November 26th with a standard deviation of 15 days. The average date for the occurrence of complete freeze-up was December 11th with a standard deviation of 11 days.

2. ***Duration of Freeze-Up:*** Nearshore freeze-up and complete freeze-up both occurred 72 days after first ice. During the nine years covered by recent freeze-up studies, the duration of freeze-up (from first ice to complete freeze-up) averaged 63 with a standard deviation of ten days.

3. ***Wind Regime:*** Easterlies outnumbered westerlies in November, December, and January, while westerlies prevailed in October and February. Over the entire five-month study period, easterlies outpaced westerlies by a margin of 55% to 45%. The monthly average speeds declined over the course of freeze-up, decreasing from 13 kt (7 m/s) in October and November to 11 kt (6 m/s) in December, 9 kt (5 m/s) in January, and 7 kt (4 m/s) in February.

4. ***Storm Events:*** Thirteen storm events took place from October through February, consisting of nine easterlies and four westerlies. The easterlies produced 16 storm-days while the westerlies produced 7 storm-days. The numbers of easterly storm-days (16) and total storm days (23) represented historical minima relative to 2009-10 through 2016-17. As in the case of the Beaufort, storm duration was low, averaging 1.8 days/event for both easterlies and westerlies.

5. ***Landfast Ice:*** The first traces of landfast ice appeared in Kasegaluk Lagoon, the Kuk River Inlet, and Peard Bay in mid-November. Although several small patches of landfast ice formed in the exposed waters adjacent to the coast during the first half of December, a continuous strip encompassing the entire length of the study area between Point Barrow and Point Lay did not develop until month-end. Most of the newly-formed landfast ice was lost during the first half of January, a period in which winds with a significant offshore component prevailed. A partial rebound occurred during the second half of January, when westerly winds resulted in the re-establishment of a continuous strip. Additional expansion followed in February, causing the landfast ice to reach Blossom Shoals, its customary anchor point, by mid-month. At the end of the month, the width of the landfast ice zone ranged from less than 1 nm (2 km) off South Kasegaluk Lagoon and Point Belcher to 21 nm (39 km) off North Kasegaluk Lagoon.

6. ***Coastal Flaw Lead:*** From December 2019 through February 2020, the distinctive flaw lead that forms off the Chukchi Sea coast in response to offshore winds opened on seven different occasions. The frequency of occurrence, which averaged 54% over the three-month period, increased from 23% in December to 65% in January and 76% in February. The maximum width, 75 nm (139 km) occurred in January, while the maximum length, 250 nm (463 km), occurred in both January and February. The lead persisted for periods that ranged from one to 20 days.

7. ***Pack Ice:*** When a reconnaissance flight was performed at the end of February, the pack ice on the west side of the flaw lead consisted primarily of first-year floes with diameters typically ranging from less than 500 m to 1 km and occasionally reaching 3 km. Deformation was moderate. Ridge and rubble heights of 2 to 3 m were common but heights to 5 m were observed in some areas, particularly in the vicinity of the flaw lead.

8. ***Ice Pile-Ups:*** Fifty-seven ice pile-ups occurred on the shoreline between Utqiagvik and Point Lay during the 2019-20 freeze-up season. Thirty-seven were located on the seaward side of the barrier islands fronting Kasegaluk Lagoon while one was located on the landward side. The remaining 19 were located between North Kasegaluk Lagoon and Utqiagvik. The dimensions were large by historical standards, with heights ranging from 1 to 20 m, encroachment distances from negligible to 30 m, and alongshore lengths from 50 m to 8 km. The block thicknesses varied from 30 to 60 cm.

9. ***Multi-Year Ice:*** Multi-year ice drifting west in the Alaskan Beaufort Sea reached the vicinity of Point Barrow at the end of November. It remained stalled at that location until mid-December, when multi-year floes began to move into the region northwest of the Point. On December 23rd, the ice drifted south of the Point after entering the first flaw lead of the freeze-up season. A larger flaw lead appeared at the end of December, allowing the ice to move within 2 nm (4 km) of Icy Cape by early January. The ice

continued to advance to the south and west of Point Barrow during the remainder of January, reaching the Hanna Shoal and Burger Prospects in mid-month and the vicinity of Point Lay at month-end. Changes in the ice edge were minimal in February, with the western boundary tending to follow the 163ºW meridian between the 70ºN and 72ºN parallels.

Trends

1. ***Air Temperatures:*** Since the 1970s, progressively warmer winter seasons have caused the number of accumulated freezing-degree days at Utqiagvik to decline at an average rate of 54 per year. The rate of warming has accelerated, with the greatest increase in temperature occurring during the early portion of freeze-up.

2. ***Winds:*** Since the early 1980s, the frequency of storm events during freeze-up has increased by about 50%. The frequency of mid-winter storms (January through April) appears to have remained stable.

3. ***Timing of Freeze-Up:*** Nearshore freeze-up currently tends to occur at the end of October in the Alaskan Beaufort Sea and during the fourth week in November in the northeastern Chukchi Sea. The former is more than three weeks later than in the 1980s, while the latter is more than one month later than in the 1970s. The rate of change has accelerated in recent years, with the date of freeze-up currently trending later by 2.3 days per year in the Beaufort and 4.6 days per year in the Chukchi. These high rates of change imply that the length of the open-water season will increase substantially in the years ahead.

4. ***Duration of Freeze-Up:*** The duration of freeze-up in the Alaskan Beaufort Sea, from first ice to complete freeze-up, currently averages 37 days with a standard deviation of 11 days. In the Chukchi, the duration is substantially longer, averaging 63 days with a standard deviation of ten days. The duration in the Beaufort is increasing at a rate of 1.0 days per year, while that in the Chukchi is increasing at 1.9 days per year.

5. ***First-Year Ice Growth:*** Based on air temperature alone, the thickness of undeformed first-year ice attained during an average winter has decreased by 25 cm (15%) since the early 1980s. However, a significant increase in snowfall may be causing an even greater reduction in the ice thickness due to its insulating effect. Other temperature-related factors, including reduced ice production in leads, decreased consolidation of ridges and rubble fields, and reduced ice strength, serve to amplify the impact of reduced thickness on ice dynamics.

6. ***Landfast Ice Development and Stability*:** In the Alaskan Beaufort Sea, the extent of the landfast ice zone to the west of Prudhoe Bay is similar to that observed in the 1980s but the landfast ice develops more slowly. To the east of Prudhoe Bay, a stable, well-

grounded shear zone is less likely to develop during freeze-up and develops more slowly in those years when it does occur. In the Chukchi, the narrow, ephemeral nature of the landfast ice zone noted in the 1980s continues to prevail today.

7. ***Coastal Flaw Lead:*** Notwithstanding trends toward warmer air temperatures, increased storminess, and slower ice growth during freeze-up, the frequencies with which the flaw lead and extended flaw lead occur off the Chukchi Sea coast have remained unchanged since the 1990s.

8. ***Multi-Year Ice in the Alaskan Beaufort Sea:*** The probability of large multi-year ice floes invading the nearshore portion of the Alaskan Beaufort Sea during freeze-up is substantially less than in the 1980s. This change has resulted in part from a reduction in the amount of multi-year ice comprising the permanent polar pack and in part from an increase in the northerly retreat of the ice edge during the summer months, both of which have reduced the opportunities for pack floes to enter the nearshore area. In addition, warmer air temperatures, longer open-water seasons, and increased storminess have decreased the likelihood that first-year ridges and rubble will survive the summer melt season to become second-year floes of any consequence. Nevertheless, as demonstrated in both 2018-19 and 2019-20, the possibility of multi-year ice invasions cannot be ruled out in the nearshore region of the Alaskan Beaufort Sea. The probability of an invasion in any given freeze-up season currently is about 20%, based on four such occurrences in the past 20 years.

9. ***Multi-Year Ice in the Chukchi Sea:*** The probability of multi-year ice entering the Chukchi Sea to the south and west of Point Barrow also has decreased since the 1980s, but to a lesser extent than in the Beaufort. Although the factors that have reduced the probability of invasions in the Beaufort apply to the Chukchi as well, their impact has been mitigated by the ability of the Multi-Year Gateway and Early-Season Entry to divert multi-year ice floes to the southwest. The probability of an invasion in any given freeze-up season currently is about 65%, based on 13 invasions in the past 20 years.

10. ***Ice Drift:*** The limited data acquired in recent years indicate that the drift rate for pack ice in the Alaskan Beaufort Sea averages about 6 nm/day (11 km/day) during the early stages of freeze-up. This value is comparable to that which prevailed in the 1980s.

TABLE OF CONTENTS

TABLE OF CONTENTS
(continued)

TABLE OF CONTENTS
(continued)

LIST OF TABLES

LIST OF TABLES
(continued)

LIST OF FIGURES

LIST OF FIGURES
(continued)

LIST OF FIGURES
(continued)

LIST OF FIGURES
(continued)

LIST OF FIGURES
(continued)

LIST OF PLATES

LIST OF PLATES
(continued)

2019-20 FREEZE-UP STUDY OF ARCTIC SEA ICE IN THE ALASKAN BEAUFORT AND CHUKCHI SEAS

1. INTRODUCTION

This report describes an investigation of the ice conditions that prevailed in the Alaskan Beaufort and Chukchi Seas during the 2019-20 freeze-up season. The study was performed on behalf of the U.S. Department of the Interior, Bureau of Safety and Environmental Enforcement (BSEE), by Coastal Frontiers Corporation and Vaudrey & Associates, Inc.

As shown in Figure 1-1, the study area includes the southern portion of the Beaufort Sea from Barter Island on the east to Point Barrow on the west, and the northeastern portion of the Chukchi Sea bounded by the shoreline between Point Barrow and Point Lay, the 74°N parallel, and the 168°W meridian. The boundaries in the Beaufort Sea were selected to encompass all existing oil and gas developments, while those in the Chukchi were selected to encompass Hanna Shoal and lease tracts of recent interest, including the Burger and Crackerjack prospects.

Despite their proximity, the ice regimes in the Beaufort and Chukchi Seas differ markedly due to factors that include geography, meteorology, and oceanography. Whereas the Beaufort Sea coast trends east-southeast to west-northwest, the Chukchi coast is oriented northeast-southwest (Figure 1-1). As a result, the easterly winds that occur frequently in both basins tend to push the ice along the Beaufort Sea coast but away from the Chukchi coast. In the Beaufort, the alongshore winds coupled with flat nearshore slopes produce an extensive zone of grounded, landfast ice bordered by a compact, well-consolidated ice canopy farther offshore. In the Chukchi, the growth of landfast ice is limited not only by the prevalence of offshore winds but also by the relatively steep slopes that exist off the coast. As a result, the landfast ice zone typically consists of a narrow strip of grounded ice that clings to the shoreline. A flaw lead frequently opens offshore of the landfast ice, and the ice canopy tends to be less consolidated and more mobile than in the Beaufort.

The pronounced difference in ice regimes that exists during the freeze-up and winter seasons also prevails during break-up and summer. Whereas the Beaufort Gyre transports pack ice from east to west in the Beaufort Sea, the Alaska Coastal Current carries warm water north from the Bering Sea and contributes to the retreat of the pack ice in the Chukchi (Figure 1-1).

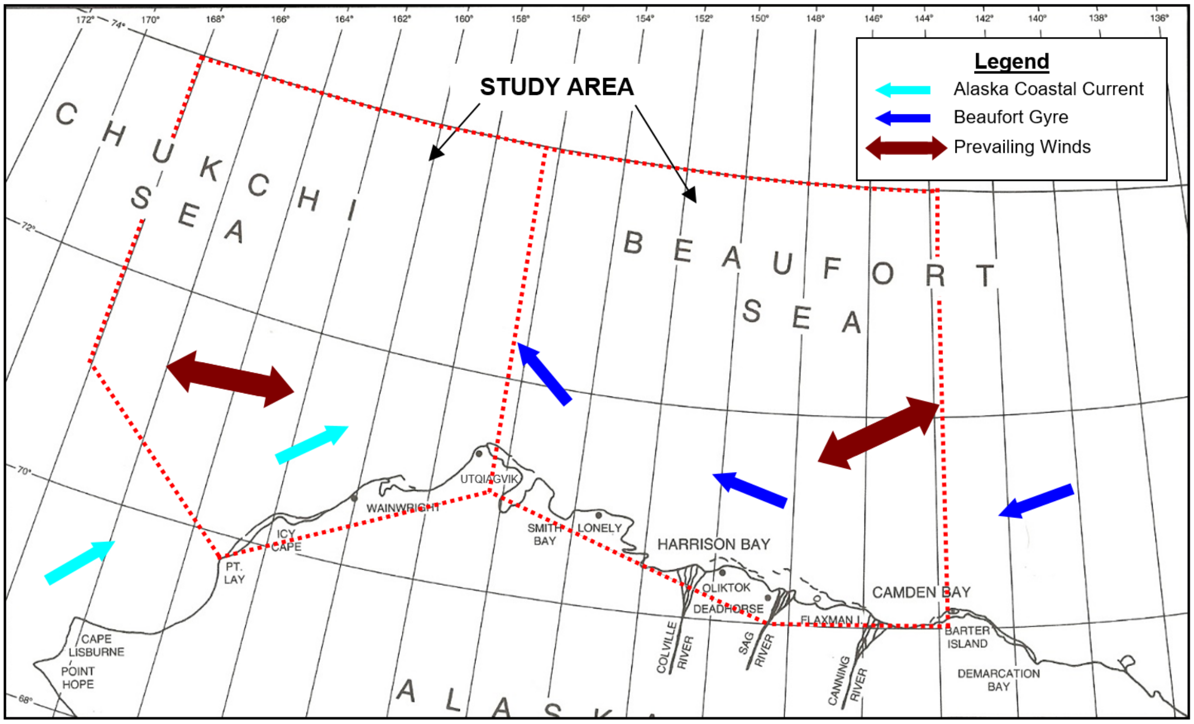

Figure 1-1. Study Area

During freeze-up, the ice cover in the study area consists primarily of thin, flexible sheets of newly-formed ice. It also may contain thicker, stronger multi-year floes that have moved into the region after surviving one or more summer melt seasons. Storms tend to disturb the first-year ice before it attains sufficient thickness to resist displacement, allowing the multi-year floes to travel great distances and attain relatively high speeds in the absence of significant confinement by the first-year canopy. Potential concerns for oil and gas facilities include impact loads on fixed structures such as man-made islands and platforms, displacement of floating structures such as drillships, and ice gouging on the routes of subsea pipelines.

The storms during freeze-up and early winter can produce significant pile-up events when moving ice encounters fixed objects such as natural shorelines and shoals, and man-made islands and causeways. The storms also can cause substantial deformation of the first-year ice, leading to the formation of ridges and rubble fields.

The foregoing phenomena, along with the impairment of vessel navigation and, in the case of the Beaufort, the use of the ice sheet as a platform for transportation and construction, imply that an understanding of freeze-up is essential for the safe design and operation of offshore oil and gas facilities. To this end, six freeze-up studies were conducted as joint-industry projects from 1980-81 through 1985-86 (Vaudrey, 1981a; 1982a; 1983; 1984; 1985a;

1986). Each was largely observational in nature, and included aerial surveys undertaken at intervals of two to three weeks from early October until early December. In some instances, an additional aerial survey was conducted at the end of January to record late freeze-up ice movements. The primary objectives of these annual studies were twofold: (1) observe and record major ice movement events and their effects on man-made structures, and (2) document the size and distribution of multi-year ice floes, the locations of major first-year ridges and rubble fields, and the zonation of the nearshore ice.

Between 1986 and 2008, freeze-up processes in the Alaskan Beaufort and Chukchi Seas were investigated primarily through analyses of satellite imagery (Vaudrey, 1988a, 1989a, 1990, 1991, 1992; Eicken, *et al*., 2006). The resulting information, although useful in its own right, lacked some of the detail provided by the earlier observational studies. Specifically, items such as the characteristics of multi-year ice floes and the locations and characteristics of ice pile-ups could not be extracted from the satellite data.

To address this shortcoming, freeze-up studies that combined remote sensing with on-site observations were initiated 2009-10 and conducted on an annual basis through 2016-17. Each of the eight studies included an analysis of meteorological data, ice charts, and satellite imagery in concert with a series of aerial reconnaissance missions to document the conditions at the end of freeze-up (Coastal Frontiers and Vaudrey, 2010; 2011; 2012a; 2013; 2014; 2015; 2016; 2017). Four of the studies (2011-12, 2012-13, 2014-15, and 2015-16) also included reconnaissance flights in late November or early December to document the conditions that prevailed in the middle of the freeze-up period.

To expand the database on the nature and interannual variability of present-day freeze-up processes, and to aid in the identification of long-term trends in those processes, a similar investigation was undertaken in 2019-20. As in each of the prior freeze-up studies, the scope of work was designed to address five specific objectives:

1. Describe the ice conditions that evolve during the freeze-up season, including the development of the landfast ice zone and early shear zone;
2. Locate and map features of potential importance for offshore exploration and production activities, including ice movement lines, substantial leads and polynyas, first-year ridges and rubble fields, and multi-year ice floes;
3. Locate, map, and characterize ice pile-ups on natural shorelines and man-made structures;
4. Correlate significant changes in the ice canopy with the corresponding meteorological conditions;

5. Using the data acquired from 2009-10 through 2016-17 and in 2020, characterize present-day freeze-up processes and compare them with those in the 1980s.

The methods were analogous to those used in the eight prior freeze-up studies, with changes limited to the addition or substitution of data sources that represented new or more reliable offerings of publicly available information. The acquisition of open-source data began in September 2019 and continued through February 2020. In addition, 20 high-resolution, proprietary RADARSAT-2 images were obtained from mid-October 2019 through the end of February 2020.

Aerial reconnaissance missions were conducted in late February 2020 to document the ice conditions at the end of the freeze-up season (when processes such as nearshore rubble formation and ice encroachment onto the shoreline typically have slowed or ceased). The missions consisted of two fixed-wing flights in the Beaufort followed by two fixed-wing flights in the Chukchi.

The remainder of this report presents a detailed account of the 2019-2020 Freeze-Up Study. The conventions and definitions adopted for the project are provided in Section 2. To provide historical context, the findings of fourteen prior studies (1980-81 through 1985-86 and 2009-10 through 2016-17) are summarized in Section 3. Data acquisition and analysis are discussed in Section 4, which covers the aerial reconnaissance missions as well as the data obtained from all other sources. Section 5 describes the progression of freeze-up in the Alaskan Beaufort Sea in 2019-20, while Section 6 provides analogous information for the Chukchi. In Section 7, trends in freeze-up are identified by characterizing present-day processes and comparing them with those in the 1980s. Conclusions are presented in Section 8, followed by references in Section 9.

Figures, tables, and plates are interspersed with the text, while three large-format drawings that display the observations made during the reconnaissance flights are provided in Appendix A. Image acquisition reports pertaining to the RADARSAT-2 images are provided in Appendix B, while a post-observation report describing the reconnaissance flights is provided in Appendix C. A technical summary of the study appears in Appendix D. The digital data files that were used to conduct the study are compiled on a DVD that constitutes Appendix E.

Throughout this report, the locations of ice features are referenced to geographic features that include bays, rivers, lagoons, points of land, natural and man-made islands, and coastal villages. For ease of reference, these geographic features are shown in Figure 1-2 (Central Beaufort Sea), Figure 1-3 (Western Beaufort Sea), and Figure 1-4 (Chukchi Sea).

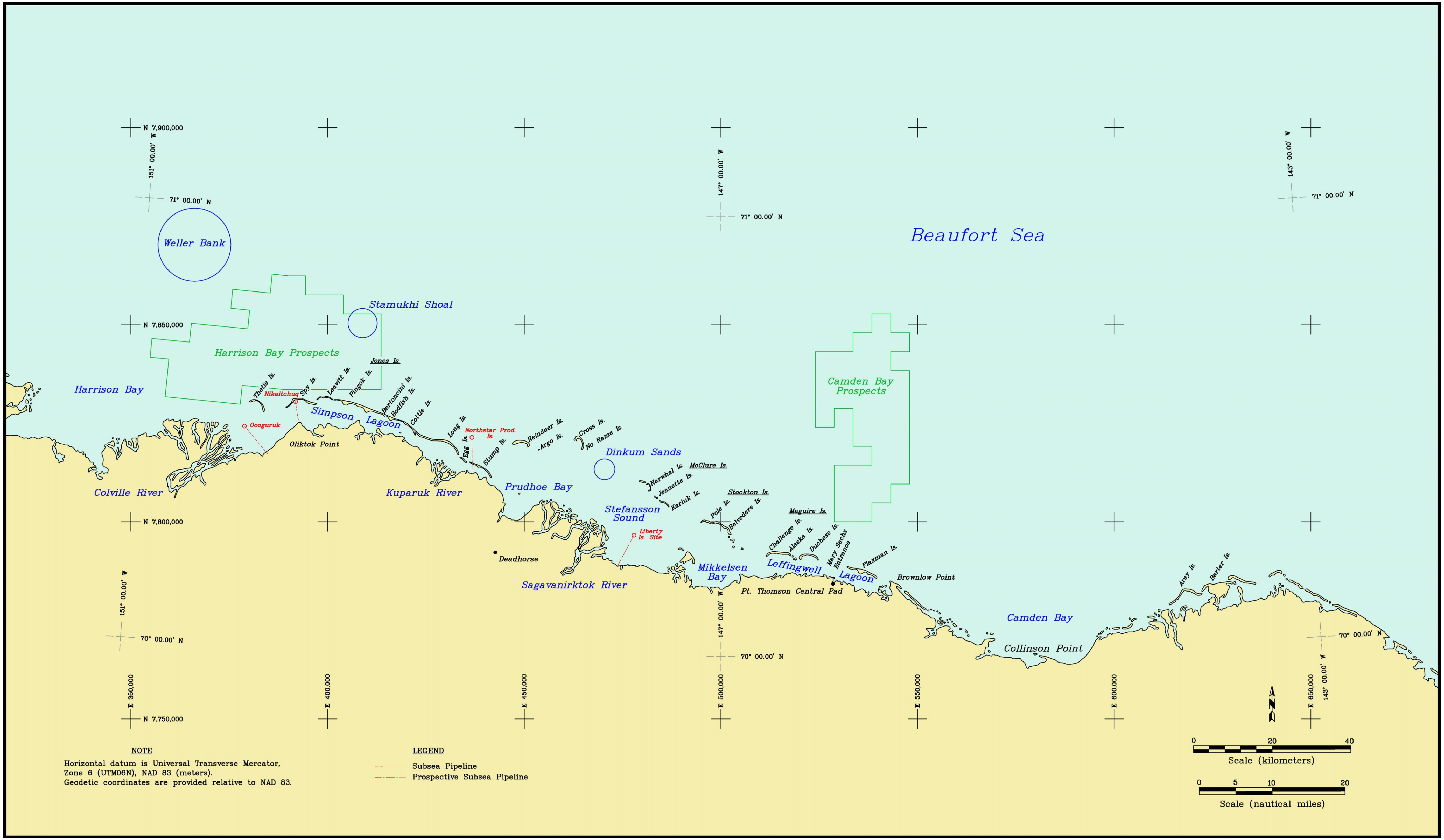

Figure 1-2. Geographic Points of Interest in Central Beaufort Sea

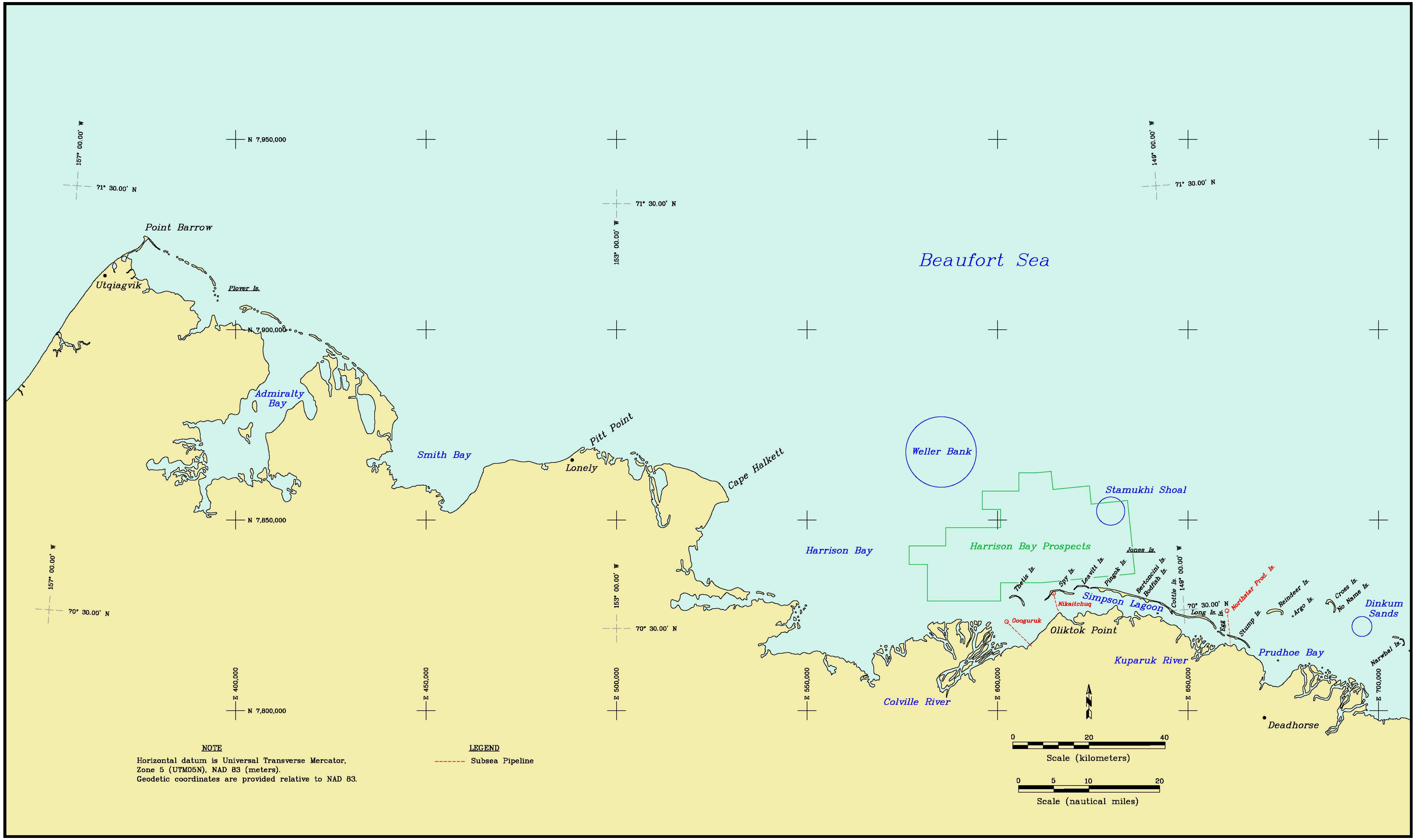

Figure 1-3. Geographic Points of Interest in Western Beaufort Sea

"THIS INFORMATION IS DISTRIBUTED SOLELY FOR THE PURPOSE OF PRE-DISSEMINATION PEER REVIEW UNDER APPLICABLE INFORMATION QUALITY GUIDELINES. IT HAS NOT BEEN FORMALLY DISSEMINATED BY BSEE. IT DOES NOT REPRESENT AND SHOULD NOT BE CONSTRUED TO REPRESENT ANY BSEE DETERMINATION OR POLICY."

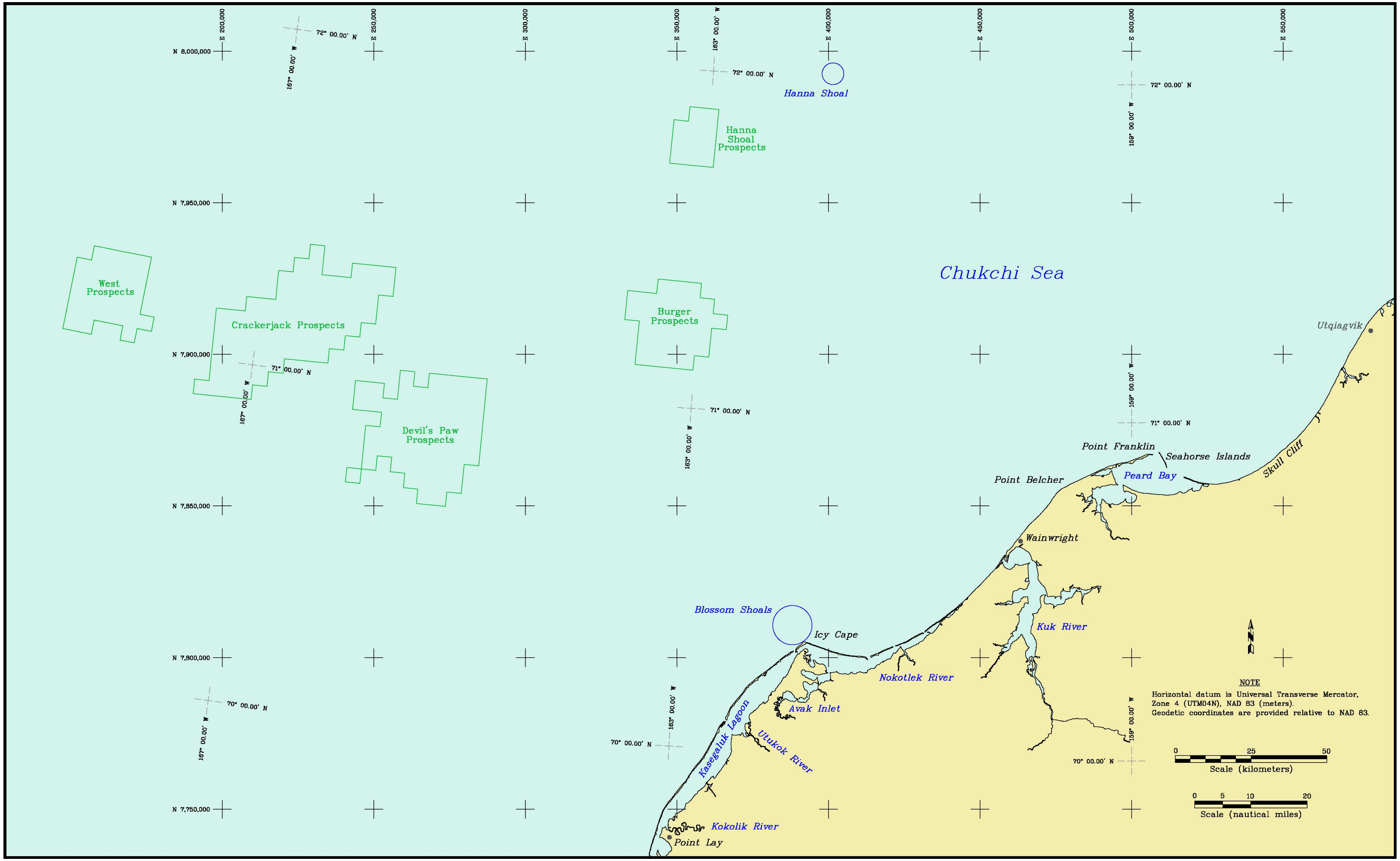

Figure 1-4. Geographic Points of Interest in Chukchi Sea

2. CONVENTIONS, DEFINITIONS, AND ACCESSIBILITY

The conventions and definitions adopted for this study are presented in Sections 2.1 and 2.2, respectively. Comments related to Accessibility follow in Section 2.3.

2.1. Conventions

- **Horizontal Datum:** The horizontal datum for all geographic coordinates is the North American Datum of 1983 (NAD 83). Many of the graphical products also include a grid referenced to the Universal Transverse Mercator (UTM) Datum, NAD 83, with units of meters. UTM Zone 6N is used in the central Beaufort Sea, UTM Zone 5N in the western Beaufort Sea, and UTM Zone 4N in the Chukchi Sea.
- **Vertical Datum:** The vertical datum is Mean Sea Level (MSL). MSL lies only 11 cm above Mean Lower Low Water (MLLW) at Prudhoe Bay, 9 cm at Utqiagvik, and 10 cm at Point Hope (National Ocean Service, 2020). For purposes of this report, the difference between MSL and MLLW (which represents the vertical datum for all National Ocean Service nautical charts of the region) is assumed to be negligible.
- **Units:** The International System of Units (SI) is used throughout this report, with three exceptions: (1) distances are provided in nautical miles (nm) to maintain consistency with the use of geographic coordinates; (2) wind speeds are provided in knots (kt), again to maintain consistency with the use of geographic coordinates; and (3) temperatures are provided in degrees Fahrenheit (°F), and freezing-degree days (FDD) are computed using the Fahrenheit rather than Celsius scale both to provide greater resolution and to maintain consistency with past freeze-up reports. In the case of nautical miles, knots, and degrees Fahrenheit, the corresponding values in SI units are provided in parentheses.
- **Winds:** Unless stated otherwise, the wind speeds discussed in the text refer to the daily average values (rather than the daily maximum values or hourly values). The wind directions indicate the orientations **from which** the wind is blowing (*i.e.*, an "easterly wind" is directed from east to west).
- **Ice Drift:** The ice drift speeds discussed in the text refer to the daily average values. The drift directions indicate the orientations **to which** the ice is moving (*i.e.*, an "easterly drift" is directed from west to east).

2.2. Definitions

The following definitions borrow heavily from, but are not identical to, those adopted by the World Meteorological Organization (WMO; 2014).

Ice Types by Location

- **Lagoon Ice:** Ice that forms in semi-protected basins adjacent to the coast, including bays, lagoons, and river entrances. Although lagoon ice typically represents a form of landfast ice, it is accounted for separately in this report.
- **Landfast Ice:** Ice that remains attached to the coast for an extended period of time (typically exceeding one week).
- **Landfast Ice Edge:** The seaward boundary of the landfast ice.
- **Pack Ice:** Sea ice that is susceptible to advection by meteorologic and oceanographic influences, other than lagoon ice or landfast ice.

Ice Types by Stage of Development

- **New Ice:** Newly-formed ice such as grease ice and slush composed of crystals that are only weakly frozen together.
- **Grease Ice:** A thin, soupy layer of ice crystals that resembles an oil slick on the sea surface.
- **Nilas:** Thin, elastic sea ice that is less than 10 cm thick.
- **Young Ice:** Sea ice in the transition stage between nilas and first-year ice, with a thickness of 10 to 30 cm.
- **First-Year Ice:** Sea ice of not more than one winter's growth that is at least 30 cm thick.
- **Multi-Year Ice:** Sea ice that has survived at least one summer melt season, including both true multi-year floes from the permanent polar pack and second-year floes that develop when grounded pieces of thick first-year ice survive the summer melt season.
- **Second-Year Ice:** Multi-year ice that has survived only one summer melt season.
- **Ice-Free:** Water in which no ice of any kind is present.

Ice Movement

- **Wind Factor:** The ratio of ice drift speed to wind speed, expressed as a percent.

Features

- **Ice Pile-Up:** A feature formed when an advancing ice sheet breaks into discrete blocks while encountering a natural shoreline, shoal, or man-made structure.
- **Ice Ridge:** A line or wall of deformed sea ice created by pressure. A pressure ridge is formed when one ice feature pushes against a second feature while moving perpendicular to their common boundary. A shear ridge is formed when one ice feature grinds past the other while moving parallel to their common boundary.
- **Ice Rubble:** An area of deformed sea ice created by pressure. A rubble pile is a grounded feature composed of ice broken into discrete blocks. A rubble field is a continuous body or region of floating (rather than grounded) ice blocks or closely-spaced ice ridges.
- **Lead:** A linear or quasi-linear opening in the sea ice that exposes sea water to the atmosphere.
- **Flaw Lead:** A lead that exists at the boundary between landfast ice and pack ice.
- **Polynya:** A non-linear opening in the sea ice that exposes sea water to the atmosphere.
- **Shear Line:** A linear boundary that forms between two ice features when one grinds past the other while moving parallel to their common boundary. Shear lines typically contain shear ridges on one or both sides of the boundary.
- **Thermal Crack:** A crack that forms in the sea ice in response to a rapid drop in air temperature. The drop causes contraction and cracking of the ice sheet while an ensuing rise can cause compression and extrusion of the refreezing slush in the crack, creating a ridge.

Freezing and Thawing

- **Freezing-Degree Day (FDD):** The difference between the daily average air temperature and the freezing point of seawater (29°F; -2°C).

Dates

- **First Ice:** The first occasion on which ice begins to form in protected or semi-protected waters at the outset of freeze-up (excluding ice that forms but subsequently melts before freeze-up begins in earnest).
- **Nearshore Freeze-Up:** The first occasion on which complete (10/10s) ice coverage occurs in the region typically occupied by landfast ice.
- **Complete Freeze-Up:** The first occasion on which complete ice coverage (10/10s) occurs in an entire oceanographic basin (Alaskan Beaufort Sea or Chukchi Sea north of Cape Lisburne).

Lagoon Extents

- **North Kasegaluk Lagoon:** That portion of Kasegaluk Lagoon that lies to the east of Icy Cape.
- **South Kasegaluk Lagoon:** That portion of Kasegaluk Lagoon that lies to the south of Icy Cape.

2.3. Accessibility

Although this report passes all checks for Section 508 compliance in Adobe Acrobat, the software incorrectly verbalizes the abbreviations for the following units:

Table 2-1. Units Incorrectly Verbalized by Adobe Acrobat

Abbreviation	Correct Verbalization	Incorrect Verbalization by Adobe
km^2	square kilometers	"k-m-2"
kt	knots	"k-t"
m	meters	"m"
m/s	meters per second	"m-slash-s"
nm	nautical miles	"nanometers"

Adobe Acrobat also struggles with the pronunciation of the Inupiat names shown in Table 2-2. Phonetic pronunciations are provided in this table.

Table 2-2. Phonetic Pronunciations of Inupiat Names

Name	Phonetic Pronunciation
Avak	AH-vak
Chukchi	CHOOK-chee
Karluk	CAR-luk
Kasegaluk	Ca-SEE-ga-luk
Kokolik	KO-ko-lik
Kuk	KOOK
Nikaitchuq	Ni-KAIT-chuk
Nokotlek	No-KOT-lek
Oliktok	O-LIK-tok
Oooguruk	OO-gu-ruk
Sagavanirktok	Sag-a-va-NIRK-tok
Tuktoyaktuk	TUK-toe-yak-tuk
Utqiagvik	OOK-key-ag-vik
Utukok	OO-too-kok

3. PRIOR STUDIES

As indicated in Section 1, six annual freeze-up studies were conducted from 1980-81 through 1985-86 (Vaudrey, 1981a; 1982a; 1983; 1984; 1985a; 1986). More recently, eight annual freeze-up studies were undertaken from 2009-10 through 2016-17 (Coastal Frontiers and Vaudrey, 2010; 2011; 2012a; 2013; 2014; 2015; 2016; 2017). The methods employed and results obtained in these prior studies are summarized below.

3.1. 1980s Freeze-Up Studies

The freeze-up studies conducted in the 1980s were made available to the present project through the courtesy of Shell International Exploration and Production, Inc. (Reece, 2009). The primary objectives of each study were twofold: (1) observe and record major ice movement events and their effects on man-made structures, and (2) document the size and distribution of multi-year floes, the locations of major first-year ridges and rubble fields, and the zonation of the nearshore ice. Each study included a series of aerial surveys conducted at two- to three-week intervals from early October until early December to monitor the progression of freeze-up.

The first three studies (1980-81 through 1982-83) were limited to the central Beaufort Sea, from Cape Halkett on the west to Flaxman Island on the east. The last three studies (1983-84 through 1985-86) were expanded significantly to include the entire region between Icy Cape in the Chukchi Sea and Barter Island in the Beaufort Sea. Occasionally, the reconnaissance flights continued east of Barter Island to the Canadian border. Each of the studies commencing in 1983, 1984 and 1985 included an additional trip at the end of January to record late freeze-up ice movements caused by storms occurring after the early-December visit. The progress of the freeze-up season was documented by reporting the ice conditions observed during each successive trip. Meteorological data, including wind speed and direction as well as air temperature, were acquired from coastal or near-coastal reporting stations at Deadhorse, Utqiagvik, and Barter Island.

Key findings from the six freeze-up studies in the 1980s are presented below:

<u>Beaufort Sea: 1980s</u>

- **Initiation of Freeze-Up:** Freeze-up occurred in the nearshore portion of the Beaufort Sea between late September and early October. Unseasonably warm air temperatures in October retarded initial ice growth by seven to ten days in 1983 and 1985, and by almost three weeks in 1984.

- **Landfast Ice and Shear Zone Development:** Persistent easterly winds during freeze-up created a grounded shear zone that provided stability for the landfast ice. In contrast, westerly winds fostered offshore movement of the ice cover and retarded the development of landfast ice. In the absence of strong westerly winds, an extensive zone of landfast ice stabilized by a grounded shear zone tended to form by the end of November.

- **Ice Pile-Ups and Rubble Formation:** The primary cause of ice pile-ups on natural shorelines and man-made facilities was found to be a reversal in the wind direction, especially during the early months of the freeze-up season. Two such ice movement sequences were documented during the six-year study period. The first, in November 1981, was caused by a westerly that loosened the landfast ice followed by an easterly that drove the ice back onto the shoreline. The second, in mid-October 1982, resulted from an easterly that created a lead offshore of the temporary fast ice followed by a strong westerly that dislodged the fast ice and drove it up the slopes and onto the work surfaces of several man-made exploration islands.

  Wind reversals also tended to create significant rubble piles offshore, especially on Stamukhi Shoal and Weller Bank. Several large rubble piles were observed 10 to 15 nm (19 to 28 km) northwest of Seal Exploration Island (the current location of Northstar Production Island) in water depths of 10 to 12 m after a strong southwesterly in late December 1983.

- **Multi-Year Ice:** Significant concentrations of multi-year ice were noted in the nearshore portion of the central Beaufort Sea during three of the six freeze-up seasons studied. The most extensive invasion occurred in late September 1980, when concentrations of 3 to 5 tenths occurred 2 to 3 nm (4 to 6 km) offshore of the barrier islands from Cross to Flaxman. During the summer of 1983, mild winds and cold air temperatures produced a substantial concentration of second-year ice in the nearshore region in early October. Two years later, in October 1985, most of the multi-year ice remained north of a line that roughly paralleled the coast 15 to 20 nm (28 to 37 km) offshore. During the other three freeze-up seasons, (1981, 1982, and 1984), multi-year ice in the nearshore region was confined to localized belts and patches of small floes and isolated ridge fragments grounded on the barrier islands and in the shear zone.

<u>Chukchi Sea: 1980s</u>

- **Initiation of Freeze-Up:** In 1983, freeze-up near Utqiagvik occurred around October 1st. This early date appears to have resulted, at least in part, from the cooling and stabilizing influence of multi-year ice present in the region. In 1984 and 1985, the nearshore waters of the Chukchi remained ice free until late October and mid-October, respectively.

- **Landfast Ice:** Landfast ice development along the Chukchi coast was found to be very limited in extent due to the predominance of easterly winds. These winds repeatedly opened a flaw lead that, in turn, produced ice when it refroze.
- **Ice Pile-Ups:** As in the Beaufort Sea, abrupt wind reversals during the freeze-up season were found to cause shoreline pile-ups on the Chukchi coast, especially near Utqiagvik and Point Belcher. However, an absence of strong winds in 1983 and a paucity of wind reversals in both 1984 and 1985 minimized the number of pile-ups observed during the three studies.
- **Multi-Year Ice:** Cold air temperatures and a lack of strong winds during the summer of 1983 produced a significant concentration of second-year ice north of the 71°N parallel in early October. In November 1984, a 2- to 3-tenths concentration of multi-year ice in the western Beaufort Sea moved into the Chukchi. It remained above the 71°N parallel through late January 1985 and was located well offshore of the prevailing 10- to 20-nm (19- to 37-km) wide coastal flaw lead. The multi-year floes typically ranged from 300 to 600 m in diameter, with a maximum horizontal extent of 4 km. In October 1985, multi-year ice attained higher concentrations and moved closer to the coast than in the Beaufort.

3.2. 2009-10 Freeze-Up Study

The scope and methods of the 2009-2010 Freeze-Up Study, which were adopted with relatively minor modifications for the 2010-11 through 2016-17 studies, are described in detail by Coastal Frontiers and Vaudrey (2010). Significant findings are as follows:

<u>Beaufort Sea: 2009-10</u>

- **Initiation of Freeze-Up:** Nearshore freeze-up occurred during the third week in October.
- **Landfast Ice and Shear Zone Development:** An intense easterly storm in late December 2009 created a grounded shear zone to the west of Prudhoe Bay that remained intact through midwinter. In contrast, westerly winds in January 2010 removed much of the landfast ice off the barrier islands to the east of Prudhoe Bay, and the ice in this region remained dynamic through mid-February.
- **Ice Pile-Ups:** Ice pile-ups were observed on or adjacent to six natural barrier islands and one man-made island during the reconnaissance flights conducted in early

February. The estimated pile-up heights ranged from 1 to 16 m. The largest pile-up exceeded 2 km in length.

- **Multi-Year Ice:** For the first time since 2001-02, multi-year ice floes invaded the nearshore waters of the Alaskan Beaufort Sea. The floes remained 10 to 20 nm (19 to 37 km) offshore as they migrated toward the west and ultimately moved into the Chukchi Sea.

Chukchi Sea: 2009-10

- **Initiation of Freeze-Up:** Freeze-up proceeded more slowly than in the Beaufort, with the ice edge advancing to the south and west during the month of November. Nearshore freeze-up occurred at the end of the month.
- **Landfast Ice:** Alternating periods of easterly (offshore) and westerly (onshore) winds repeatedly dislodged the nearshore ice between Utqiagvik and Point Lay, causing the freeze-up process to start anew. As a result, most of the coast lacked ridges and rubble fields that were sufficiently well-grounded to stabilize the landfast ice, and the ice remained susceptible to removal during easterly storms.
- **Flaw Lead:** The distinctive flaw lead that forms off the Chukchi Sea coast opened and closed repeatedly in response to the alternating easterly and westerly winds. The width of the lead varied substantially depending on the duration and intensity of the easterlies. A maximum width of 40 to 50 nm (74 to 93 km) was noted during a 25-day period from mid-February to early March, and again during a 10-day period in late March.
- **Ice Pile-Ups:** Nineteen ice pile-ups were observed on the Chukchi Sea coast during the February reconnaissance flights, including three that encroached up to 6 m onto the subaerial beach. The most significant pile-up extended 150 m alongshore and attained a maximum height of 15 m. The maximum heights of the others ranged from 4 to 10 m.
- **Multi-Year Ice:** Multi-year ice entered the northern Chukchi Sea from the western Beaufort and split into two separate branches that persisted through mid-winter: (1) a northern branch that remained above the 71.5°N parallel in the eastern and central Chukchi before dipping south, and (2) a southern branch that extended southwest from Utqiagvik to the vicinity of the 70°N parallel.

3.3. 2010-11 Freeze-Up Study

Key findings of the 2010-11 Freeze-Up Study (Coastal Frontiers and Vaudrey, 2011) are summarized below:

Beaufort Sea: 2010-11

- **Initiation of Freeze-Up:** Nearshore freeze-up occurred during the second week of October.
- **Landfast Ice and Shear Zone Development:** The landfast ice zone remained narrow and unstable throughout the 2010-11 freeze-up season due to a lack of easterly storms and sustained easterly winds. In the western Beaufort, the landfast ice edge at the end of January passed through Weller Bank but fell short of its other typical anchor point, Stamukhi Shoal. In the central Beaufort, the landfast ice edge at the end of January was located in close proximity to the barrier islands east of Prudhoe Bay and within 10 nm (19 km) of the shoreline in Camden Bay.
- **Ice Pile-Ups:** Only one ice pile-up was observed in the Alaskan Beaufort Sea in 2010-11. It was located on the Oooguruk Offshore Drillsite in the shallow waters of the Colville River Delta, and consisted of 10- to 15-cm thick plates that were stacked against the south corner and southwest side in multiple waves with heights to 3 m. The pile-up did not encroach past the waterline of the island's gravel-bag armor.
- **Multi-Year Ice:** In contrast to 2009-2010, large multi-year ice floes did not invade the nearshore region of the Alaskan Beaufort Sea during the 2010-11 freeze-up season. Between November 2010 and mid-February 2011, such floes remained north of the 71°N parallel in the eastern Beaufort and 72°N parallel in the western Beaufort. However, fragments of multi-year ice with diameters ranging from 1 to 6 m were observed on the shorelines of many of the barrier islands. The fragments originated from a band of grounded ice between Flaxman Island and Smith Bay that persisted for the duration of the 2010 open-water season.

Chukchi Sea: 2010-11

- **Initiation of Freeze-Up:** Freeze-up in the Chukchi Sea began during the first week in October but progressed slowly due to above-normal air temperatures and a prolonged easterly storm that dislodged the newly-formed ice from the coast in mid-month. Complete freeze-up occurred during the first week in December.
- **Landfast Ice:** Except in Peard Bay, Kasegaluk Lagoon, and the semi-protected embayment east of Point Franklin, landfast ice between Utqiagvik and Point Lay

was confined to a narrow strip that remained unstable through mid-February 2011. A paucity of westerly storms through mid-January limited the production of grounded rubble, thereby leaving the nearshore ice susceptible to break-out and removal during periods of easterly winds.

- **Flaw Lead:** The coastal flaw lead was detected on five occasions during the 2010-11 freeze-up season: late December, early January, late January, and twice in the first half of March. The dimensions of the lead varied substantially, from an estimated 50 nm (93 km) long and 5 nm (9 km) wide in late December to 140 nm (259 km) long and 60 nm (111 km) wide in late January. The feature's persistence also varied, from as little as several days during each appearance in March to about a week in early January.
- **Ice Pile-Ups:** Twenty-seven pile-ups were observed on the Chukchi Sea coast in February 2011, representing eight more than in 2010. The largest pile-ups were located between Point Belcher and Wainwright, where one ice pile attained both the maximum height of 8 m and maximum encroachment distance of 40 m onto the subaerial beach. The longest ice pile, stretching 2.3 km alongshore with a height of 3 m, also occurred in this region.
- **Multi-Year Ice:** Large multi-year ice floes remained well offshore throughout the 2010-11 freeze-up season, with the southern boundary located approximately 60 nm (111 km) north of Point Barrow at the end of December and 180 nm (333 km) north at the end of March. Nevertheless, fragments of old ice embedded in first-year floes were observed in Shell's Burger Prospects in February 2011. They comprised less than 5% of the ice cover, with maximum horizontal dimensions that ranged from one hundred to several hundred meters.

3.4. 2011-12 Freeze-Up Study

The results of the 2011-12 Freeze-Up Study (Coastal Frontiers and Vaudrey, 2012a) are summarized below:

Beaufort Sea: 2011-12

- **Initiation of Freeze-Up:** Freeze-up began during the second week in October, when ice began to form along the coast. Nearshore freeze-up occurred on October 26th, followed soon thereafter by complete freeze-up on November 1st.
- **Landfast Ice and Shear Zone Development:** After remaining narrow in November, the landfast ice zone grew dramatically in December in response to three easterly storms. The ice remained firmly grounded on Weller Bank and Stamukhi

Shoal through mid-winter, but failed to achieve stability seaward of the 11-m isobath to the east of Prudhoe Bay.

- **Ice Pile-Ups:** Ten ice pile-ups occurred in the central portion of the Alaskan Beaufort Sea during the 2011-12 freeze-up season. Nine were located on natural barrier islands and one on Northstar Production Island. The heights ranged from 2 to 7.6 m, the encroachment distances from 0 to 20 m, and the alongshore lengths from 200 m to 1.2 km.
- **Multi-Year Ice:** Except in the immediate vicinity of Point Barrow, multi-year ice remained well offshore in the Alaskan Beaufort Sea throughout the 2011-12 freeze-up season.

Chukchi Sea: 2011-12

- **Initiation of Freeze-Up:** Freeze-up commenced during the first week in October but developed slowly in the weeks that followed. Complete freeze-up occurred on November 30th.
- **Landfast Ice:** The landfast ice in the northeast Chukchi Sea remained unstable and discontinuous until January, when a predominance of westerly winds coupled with two westerly storms produced a narrow but continuous strip from Utqiagvik to Point Lay. This configuration persisted through February despite the frequent occurrence of easterly winds, indicating that the ice had become well-grounded during the westerly winds in January.
- **Flaw Lead:** The coastal flaw lead was present during a significant portion of the 2011-12 freeze-up season, including a majority of the time in both December and February. The width typically ranged from 10 to 30 nm (19 to 56 km) but expanded to as much as 60 nm (111 km) in December. The length, typically between 120 and 180 nm (222 and 334 km), equaled or exceeded 200 nm (371 km) on several occasions.
- **Ice Pile-Ups:** Thirty-one ice pile-ups were detected on the coast between Point Barrow and Point Lay. The highest concentrations were located on the Point Franklin spit and the barrier islands that bracket Icy Cape. The heights ranged from 3 to 18 m, the encroachment distances from 0 to 40 m, and the alongshore lengths from 100 m to 5.4 km. All of the maximum dimensions were associated with a massive pile-up that overtopped the 15-m high bluff at Skull Cliff and spilled 3 m onto the surface of the tundra.
- **Multi-Year Ice:** Large multi-year ice floes began streaming into the region south and west of Point Barrow in mid-December when they entered a northeasterly

extension of the coastal flaw lead. This phenomenon, in which multi-year floes are diverted to the southwest by an extended flaw lead, produced another substantial multi-year ice invasion in late March. Between December and March, floes with diameters as large as 20 km moved as far south as the 68°N parallel and attained concentrations as high as 90%.

- **Grounded Ice Features:** Two grounded ice features believed to be icebergs from the Canadian Arctic Archipelago were discovered off the Chukchi Sea coast in February 2012. The larger of the two, located approximately 3 nm (6 km) off Point Belcher in a charted water depth of 32 m, was estimated to be 80 m long and 40 m wide, and to extend 20 m above sea level.

3.5. 2012-13 Freeze-Up Study

Key findings from the 2012-13 Freeze-Up Study (Coastal Frontiers and Vaudrey, 2013) are as follows:

Beaufort Sea: 2012-13

- **Initiation of Freeze-Up:** Ice began to form in the brackish waters off river deltas and in semi-protected bays and lagoons during the second week in October. Nearshore freeze-up took place on November 5th; complete freeze-up occurred one week later on November 12th.
- **Ice Fracture Event:** From late January through late March, the ice canopy in the Beaufort Sea was disturbed by a massive fracture event that ultimately extended from Banks Island, Canada, on the east to well past Point Barrow on the west. Driven by sustained easterly winds and a series of easterly storms, the event caused large pieces of the pack ice to break free and rotate to the west.
- **Landfast Ice and Shear Zone Development:** The landfast ice zone remained narrow and poorly-developed through mid-December, but expanded dramatically from mid-December through late January in response to the same sustained easterly winds and storms that caused the fracture event. In mid-March, the fracture event removed the outer portion of the landfast ice, and the seaward edge retreated to the vicinity of the 18-m isobath.
- **Ice Pile-Ups:** Thirty-eight ice pile-ups were noted in the central portion of the Alaskan Beaufort Sea, consisting of thirty-four on barrier islands, three on Northstar Production Island, and one on the mainland shore. The heights ranged from 2 to 10 m, the encroachment distances from 0 to 10 m, and the alongshore lengths from 100 m to 2.2 km.

- **Multi-Year Ice:** As in 2010-11 and 2011-12, multi-year ice failed to invade the nearshore region of the Alaskan Beaufort Sea during the 2012-13 freeze-up season.

Chukchi Sea: 2012-13

- **Initiation of Freeze-Up:** Freeze-up began during the second week in October with the formation of ice in Kasegaluk Lagoon, the Kuk River Inlet, and Peard Bay. Nearshore freeze-up occurred on November 15th, followed by complete freeze-up on November 28th.
- **Flash-Freeze Event:** On October 31st, a flash freeze occurred off Wainwright in a large area bounded by the 71°N and 72.5°N parallels, and the 160°W and 165°W meridians. The ice patch, which was surrounded by open water, covered all of the Hanna Shoal Prospects and portions of the Burger Prospects.
- **Landfast Ice:** At the end of November, a narrow strip of landfast ice extended from Utqiagvik to the vicinity of Wainwright, and another narrow strip encircled Icy Cape. During the next four months, in the absence of westerly storms, the landfast ice zone alternated between a narrow, continuous strip and an even narrower, discontinuous strip.
- **Flaw Lead:** The coastal flaw lead remained open for about half of the month of December, three quarters of the month of January, the entire month of February, and half of the month of March. During the 46-day period from January 31st through March 17th, it never closed. Maintained by a combination of sustained easterly winds, energetic easterly storms, and the massive ice fracture event in the Beaufort, the lead reached a maximum width of 150 nm (278 km) while stretching from Cape Lisburne to well northeast of Point Barrow.
- **Ice Pile-Ups:** Thirty-two ice pile-ups were observed on the Chukchi Sea coast between Point Barrow and Point Lay, with the highest concentration located on the barrier islands that lie to the south of Icy Cape. The pile-ups were relatively small, with heights ranging from 2 to 4 m, encroachment distances from 0 to 8 m, and alongshore lengths from 100 m to 3.8 km.
- **Multi-Year Ice:** As in the case of the Beaufort, multi-year ice remained absent from the region south and west of Point Barrow during the 2012-13 freeze-up season.

3.6. 2013-14 Freeze-Up Study

The 2013-14 Freeze-Up Study (Coastal Frontiers and Vaudrey, 2014) produced the following results:

Beaufort Sea: 2013-14

- **Initiation of Freeze-Up:** Ice began to form in the semi-protected waters adjacent to the coast in late September. Nearshore freeze-up occurred on October 26th, followed by complete freeze-up on November 20th.
- **Landfast Ice and Shear Zone Development:** The landfast ice zone remained narrow and poorly-developed through the end of December. The situation changed in January, when persistent easterly winds caused the ice to expand past the 18-m isobath from Point Barrow to Barter Island. In February and March, the landfast ice edge advanced in response to easterly winds and retreated in response to westerly winds but tended to retreat no farther than the 18-m isobath due to the existence of a well-grounded shear zone.
- **Ice Pile-Ups:** Of the forty-six ice pile-ups that occurred in the central portion of the Alaskan Beaufort Sea, thirty-nine were located on natural barrier islands, four on man-made facilities, and three on the mainland shore. The heights ranged from 1 to 8 m, the encroachment distances from 0 to 20 m, and the alongshore lengths from 50 m to 2.6 km.
- **Multi-Year Ice:** Multi-year ice was present in the offshore portion of the Alaskan Beaufort Sea throughout freeze-up and early winter but remained absent from the nearshore region except in the immediate vicinity of Point Barrow.

Chukchi Sea: 2013-14

- **Initiation of Freeze-Up:** Freeze-up in the Chukchi Sea began during the first week in October but proceeded slowly in response to unseasonably warm air temperatures that persisted through mid-November. Nearshore freeze-up occurred on November 26th. Complete freeze-up took place on December 14th.
- **Flash-Freeze Event:** On or about November 12th, a flash freeze created a patch of ice centered 130 nm (241 km) west of Icy Cape. Although much smaller than that which formed off Wainwright in October 2013, it nevertheless marked the second documented occurrence of flash freezing in the Chukchi Sea in five freeze-up seasons.
- **Landfast Ice:** At the end of November, the landfast ice zone between Utqiagvik and Point Lay consisted of a narrow, discontinuous strip. It remained narrow in December except for an advance to Blossom Shoals that occurred at the end of the month and persisted for the remainder of the study period. In mid-January, a prolonged easterly storm dislodged virtually all of the landfast ice north of the

Nokotlek River Mouth. Subsequently, the width of the landfast ice zone ranged from negligible to 20 nm (37 km) in response to changing wind conditions. At the end of March, landfast ice was confined to a narrow strip located inside the 11-m isobath in most areas.

- **Flaw Lead:** The flaw lead was present on 57% of the days from December 2013 through March 2014. The maximum width of 100 nm (185 km) occurred in February, when the lead encompassed all of the Burger and Crackerjack Prospects and parts of the Hanna Shoal and West Prospects. The maximum length, 250 nm (463 km), occurred on repeated occasions in February and March. The maximum persistence of 15 days took place from mid-February to early March.
- **Ice Pile-Ups:** Twenty-two ice pile-ups were detected between Utqiagvik and Point Lay, with the highest concentration located on the barrier islands to the east of Icy Cape. The pile-up heights, which varied from 1 to 3 m, were smaller than those recorded during the prior four freeze-up seasons. All 22 pile-ups encroached onto the subaerial beach, with the encroachment distances ranging from 5 to 20 m and the alongshore lengths from 100 m o 7.8 km.
- **Multi-Year Ice:** Multi-year ice remained north of Point Barrow until mid-December. During the month that followed, multi-year floes were channeled into the region south and west of the Point on four occasions by a northeasterly extension of the flaw lead. The last invasion, which occurred in mid-January, produced a significant southerly displacement of the multi-year ice edge. The ice continued to advance slowly to the south in February and March, crossing the 71°N parallel in late February and reaching the vicinity of Icy Cape in mid-March.

3.7. 2014-15 Freeze-Up Study

Salient findings from the 2014-15 Freeze-Up Study (Coastal Frontiers and Vaudrey, 2015) are summarized below:

Beaufort Sea: 2014-15

- **Initiation of Freeze-Up:** Freeze-up commenced in early October, when ice began to form in the semi-protected bays and lagoons adjacent to the coast. Nearshore freeze-up occurred on October 30th, followed soon thereafter by complete freeze-up on November 5th.
- **Landfast Ice and Shear Zone Development:** Landfast ice, which began to form during the second week in October, advanced to the 11-m isobath in late November, the 18-m isobath in late December, and well beyond the 18-m isobath in mid-

January, with each advance precipitated by one or more easterly storms. Westerly storms in late January produced significant losses, with the ice remaining grounded on Weller Bank and Stamukhi Shoal but retreating to the vicinity of the 11-m isobath on either side. Subsequently, in February and March, the landfast ice edge advanced in response to easterly winds and retreated in response to westerly winds but remained between the 11- and 18-m isobaths.

- **Ice Pile-Ups:** Thirty-five ice pile-ups occurred in central portion of the Alaskan Beaufort Sea during the 2014-15 freeze-up season. Thirty-one were located on natural barrier islands, three on man-made islands, and one on a spit emanating from the mainland shore. The heights ranged from 1 to 15 m, the encroachment distances from 0 to 25 m, the alongshore lengths from 50 m to 1.5 km, and the ice block thicknesses from 30 to 90 cm.
- **Multi-Year Ice:** For the fifth consecutive year, multi-year ice failed to invade the nearshore region of the Alaskan Beaufort Sea. It remained well offshore, never less than 90 nm (167 km) from the coast at the U.S.-Canadian border, 75 nm (139 km) from Cross Island, and 25 nm (46 km) from Point Barrow.

Chukchi Sea: 2014-15

- **Initiation of Freeze-Up:** Freeze-up began in early October but was delayed by a severe easterly storm in mid-month. Nearshore freeze-up occurred on November 28th; complete freeze-up occurred nearly three weeks later on December 17th. These dates were later than in any of the five prior freeze-up seasons.
- **Landfast Ice:** Landfast ice began to form in late October. During the next three months, the landfast ice zone expanded and contracted in response to changing wind conditions but remained narrow and discontinuous. Westerly winds and a westerly storm produced a significant expansion during the first half of February, but easterly winds and two easterly storms erased this gain by month-end. Another major expansion followed in mid-March, again in response to westerly winds. This time, however, the ice became sufficiently well-grounded to resist displacement during the easterly winds that followed at the end of the month.
- **Flaw Lead:** The flaw lead was present 64% of the time from December through March. The frequency of occurrence varied with the wind direction, peaking at 90% in December when easterlies prevailed 90% of the time, and falling to 46% in February when easterlies prevailed only 54% of the time. The maximum width, 110 nm (204 km), occurred in February, when the lead encompassed all of the

"THIS INFORMATION IS DISTRIBUTED SOLELY FOR THE PURPOSE OF PRE-DISSEMINATION PEER REVIEW UNDER APPLICABLE INFORMATION QUALITY GUIDELINES. IT HAS NOT BEEN FORMALLY DISSEMINATED BY BSEE. IT DOES NOT REPRESENT AND SHOULD NOT BE CONSTRUED TO REPRESENT ANY BSEE DETERMINATION OR POLICY."

Burger Prospects and the southern portion of the Crackerjack Prospects. The maximum length, 250 nm (463 km), occurred in both December and March. The maximum persistence of 27 days took place in December.

- **Ice Pile-Ups:** Fifty-five ice pile-ups were observed on the coast during the 2014-15 freeze-up season. The highest concentrations were located between Utqiagvik and Peard Bay, and on the barrier islands east of Icy Cape. The pile-up heights ranged from 1 to 8 m, the encroachment distances from 0 to 30 m, and the alongshore lengths from 50 m to 9.5 km. The block thicknesses were estimated to vary from 2 to 60 cm.
- **Multi-Year Ice:** Multi-year ice briefly entered the region south and west of Point Barrow in mid-November, when a small tongue of such floes advanced to within 25 nm (46 km) of Point Belcher. By the end of November, however, the southern boundary had retreated to the 73°N parallel. It remained well north of Point Barrow, between the 72°N and 73°N parallels, from December through March.

3.8. 2015-16 Freeze-Up Study

Key findings from the 2015-16 Freeze-Up Study (Coastal Frontiers and Vaudrey, 2016) are as follows:

Beaufort Sea: 2015-16

- **Initiation of Freeze-Up:** Freeze-up began in late September with the formation of ice adjacent to the coast. Nearshore freeze-up occurred on October 26th, followed five days later by complete freeze-up on October 31st.
- **Landfast Ice and Shear Zone Development:** Landfast ice began to form in mid-October, and grew to cover all of Stefansson Sound, the central portion of Harrison Bay, and the southern portion of Camden Bay in early November. The next major expansion, which was triggered by an easterly storm in late November and early December, caused the ice to become grounded on its customary anchor points, Weller Bank and Stamukhi Shoal. In January, the landfast ice edge advanced seaward of the 18-m isobath over the entire length of the study area. This configuration persisted virtually unchanged through mid-March in response to a predominance of easterly winds coupled with a complete absence of westerly storms.
- **Ice Pile-Ups:** Only four ice pile-ups occurred in central portion of the Alaskan Beaufort Sea during the 2015-16 freeze-up season. Two were located on natural barrier islands to the west of Prudhoe Bay, one on the Nikaitchuq Spy Island Drillsite (SID), and one on Northstar Production Island. The pile-ups were small by historical

standards, with heights of 2 to 5 m, alongshore lengths of 100 to 900 m, encroachment distances of 0 to 5 m, and ice block thicknesses of 20 to 40 cm.

- **Multi-Year Ice:** Except in the immediate vicinity of Point Barrow, multi-year pack ice remained absent from the nearshore portion of the Alaskan Beaufort Sea throughout freeze-up. However, numerous small fragments of first-year ice survived the 2015 open-water season and became grounded on and around the barrier islands at the outset of freeze-up. At Point Barrow, low concentrations of multi-year ice entered the nearshore region during the first week in November and remained within 15 nm (28 km) of the coast until mid-January.

Chukchi Sea: 2015-16

- **Initiation of Freeze-Up:** Ice began to form in Kasegaluk Lagoon, the Kuk River Inlet, and Peard Bay during the second week in October. Complete coverage of these semi-enclosed basins took place during the third week, along with initial ice growth in the exposed waters adjacent to the coast. Nearshore freeze-up was delayed by a combination of relatively warm air temperatures and easterly storms. It finally occurred on December 5th after several days of low temperatures and moderate winds. Complete freeze-up followed a week later, on December 12th.
- **Landfast Ice:** Landfast ice remained narrow and ephemeral throughout the study period, reflecting the disruptive influence of easterly storms and a complete absence of westerly storms. The first landfast ice appeared in late October, when small strips formed off Peard Bay, the Kuk River Inlet, and North Kasegaluk Lagoon. Modest growth followed in November and December, producing a narrow, near-continuous strip from Point Barrow to Icy Cape and a narrow, intermittent strip from Icy Cape to Point Lay. This configuration persisted through January, but strong easterly storms in February completely removed the ice at the base of Skull Cliff. In the remainder of the study area, the thin strip remained in place through February and the first half of March, indicating that the ice had become sufficiently well-grounded to resist displacement.
- **Flaw Lead:** From December 2015 through March 2016, the flaw lead opened on seven different occasions. The frequency of occurrence, which averaged 83% over the four-month period, varied from a low of 61% in March to a high of 100% in February. The maximum width, 80 nm (148 km), occurred in March while the maximum length, 250 nm (463 km), occurred in both December and January. The lead persisted for periods that ranged from one day to an extraordinary 64 consecutive days (from January 10th through March 13th).

- **Ice Pile-Ups:** Fifty-two ice pile-ups were observed on the shoreline between Utqiagvik and Point Lay during the 2015-16 freeze-up season, with more than half located between Utqiagvik and Peard Bay. The dimensions were unexceptional: the heights ranged from 1 to 8 m, the encroachment distances from 0 to 10 m, the alongshore lengths from 100 m to 4.4 km, and the ice block thicknesses from 20 to 60 cm.
- **Multi-Year Ice:** Multi-year pack ice moved south to the vicinity of Point Barrow in late October and began streaming into the region south and west of the Point in mid-November. This early-season invasion consisted of low concentrations of small floes entering an area of predominantly open water. Multi-year floes continued to move south and west of Point Barrow for the next two and a half months. From mid-November until mid-December, the concentrations remained at or below 10% as the ice advanced to the 70°N parallel off Point Lay. From mid-December until the end of January, the concentrations increased to as much as 50%. The invasion ceased in early February, when the southern boundary of the multi-year ice retreated rapidly to the north. The ice that already had entered the region south and west of Point Barrow continued to drift to the west, moving past the 168°W meridian in late February.

3.9. 2016-17 Freeze-Up Study

The findings of the 2016-17 Freeze-Up Study (Coastal Frontiers and Vaudrey, 2017) are summarized below:

<u>Beaufort Sea: 2016-17</u>

- **Initiation of Freeze-Up:** Freeze-up commenced in mid-October when ice appeared in the semi-protected waters adjacent to the coast. Nearshore freeze-up occurred on November 7th, while complete freeze-up occurred about two weeks later on November 23rd.
- **Landfast Ice and Shear Zone Development:** Landfast ice began to develop during the last week in October and expanded to cover all of the coastal lagoons and a significant portion of Harrison Bay over the course of November. The expansion stalled in December, with gains during the first half of the month erased by losses during the second. The next major advance occurred in late January, when easterly winds propelled the ice edge to the vicinity of the 11-m isobath. After another period of minimal change, the ice edge moved to the 18-m isobath in late February, finally reaching its customary anchor points on Weller Bank and Stamukhi Shoal.

- **Ice Pile-Ups:** Thirty-eight ice pile-ups formed in the central portion of the Alaskan Beaufort Sea during the 2016-17 freeze-up season. One was located on the Oooguruk Offshore Drillsite (ODS), one on the Spy Island Drillsite (SID), one on Northstar Production Island, two on Thetis Island (a natural barrier island in Harrison Bay), and 33 on natural barrier islands and shoals to the east of Prudhoe Bay. The dimensions of the pile-ups tended to be unexceptional by historical standards, with heights of 1 to 8 m, encroachment distances of 0 to 12 m, and block thicknesses of 20 to 40 cm. Several of the features extended alongshore for substantial distances, however, including a maximum length of 5.9 km on the spit that emanates from Brownlow Point.
- **Multi-Year Ice:** With the exception of two small patches of second-year ice that drifted away from Point Barrow in October, multi-year ice remained absent from the nearshore region of the Alaskan Beaufort Sea throughout freeze-up. The minimum separation between the ice and the coast, 170 nm (315 km), occurred off Barter Island at the end of February.

<u>**Chukchi Sea: 2016-17**</u>

- **Initiation of Freeze-Up:** Ice began to appear in Kasegaluk Lagoon, the Kuk River Inlet, and Peard Bay during the third week in October, but freeze-up proceeded slowly in the weeks that followed due to air temperatures that hovered near freezing. The pack ice, after advancing rapidly to the south during the first week in November, reached the vicinity of Point Barrow during the second week and began to coalesce with a nascent strip of coastal ice. On or about December 7th, a flash-freeze created an isolated patch of ice centered approximately 150 nm (278 km) west of Icy Cape. Nearshore freeze-up took place three days later, on December 10th, followed by complete freeze-up on December 27th.
- **Landfast Ice:** Landfast ice first appeared at the end of October but remained narrow and discontinuous for the next two months in response to a predominance of easterly winds. The situation changed in January, when an increased frequency of westerly winds coupled with several westerly storms produced a continuous band of ice up to 10 nm (19km) wide off Skull Cliff and 8 nm (15 km) wide between Icy Cape and Point Lay. During the second half of January, the ice grounded on Blossom Shoals, its customary anchor point off Icy Cape. Additional expansion followed in early February, producing a maximum width of 20 nm (37 km) between Wainwright and the Nokotlek River mouth. Subsequently, at the end of February, a strong easterly storm dislodged the newly-accumulated ice and caused the landfast ice edge to retreat to its location at the beginning of the month.

- **Flaw Lead:** From December 2016 through February 2017, the flaw lead opened on nine different occasions. The frequency of occurrence, which averaged 51% over the three-month period, increased from 42% in December to 52% in January and 61% in February. The maximum width, 50 nm (93 km), and maximum length, 250 nm (463 km), both occurred during a single event that began in late January and continued into early February. The lead persisted for periods that ranged from one to 15 days.
- **Ice Pile-Ups:** Sixty-three ice pile-ups occurred on the shoreline between Utqiagvik and Point Lay during the 2016-17 freeze-up season. Fifty-two were located to the south of Point Belcher, while 11 were located to the north. Their dimensions were relatively small compared to those observed in past years, with heights of 1 to 5 m, encroachment distances of 0 to 10 m, and alongshore lengths of 50 m to 4 km. The block thicknesses were estimated to vary from 30 to 40 cm.
- **Multi-Year Ice:** With the exception of the two small patches of second-year ice that drifted away from Point Barrow in October (discussed above in relation to the Beaufort Sea), multi-year ice remained completely absent from the Chukchi Sea study area during the five-month study period.

4. DATA ACQUISITION AND ANALYSIS

As discussed in Section 1, the 2019-20 Freeze-Up Study was conducted using a combination of remotely-sensed data and on-site observations. This section describes the sources of data and methods of analysis in terms of the following five categories: meteorological data (Section 4.1), ice charts (Section 4.2), satellite imagery (Section 4.3), drift buoy data (Section 4.4), and aerial reconnaissance missions (Section 4.5). The underlying digital data are provided in Appendix E.

4.1. Meteorological Data

Meteorological conditions during the nine-month period from September 2019 through May 2020 were derived from the *Local Climatological Data* (LCD) for the Deadhorse and Utqiagvik Airport Automated Surface Observing System stations compiled by the National Oceanographic and Oceanic Administration (NOAA, 2020a). The LCD includes hourly observations and daily summaries of temperature, pressure, humidity, precipitation and winds. Raw daily and hourly data are provided in Appendix E in PDF format. Excel spreadsheets with monthly summaries of the meteorological conditions also are included in Appendix E.

The wind data were used to identify storms and changes in wind direction that could impact the ice canopy. Such impacts included the development and loss of landfast ice, the opening and closing of the Chukchi Sea flaw lead, and the generation of ice pile-ups. The air temperature data were used to derive freezing-degree days (FDD), which were computed for each day as the difference between the freezing point of seawater (29°F; -2°C) and the average air temperature. Days in which the temperature exceeded 29°F produced negative FDD. The daily values were summed over the period that produced the maximum number of accumulated FDD: October 20th through May 21st at Utqiagvik Airport, and October 7th through May 21st at Deadhorse Airport. The results are shown in Table 4-1.

Table 4-1. Accumulated Freezing-Degree Days (<29°F) at Utqiagvik and Deadhorse Airports in 2019-20

Site	Sep	Oct	Nov	Dec	Jan	Feb	Mar	Apr	May
Utqiagvik	0	48	406	1,318	2,621	4,224	5,284	5,907	6,122
Deadhorse	0	162	696	1,881	3,480	5,162	6,305	6,958	7,143

To provide historical perspective, the normal range of daily air temperatures at each weather station defined by the average values of the daily highs and lows from 1980-81

"THIS INFORMATION IS DISTRIBUTED SOLELY FOR THE PURPOSE OF PRE-DISSEMINATION PEER REVIEW UNDER APPLICABLE INFORMATION QUALITY GUIDELINES. IT HAS NOT BEEN FORMALLY DISSEMINATED BY BSEE. IT DOES NOT REPRESENT AND SHOULD NOT BE CONSTRUED TO REPRESENT ANY BSEE DETERMINATION OR POLICY."

through 2009-10 was obtained from NOAA (Arguez, *et al.*, 2010). The appropriate range is included in each plot of daily average air temperature that appears in Sections 5 and 6. It should be noted that the "normal ranges" used for the five freeze-up studies from 2009-10 through 2013-14 were derived from the period from 1970-71 through 1999-2000 rather than 1980-81 through 2009-10.

As in each of the prior eight freeze-up studies, Utqiagvik Airport was adopted as the primary source of weather data for the Chukchi Sea. Although the data from Wainwright Airport have become sufficiently reliable to warrant consideration, a comparison with the Utqiagvik data for the 2014-15 freeze-up season indicated that the differences were relatively minor (Coastal Frontiers and Vaudrey, 2015). As a result, to maintain continuity with the prior studies, all of the wind and temperature data presented in Section 6 were obtained from Utqiagvik.

To supplement the data from Deadhorse Airport, monthly plots of wind speed, wind direction, air temperature and barometric pressure measured at the Prudhoe Bay West Dock Seawater Treatment Plant (STP) were downloaded from the National Ocean Service website (NOS, 2020) for the period from October 2019 through February 2020. These plots are included as PNG files in Appendix E.

4.2. Ice Charts

Weekly ice charts pertaining to the study area were downloaded from two government sources: the Canadian Ice Service (CIS; 2019, 2020) and the National Ice Center (NIC; 2019, 2020). Daily ice charts from the National Weather Service (NWS; 2020) also were downloaded. Although the charts from all three organizations provide similar information, the CIS products tend to incorporate greater detail. However, coverage is limited to the Beaufort Sea and extreme northeast portion of the Chukchi Sea whereas the NIC and NWS charts encompass the entire Chukchi as well as the Beaufort.

Twenty-two ice charts were obtained from the CIS for the period from September 30, 2019, through February 24, 2020. The charts are provided in Appendix E in shapefile and image (PNG) format. For clarity, the CIS provides two images for each ice chart: one showing the ice concentration and the other showing the stage of development. Figure 4-1 presents the CIS stage of development chart for November 25, 2019, shortly after complete freeze-up had occurred in the Alaskan Beaufort Sea.

Type text here

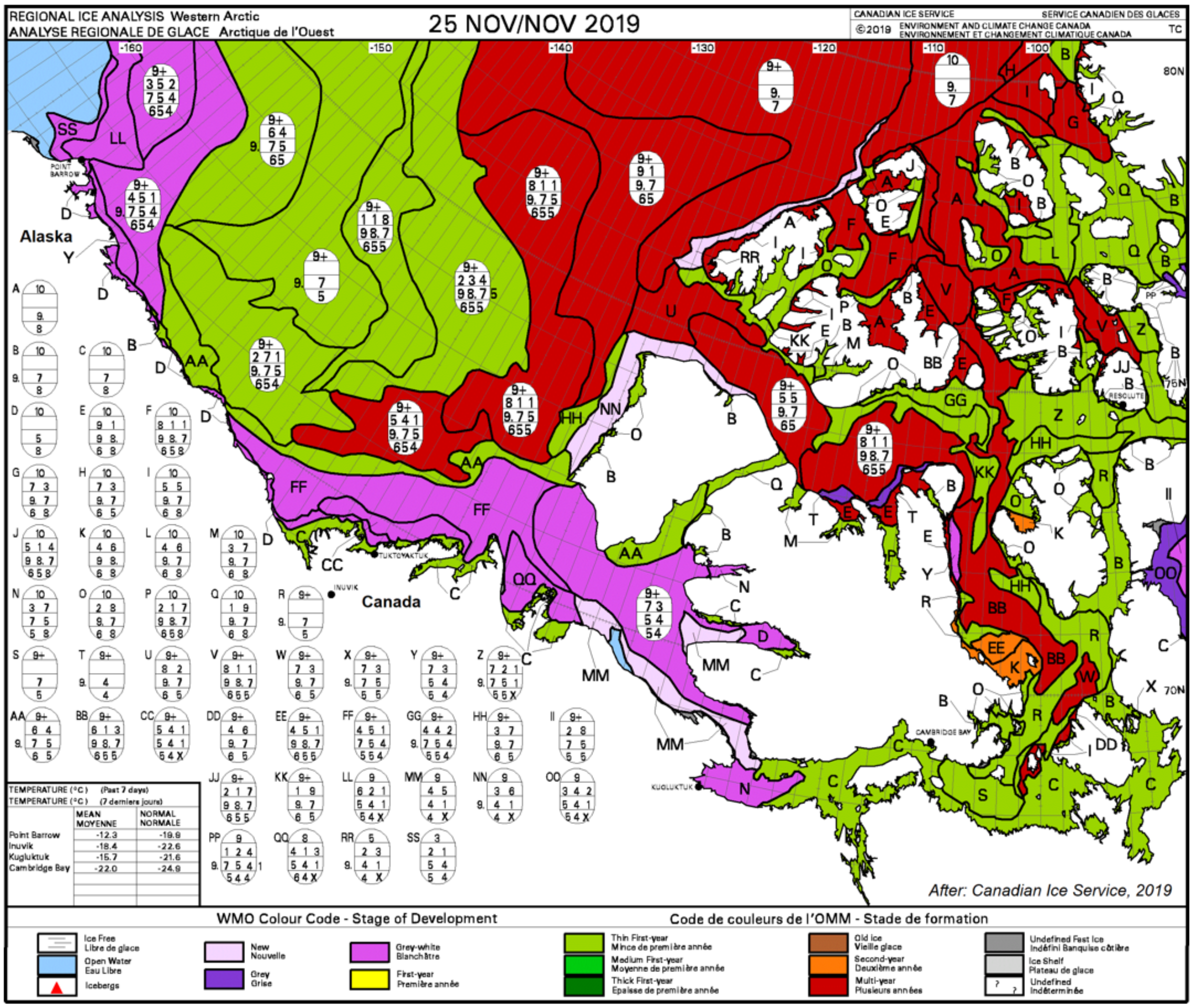

After: Canadian Ice Service, 2019

Figure 4-1. CIS Ice Stage of Development Chart of Beaufort Sea for November 25, 2019

Twenty-two weekly ice charts covering the period from October 3, 2019, through February 27, 2020 were obtained from the NIC. The NIC charts are available in shapefile and image format and, similar to the CIS, the NIC provides two images for each ice chart: one showing ice concentration, and one displaying stage of development. The NIC charts are included in Appendix E in both shapefile and image (PNG) format. Figure 4-2 presents the NIC stage of development chart for February 27, 2020, at the end of the study period.

Background information on the progression of freeze-up in the entire Arctic region was obtained from the NIC Arctic Marginal Ice Zone charts, which depict the extent of the pack ice and marginal ice zone on a daily basis. For the purpose of preparing these charts, pack ice is assumed to occupy the region with eight tenths or more coverage, while the marginal ice zone is the transition between the open ocean (ice free) and pack ice (NIC, 2020). A representative example corresponding to December 4, 2019, after basin-wide freeze-up had

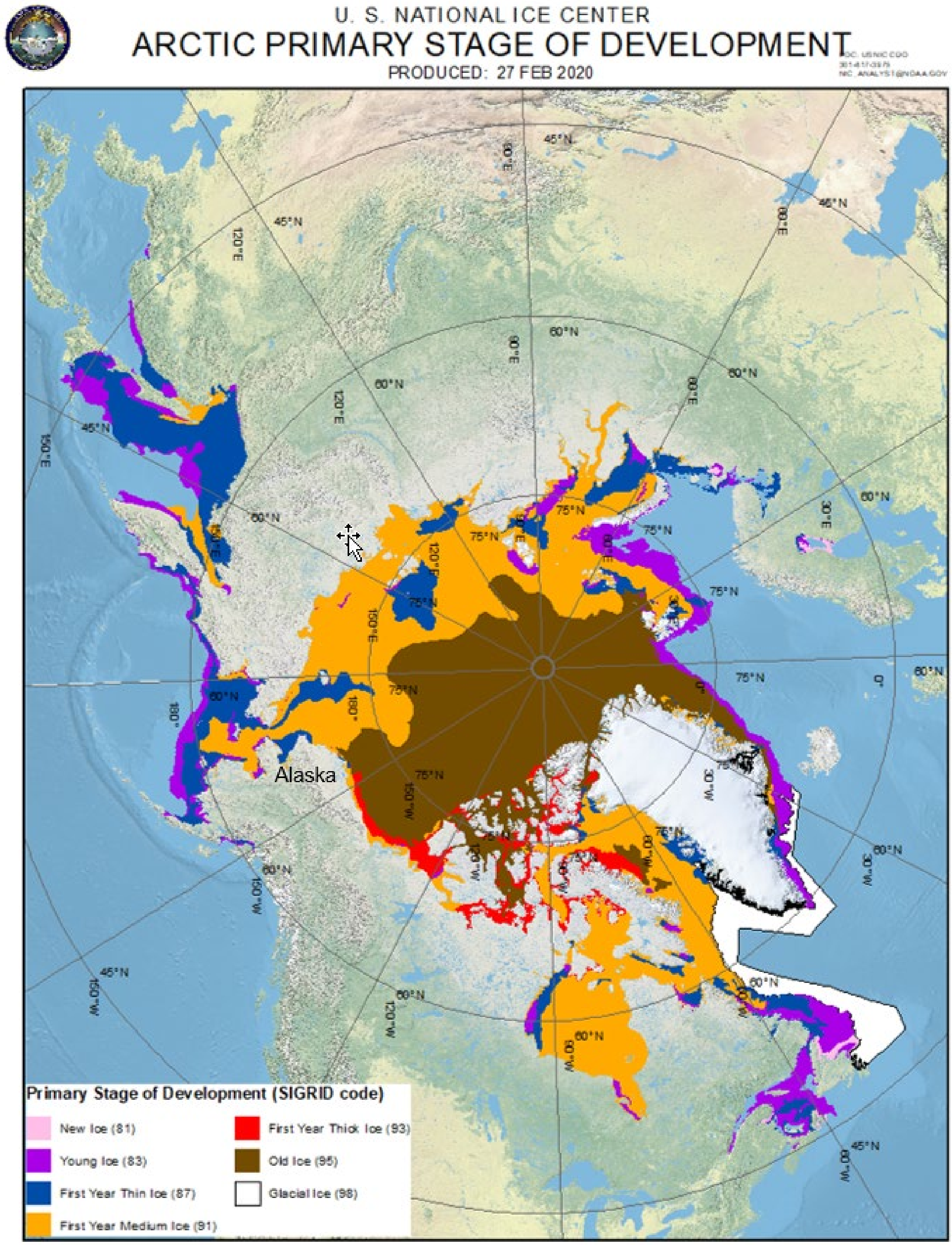

After: National Ice Center, 2020

Figure 4-2. NIC Arctic Ice Stage of Development Chart for February 27, 2020

occurred in the Beaufort but not in the Chukchi, is provided in Figure 4-3. PNG files of the NIC Arctic Marginal Ice Zone charts beginning on October 1, 2019 and ending on February 29, 2020, are included in Appendix E.

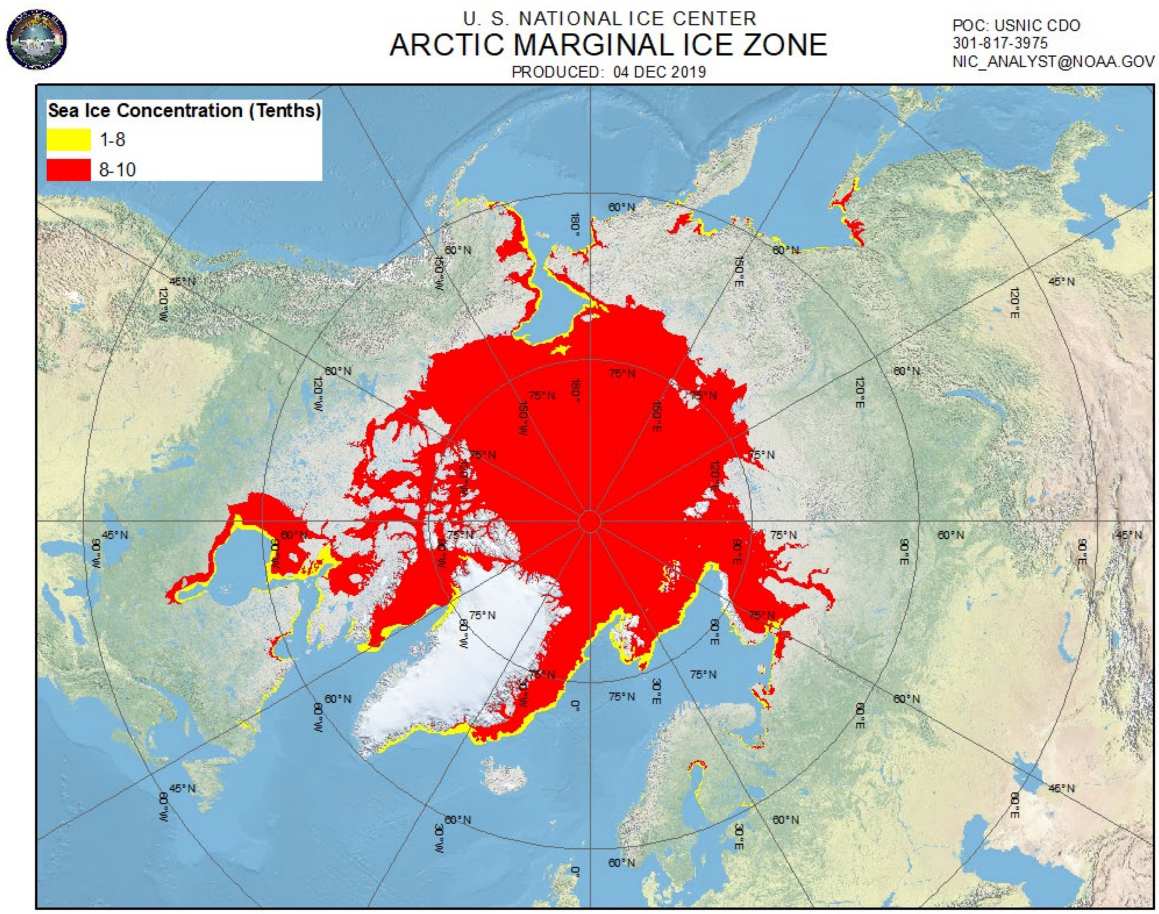

Source: National Ice Center, 2020

Figure 4-3. NIC Arctic Marginal Ice Zone Chart for December 4, 2019

The data obtained from the CIS and NIC were supplemented with daily ice charts produced by the National Weather Service for the period from October 2019 through February 2020. Because the NWS charts often differed from the corresponding CIS and NIC charts as well as from the satellite images obtained for this project, they were used only sparingly. They are included in image (JPG) and shapefile format in Appendix E.

The ice charts described above were used to track the evolution of freeze-up on a coarse scale, particularly during the early stages of the process. They were not sufficiently detailed to support the investigation of fine-scale features such as individual ice floes, rubble fields, and ice movement lines.

4.3. Satellite Imagery

Three different types of satellite imagery were used to study the ice conditions that prevailed during the 2019-20 freeze-up season: RADARSAT-2, VIIRS (Visible Infrared Imaging Radiometer Suite), and MODIS (Moderate Resolution Imaging Spectro-radiometer). The RADARSAT-2 imagery served as the primary source of ice data, while the VIIRS imagery played a supplemental role. The MODIS imagery was used only sparingly.

General information about the progress of freeze-up was obtained from 22 publicly available RADARSAT-2 mosaics compiled by the CIS for the period from October 7, 2019, through February 24, 2020. The mosaics, which were produced on a weekly basis, are provided as GIF files in Appendix E. Although the resolution was inadequate to support detailed analysis, the composite images provided useful data on synoptic-scale ice conditions. A representative example from mid-December, 2019 is provided as Figure 4-4 (CIS, 2020).

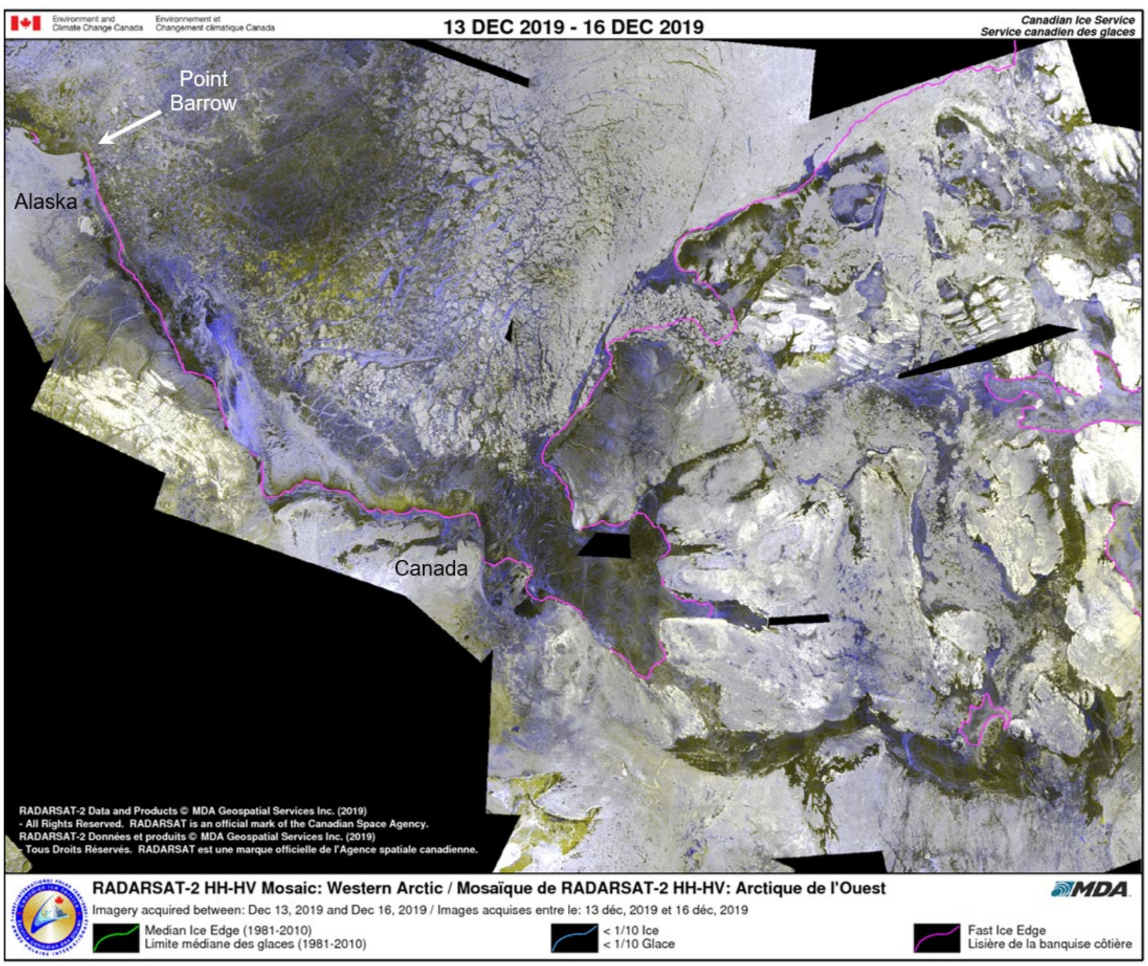

After: Canadian Ice Service, 2019

Figure 4-4. CIS RADARSAT-2 Mosaic for December 13-16, 2019

The most useful RADARSAT-2 images were the 20 high-resolution, georeferenced scenes captured using the ScanSAR Wide beam mode, which provides a nominal resolution of 100 m over a nominal area of 270 x 270 nm (500 x 500 km; MacDonald, Dettwiler and Associates, 2020). The data set consisted of 10 images of the Beaufort Sea obtained between October 17, 2019, and February 28, 2020, and 10 images of the Chukchi Sea obtained between October 19, 2016, and February 26, 2020. In each case, the interval between successive images was approximately two weeks. The image characteristics were sufficient not only to track the general evolution of the ice cover during freeze-up, but also to support detailed investigations of features and phenomena that included the development of the landfast ice zone, large multi-year ice floes, leads, and ice movement.

As the licensing agreement for the RADARSAT-2 images prohibits the distribution of the original georeferenced TIFF files (MDA Geospatial Services, 2019), each scene is provided in Appendix E in PDF format. A sample image of the Chukchi Sea that was acquired on December 16th, 2019 is provided as Figure 4-5. Image acquisition reports prepared following the receipt and processing of each pair of images (consisting of one image of the Beaufort and one of the Chukchi) are provided in Appendix B.

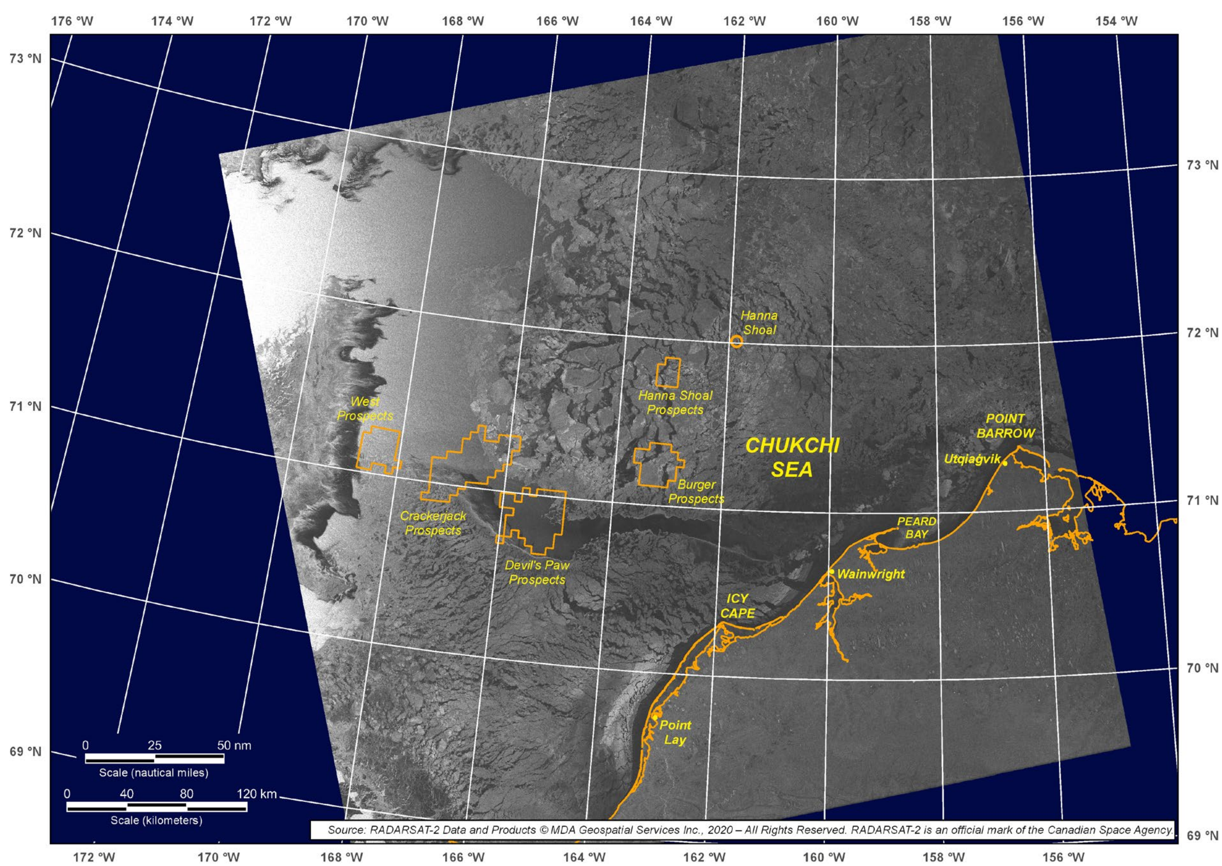

Figure 4-5. RADARSAT-2 Image of Chukchi Sea Acquired on December 16, 2019

To bridge the chronological gaps between RADARSAT-2 scenes, 148 VIIRS images were obtained on a daily basis from October 1, 2019, through February 29, 2020. Although AVHRR (Advanced Very High Resolution Radiometer) imagery was used to complement the RADARSAT-2 products in prior freeze-up studies, VIIRS was adopted for the current study due to its improved spatial resolution. Data were downloaded from NOAA's Regional and Mesoscale Meteorology Branch (RAMMB, 2019 and 2020) and from the Geographic Information Network of Alaska (GINA, 2019 and 2020).

The primary VIIRS product used for this study was I5-band longwave infrared imagery (I5 Band), but scenes corresponding to the Day-Night Band (DNB), which uses light in the visual spectrum, also were employed. The utility of this imagery was limited by the sensors' spatial resolution (375 m for the I5 Band, and 750 m for the DNB) and inability to penetrate cloud cover. Notwithstanding these drawbacks, the high frequency of image capture (multiple scenes per day subject to suitable weather conditions) allowed large-scale changes in the ice canopy to be tracked on a short-term basis. The imagery was particularly useful in determining the status of the coastal flaw lead in the Chukchi.

Some of the VIIRS images are provided as PNG files and others as TIFF files in Appendix E. A representative example in Figure 4-6 shows the coastal flaw lead in the Chukchi Sea on January 8, 2020.

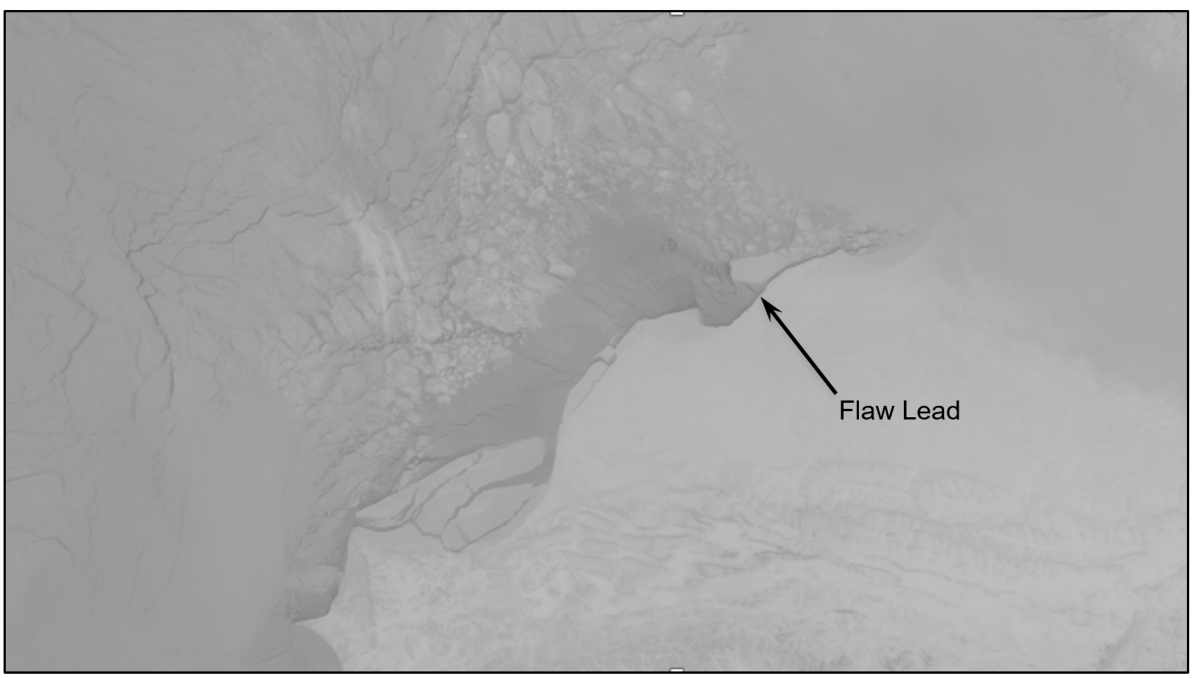

After: GINA, 2020

Figure 4-6. VIIRS I5-Band Image of Alaskan Chukchi Sea Acquired on January 8, 2020

MODIS imagery, like that from VIIRS, was acquired to supplement the RADARSAT-2 scenes. Unfortunately, the sensor’s maximum resolution of 250 m was outweighed by its inability to penetrate cloud cover and darkness, and its dependence on light in the visible spectrum. As a result, useful scenes were confined to two periods: (1) prior to the onset of darkness (October 1 through November 5, 2019) and (2) following the return of daylight (February 10 through 29, 2020). The fifty-six MODIS images that were obtained from the NASA Worldview Snapshots tool (NASA, 2019 and 2020) are provided as georeferenced JPG files in Appendix E.

Figure 4-7 presents a MODIS image acquired on October 26th, when ice had begun to form in the semi-protected, nearshore waters of both basins.

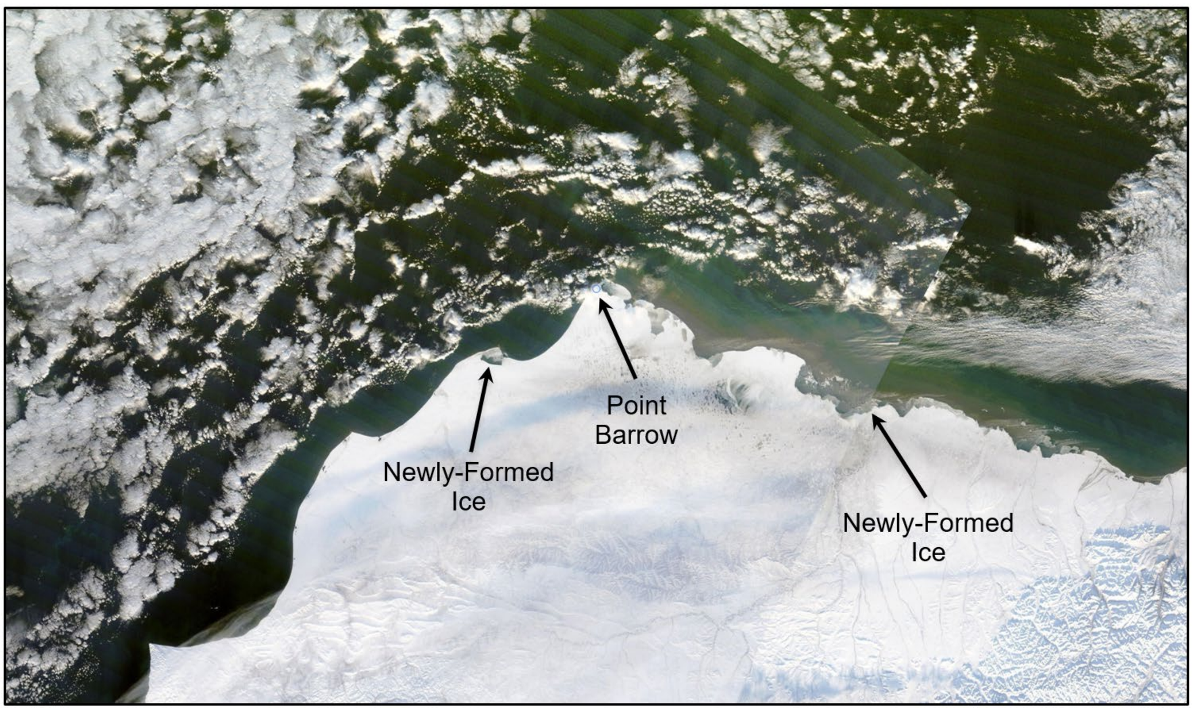

After: NASA, 2019

Figure 4-7. MODIS Image Acquired on October 26, 2019

4.4. Drift Buoys

As in previous freeze-up studies (Coastal Frontiers and Vaudrey, 2014; 2015; 2016; 2017), information on ice drift was obtained from telemetry buoys monitored through the International Arctic Buoy Programme (“IABP”; Rigor, 2020). Three such buoys were present in the study area when freeze-up data acquisition began on October 1st. Their characteristics are summarized in Table 4-2. Note that the lengthy buoy identification numbers used by the IABP have been replaced by one-letter designations in this study in the interest of simplicity.

Table 4-2. IABP Drift Buoy Characteristics

Buoy Identifier in this Report	IABP Buoy Identifier	Sponsor	Period of Ice Drift Data[1]	Basin
X	300234060738030	Environment Canada	Nov 30, 2019 – Dec 24, 2019 Dec 24, 2019 – Feb 29, 2020	Beaufort Chukchi
Y	300234067522560	USIABP[2]	Nov 30, 2019 – Feb 29, 2020	Beaufort
Z	300234063983340	USIABP[2]	Dec 31, 2019 – Feb 29, 2020	Beaufort

Notes:

1 The period in which the movement of each buoy could be used to quantify ice drift was determined by superimposing its trajectory on available satellite imagery and ice charts.

2 U.S. Interagency Buoy Program.

To determine the period in which the motion of a particular buoy could be used to quantify ice drift, its track was superimposed on the available RADARSAT-2 and VIIRS satellite images, as well as on CIS ice concentration charts (Section 3.3). Those portions that corresponded to open water or partial ice cover were discarded, while those portions that corresponded to complete ice cover were retained. The resulting on-ice drift tracks are shown in Figure 4-8, which was constructed from the daily position of each buoy at midnight.

4.5. Aerial Reconnaissance Missions

Four aerial reconnaissance missions were undertaken in the Beaufort and Chukchi Seas in late February to observe the conditions that prevailed at the end of freeze-up. The specific objectives of the missions were as follows:

- Obtain ground truth information to confirm and expand upon the conclusions drawn from satellite imagery;
- Investigate major features identified in the satellite imagery, such as leads, landfast ice and well-developed shear lines;
- Detect, investigate, and document small-scale features that were beneath the resolution of the satellite imagery, including ridges, rubble fields, and pile-ups.

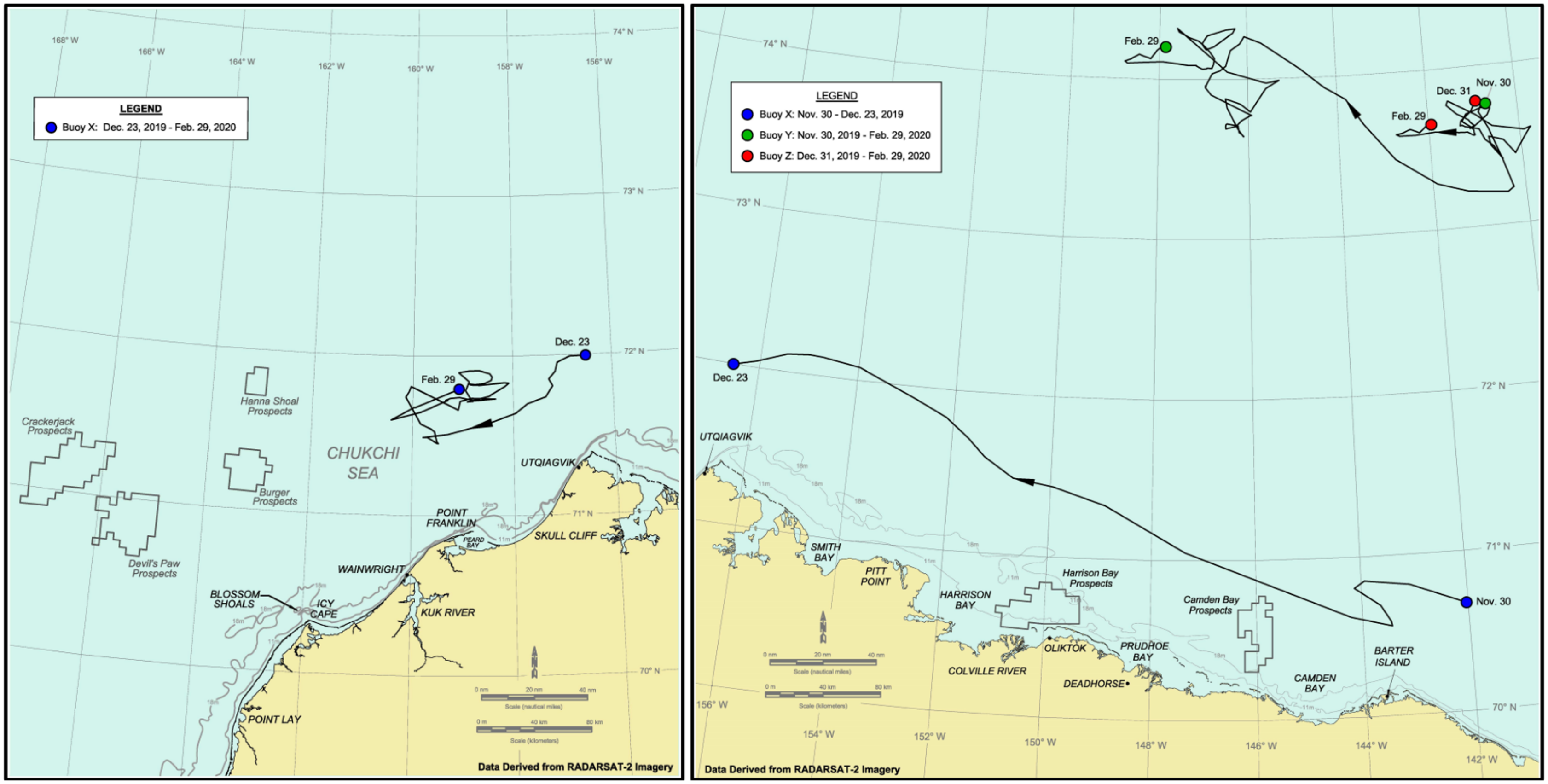

Data Source: Rigor, 2020

Figure 4-8. On-Ice Drift Buoy Tracks during 2019-20 Freeze-Up Season

All of the flights were conducted using an Aero Commander 690 (Plate 4-1). This fixed-wing aircraft offers the benefits of an extended range, an ability to fly at relatively low speeds, a high wing that facilitates unobstructed views of the ice below, and a moderate cost per flight hour.

Plate 4-1. Aero Commander 690 at Utqiagvik Airport (February 24, 2020)

Each flight path was mapped using a Garmin GPSMap 196. To improve the accuracy of the position data, differential corrections broadcast in real time via satellite by the U.S. Government's Wide Area Augmentation System (WAAS) were received by the GPS unit when available. Static position checks conducted at North Slope survey monuments in the past have indicated that the accuracy attainable with WAAS is less than 1 m (*e.g.*, Coastal Frontiers, 2015). When operated in the stand-alone mode, the GPS accuracy typically is on the order of 10 m. The GPS position data were displayed on a base map of the study area in real time using a laptop computer and Hypack survey software. This arrangement allowed the field crew both to direct the aircraft to locations of interest identified in advance in the satellite imagery, and to record the positions of small-scale features noted during the flight.

The flight paths are shown in Drawings CFC-1070-01-001, -002 and -003 (Appendix A). The drawings display the locations of ice features observed during the flights as well as those of photographs and videos taken during the flights. Each photo is identified by a unique number such as "B1-15", and each video by unique number such as "C2-V5". The first letter, "B" or "C", indicates whether the flight was conducted in the Beaufort or Chukchi; the number that follows indicates which flight in that basin was involved. The second number indicates the order in which the photo or video was obtained during that flight.

"THIS INFORMATION IS DISTRIBUTED SOLELY FOR THE PURPOSE OF PRE-DISSEMINATION PEER REVIEW UNDER APPLICABLE INFORMATION QUALITY GUIDELINES. IT HAS NOT BEEN FORMALLY DISSEMINATED BY BSEE. IT DOES NOT REPRESENT AND SHOULD NOT BE CONSTRUED TO REPRESENT ANY BSEE DETERMINATION OR POLICY."

Hence, C2-V5 designates the 5th video acquired during the second Chukchi Sea reconnaissance flight.

The photographs and videos are provided in digital form in Appendix E, with the file names corresponding to the identification numbers shown on the drawings. The ice features observed during the flights are denoted on the drawings using the abbreviations listed in Table 4-3, while the objective and path of each flight are summarized below.

Table 4-3. Abbreviations for Ice Features

Ice Feature	Abbreviation
Active Shear Line	ASL
Broken Ice	BRK
Crack	CRK
Finger Rafting	FR
Inactive Shear Line	ISL
Lead	LD
Landfast Ice Edge	LFI
Multi-Year Ice (concentration in %)	MYI (_%)
Nilas (< 10 cm)	NLS
Pancake Ice	PNK
Pile-Up (height, encroachment in m)	P/U (_, _m)
Polynya	PLY
Refrozen Lead	RFL
Ridge (height in m)	RDG (_m)
Rubble (height in m)	RBL (_m)
Thermal Crack Ridge (height in m)	TCK (_m)
Undeformed Ice	UDI
Young Ice (10-30 cm)	YNG

Note: The prefixes "i" and "m" are used to indicate intermittent features and multiple features, respectively (*i.e.*, "iRBL" indicates intermittent rubble).

February 2020 Beaufort Sea Flight No. 1 ("B1" on Drawing CFC-1070-01-001)

The first reconnaissance flight was undertaken on February 22nd to observe the ice conditions in the Central Beaufort Sea. Low light conditions prevailed due to the presence of complete cloud cover. The route was as follows:

- Deadhorse Airport
- Transit northeast
- Liberty Development prospective island site
- Endicott Project
- Transit north
- Barrier islands from Cross to North Star (heading east-northeast)
- Sivulliq Development prospective pipeline route
- Flaxman Island, Brownlow Point, and adjacent spit
- Transit east-northeast across southern Camden Bay to Barter Island
- Transit west-northwest across northern Camden Bay
- Camden Bay Prospects
- Zigzag west at distances of 5 to 20 nm (9 to 37 km) off the barrier islands
- Northstar Production Island
- Transit south
- Deadhorse Airport
- Flight time = 2.4 hours.

Although the original intent was to continue west to Stamukhi Shoal after passing through the Camden Bay Prospects, the visibility was severely reduced by falling snow when the aircraft reached the vicinity of Northstar Island. As a result, the mission was terminated at this location and the aircraft returned to Deadhorse. Stamukhi Shoal was added to the flight path for the Western Beaufort, as indicated below.

February 2020 Beaufort Sea Flight No. 2 ("B2" on Drawing CFC-1070-01-002)

The second reconnaissance flight was undertaken on February 23rd to observe the ice conditions in the Western Beaufort Sea. Cloud cover at the beginning of the mission gave way to clear skies soon after departing Deadhorse, and excellent visibility prevailed thereafter. The flight path is summarized below:

- Deadhorse Airport
- Transit north
- West Dock Causeway
- Barrier islands from Stump to Long (heading west-northwest)
- Northstar Production Island
- Transit east

- Reindeer and Argo Islands
- Transit west-southwest
- Barrier islands from Long to Spy (heading west-northwest)
- Oliktok Point
- Transit west-southwest
- Oooguruk Offshore Drillsite (ODS)
- Thetis Island
- Spy Island Drillsite (SID)
- Harrison Bay Prospects
- Stamukhi Shoal
- Harrison Bay Prospects
- Weller Bank
- Zigzag west-northwest at distances of 5 to 30 nm (9 to 56 km) offshore
- Transit southwest
- Utqiagvik Airport
- Flight time = 2.4 hours.

February 2020 Chukchi Sea Flight No. 1 ("C1" on Drawing CFC-1070-01-003)

The first reconnaissance mission in the Alaskan Chukchi Sea was undertaken on February 24th under clear skies. The flight, which covered the offshore region to the northwest and west of Point Barrow, proceeded in the following manner:

- Utqiagvik Airport
- Transit northwest, altering course as necessary to investigate possible multi-year ice floes
- Hanna Shoal
- Transit southwest
- Hanna Shoal Prospects
- Transit south
- Burger Prospects
- Transit 15 nm (28 km) south
- Transit east, altering course as necessary to investigate possible multi-year ice floes
- Utqiagvik Airport
- Flight time = 2.7 hours.

February 2020 Chukchi Sea Flight No. 2 ("C2" on Drawing CFC-1070-01-003)

The second reconnaissance flight in the Alaskan Chukchi Sea was undertaken on February 25th to observe nearshore ice conditions and shoreline pile-ups between

Utqiagvik and Point Lay, a region where pipelines from the offshore prospects could make landfall. The flight, which was conducted under clear skies, described the following path:

- Utqiagvik Airport
- Transit southwest to Point Lay at distances of 7 to 17 nm (13 to 32 km) offshore, altering course on several occasions to cross the landfast ice edge
- Barrier islands fronting South Kasegaluk Lagoon
- Icy Cape and Blossom Shoals
- Barrier islands fronting North Kasegaluk Lagoon
- Shoreline from North Kasegaluk Lagoon to Point Franklin
- Seahorse Islands and Peard Bay
- Shoreline from Peard Bay to Utqiagvik
- Utqiagvik Airport
- Flight time = 2.7 hours.

A Post-Observation Freeze-Up Progress Report that summarizes the objectives, area of observation and significant findings of the flights is provided in Appendix C.

As in each of the eight prior freeze-up studies (Coastal Frontiers and Vaudrey, 2010; 2011; 2012a; 2013; 2014; 2015; 2016; 2017), the reconnaissance flights provided invaluable opportunities to confirm and refine the findings derived from satellite imagery, and to expand upon those findings with respect to small-scale features and processes.

5. BEAUFORT SEA FREEZE-UP

Section 5.1 provides an overview of the 2019-20 freeze-up season in the Alaskan Beaufort Sea, while Sections 5.2 through 5.5 present a more in-depth analysis of the conditions that prevailed from late summer 2019 through February 2020.

5.1 Overview

Air Temperatures: The air temperatures at Deadhorse Airport cycled through two distinct phases during the five-month study period: a warm phase at the beginning and a cold phase at the end. The characteristics of each phase are summarized below:

- *Warm Phase (October 1st - December 18th)*: The daily average air temperatures exceeded the normal range (the long-term daily average maximum and minimum values for the 30-year period from 1981 through 2010) on 57 occasions while never falling below;

- *Cold Phase (December 24th - February 29th)*: The daily average air temperatures exceeded the normal range on only six occasions while falling below on 41. On nine days, the daily average was less than or equal to -40°F (-40°C), including a minimum of -45°F (-43°C) on January 6th.

Over the entire five-month study period (October through February), the daily average air temperature exceeded the normal range on 63 days (41% frequency) and dropped below on 41 days (27% frequency).

Winds: Table 5-1 presents the daily average wind speeds and directions recorded at Deadhorse Airport during the 2019-20 freeze-up season. Westerlies predominated in each of the five months, with frequencies of occurrence ranging from 55% in December to 79% in February. Over the entire study period, westerlies outnumbered easterlies by a margin of 64% to 36%. The average monthly speeds were tightly clustered and relatively low by historical standards, with values of 11 kt (6 m/s) recorded in October, November, and December, and 9 kt (5 m/s) in January and February.

Storms: The characteristics of all storms with a daily average sustained wind speed exceeding 15 kt (8 m/s) at Deadhorse Airport are presented in Table 5-2. Nine such events occurred from October 2019 through February 2020, consisting of four easterlies and five westerlies. The most severe easterly, with a maximum wind speed of 29 kt (15 m/s) and duration of two days, occurred in mid-December, while the most severe westerly, with a maximum wind speed of 25 kt (13 m/s) and duration of five days, occurred in late October and early November. Seven of the nine storms and 16 of the 18 storm-days took place prior to the end of December.

Table 5–1. Beaufort Sea Wind Characteristics, October 2019 – February 2020

Month	Easterly Wind Predominance (days)	Westerly Wind Predominance (days)	Average Speed (kt)
October	12	19	11
November	12	18	11
December	14	17	11
January	10	21	9
February	6	23	9
Total Days	**54**	**98**	n/a
Frequency (%)	**36**	**64**	n/a

Note: Table 5–1 is based on the daily average values recorded at Deadhorse Airport.

Table 5–2. Beaufort Sea Storm Characteristics, October 2019 – February 2020[1]

Month	Day	Duration (days)	Maximum Easterly Wind Speed[2] (kt)	Maximum Westerly Wind Speed[2] (kt)
October	17-19	3	26	-
October	Oct 30-Nov 3[3]	5	-	25
November	8	1	17	-
December	4	1	-	20
December	8-10	3	22	-
December	17-18	2	29	-
December	28	1	-	17
January	14	1	-	19
February	28	1	-	16
Total Duration	n/a	**18**	n/a	n/a
Total Number of Events	n/a	n/a	**4**	**5**

Notes:

1 Table 5–2 includes all storm events with a daily average sustained wind speed exceeding 15 kt (8 m/s) at Deadhorse Airport.

2 "Maximum Wind Speed" refers to highest daily average sustained wind speed that occurred during each storm event.

3 The daily average wind speed decreased to 12 kt on November 2nd but freshened to 26 kt on November 3rd.

Ice Cover: First-ice occurred in mid-October, when ice appeared along the coast between Admiralty Bay and Point Brownlow. Nearshore freeze-up took place on November 11th, followed by complete freeze-up in the Alaskan Beaufort Sea on November 24th.

Ice Thickness: The thickness of undeformed first-year ice at the end of each month was estimated using the relationship of Lebedev (Bilello, 1960) in concert with the freezing-degree days (FDD) accumulated at Deadhorse Airport (Table 4-1). The relationship is as follows:

$$t = 0.94(\sum FDD)^{0.58} \qquad (1)$$

where:

t = ice thickness in cm
ΣFDD = accumulated freezing-degree days relative to 29°F

Although Lebedev originally calculated FDD relative to 32°F, ice thickness measurements in the Beaufort Sea obtained by Vaudrey and Associates, Inc., have indicated that Equation (1) provides more accurate results if FDD are referenced to 29°F, the approximate freezing point of sea water.

The computed values of ice thickness for the entire 2019-20 winter season are provided in Table 5–3, which indicates that undisturbed first-year ice attained a maximum thickness of 162 cm on May 21st. Subsequent to that date, the daily average air temperatures equaled or exceeded 29°F.

Table 5–3. Beaufort Sea Computed Ice Thickness, September 2019 – May 2020[1]

Date	Accumulated FDD	Ice Thickness[2] (cm)
30 September 2019	0	0
31 October 2019	162	18
30 November 2019	696	42
31 December 2019	1,881	75
31 January 2020	3,480	106
29 February 2020	5,162	134
31 March 2020	6,305	150
30 April 2020	6,958	159
21 May 2020	7,143	162

Notes:
1 Table 5–3 is based on the daily average air temperature data recorded at Deadhorse Airport.
2 Ice thickness is computed from accumulated FDD using method of Lebedev (Bilello, 1960).

Landfast Ice: The formation of landfast ice was delayed by warm air temperatures and westerly winds in October. It began to develop during the first week in November, with growth occurring first in the western portion of the study area and subsequently in the eastern portion. At the end of November, the landfast ice zone included Admiralty Bay, Smith Bay, Harrison Bay, Simpson Lagoon, Gwyder Bay, and most of Stefansson Sound as well as a narrow strip along the coast of Camden Bay.

During the first half of December, aided by the occurrence of two easterly storms, the landfast ice edge advanced seaward by distances that ranged from negligible in Camden Bay to 10 nm (19 km) off Smith Bay. The advance stalled, however, with minor gains occurring in some areas and minor losses in others over the remainder of the month.

Substantial expansion followed in January, causing the landfast ice edge to reach one of its customary anchor points, Weller Bank, by mid-month and a second, Stamukhi Shoal, by early February. The maximum gain, 18 nm (33 km), took place off Oliktok Point. The advance continued through the first three weeks in February, a period marked by light winds and an absence of westerly storms. A reversal occurred at the end of the month, however, when a brief westerly storm (Table 5–2) caused the ice edge to retreat by distances up to 20 nm (37 km) between Weller Bank and the eastern edge of the study area. Although the ice remained grounded on Weller Bank, it was displaced from Stamukhi Shoal - a development that underscored the absence of a well-developed, firmly-grounded shear zone during the 2019-20 freeze-up season.

Ice Pile-Ups: Thirty-two ice pile-ups formed in the central portion of the Alaskan Beaufort Sea during the 2019-20 freeze-up season (Table 5–4). Two were located on the Endicott Project’s Endeavor Island, two on Northstar Production Island, one on the Oooguruk Offshore Drillsite (ODS), one on the Spy Island Drillsite (SID), and 26 on natural barrier islands and shoals stretching from Duchess Island on the east to Thetis Island on the west.

The dimensions of the pile-ups were unexceptional by historical standards, with heights ranging from 1 to 7 m above sea level, encroachment distances from negligible to 20 m onto the subaerial beach, and lengths from 50 m to 2 km alongshore. Fifteen of the pile-ups arrived from the northeast quadrant, three from the southeast quadrant, and seven from each of the southwest and northwest quadrants. The thicknesses of the ice blocks comprising the piles were estimated to range from 20 to 50 cm.

As discussed by Coastal Frontiers and Vaudrey (2012b), pile-ups tend to form when the ice loses confinement, typically in response to abrupt changes in wind direction accompanied by speeds greater than or equal to 15 kt (8 m/s). The pile-ups listed in Table 5–4 are believed

Table 5–4. Ice Pile-Ups on Beaufort Sea Coast during 2019-20 Freeze-Up Season

No.	Location	Formation Date	Arrived From	Length[1] (m)	Height[2] (m)	Encroachment[3] (m)
1	Endeavor Island	Nov 23 – Dec 9	NE	150	2	1
2	Endeavor Island	Nov 23 – Dec 9	NW	50	1	0
3	Cross Island	Nov 23 – Dec 9	NW	650	2	5
4	Dinkum Sands	Oct 25 - 30	SW	150	7	0
5	Dinkum Sands	Oct 25 - 30	SW	200	5	0
6	Narwhal Island	Nov 23 – Dec 9	NW	1,750	2	5
7	Narwhal Island	Nov 23 – Dec 9	NE	100	2	5
8	Karluk Island	Nov 23 – Dec 9	NE	150	1	3
9	Pole Island	Nov 23 – Dec 9	NW	1,150	4	7
10	Pole Island	Nov 23 – Dec 9	NW	1,350	7	8
11	Pole/Belvedere	Nov 23 – Dec 9	NE	1,850	3	5
12	Stockton Shoals	Nov 23 – Dec 9	NE	200	3	0
13	Duchess Island	Nov 23 – Dec 9	NE	750	2	3
14	Stump Island	Nov 23 – Dec 9	NE	950	1	3
15	Egg Island Shoal	Nov 23 – Dec 9	NE	100	2	0
16	Northstar Prod.	Nov 23 – Dec 9	NE	150	4	10
17	Northstar Prod.	Nov 23 – Dec 9	SW	150	5	0
18	Reindeer Island	Nov 23 – Dec 9	NE	200	3	5
19	Reindeer Island	Oct 25 - 30	SE	200	7	0
20	Argo Island	Oct 25 - 30	SE	200	7	20
21	Long Island	Nov 23 – Dec 9	NE	50	2	5
22	Long Island	Nov 23 – Dec 9	NE	100	3	3
23	Bertoncini Is.	Nov 23 – Dec 9	NE	500	4	6
24	Pingok Island	Oct 25 - 30	SW	50	1	1
25	Pingok Island	Oct 25 - 30	SW	1,750	2	5
26	Leavitt Island	Nov 23 – Dec 9	NE	400	2	5
27	Leavitt Island	Oct 25 - 30	SW	600	2	7
28	Spy Island	Oct 25 - 30	SW	850	4	5
29	Oooguruk ODS	Nov 23 – Dec 9	NW	50	4	5

(continued)

Table 5–4. Ice Pile-Ups on Beaufort Sea Coast during 2019-20 Freeze-Up Season (continued)

No.	Location	Formation Date	Arrived From	Length[1] (m)	Height[2] (m)	Encroachment[3] (m)
30	Thetis Island	Nov 23 – Dec 9	NW	100	7	5
31	Thetis Island	Nov 23 – Dec 9	NE	2,000	3	5
32	Nikaitchuq SID	Oct 25 - 30	SE	150	4	1

Notes:
[1] "Length" indicates alongshore extent of pile-up.
[2] "Height" indicates maximum height of pile-up relative to MSL.
[3] "Encroachment" indicates distance ice advanced onto subaerial beach.

to have resulted from two such sequences, the first of which took place from October 25th through 30th. During this six-day period, when the calculated thickness of undeformed first-year ice was less than 20 cm, southwesterly winds with one-hour sustained speeds to 17 kt (9 m/s) shifted to easterly and attained the same peak speed before veering back to southwesterly while freshening to 32 kt (16 m/s). As the ice in the lagoon areas was relatively thin and weak at this early stage of freeze-up, it is likely that the nine pile-ups noted on the south sides of barrier islands, shoals, and the Nikaitchuq SID occurred at this time.

The remaining 23 pile-ups are believed to have formed between November 23rd and December 9th, a 17-day period in which the winds alternated between easterly and westerly on 11 occasions. The one-hour sustained speeds peaked at 37 kt (19 m/s) for the easterlies and 24 kt (12 m/s) for the westerlies. The calculated thickness of first-year ice ranged from 37 cm at the beginning of this period to 50 cm at the end.

Multi-Year Ice: Multi-year ice began to drift west into the Alaskan Beaufort Sea study area during the second week in October, extending as far south as the 70°50'N parallel and as far west as the 145°25'W meridian at month-end. In the absence of a well-developed first-year ice canopy, the multi-year floes advanced rapidly to the west in November. Some of the ice at the southern boundary was incorporated into the landfast ice zone in late November and early December, and remained there through the end of the freeze-up study period in February. The concentrations typically were less than 10%. Farther offshore, where the multi-year floes tended to be larger, the concentrations ranged from less than 10% to 50% in December, less than 10% to 60% in January, and less than 10% to 70% in February. The only region lacking multi-year ice for an extended period of time was a tongue of first-year ice that developed between the U.S.-Canadian border and Harrison Bay in mid-December, and persisted through February just offshore of the landfast ice zone.

Ice Drift: The movements of 11 multi-year ice floes were tracked using RADARSAT-2 images, and an average monthly speed was derived for each floe for each month in which the period of record in the Alaskan Beaufort Sea exceeded 15 days. The speed was computed on the basis of the net displacement that occurred during the period of record. The results are summarized in Table 5–5. Despite the prevalence of westerly winds (Table 5–1), all of the floes experienced net displacements to the west. Factors contributing to this outcome included the westerly set of the Beaufort Gyre (Figure 1-1), the absence of significant confinement to the west of the advancing pack ice in November, and the occurrence of two easterly storms in December (Table 5–2). The highest average monthly floe speed, 10.4 nm/day (19.3 km/day), occurred in November, while the lowest, 1.1 nm/day (2.0 km/day), occurred in both January and February in response to persistent westerly winds (Table 5–1). The mean value of the average monthly floe speeds recorded from November through February was 4.5 nm/day (8.3 km/day).

Table 5–5. Multi-Year Ice Floe Average Monthly Speeds in Beaufort Sea, November 2019 - February 2020

Month	No. of Floes	Maximum Speed (nm/day)	Minimum Speed (nm/day)	Average Speed (nm/day)
November	1	10.4	10.4	10.4
December	6	9.6	2.3	4.9
January	5	1.8	1.1	1.5
February	4	1.5	1.1	1.3
Average	n/a	n/a	n/a	**4.5**

Note: Average monthly speeds were derived from the net displacements that occurred over periods ranging from 17 to 31 days (depending on the availability of RADARSAT-2 images).

5.2 Late Summer 2019

The ice cover in the Alaskan Beaufort Sea diminished rapidly in July and early August (Vinas, 2019), reflecting the prevalence of warm air temperatures and clear skies (National Snow and Ice Data Center, 2019a; 2019b). On August 12th, ice-free conditions prevailed in a band that averaged 150 nm (278 km) wide off the coast between Point Barrow and Barter Island (Figure 5-1).

The loss of ice cover proceeded more slowly from mid-August through mid-September, a period in which severe storms capable of fragmenting the weakened pack ice remained conspicuously absent. The minimum ice extent, 4.15 million km^2 (Figure 5-2), occurred on

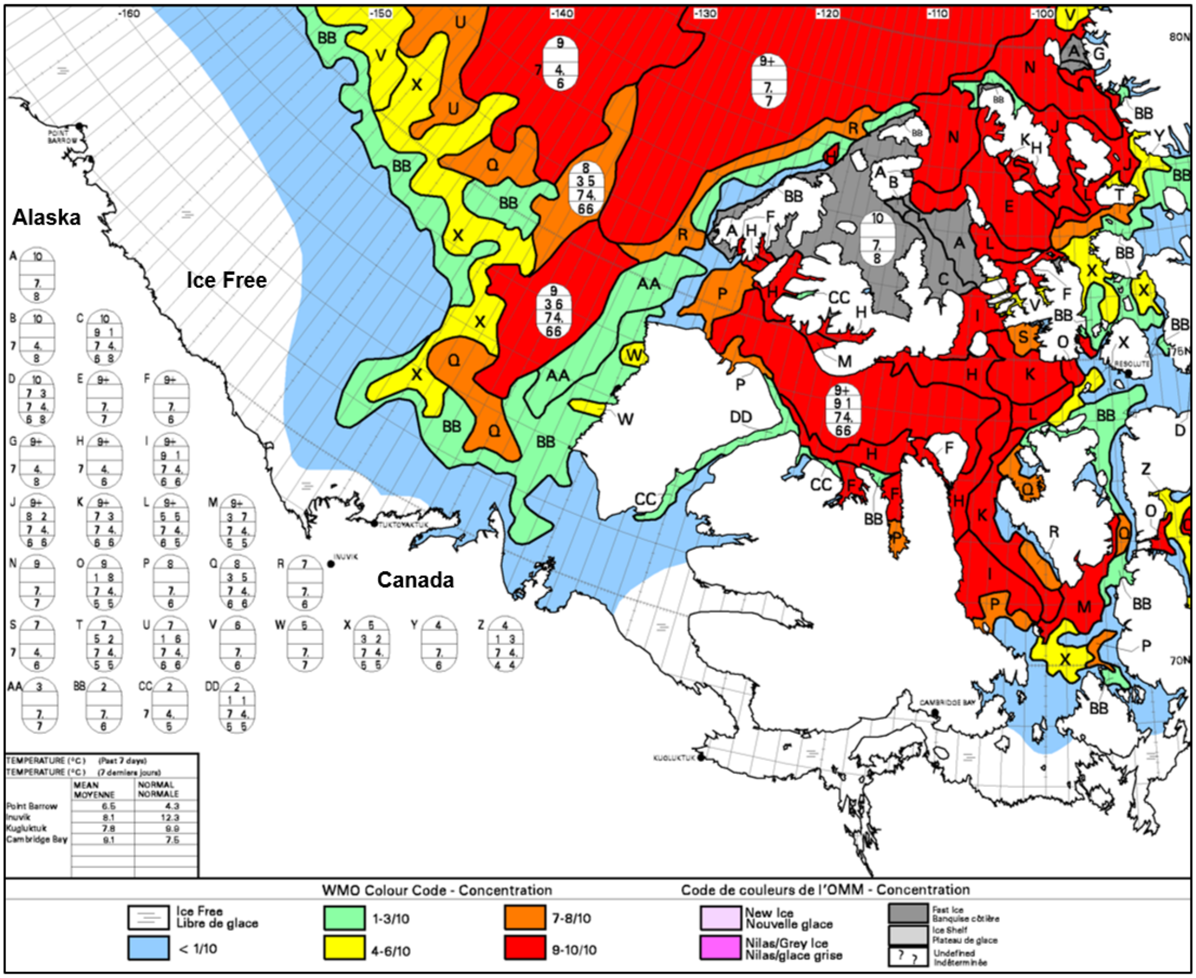

After: Canadian Ice Service, 2019

Figure 5-1. Beaufort Sea Ice Concentrations on August 12, 2019

September 18th; (National Snow and Ice Data Center, 2019c; "extent" refers to the area in which ice covers at least 15% of the ocean surface). This area essentially ties those in 2007 and 2016 as the second lowest since the acquisition of satellite-based data began in 1979. The smallest extent, 3.39 km^2, occurred in 2012 (Table 5–6). It is noteworthy that the ice extents recorded in each of the last 13 years represent the 13 lowest values on record.

Based on satellite data compiled by the National Snow and Ice Data Center (2019d), the average extent of the Arctic sea ice in September decreased at a rate of 82,400 km^2/yr, or 12.9% per decade, between 1979 and 2019 (Figure 5-3). Notwithstanding this rapid rate of decline, it is noteworthy that (1) substantial interannual variations have occurred around the long-term trend, and (2) during the past 13 years (2007-2019), the trend line has been essentially flat (*i.e.*, no significant loss in sea ice extent).

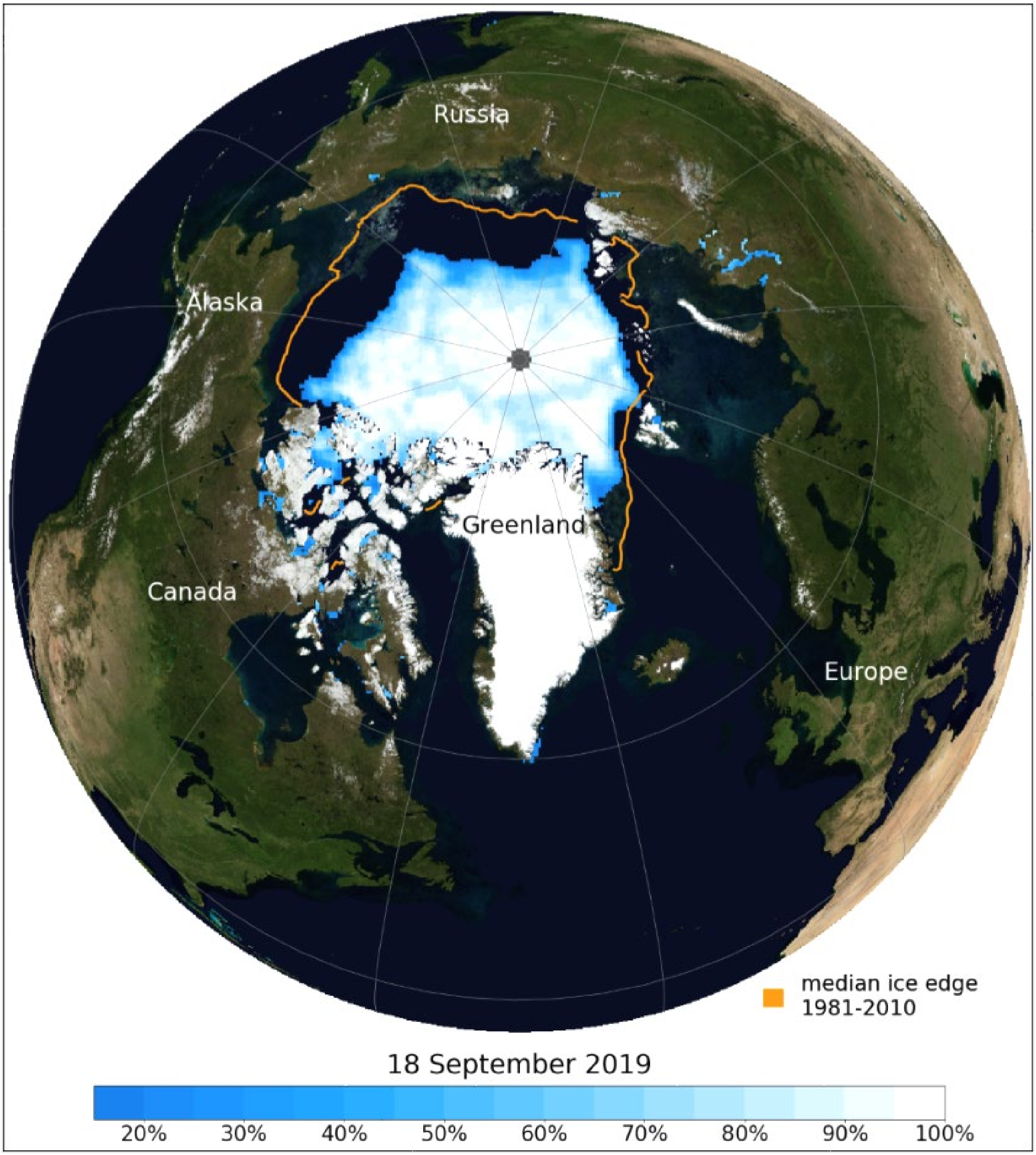

Source: National Snow and Ice Data Center, 2019c

Figure 5-2. Sea Ice Minimum Extent on September 18, 2019

Table 5–6. Minimum Arctic Sea Ice Extent, 2007-2019

Rank	Year	Minimum Ice Extent (km^2)	Date
1	2012	3.39	Sep 17
2	2019	4.15	Sep 18
2	2007	4.16	Sep 18
2	2016	4.17	Sep 10
5	2011	4.34	Sep 11
6	2015	4.43	Sep 9
7	2008	4.59	Sep 19
7	2010	4.62	Sep 21
9	2018	4.66	Sep 23
9	2017	4.67	Sep 13
11	2014	5.03	Sep 17
11	2013	5.05	Sep 13
13	2009	5.12	Sep 13
Average	n/a	**4.45**	**Sep 16**

After: National Snow & Ice Data Center, 2019d

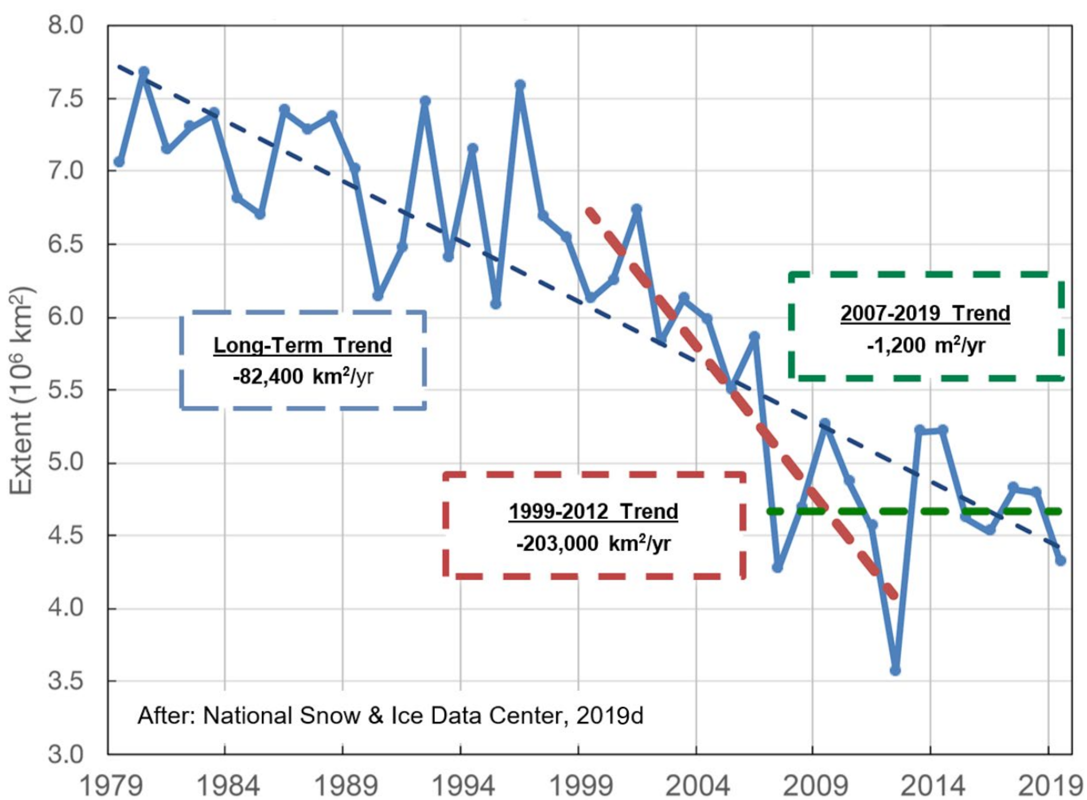

Figure 5-3. Average Arctic Sea Ice Extent in September, 1979-2019

5.3 Early Freeze-Up

5.3.1 October 2019

<u>Meteorological Conditions</u>: The daily values of average sustained wind speed, maximum sustained wind speed, average wind direction, and average air temperature at Deadhorse Airport are shown in Figure 5-4 along with the normal range of air temperatures defined by the average values of the daily highs and lows from 1981 through 2010. The significance of the red and blue color bands in this and all subsequent meteorological plots is explained in Table 5–7. Unless stated otherwise, the wind speeds discussed in the text refer to the daily average values rather than the daily maximum values or hourly average values.

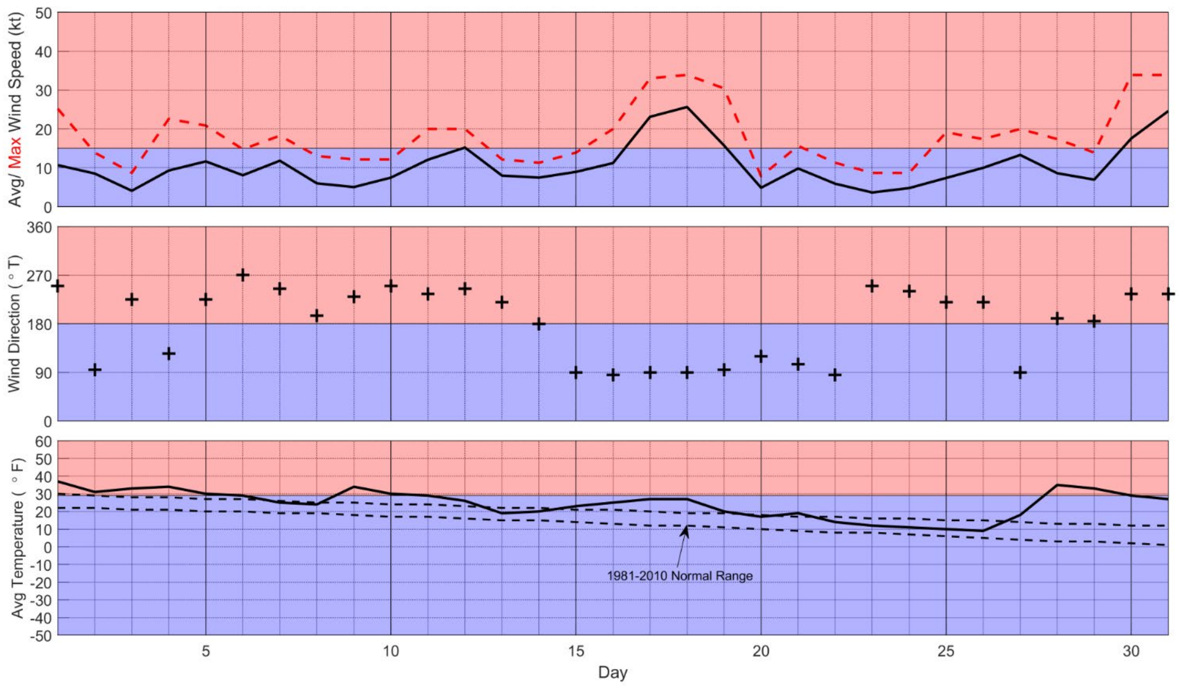

Figure 5-4 Meteorological Conditions at Deadhorse Airport in October 2019

Table 5–7. Significance of Color Bands in Plots of Meteorological Conditions

Parameter	Blue Band	Red Band
Wind Speed	≤ 15 kt	> 15 kt (Storm)
Wind Direction	Easterly	Westerly
Air Temperature	≤ 29°F (Freezing Point of Seawater)	>29°F

The air temperatures in October were exceptionally warm by historical standards, with the daily average values exceeding the normal range on 21 occasions and never falling below. The warm weather peaked on the 28th, when the daily average temperature of 35°F (2°C) exceeded the long-term average by 22°F (12°C). The average temperature for the month was 24°F (-4°C).

Westerly winds predominated in October, occurring on 19 days versus 12 days for easterlies. The speeds were moderate, with an average monthly value of 11 kt (6 m/s) and only two storm events (Table 5–2):

- October 17th-19th: three-day easterly with maximum speed of 26 kt (13 m/s);
- Oct 30th-Nov 3rd: five-day westerly with maximum speed of 25 kt (13 m/s).

The second storm, which began in late October and continued into early November, was the most severe westerly of the five-month study period in terms of both maximum wind speed (25 kt; 13 m/s) and duration (five days). It was attributed to the month of October because the peak wind speed occurred on October 31st.

Ice Cover: The formation of first-year ice was delayed not only by the aforementioned warm air temperatures, but also by anomalously high sea surface temperatures (National Snow and Ice Data Center, 2019c). As shown in Figure 5-5 and Figure 5-6, the mean sea surface temperature in October remained well above the freezing-point of seawater (29°F; -2°C) throughout most of the Alaskan Beaufort Sea, and exceeded the long-term average values derived for the period 1982-2011 by 1 to 4°F (1 to 2°C).

First-ice occurred on October 14th, when ice appeared along the coast between Admiralty Bay and Brownlow Point. The ice in the nearshore region expanded slowly during the remainder of the month, with the majority of the growth confined to the semi-protected waters in bays and lagoons. Offshore, pack ice entered the Beaufort Sea study area (Figure 1-1) from the Canadian waters to the east during the second week of the month. It drifted slowly to the west in the weeks that followed, extending as far south as the 70°50'N parallel and as far west as the 145°25'W meridian at month-end. The rest of the offshore region remained ice-free throughout the month.

Ice Thickness: FDD began to accumulate on October 7th, when the daily average air temperature dropped to 25°F (-4°C) As indicated in Table 5–3, the computed thickness of undisturbed first-year ice at the end of October was 18 cm.

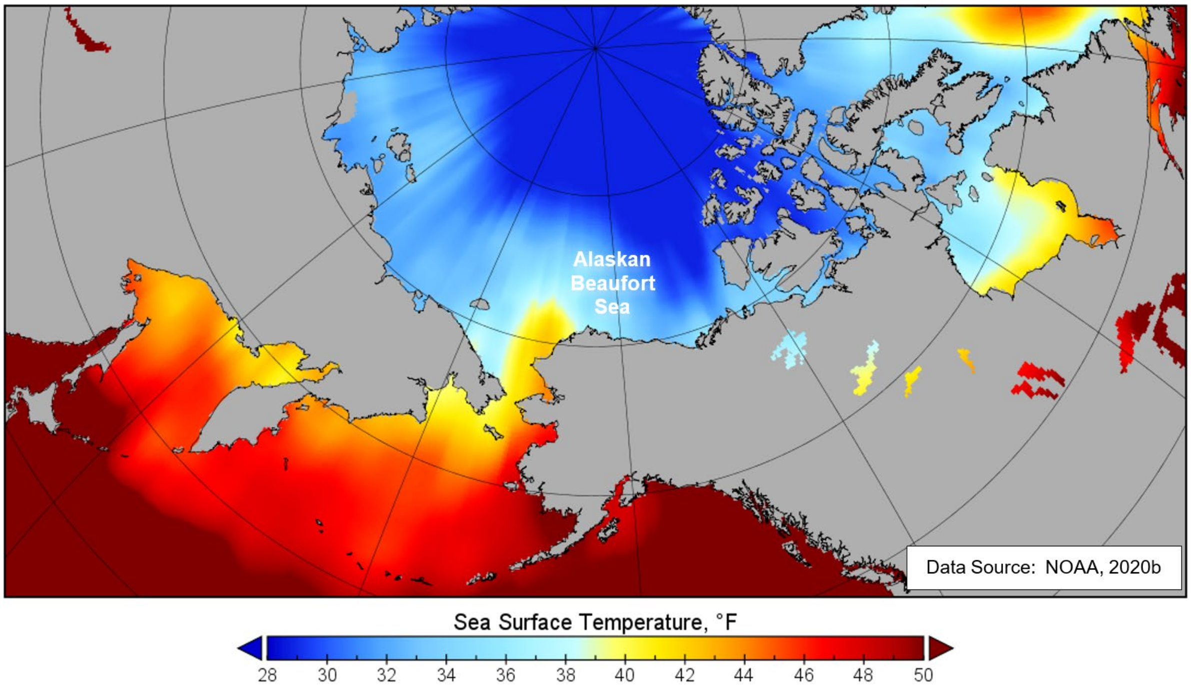

Figure 5-5. Mean Sea Surface Temperature in October 2019

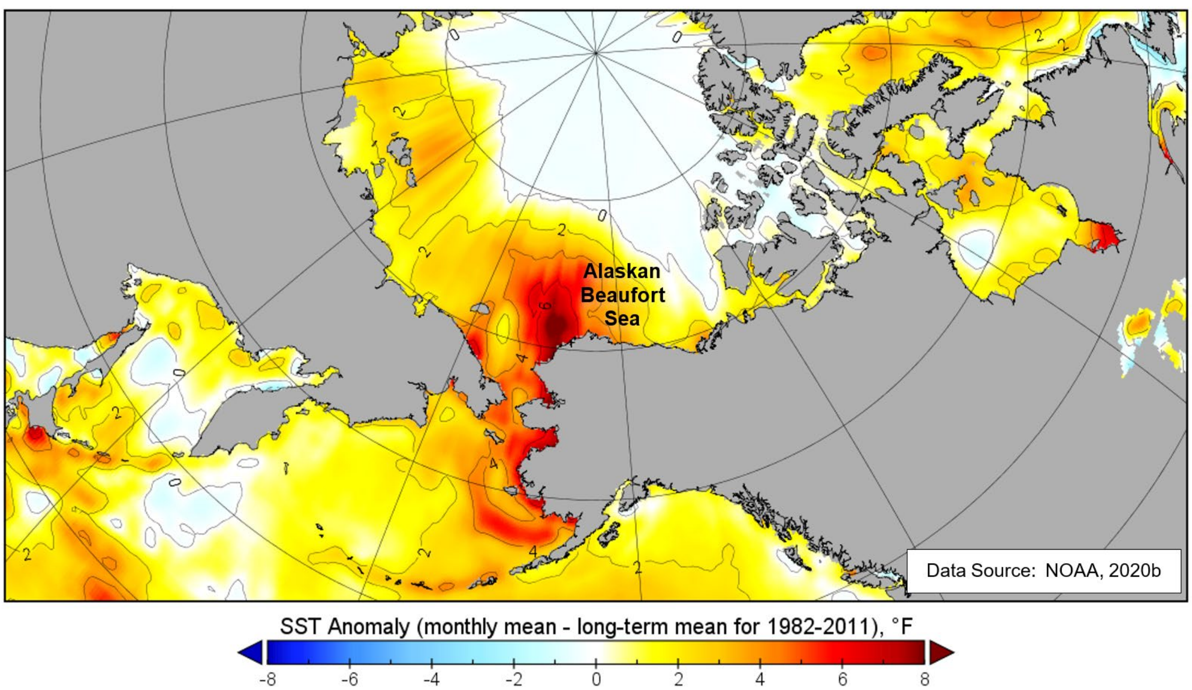

Figure 5-6. Mean Sea Surface Temperature Anomaly in October 2019

Landfast Ice: Landfast ice remained absent from the nearshore region in October, reflecting both the anemic development of first-year ice and the prevalence of westerly winds (which tend to push the nascent ice canopy away from the coast).

Ice Pile-Ups: As discussed in Section 5.1, nine of the 32pile-ups noted during the February 2020 reconnaissance flights were located on the south sides of barrier islands, shoals, and the Nikaitchuq SID. They probably formed between October 25th and 30th, when southwesterly winds with one-hour sustained speeds to 17 kt (9 m/s) shifted to easterly and attained the same peak speed before veering back to southwesterly and freshening to 32 kt (16 m/s). The calculated thickness of undeformed first-year ice was less than 20 cm at this early stage of freeze-up, rendering the ice susceptible to displacement. Had the identical sequence of wind shifts occurred later in the freeze-up season, when the ice thickness had increased to 30 cm or more, it is unlikely that displacement would have occurred in the confined spaces of the lagoons. The locations and characteristics of the nine pile-ups that occurred in October are summarized in Table 5-4.

Multi-Year Ice: Multi-year ice floes embedded in the pack ice began to drift west into the Alaskan Beaufort Sea study area during the second week in October. Like the remainder of the pack, they moved slowly to the west during the remainder of the month. As shown in Figure 5-7, the edge of the multi-year ice was identical to that of the pack ice at month-end, and was located as far south as the 70°50'N parallel and as far west as the 145°25'W meridian.

5.3.2 November 2019

Meteorological Conditions: The meteorological conditions at Deadhorse Airport are summarized in Figure 5-8. The unseasonably warm air temperatures that prevailed in October persisted throughout November, producing 26 days on which the average value exceeded the normal range and none on which it fell below. The average temperature for the month was 11°F (-12°C).

The wind regime was similar to that in October, with westerlies recorded on 18 of the 30 days and an average monthly speed of 11 kt (6 m/s). Excluding the westerly event that peaked in late October and continued into early November (Section 5.3.1), the sole storm was a mild easterly of short duration (Table 5-2):

- November 8th: one-day easterly with maximum speed of 17 kt (9 m/s).

Ice Cover: The pack ice advanced rapidly to the west and south in November, while the band of first-year ice along the coast expanded slowly to the north. Based on the

“THIS INFORMATION IS DISTRIBUTED SOLELY FOR THE PURPOSE OF PRE-DISSEMINATION PEER REVIEW UNDER APPLICABLE INFORMATION QUALITY GUIDELINES. IT HAS NOT BEEN FORMALLY DISSEMINATED BY BSEE. IT DOES NOT REPRESENT AND SHOULD NOT BE CONSTRUED TO REPRESENT ANY BSEE DETERMINATION OR POLICY.”

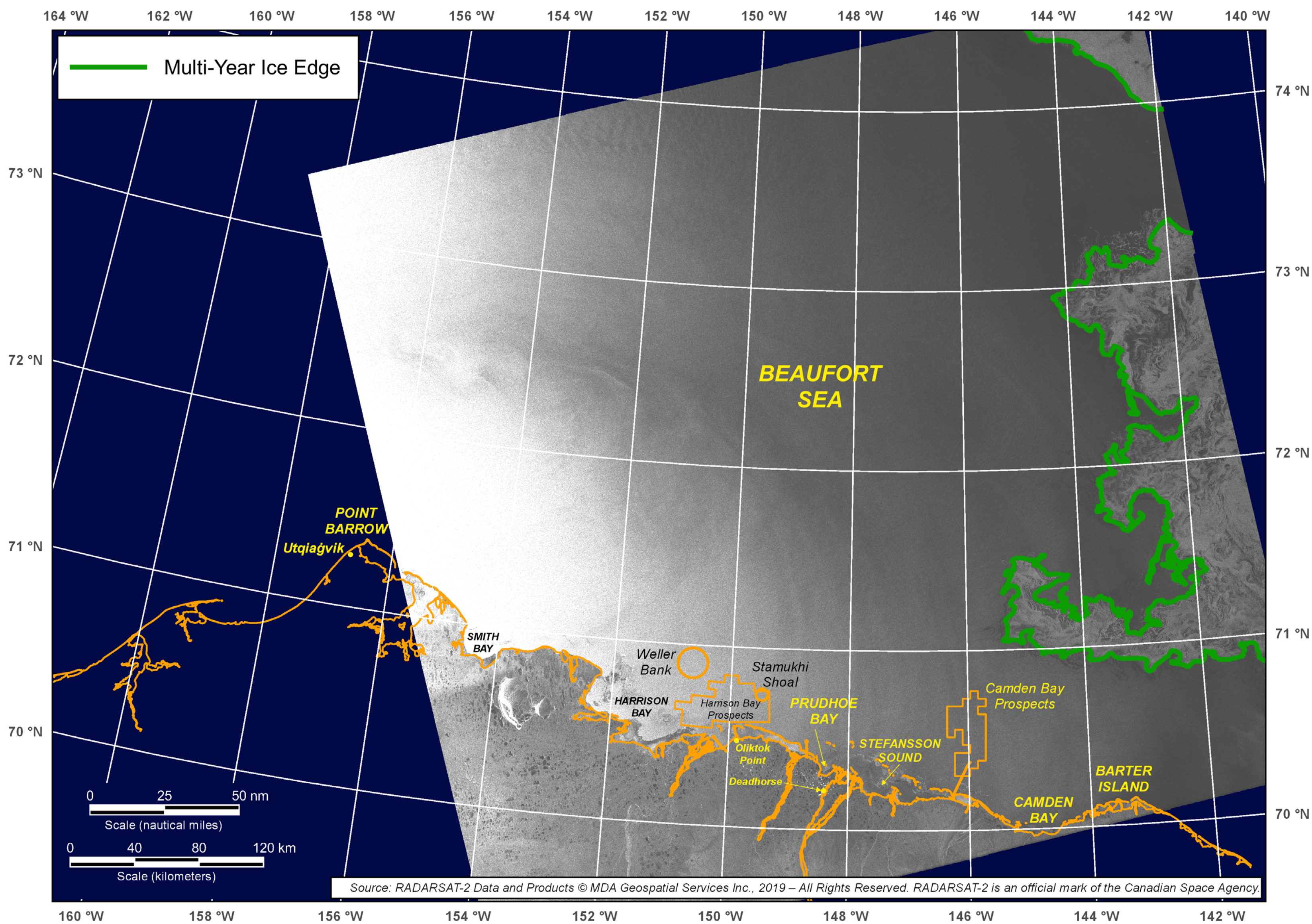

Figure 5-7. RADARSAT-2 Image of Beaufort Sea Acquired on October 31, 2019

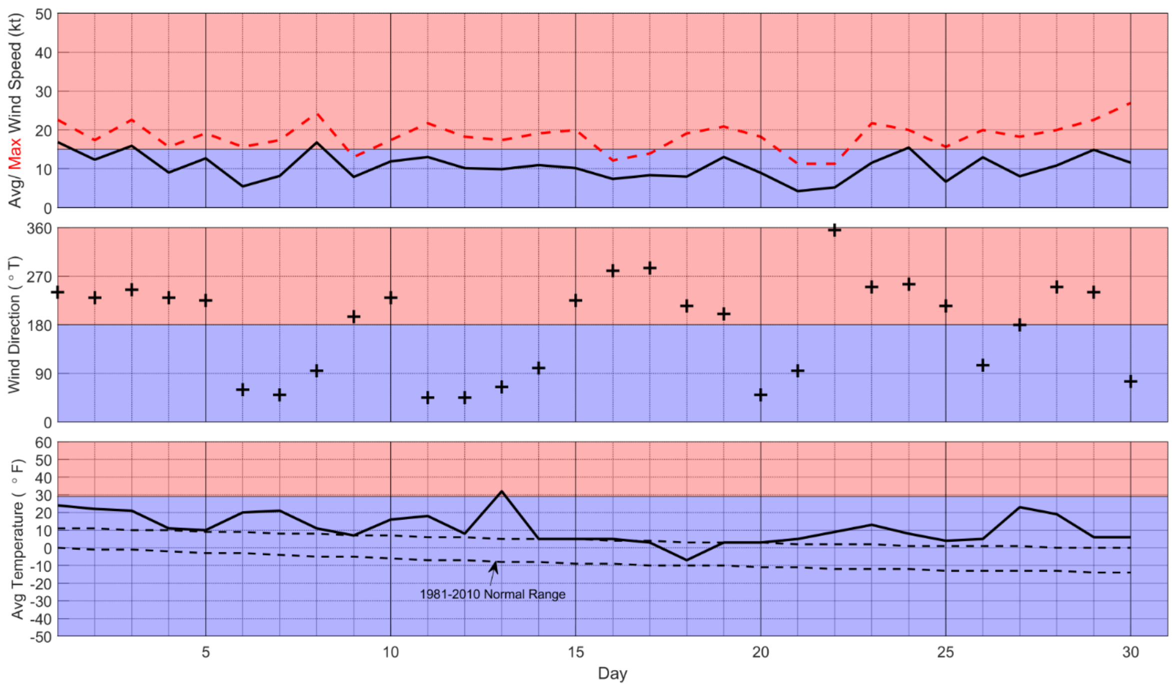

Figure 5-8. Meteorological Conditions at Deadhorse Airport in November 2019

information presented in the CIS ice charts (CIS, 2019; Figure 5-9), nearshore freeze-up occurred on or about November 11th, when 300 FDD had accumulated at Deadhorse Airport. Complete freeze-up in the Alaskan Beaufort Sea followed two weeks later, on November 24th, when the pack ice coalesced with the coastal ice over the entire length of the study area. A total of 585 FDD had accumulated at Deadhorse Airport on this date. With the exception of leads and polynyas, the nascent ice canopy remained intact thereafter.

Ice Thickness: The calculated thickness of undisturbed first-year ice increased from 18 cm at the beginning of the month to 42 cm at the end (Table 5–3).

Landfast Ice: Landfast ice began to develop in early November, appearing first in the western portion of the Beaufort Sea study area before expanding to the east. As shown in Figure 5-10, which was derived from the RADARSAT-2 images obtained on November 17th and December 4th, the landfast ice zone at mid-month included virtually all of Admiralty Bay, Smith Bay, Simpson Lagoon, Gwydyr Bay, and Prudhoe Bay; most of Harrison Bay; and a narrow strip along the mainland coast of Stefansson Sound.

During the second half of the month, the landfast ice experienced modest expansion that produced complete coverage in Harrison Bay, near-complete coverage in Stefansson Sound, and a narrow strip along the coast of Camden Bay. The lack of robust growth is consistent

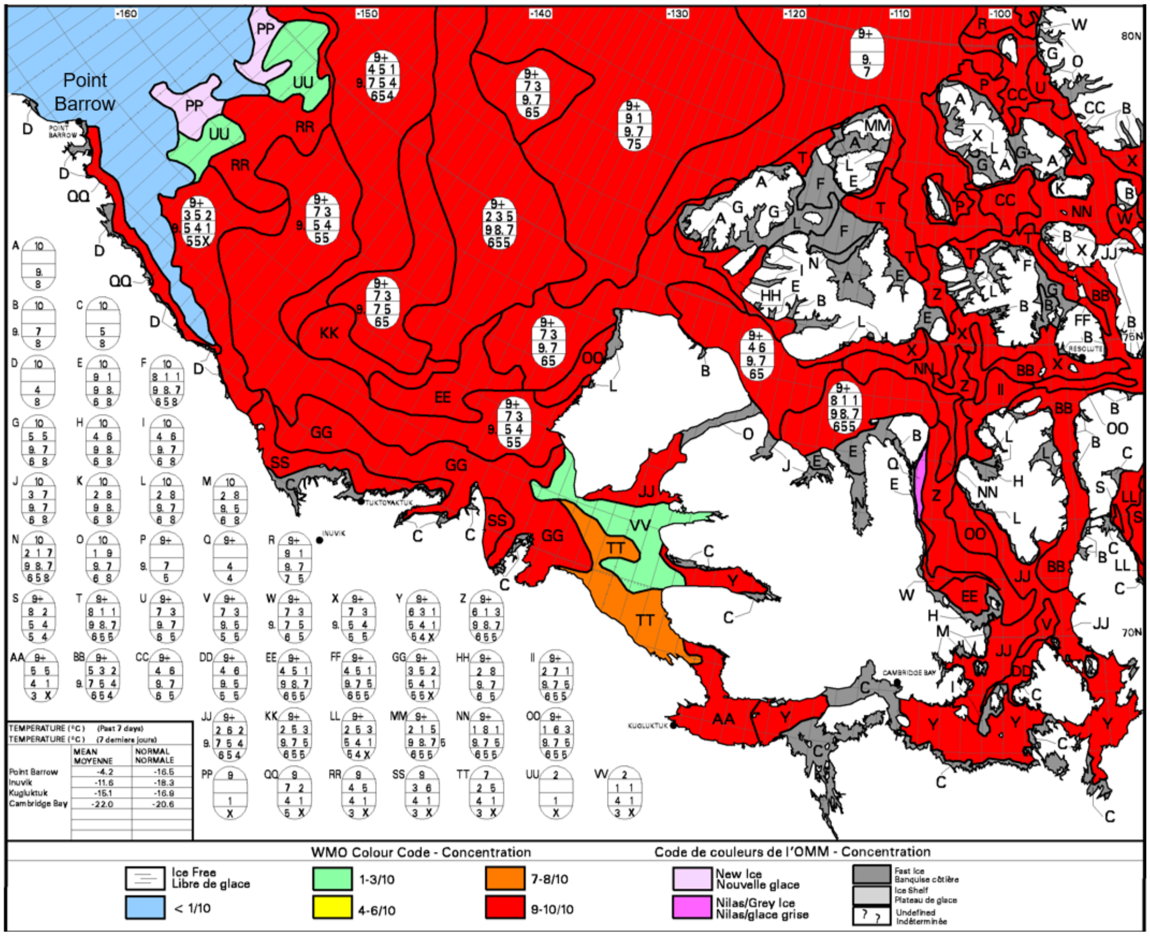

After: Canadian Ice Service, 2019

Figure 5-9. Beaufort Sea Ice Concentrations at Time of Nearshore Freeze-Up (November 11, 2019)

with the prevalence of westerly winds (Figure 5-8), which tend to retard the development of landfast ice by pushing the ice offshore.

Ice Pile-Ups: The 23 pile-ups in Table 5–4 that were caused by ice approaching from the northeast and northwest are believed to have formed between November 23rd and December 9th, a 17-day period in which the winds alternated between easterly and westerly on 11 occasions. The one-hour sustained speeds peaked at 37 kt (19 m/s) for the easterlies and 24 kt (12 m/s) for the westerlies. The calculated thickness of first-year ice increased from 37 cm at the beginning of this period to 50 cm at the end.

Multi-Year Ice: In the absence of a well-developed first-year ice canopy in the Alaskan Beaufort Sea (Figure 5-7), the multi-year ice arriving from the Canadian Beaufort advanced rapidly to the west over the course of November. On November 17th, the southern boundary

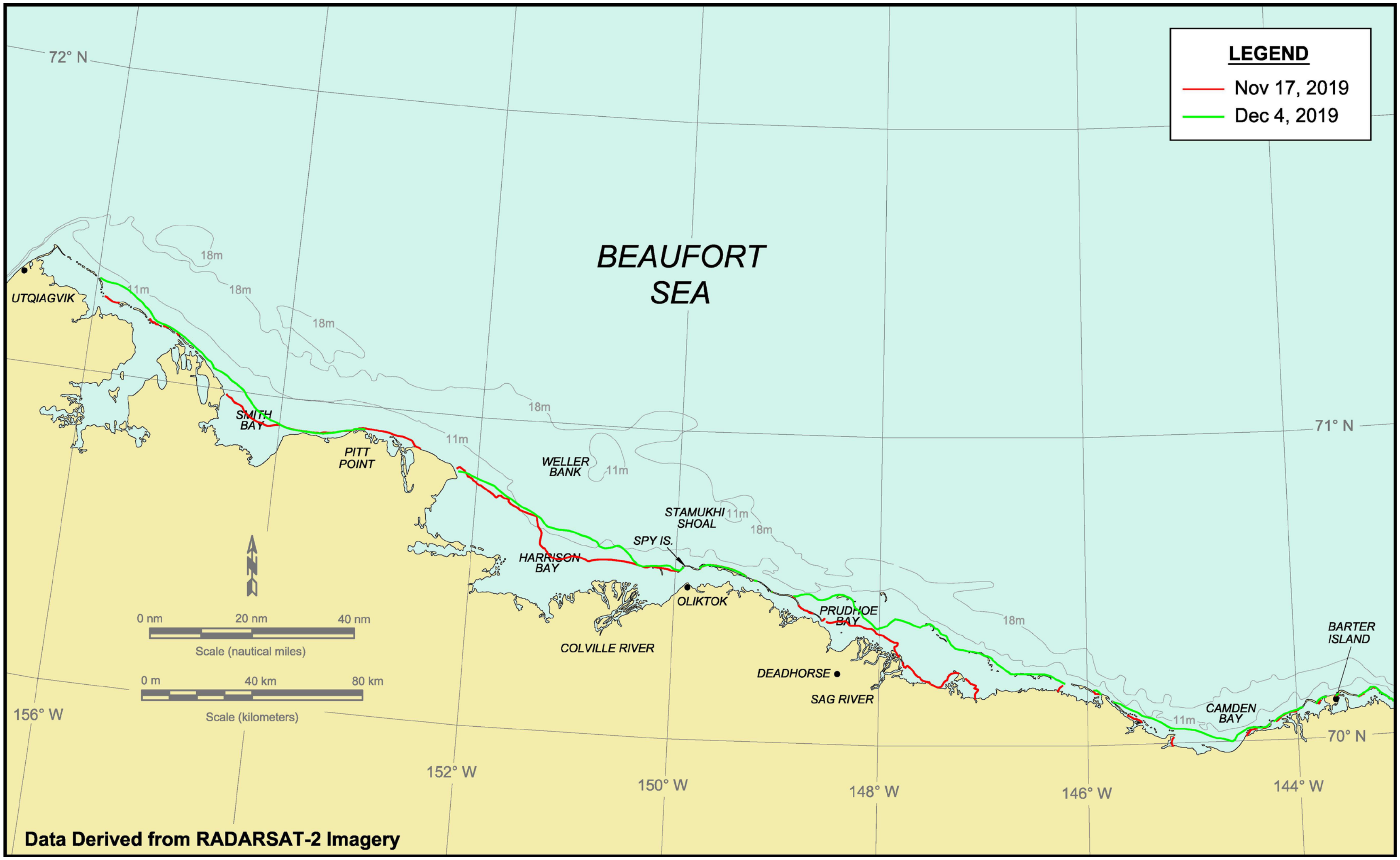

Figure 5-10. Beaufort Sea Landfast Ice Edge in November 2019

was located only 10 to 12 nm (19 to 22 km) off the shoreline of Camden Bay and 1.5 to 12 nm (2.8 to 22 km) off the barrier islands between Camden and Harrison Bays (Figure 5-11). The western boundary meandered between the 150°W and 154°W meridians.

The multi-year ice continued to advance to the west and south in the weeks that followed, with some of the ice at the southern boundary becoming incorporated into the landfast ice zone to the east of Prudhoe Bay between November 18th and 25th, and to the west of Prudhoe Bay between November 25th and December 2nd (CIS, 2019). The net result is displayed in Figure 5-12, which shows the southern boundary in close proximity to the coast over the entire length of the Beaufort Sea study area, and the western boundary at the 156°45'W meridian off Point Barrow. The multi-year ice concentrations in the landfast ice zone typically were less than 10%, while those to the north of the landfast ice zone reached values as high as 20%.

Ice Drift: The rate of ice drift was quantified by comparing the positions of a large multi-year floe ("Floe A", with a diameter of approximately 10 km) evident in the RADARSAT-2 images obtained on November 17th and December 4th. During this 17-day period, the floe advanced 177 nm (32 km) to the west-northwest (Figure 5-13). The average speed, 10.4 nm/day (19.3 km/day), was the highest average monthly value recorded during the freeze-up study period. (Note: as discussed in Section 5.1, an average monthly speed was computed for each floe for each month in which the period of record in the Alaskan Beaufort Sea exceeded 15 days.) Easterly storms were absent and westerly winds outnumbered easterlies during the 17 days, suggesting that the westerly set of the Beaufort Gyre (Figure 1-1) coupled with the absence of confinement to the west (Figure 5-11) were primarily responsible for the high drift rate.

5.4 Late Freeze-Up

5.4.1 December 2019

Meteorological Conditions: The wind and temperature data recorded at Deadhorse Airport in December 2019 are provided in Figure 5-14. The warm air temperatures that characterized October and November continued through December 18th before falling back into the normal range. Only six days later, on the 24th, they dropped below the normal range to mark the start of a cold phase that persisted for the remainder of the freeze-up study period. The net result was ten days in December in which the daily average air temperature exceeded the normal range and six days in which it fell below. The average value for the month was -9°F (-23°C).

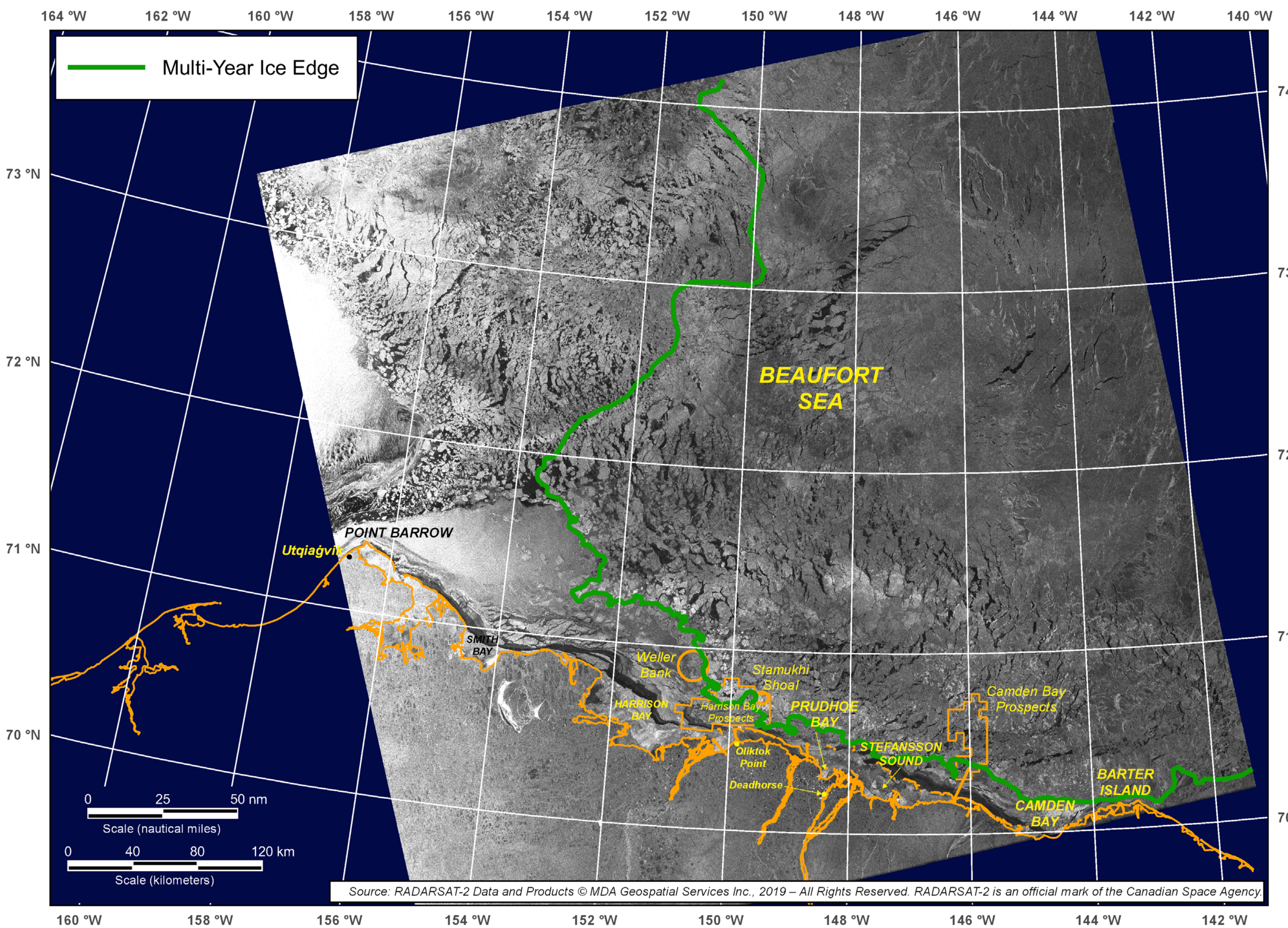

Figure 5-11. RADARSAT-2 Image of Beaufort Sea Acquired on November 17, 2019

“THIS INFORMATION IS DISTRIBUTED SOLELY FOR THE PURPOSE OF PRE-DISSEMINATION PEER REVIEW UNDER APPLICABLE INFORMATION QUALITY GUIDELINES. IT HAS NOT BEEN FORMALLY DISSEMINATED BY BSEE. IT DOES NOT REPRESENT AND SHOULD NOT BE CONSTRUED TO REPRESENT ANY BSEE DETERMINATION OR POLICY.”

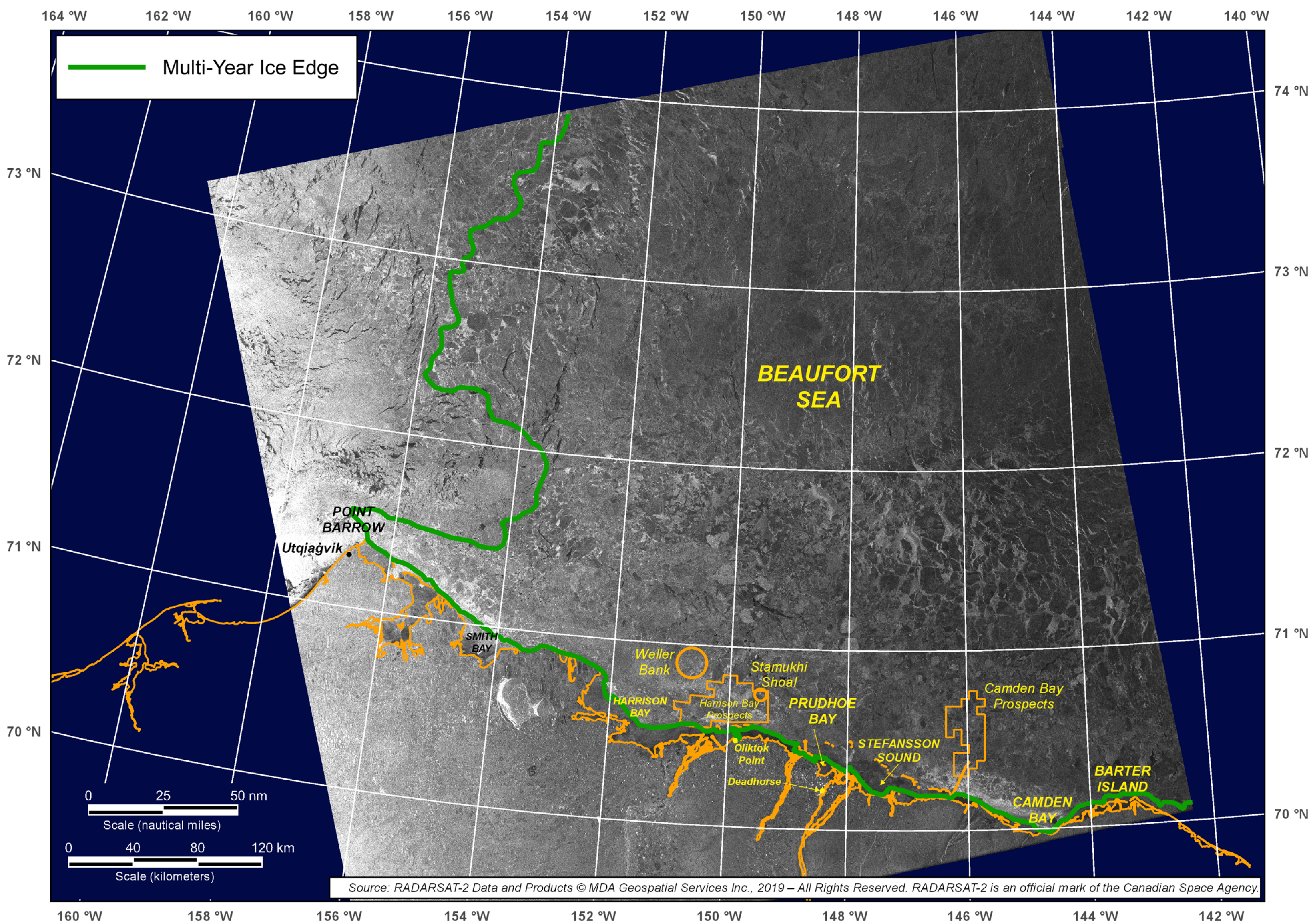

Figure 5-12. RADARSAT-2 Image of Beaufort Sea Acquired on December 3, 2019

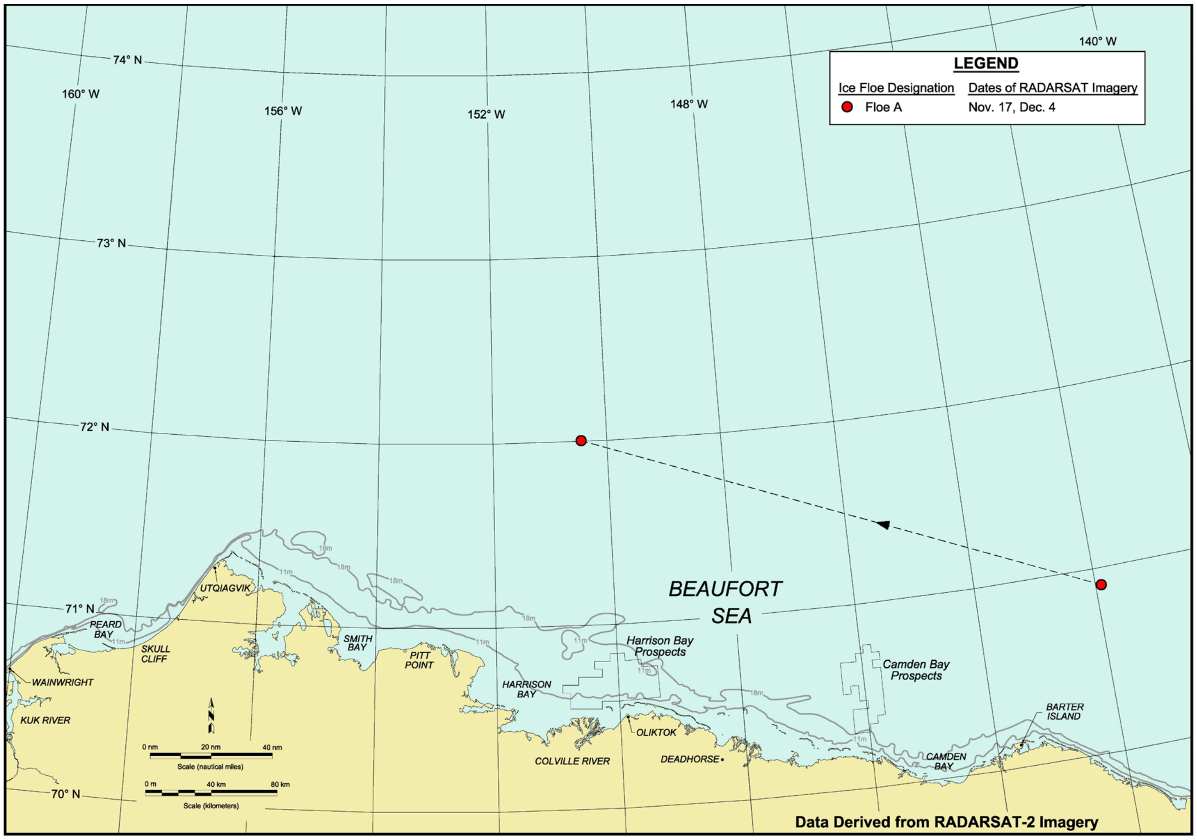

Figure 5-13. Beaufort Sea Multi-Year Ice Floe Displacement in November 2019

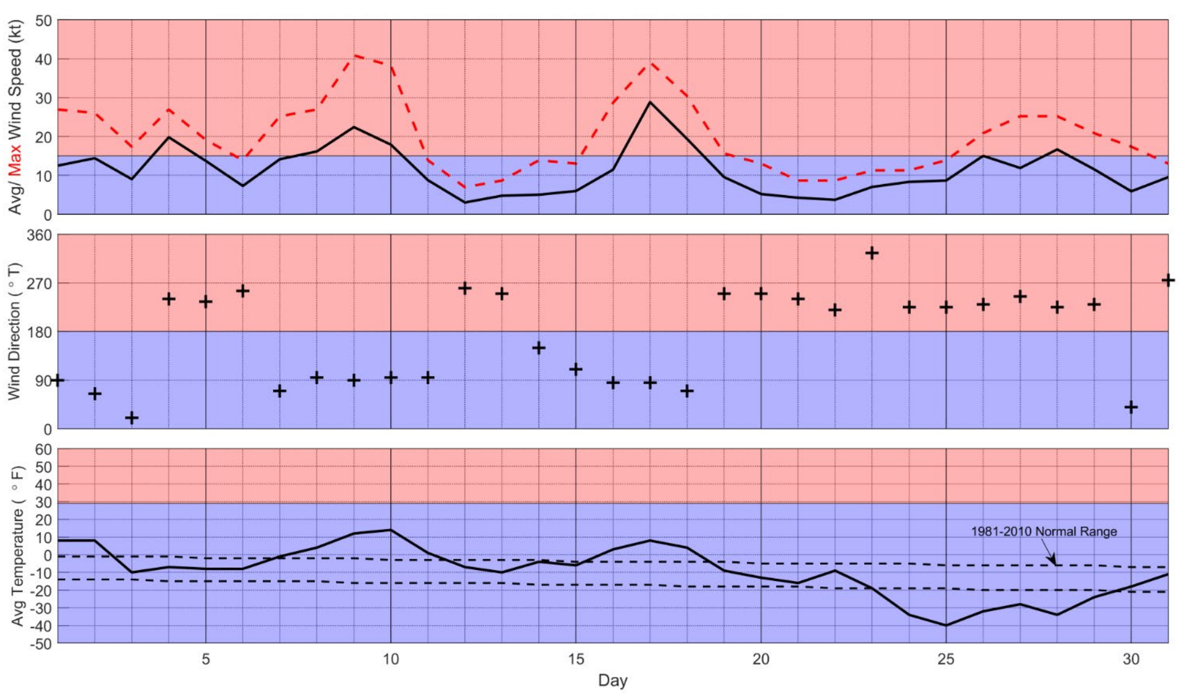

Figure 5-14. Meteorological Conditions at Deadhorse Airport in December 2019

Westerly winds outnumbered easterlies, but the difference was the smallest recorded during any month in the study period with westerlies prevailing on 17 days and easterlies on 14. As in October and November, the average wind speed was 11 kt (6 m/s). The storm population consisted of two brief, relatively mild westerly events and two easterly events of greater intensity and duration:

- December 4th: one-day westerly with maximum speed of 20 kt (10 m/s);
- December 8th-10th: three-day easterly with maximum speed of 22 kt (11 m/s);
- December 17th-18th: two-day easterly with maximum speed of 29 kt (15 m/s);
- December 28th: one-day westerly with maximum speed of 17 kt (9 m/s).

Ice Thickness: The calculated thickness of undisturbed first-year ice increased by 33 cm over the course of the month, from 42 to 75 cm.

Landfast Ice: The locations of the landfast ice edge were estimated from RADARSAT-2 images obtained on December 4th, December 18th, and January 4th. The results are presented in Figure 5-15. Between December 4th and 18th, a period dominated by easterly winds and two easterly storms (Table 5–2), the ice edge advanced to the vicinity of the 11-m isobath from the western side of Camden Bay to Point Barrow. The greatest gain, 10 nm (19 km), occurred off Smith Bay.

Between December 8th and January 4th, mild to moderate westerly winds prevailed. The only exception consisted of a one-day westerly storm on December 28th. The landfast ice edge experienced only minor changes during this period, indicating that the ice, although of limited areal extent, had become sufficiently well-grounded to resist displacement.

Multi-Year Ice: The multi-year ice in the landfast ice zone remained stationary throughout December at concentrations typically less than 10%. Farther offshore, where the multi-year floes tended to be larger, the maximum concentrations increased over the course of the month from 20% at the beginning to 50% at the end. The only region lacking multi-year ice was a tongue of first-year ice that developed between the U.S.-Canadian border and Harrison Bay in mid-December (Figure 5-16), and persisted for the remainder of the freeze-up study period just offshore of the landfast ice zone.

Ice Drift: Ice drift rates were derived from the successive positions of 11 large multi-year floes identified in RADARSAT-2 images obtained on December 4th, December 18th, January 2nd, and January 4th. The tracking periods for individual floes ranged from 12 to 29 days, while the average floe diameters ranged from 3 to 17 km. It should be noted that if a floe moved west from the Beaufort into the Chukchi between images, its motion during the

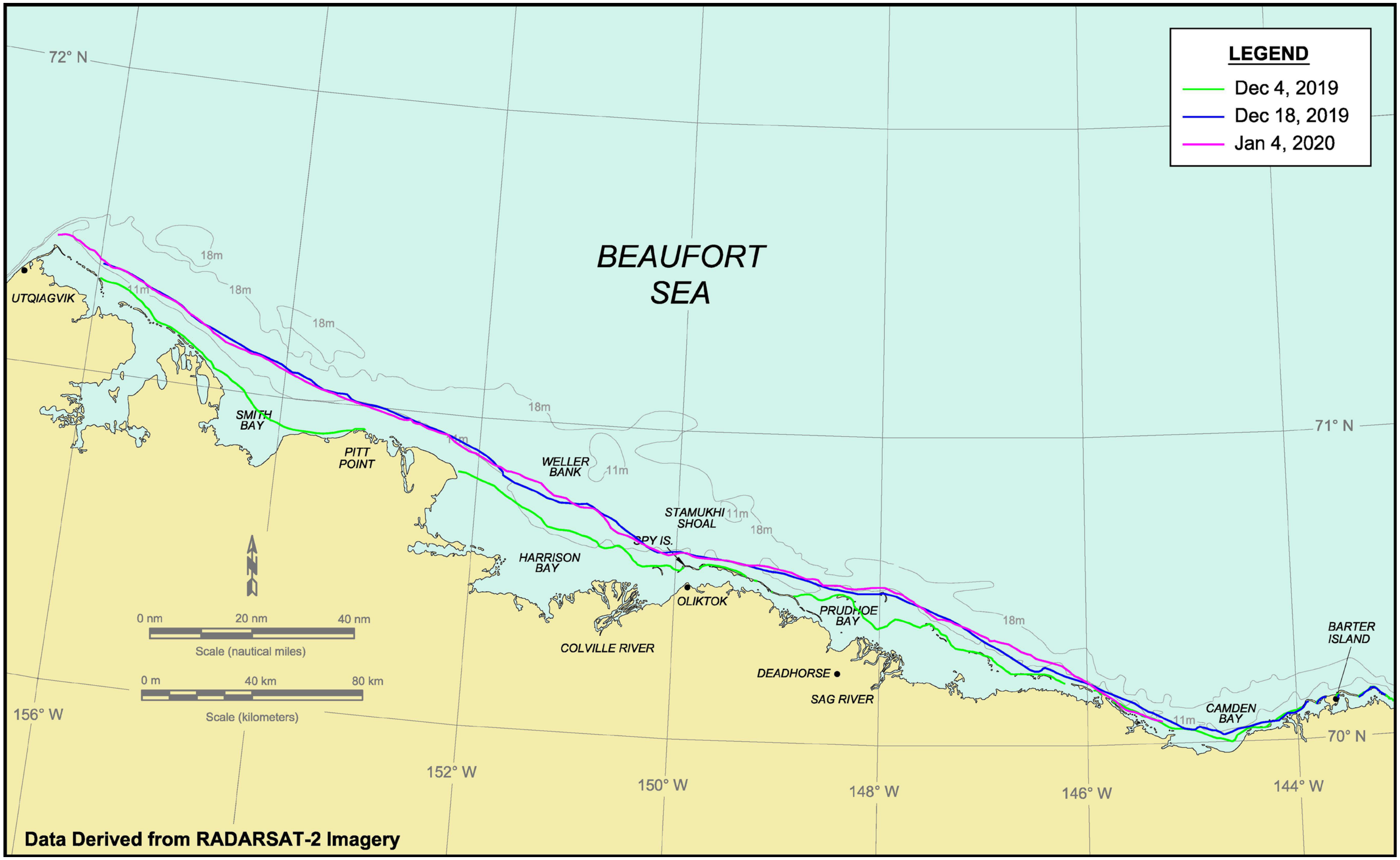

Figure 5-15. Beaufort Sea Landfast Ice in December 2019

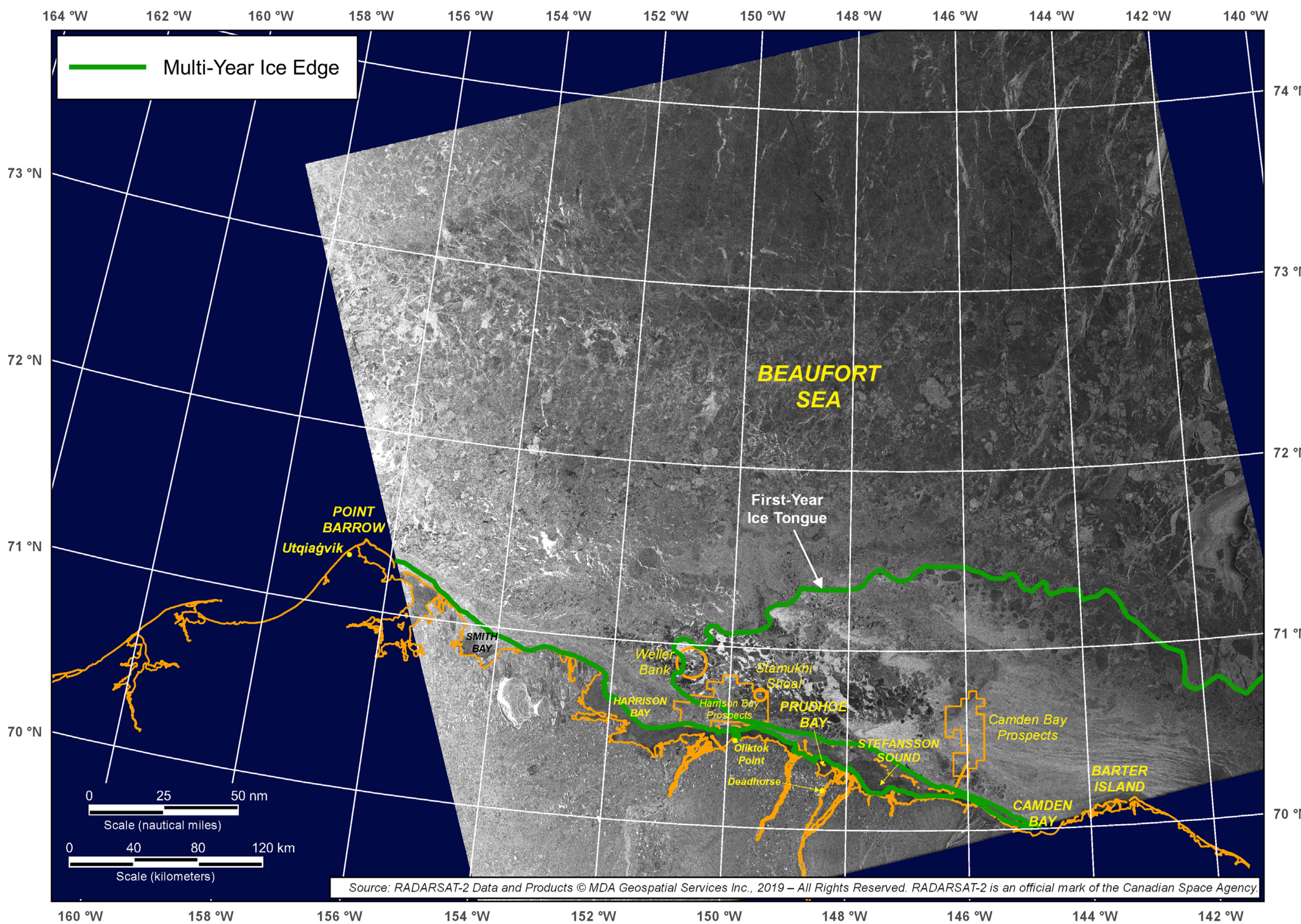

Figure 5-16. RADARSAT-2 Image of Beaufort Sea Acquired on December 18, 2019

intervening period was attributed to whichever basin contained the larger displacement. Displacements that occurred primarily in the Chukchi will be discussed in Section 6.

All 11 floes moved to the west (Figure 5-17), but the drift rates varied with the wind regime. The highest speeds occurred between December 4th and 18th in response to the aforementioned predominance of easterly winds punctuated by two easterly storms. For the six floes tracked within this period (Floe A and Floes G through K), the along-track speeds ranged from 12.5 nm/day (23.2 km/day; Floes A and I) to 14.1 nm/day (26.1 km/day; Floe G). The latter represented the highest value obtained from the RADARSAT-2 images of both basins during the entire study period. Lower speeds occurred between December 18th and early January, when westerly winds slowed the westward set of the Beaufort Gyre. The six floes tracked during this period (Floes B through G) registered along-track speeds that varied between 2.3 nm/day (4.3 km/day; Floe B) and 6.2 nm/day (11.5 km/day; Floe F).

Average monthly speeds were computed from the net displacements of the six floes with tracking periods that exceeded 15 days (Floes B through G). Floe G, which was tracked for the entire month (December 4th - January 2nd), averaged 9.6 nm/day (17.8 km/day). The other five floes, which were tracked only during the second half of the month (December 18th - January 4th) averaged between 2.3 and 6.2 nm/day (4.3 and 11.5 km/day, respectively). As shown in Table 5–5, the mean monthly value for all six floes was 4.9 nm/day (9.1 km/day) – a relatively low value that reflects a bias toward data obtained during the second half of the month.

Additional data on ice drift were derived from the daily positions of IABP Buoys X and Y (Section 4.4). Their tracks and daily average speeds are provided in Figure 5-18 and Figure 5-19, respectively. Buoy X moved rapidly to the west over the course of the month, passing north of Point Barrow on December 23rd. Its net displacement between midnight on November 30th and midnight on December 23rd was 290 nm (537 km) to the west-northwest, yielding an average speed of 12.6 nm/day (23.3 km/day). The peak speed between successive daily positions, 34.9 nm/day (64.7 km/day), occurred on December 10th on the final day of a three-day easterly storm (Figure 5-19). If this speed is expressed in knots (1.5 kt; 0.8 m/s) and compared with the daily average wind speed measured at Deadhorse Airport at the peak of the storm (22 kt or 11 m/s on December 9th), a wind factor of 6.8% is obtained. This high value is nearly identical to that of 6.7% recorded during the 2012-13 Freeze-Up Study (Coastal Frontiers and Vaudrey, 2013), comparable to those measured during an investigation of multi-year ice floes in 1984 (Tekmarine, *et al.*, 1985), and slightly greater than that of about 5% recorded by a multi-year floe in the nearshore region of the Alaskan Beaufort Sea in 1985 (Vaudrey, 1987b). As discussed in the Tekmarine report, nearshore current speeds

“THIS INFORMATION IS DISTRIBUTED SOLELY FOR THE PURPOSE OF PRE-DISSEMINATION PEER REVIEW UNDER APPLICABLE INFORMATION QUALITY GUIDELINES. IT HAS NOT BEEN FORMALLY DISSEMINATED BY BSEE. IT DOES NOT REPRESENT AND SHOULD NOT BE CONSTRUED TO REPRESENT ANY BSEE DETERMINATION OR POLICY.”

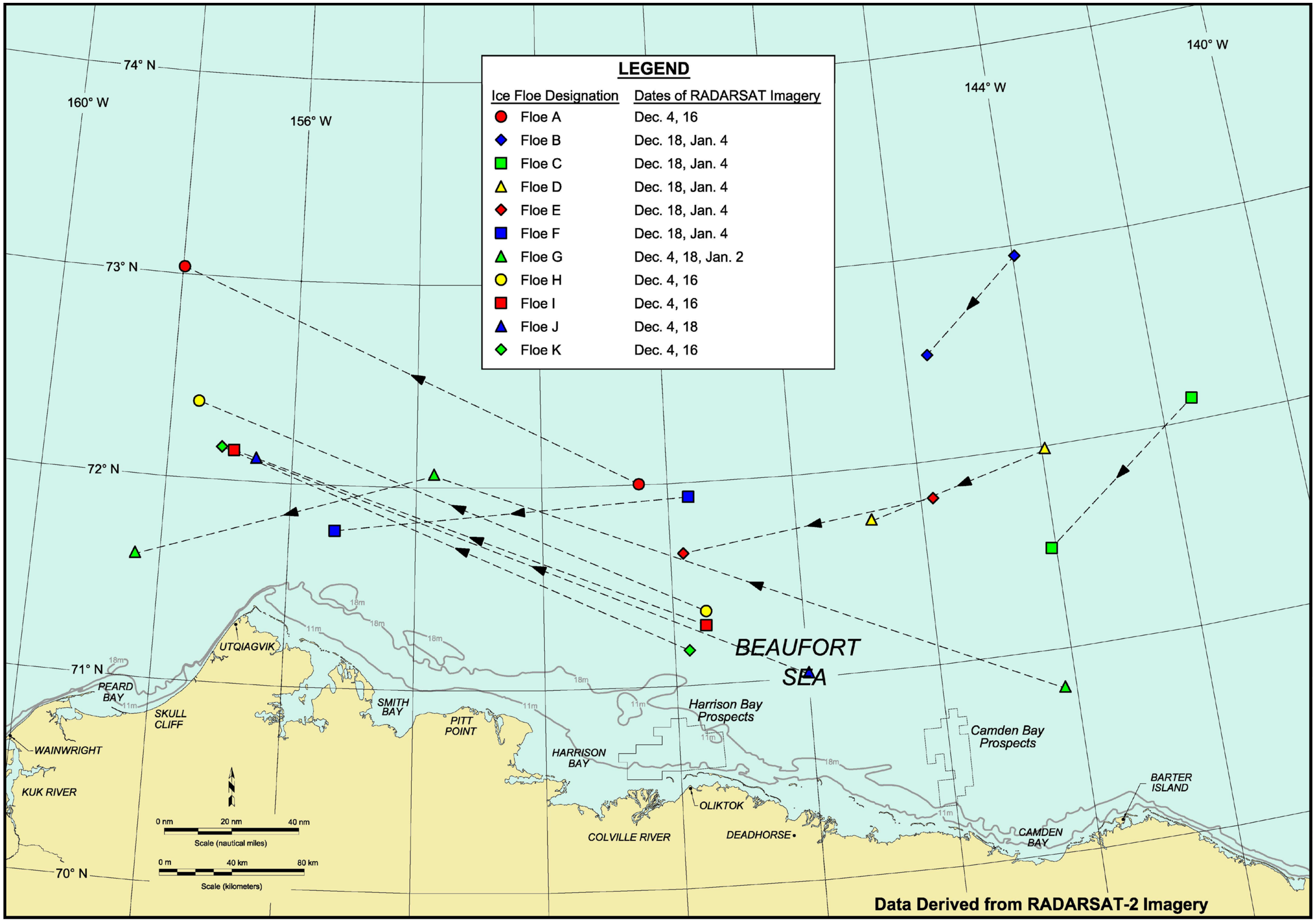

Figure 5-17. Beaufort Sea Multi-Year Ice Floe Displacements in December 2020

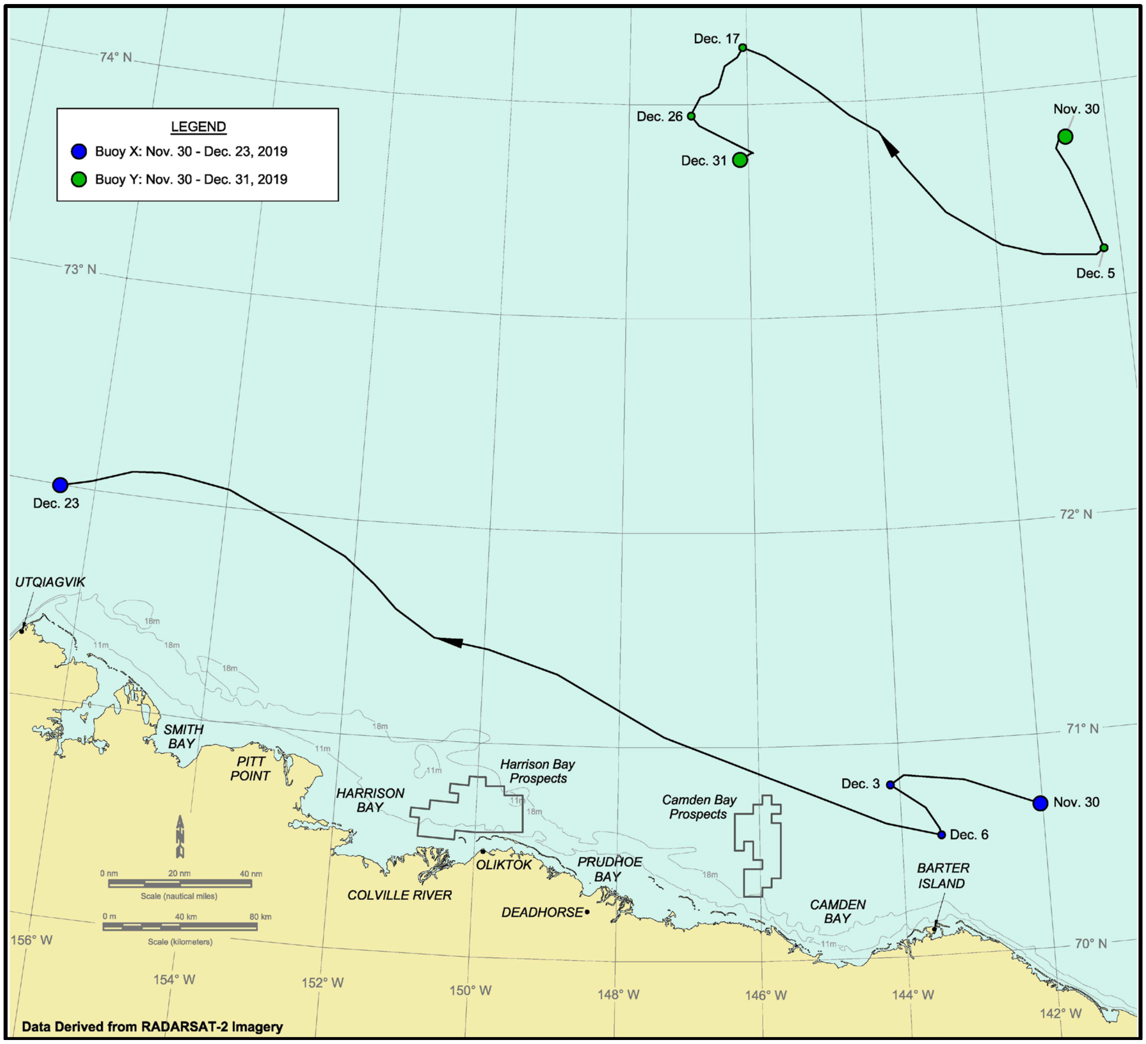

Figure 5-18. Beaufort Sea Drift Buoy Tracks in December 2019

tend to be higher than those in deep water due to the coastal boundary effect known as the “coastal jet” (Csanady, 1982).

Buoy Y, like Buoy X, experienced a net displacement to the west over the course of the month but at a substantially lower rate. The net displacement between midnight on November 30th and midnight on December 31st was a modest 92 nm (171 km), producing an average speed of 3.0 nm/day (5.6 km/day). The peak speed between successive daily positions was 18.3 nm/day (33.9 km/day) and occurred on December 10th. The lower speed attained by Buoy Y relative to Buoy X may be explained, at least in part, by the fact that it was deeply embedded in the pack ice and therefore subject to greater confinement. An additional factor that reduced its net displacement to the west was the one-day westerly storm on December 28th (Figure 5-19). As shown in Figure 5-18, the storm caused Buoy Y to reverse course and move to the east after Buoy X had moved out of the Beaufort and into the Chukchi.

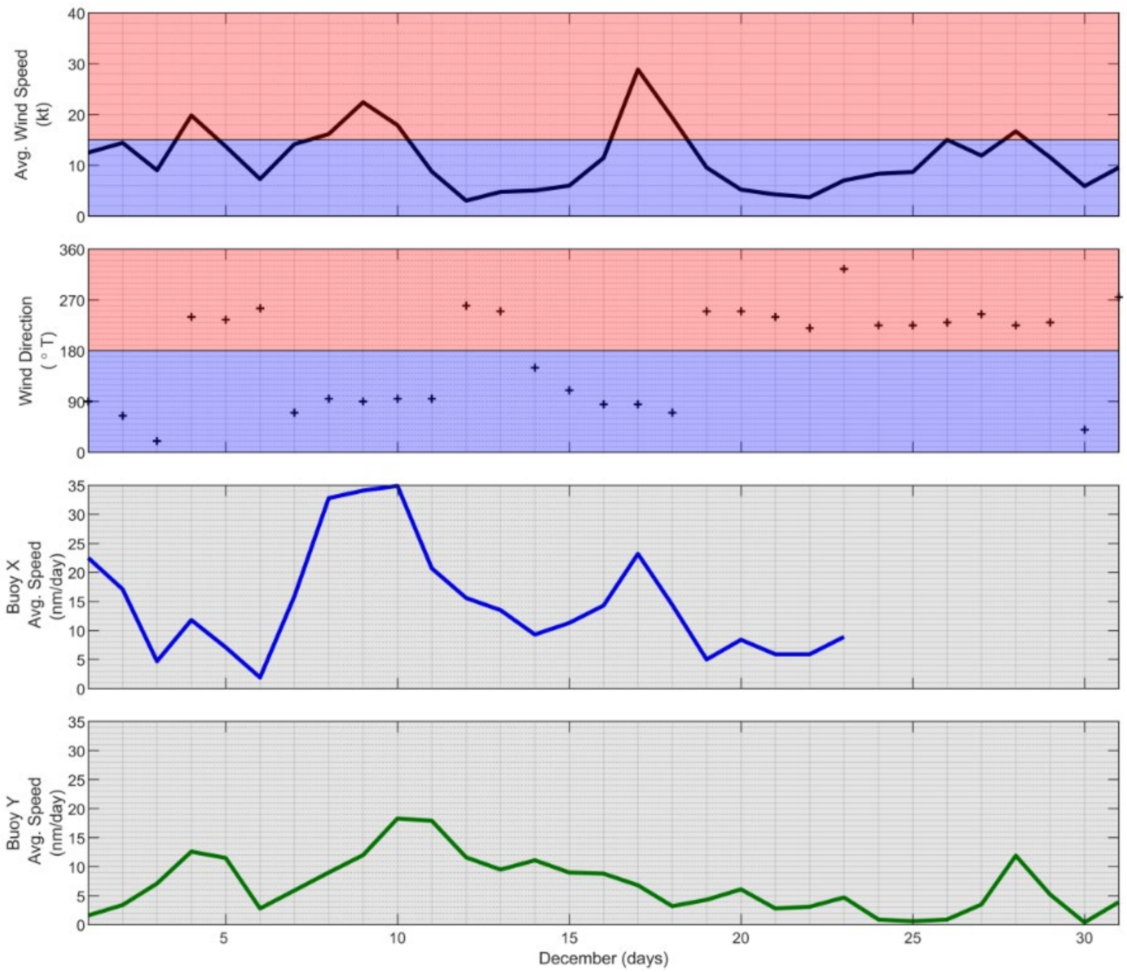

Figure 5-19. Beaufort Sea Drift Buoy Daily Average Speeds in December 2019

5.4.2 January 2020

Meteorological Conditions: Figure 5-20 presents the wind and temperature data recorded at Deadhorse Airport in January 2020. The cold air temperatures that began in late December persisted in January, producing 16 days in which the daily average value dropped below the normal range and only four days in which it rose above. The average temperature for the month was -23°F (-31°C). The minimum temperature, -45°F (-43°C) on January 6th, was the lowest recorded during the study period.

Westerly winds outnumbered easterlies by a ratio of more than 2 to 1, occurring on 23 of the 31 days. The speeds tended to be low, averaging only 9 kt (5 m/s) for the month. The sole storm was a brief, relatively mild westerly that occurred at mid-month:

- January 14th: one-day westerly with maximum speed of 19 kt (10 m/s).

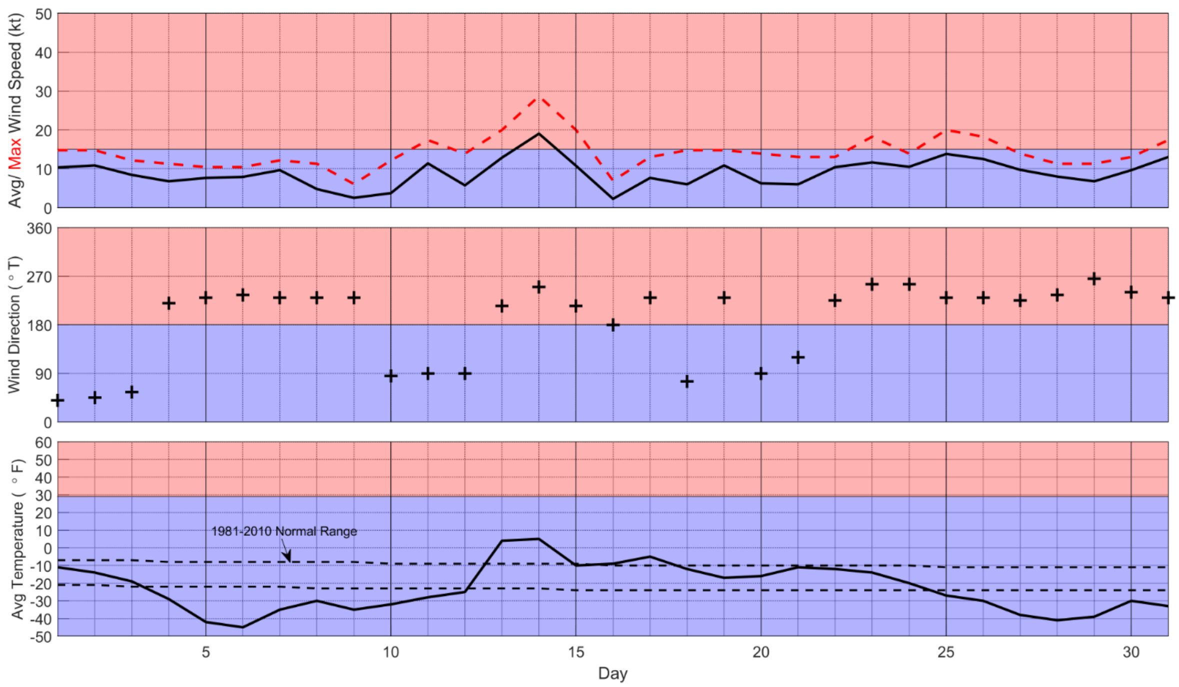

Figure 5-20. Meteorological Conditions at Deadhorse Airport in January 2020

Ice Thickness: The calculated thickness of undisturbed first-year ice increased from 75 cm at the beginning of January to 106 cm at the end, a robust gain of 31 cm.

Landfast Ice: Figure 5-21 illustrates the locations of the landfast ice edge derived from RADARSAT-2 images obtained on January 2nd, January 18th, and February 4th. During the first interval, which was dominated by light westerly winds but also contained several days of light easterly winds and the one-day westerly storm on the 14th, the ice edge retreated by as much as 7 nm (13 km) between Point Barrow and Smith Bay, advanced by as much as 10 nm (19 km) between Smith Bay and Prudhoe Bay, and remained static to the east of Prudhoe Bay. The advance, which was centered on Harrison Bay, appears to have been caused by pack ice grounding on Weller Bank. As noted in past freeze-up reports (*e.g.*, Coastal Frontiers and Vaudrey, 2017), Weller Bank typically serves as an anchor point for landfast ice in the western portion of the Alaskan Beaufort Sea.

During the second interval, from January 18th through February 4th, the landfast ice edge moved offshore along much of the Beaufort Sea coast. At the end of this period, it was located between the 11-m and 18-m isobaths from Point Barrow to Smith Bay, and in the vicinity of the 18-m isobath from Smith Bay to Prudhoe Bay and also in Camden Bay. The sole area in which the landfast ice edge remained static was the region the east of Prudhoe Bay, where it followed the 11-m isobath. The greatest advance, which peaked at 18 nm (33 km) off eastern Harrison Bay, caused the landfast ice zone to reach its other customary anchor

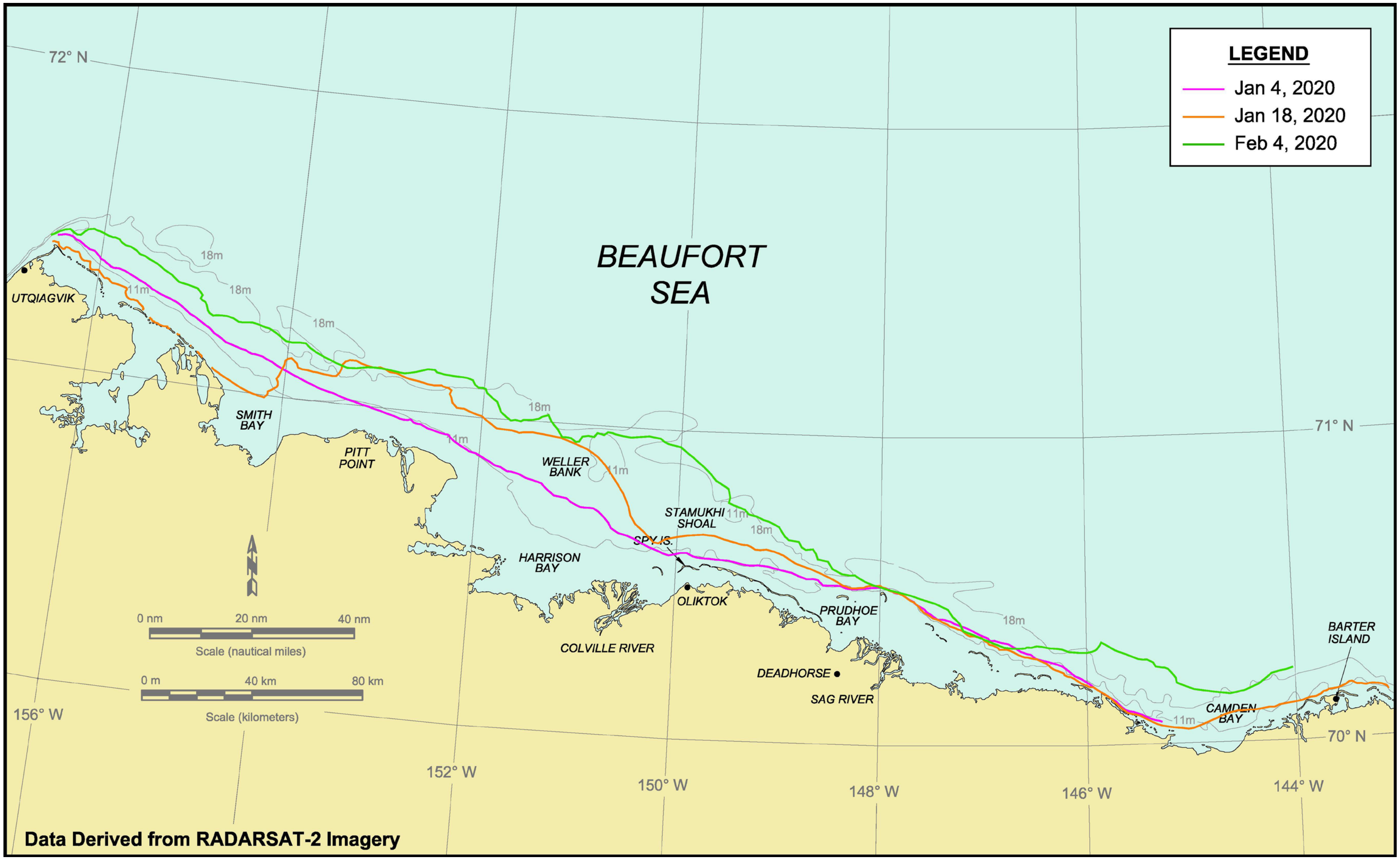

Figure 5-21. Beaufort Sea Landfast Ice in January 2020

point in the region, Stamukhi Shoal. Light westerly winds prevailed on 15 of the 17 days in this period, while the remaining two days were marked by light easterlies. In the absence of energetic easterly winds, it appears that the seaward advance of the ice edge resulted from the westerly set of the Beaufort Gyre.

Multi-Year Ice: Reflecting the absence of severe storms and persistent easterly winds (which reinforce the westerly set of the Beaufort Gyre), the distribution of multi-year ice in early January resembled that in late December (Section 5.4.1) and experienced only modest changes over the course of the month. Key characteristics are summarized below:

- *Landfast Ice:* The multi-year ice that had become incorporated into the landfast ice zone in late November and early December remained stationary in January at concentrations typically less than 10%.
- *Pack Ice:* Multi-year ice concentrations in the pack ice ranged from less than 10% to 60% throughout the month, with the largest floes and highest concentrations located to the east of Harrison Bay (Figure 5-22).
- *First-Year Ice Tongue:* The tongue of first-year ice that developed between the U.S.-Canadian border and Harrison Bay just offshore of the landfast ice zone in mid-December persisted throughout January (Figure 5-22), but narrowed from an average width of about 50 nm (93 km) at the beginning of the month to 10 nm (19 km) at the end.

Ice Drift: Five of the multi-year floes tracked in December (Floes B through F) remained in the Beaufort at the start of January. They were used to investigate ice movement rates based on RADARSAT-2 images obtained on January 4th, 16^{th,} and 18th, and February 2nd and 4th.

The westerly winds, absence of easterly storms, and high degree of confinement that prevailed in January produced net displacements and corresponding average monthly speeds that were substantially lower than those in December. As shown in Figure 5-23, all five floes moved to the northwest – a pattern consistent with the fact that most of the wind directions during this period contained a strong southerly component (Figure 5-20). The average monthly speeds ranged from 1.1 nm/day (2.0 km/day; Floe F) to 1.8 nm/day (3.3 km/day; Floe D), with a mean value of 1.5 nm/day (2.8 km/day) for all five floes.

The along-track speeds in January, like the average monthly speeds, were low relative to those in December. The maximum value, 5.9 nm/day (10.9 km/day), was recorded by Floe F between January 16th and 18th (soon after the month's sole westerly storm; Figure 5-20). Floe F also logged the minimum along-track speed, 1.1 nm/day (2.0 km/day),

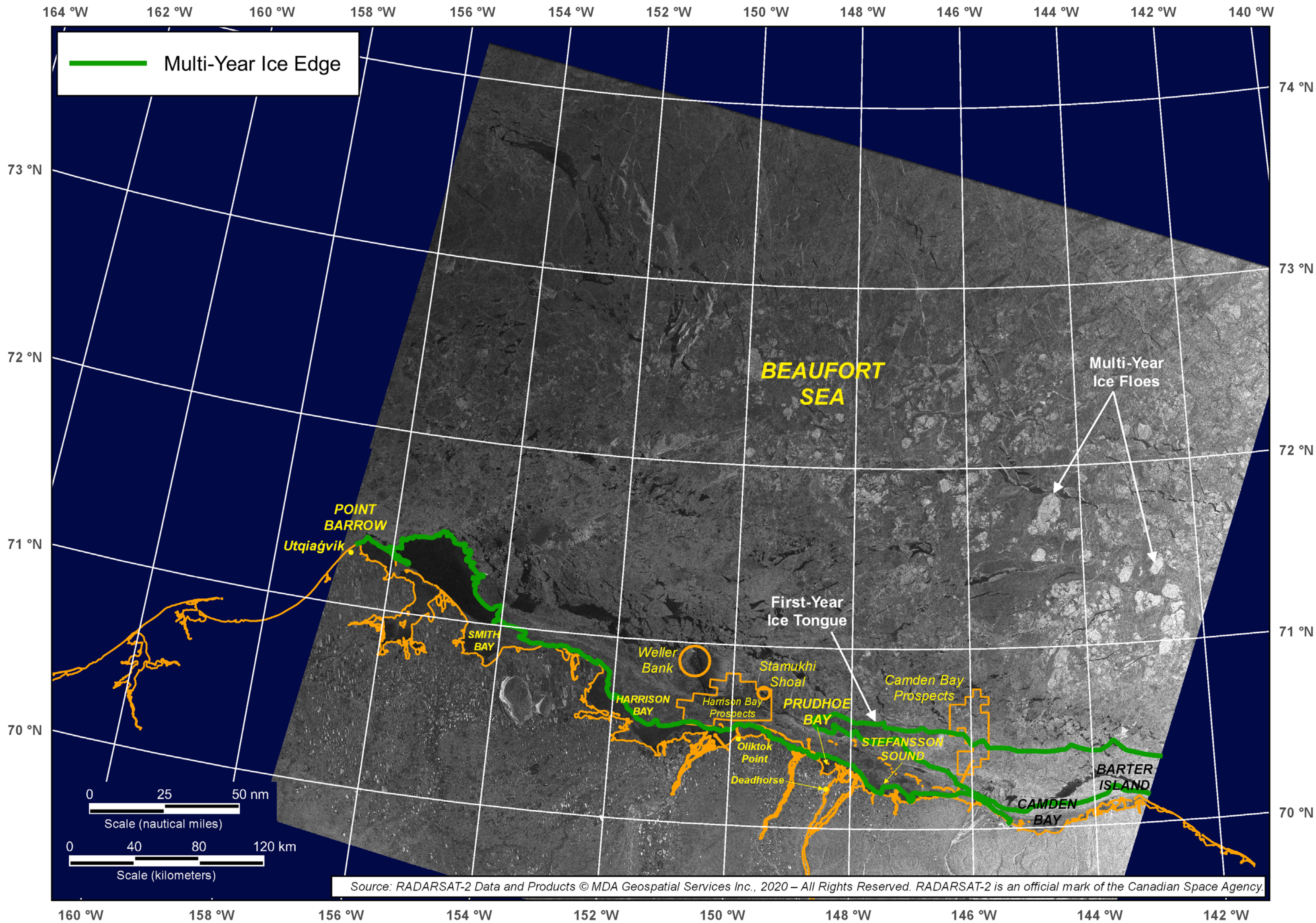

Figure 5-22. RADARSAT-2 Image of Beaufort Sea Acquired on January 18, 2020

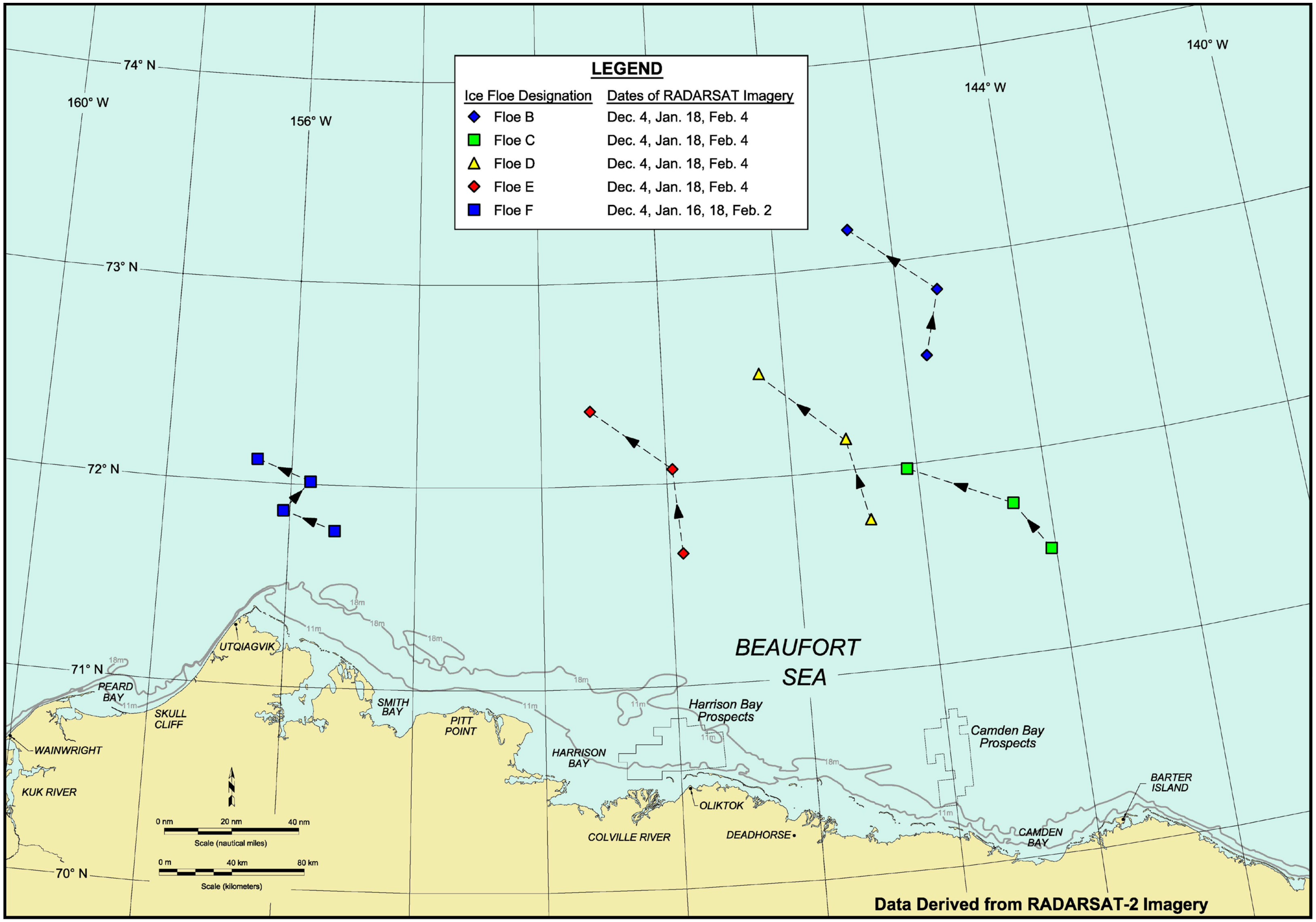

Figure 5-23. Beaufort Sea Multi-Year Ice Floe Displacements in January 2020

during the period that followed (January 18th-Februry 2nd). It is likely that the other floes moved at similar speeds during these two periods, but data are unavailable because unlike Floe F, their positions were not captured by the RADARSAT-2 image of the Chukchi Sea obtained on the 16th.

Two IABP drift buoys were present in the Beaufort Sea study area at the start of January: Buoy Y, which remained from December, and Buoy Z, which represented a new arrival. As shown in Figure 5-24, both were located near the northern boundary, in the vicinity of the 74°N parallel, and both experienced small net displacements over the course of the month. Their trajectories differed, however, in that Buoy Y ended the month 30 nm (56 km) to the northwest of its initial position whereas Buoy Z ended up 11 nm (20 km) to the south. This outcome, as well as the associated average monthly speeds of only 1.0 nm/day (1.9 km/day) for Buoy Y and 0.3 nm/day (0.6 km/day) for Buoy Z, indicate that their movement was constrained by the dense pack ice in the vicinity.

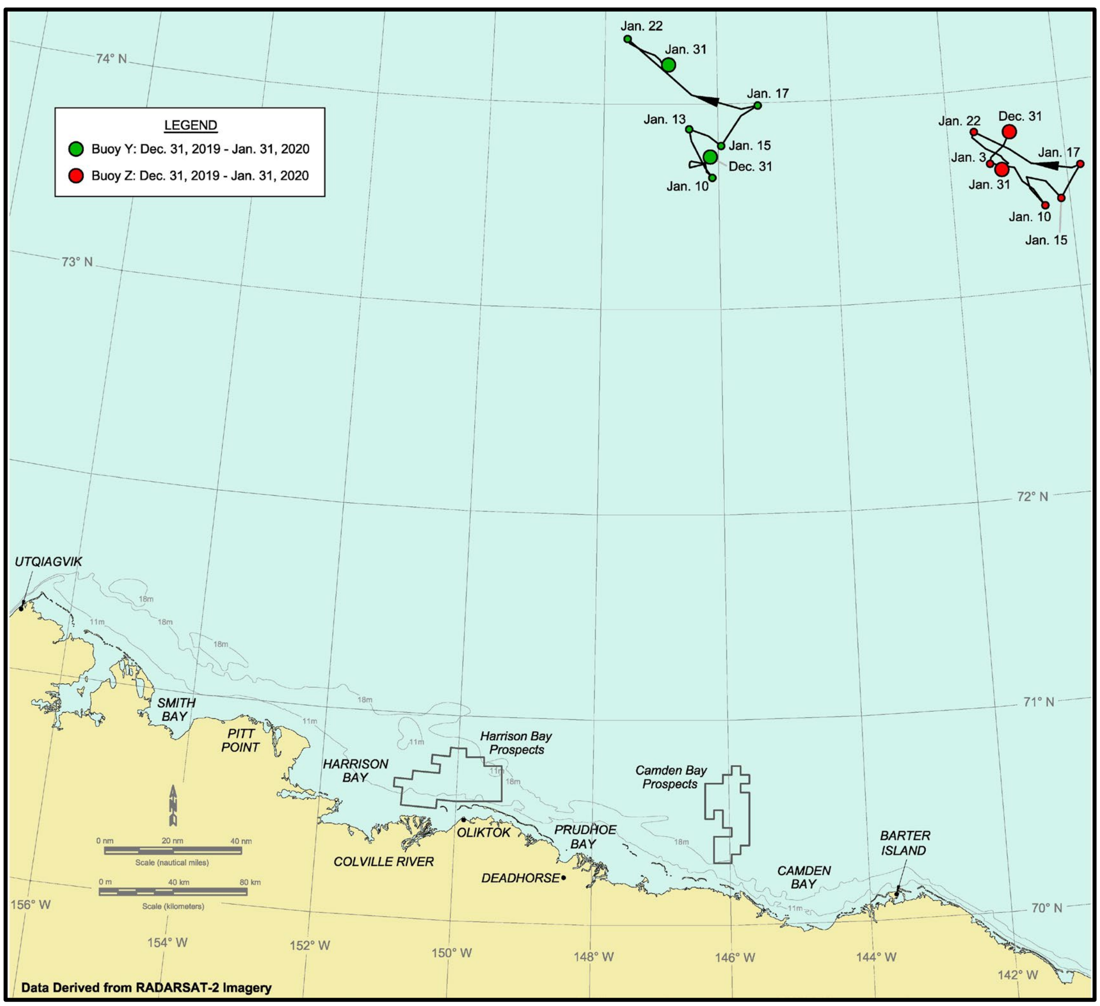

Figure 5-24. Beaufort Sea Drift Buoy Tracks in January 2020

The daily average speeds of the two buoys are plotted in Figure 5-25. In both cases, the peak values – 15.2 nm/day (28.2 km/day) for Buoy Y and 12.1 nm/day (22.4 km/day) for Buoy Z – resulted from westerly displacements that occurred on January 19th. The winds shifted from westerly to easterly and back to westerly between the 18th and 20th, suggesting that the relatively drift high speeds were caused by a temporary loss of confinement.

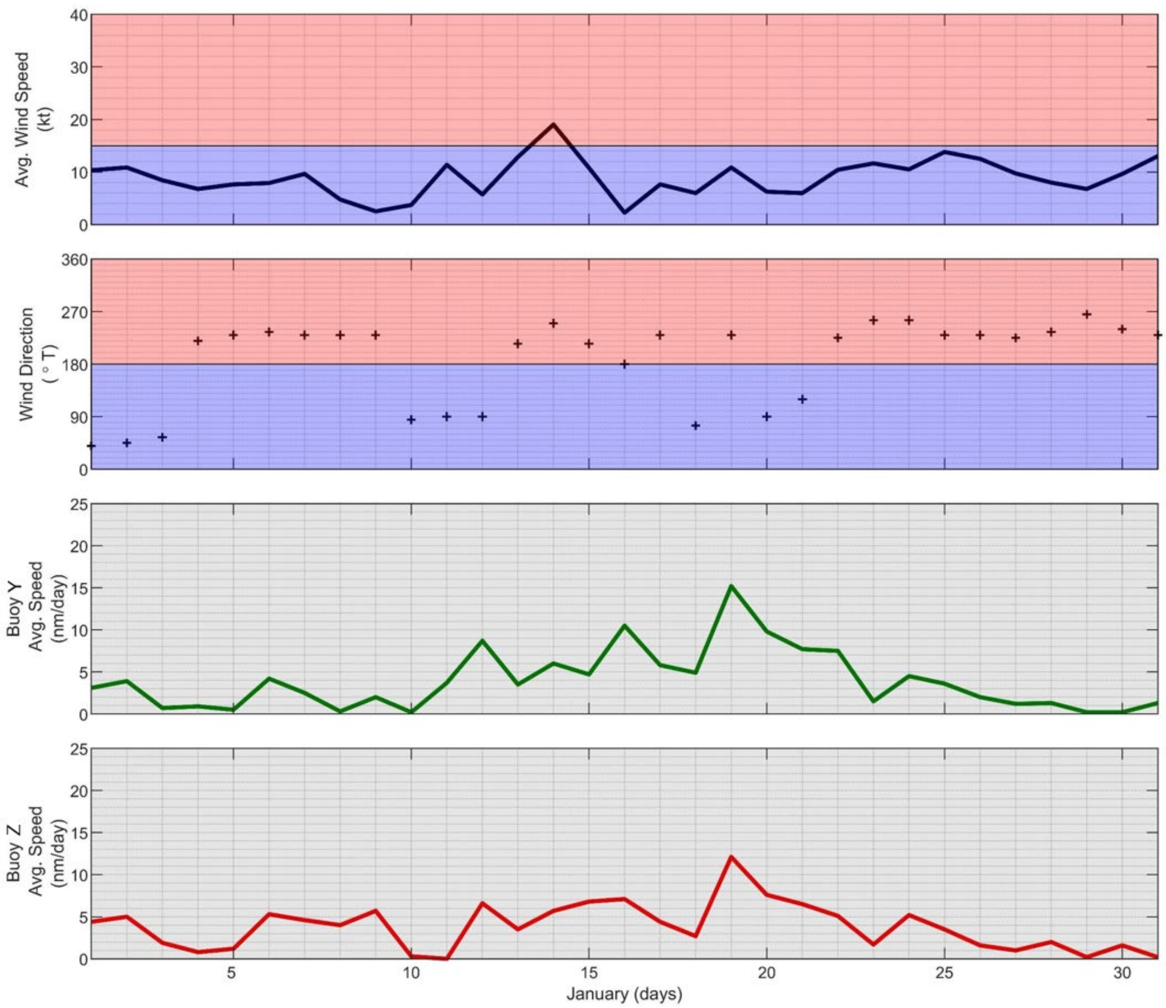

Figure 5-25. Beaufort Sea Drift Buoy Daily Average Speeds in January 2020

5.4.3 February 2020

Meteorological Conditions: The meteorological conditions at Deadhorse Airport in February are displayed in Figure 5-26. Unseasonably cold air temperatures prevailed, extending the pattern that began in late December and continued unabated in January. Over the course of the month, the daily average values were below the normal range on 19 days and above on only two. Daily average temperatures of -40°F (-40°C) or below were recorded on five occasions, while the average monthly temperature was -29°F (-34°C).

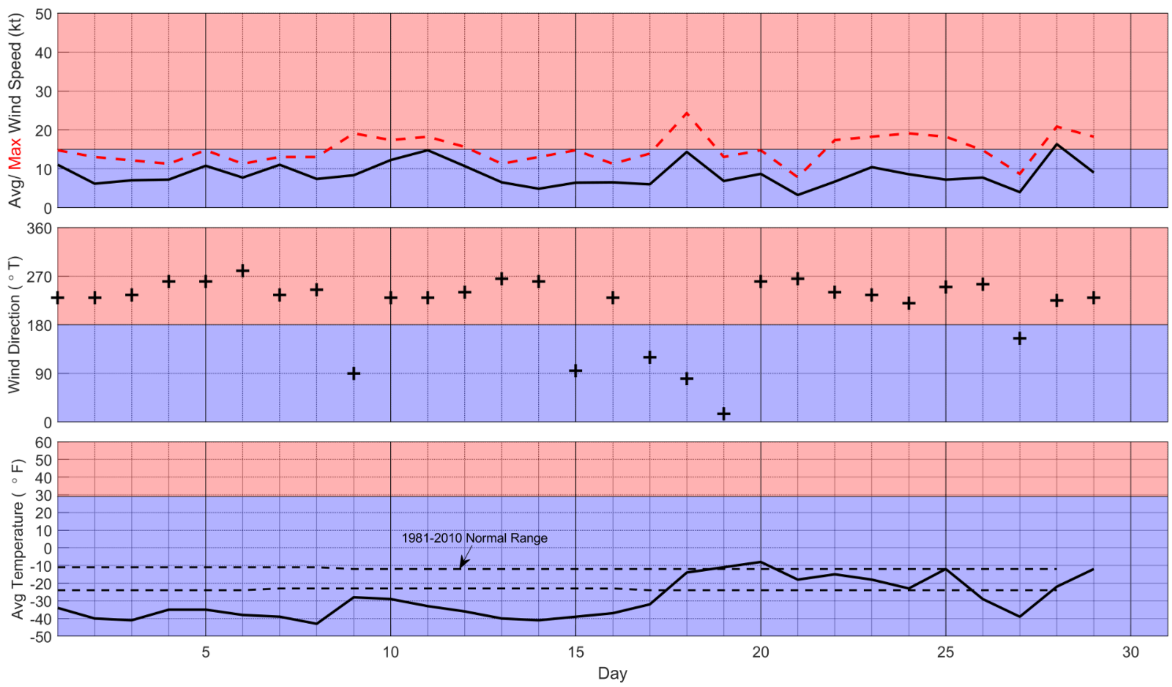

Figure 5-26. Meteorological Conditions at Deadhorse Airport in February 2020

As in each of the prior four months, westerly winds predominated in February, occurring on 23 of the 29 days. The average speed was 9 kt (5 m/s), which was identical to that in January. The only storm, a one-day westerly event, occurred at month-end:

- February 28th: one-day westerly with maximum speed of 16 kt (8 m/s).

Ice Thickness: The calculated thickness of undisturbed first-year ice increased by 28 cm, from 106 to 134 cm.

Landfast Ice: Figure 5-27 presents the locations of the landfast ice edge derived from RADARSAT-2 images obtained on February 4th, 21st (Figure 5-28), and 28th (Figure 5-29). During the interval between the first two images, the landfast ice zone expanded offshore by distances that ranged from less than 1 nm (2 km) off Point Barrow to 16 nm (30 km) off Stefansson Sound. Although light to moderate westerly winds predominated, three days of easterly winds that peaked at 14 kt (7 m/s) on the 18th were sufficient to cause the expansion. The resulting ice edge tended to follow the 18-m isobath to the west of Harrison Bay, and to lie farther offshore to the east.

During the one-week period between the 21st and 28th, the wind directions remained clustered in a narrow range between 155 and 265°T and therefore were not conducive to further expansion of the landfast ice zone. On the last day, February 28th, the southwesterly

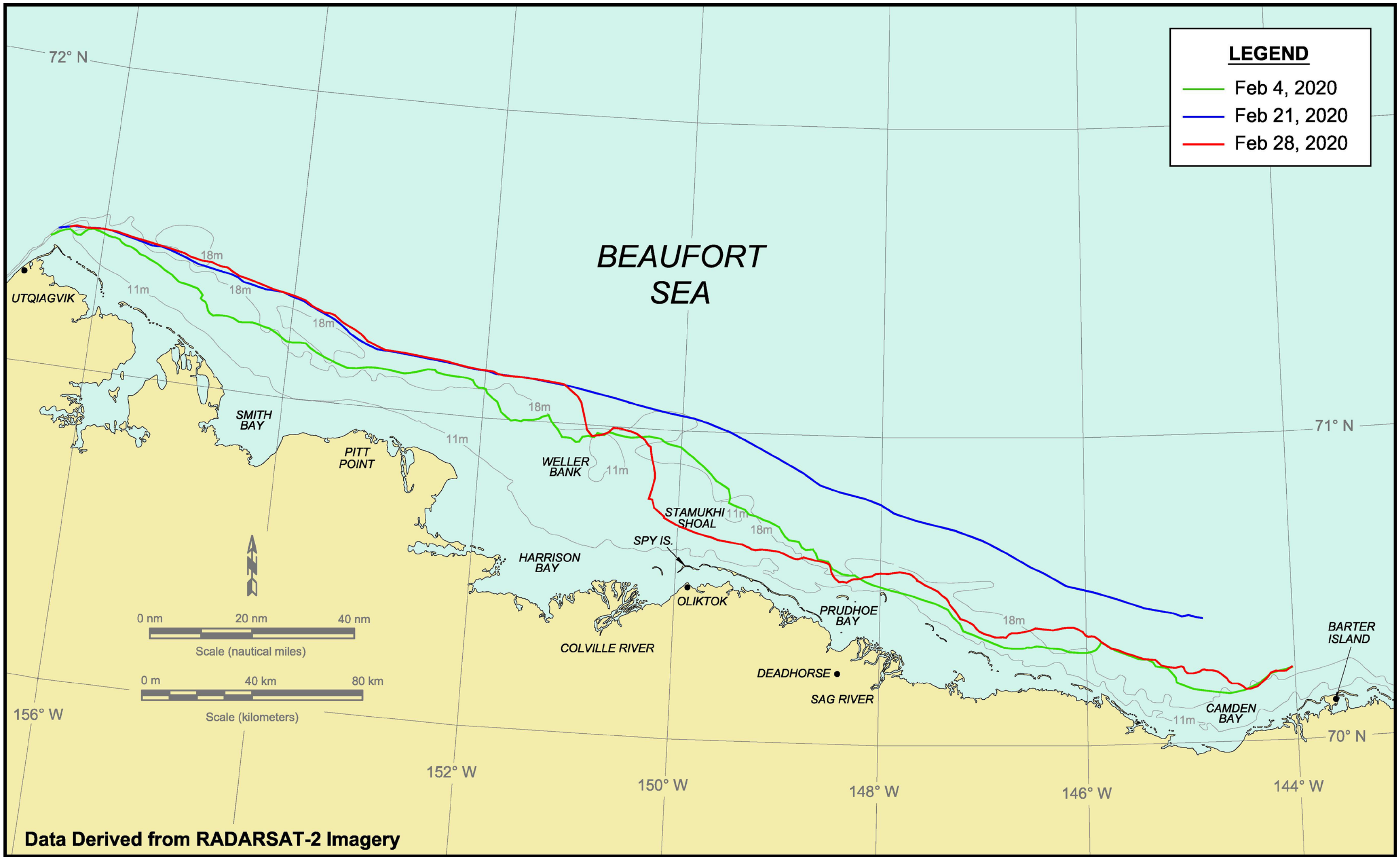

Figure 5-27. Beaufort Sea Landfast Ice in February 2020

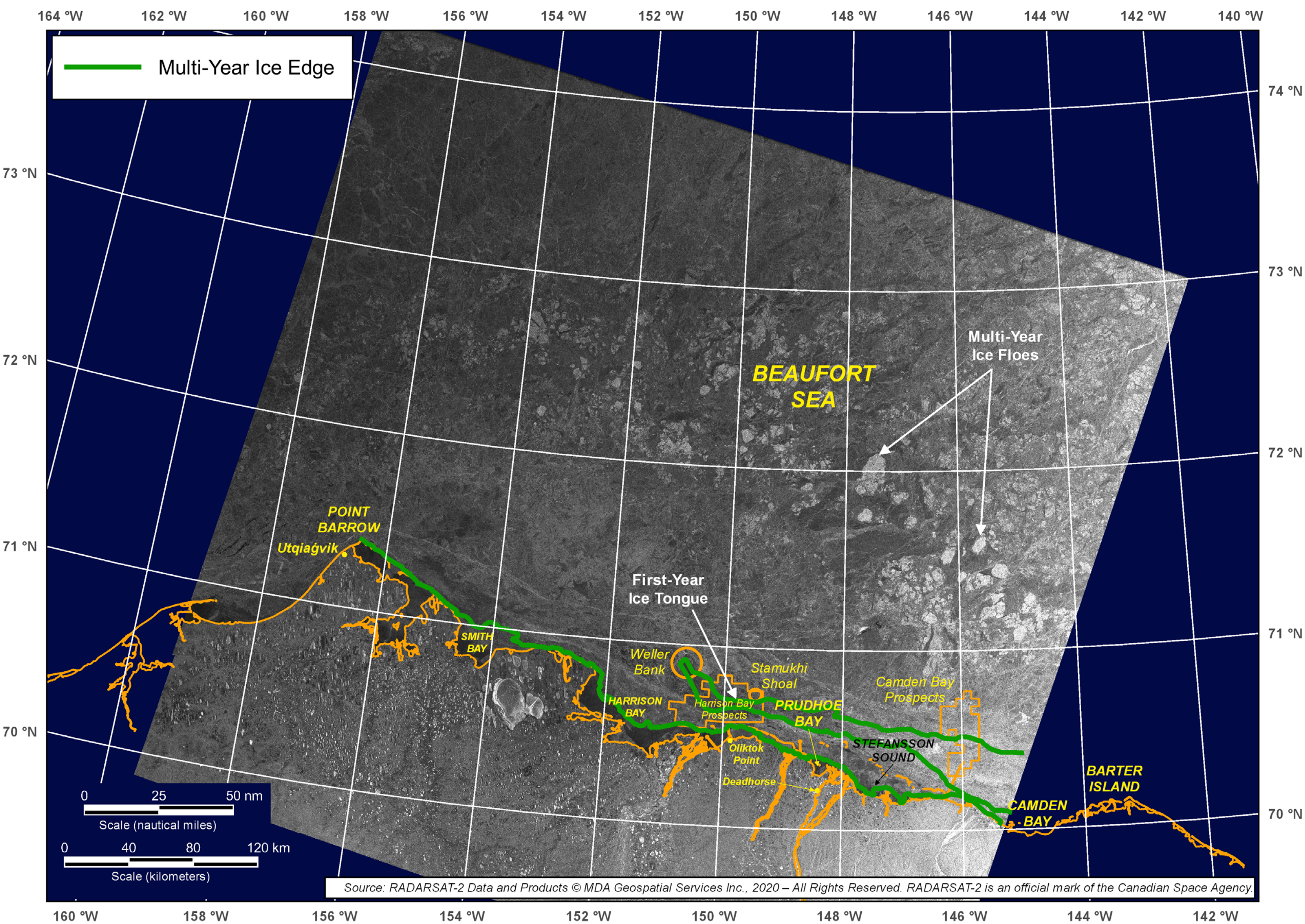

Figure 5-28. RADARSAT-2 Image of Beaufort Sea Acquired on February 21, 2020

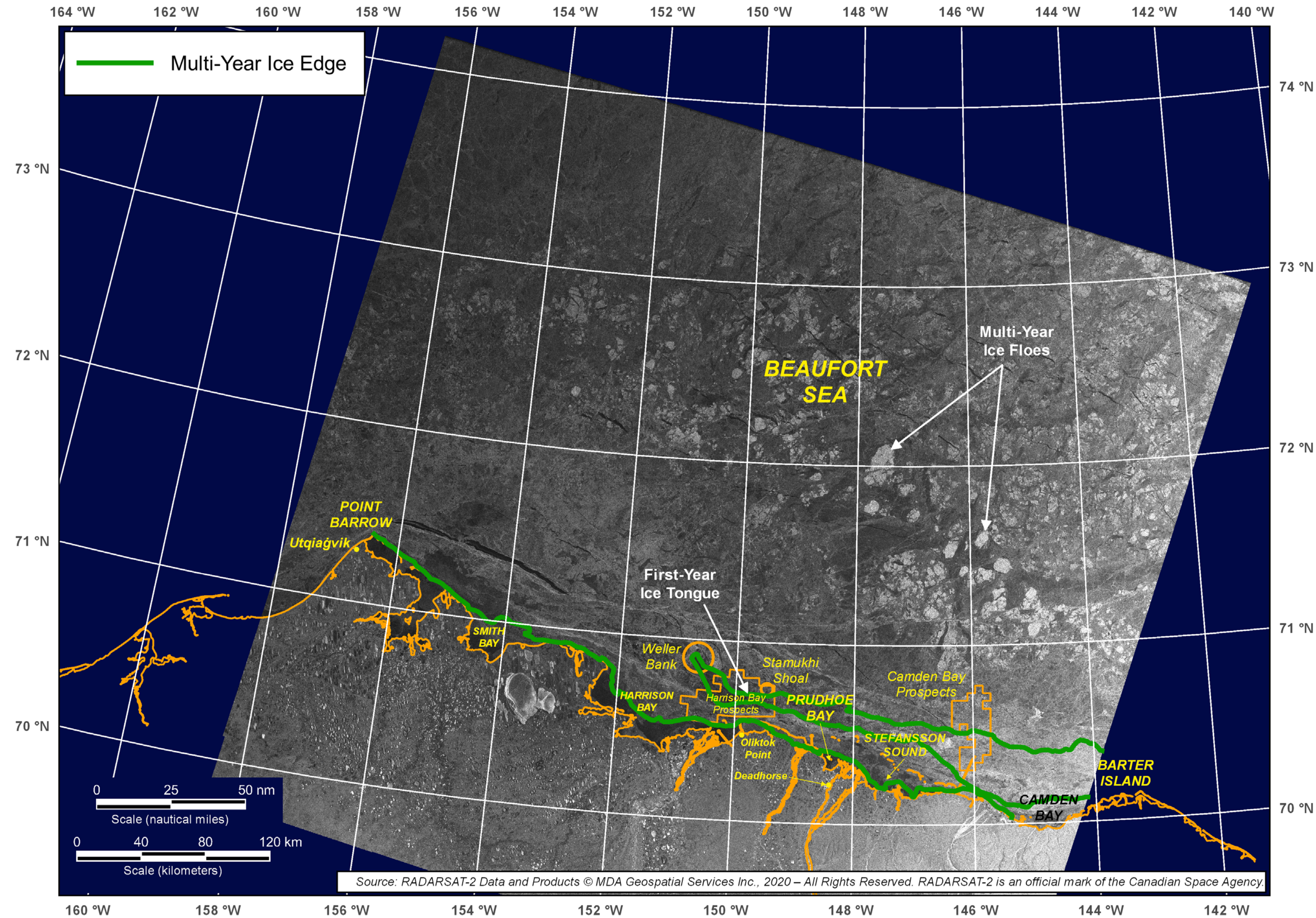

Figure 5-29. RADARSAT-2 Image of Beaufort Sea Acquired on February 28, 2020

winds that constituted the month's sole storm event removed a substantial portion of the landfast ice between Harrison and Camden Bays. The greatest loss, 20 nm (37 km) occurred in the eastern portion of Harrison Bay between Weller Bank and Stamukhi Shoal. It is noteworthy that although the landfast ice remained grounded on the former, it was completely dislodged from the latter (Figure 5-27). This outcome suggests that in the absence of easterly storms in January and February, the ice never became firmly grounded on Stamukhi Shoal. It also suggests that the expansion that occurred prior to February 21st represented a "stable extension" (Mahoney, *et al*., 2012), in which the ice edge was maintained primarily by compression rather than grounding.

Multi-Year Ice: As in January, an absence of severe storms coupled with a paucity of easterly winds caused the distribution of multi-year ice to remain nearly static in February. Details are provided below:

- *Landfast Ice:* The multi-year ice in the landfast ice zone remained stationary in February at concentrations typically less than 10%.
- *Pack Ice:* Multi-year ice concentrations in the pack ice ranged from less than 10% to 70%. Although the ice drifted slowly to the west, the largest floes and highest concentrations continued to remain to the east of Harrison Bay (Figure 5-28 and Figure 5-29).
- *First-Year Ice Tongue:* The tongue of first-year ice that stretched from the U.S.-Canadian border to Harrison Bay just offshore of the landfast ice zone remained unchanged in February with an average width of about 10 nm (19 km).

Ice Drift: Ice drift was investigated using multi-year ice Floes B through E, which were evident in the RADARSAT-2 images obtained on February 4th, 21st, and 28th. As illustrated in Figure 5-30, all four floes experienced net displacements to the west during the first interval between images before stopping (Floe C) or reversing course (Floes B, D, and F) during the second. Their stoppage/reversal indicates that persistent westerly winds, including the one-day westerly storm on the 28th, were sufficiently strong to overcome the westerly set of the Beaufort Gyre.

The average monthly speeds (derived from the net displacements that occurred between the 4th and 28th) tended to be slightly lower than those in January:

- Maximum Average Monthly Speed: 1.5 nm/day (2.8 km/day; Floe E);
- Minimum Average Monthly Speed: 1.1 nm/day (2.0 km/day; Floe C);
- Mean Average Monthly Speed*:* 1.3 nm/day (2.4 nm/day).

"THIS INFORMATION IS DISTRIBUTED SOLELY FOR THE PURPOSE OF PRE-DISSEMINATION PEER REVIEW UNDER APPLICABLE INFORMATION QUALITY GUIDELINES. IT HAS NOT BEEN FORMALLY DISSEMINATED BY BSEE. IT DOES NOT REPRESENT AND SHOULD NOT BE CONSTRUED TO REPRESENT ANY BSEE DETERMINATION OR POLICY."

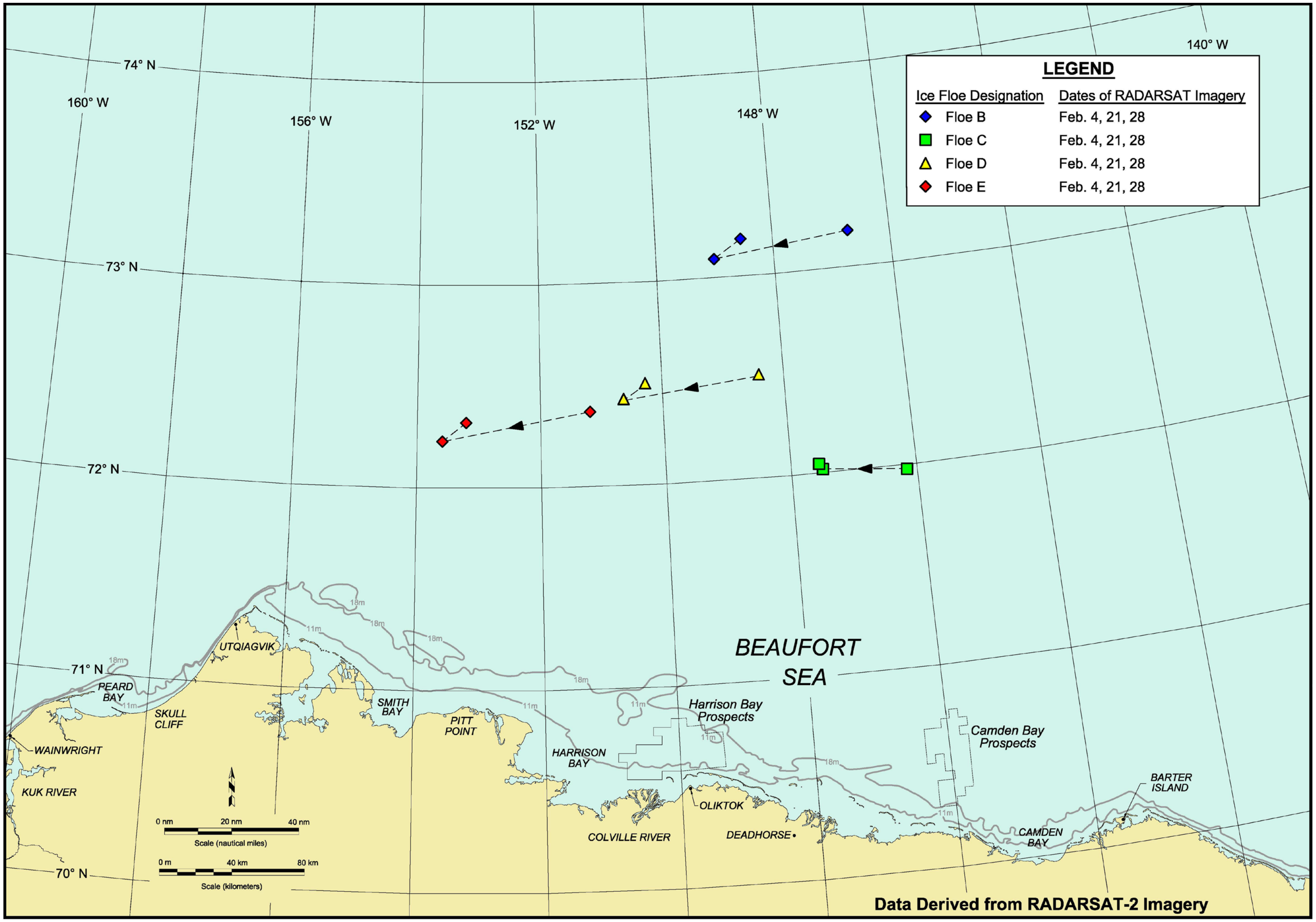

Figure 5-30. Beaufort Sea Multi-Year Ice Floe Displacements in February 2020

The along-track speeds that occurred between February 4th and 21st, although higher than those between the 21st and 28th, were relatively low. The maximum speed, 2.6 nm/day (4.8 km/day; Floe E), occurred during the former while the minimum, 0.3 nm/day (0.6 km/day; Floe C), occurred during the latter.

As in January, IAPB Buoys Y and Z remained in the Beaufort Sea study area throughout February (Figure 5-31). Both described similar trajectories consisting of a small counterclockwise loop between the 1st and 11th, a linear leg to the west between the 11th and 22nd, and a zigzag leg to the east-northeast between the 22nd and 29th. The net westerly displacements and average speeds for the month were small: 16 nm (30 km), which is equivalent to 0.6 nm/day (1.1 km/day), for Buoy Y, and 15 nm (28 km), which is equivalent to 0.5 nm/day (0.9 km/day), for Buoy Z.

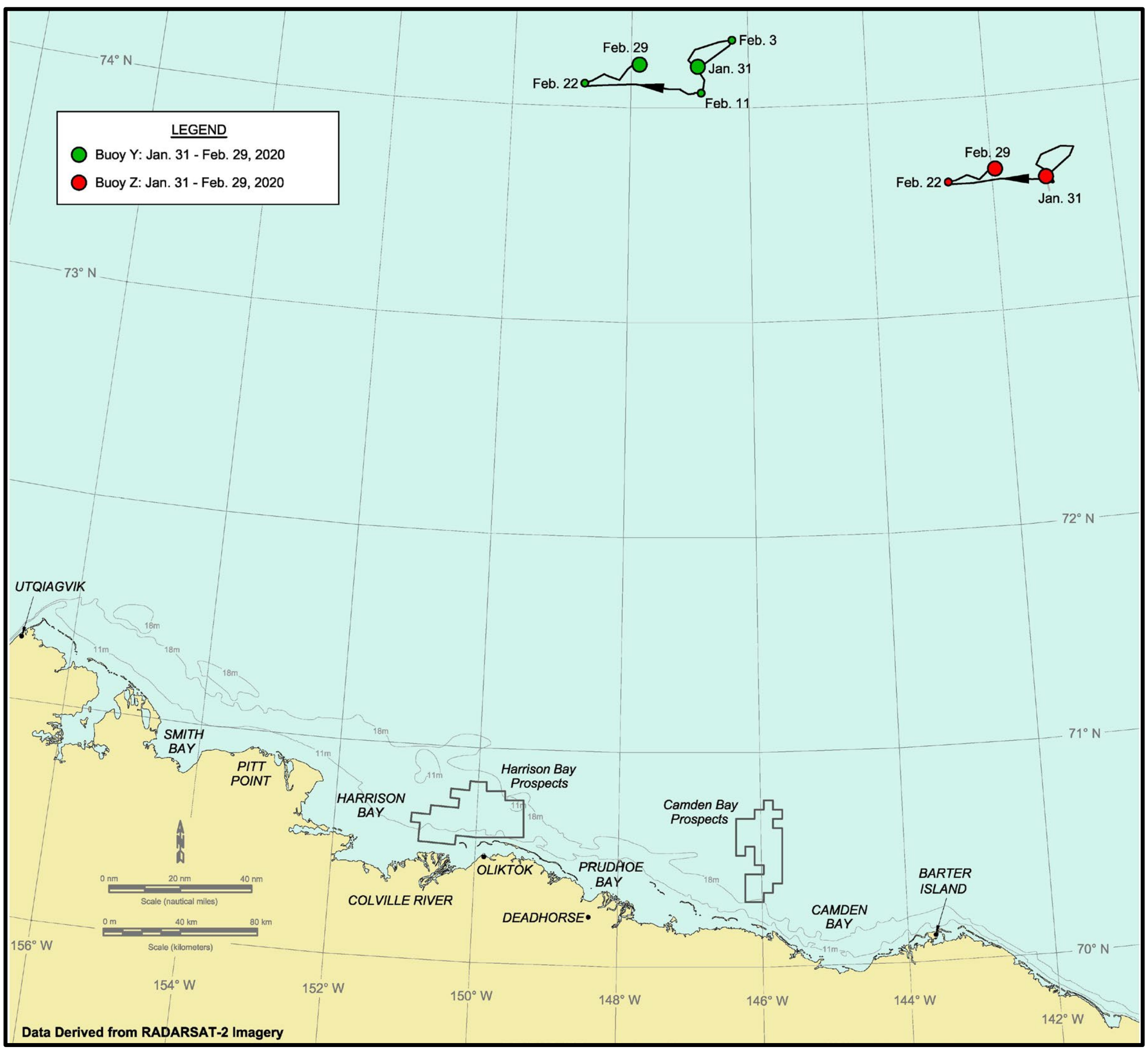

Figure 5-31. Beaufort Sea Drift Buoy Tracks in February 2020

The daily average speeds of the two buoys are plotted in Figure 5-32. The peak values, 9.5 nm/day (17.6 km/day) for Buoy Y and 9.2 nm/day (17.0 km/day) for Buoy Z, both occurred on February 19th. The average daily wind speed at Deadhorse Airport was only 7 kt (4 m/s) on this date, suggesting that the relatively high speeds resulted either from the release of stress in the pack ice occasioned by a change in wind direction, or from wind conditions that were distinctly different than those at Deadhorse.

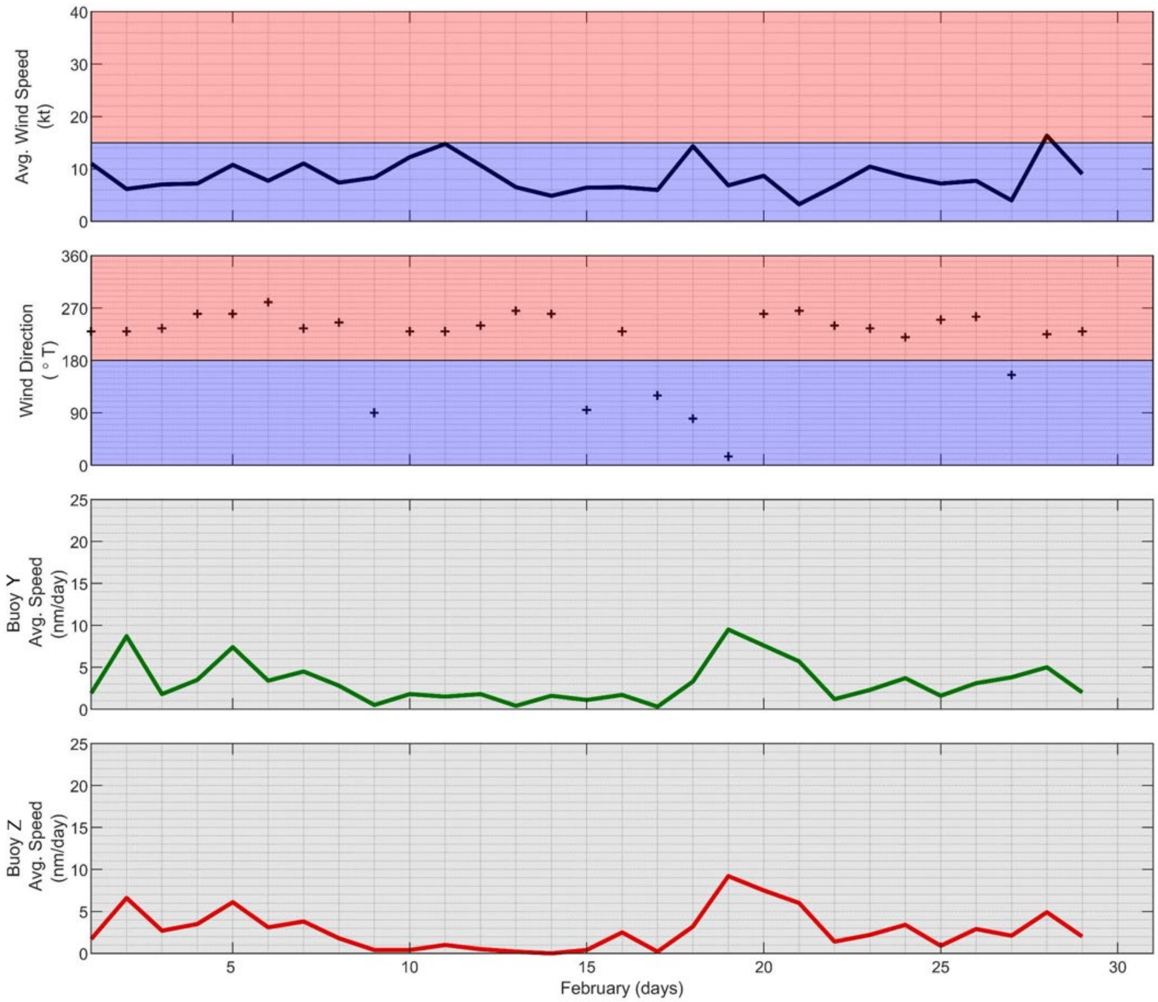

Figure 5-32. Beaufort Sea Drift Buoy Daily Average Speeds in February 2020

5.5 Reconnaissance Flights

As discussed in Section 4.5, aerial reconnaissance missions were undertaken on February 22nd and 23rd to document the ice conditions that prevailed in the Alaskan Beaufort Sea at the end of the freeze-up study period. Beaufort Sea Flight No. 1 (Flight "B1" on Drawing CFC-1070-01-001) was conducted in the Central Beaufort when overcast skies and light southwesterly winds prevailed. Beaufort Sea Flight No. 2 (Flight "B2" on

Drawing CFC-1070-01-002) took place in the Western Beaufort under similar wind conditions, but clear skies. As shown in Figure 5-26, the flights were preceded by an extended period of unseasonably cold temperatures, a predominance of mild to moderate southwesterly winds, and a complete absence of storms. The only wind event of note was a series of changes in direction that began with southwesterlies on February 16th, progressed through southeasterlies, easterlies and north-northeasterlies on the three days that followed, and ended with westerlies on the 20th. RADARSAT-2 images that bracket the flights are provided in Figure 5-28 and Figure 5-29.

5.5.1 Lagoon Ice

The ice in the semi-protected lagoons behind the barrier islands was primarily flat and featureless (Plate 5-1 and Plate 5-2). The most significant relief consisted of widely scattered ridges and rubble with heights to 1 m, and thermal cracks. As discussed in the 2010-11 Freeze-Up Study report (Coastal Frontiers and Vaudrey, 2011), thermal cracks tend to form when a rapid drop in air temperature is followed by a rapid rise. The drop causes contraction and cracking of the ice sheet, while the ensuing rise causes compression and extrusion of the refreezing slush in the crack, creating a ridge.

Twenty-two thermal cracks were observed during the reconnaissance flights, representing the largest quantity noted during any of the nine freeze-up studies conducted since 2009-10. As illustrated in Drawings CFC-1070-01-001 and -002, half of the cracks were located in Stefansson Sound while the other half were located in the region between Prudhoe and Harrison Bays. The heights of the associated ridges ranged from 0.5 to 2 m, with the latter exceeding any of the values recorded during the prior eight freeze-up studies.

The large number of cracks and exceptional ridge height of 2 m may have resulted from the extremely cold air temperatures that began in late December and continued through February. Prior to that time, the ice was too warm and therefore too flexible to be susceptible to the formation of significant cracks. Based on a review of the temperature data at Deadhorse Airport, the cracks probably formed on one or more of the following three occasions:

- December 27th-30th: Air temperature fell 22°F (12°C) before rising 30°F (17°C);
- January 4th-8th: Air temperature fell 28°F (16°C) before rising 22°F (12°C);
- February 6th-9th: Air temperature fell 20°F (11°C) before rising 28°F (16°C).

The primary importance of thermal cracks from the standpoint of offshore development is their potential to disrupt on-ice activities such as transportation and construction. This circumstance arose in 1982, when thermal cracks in Stefansson Sound interrupted ice road operations during the construction of Tern Island (Vaudrey, 1982b).

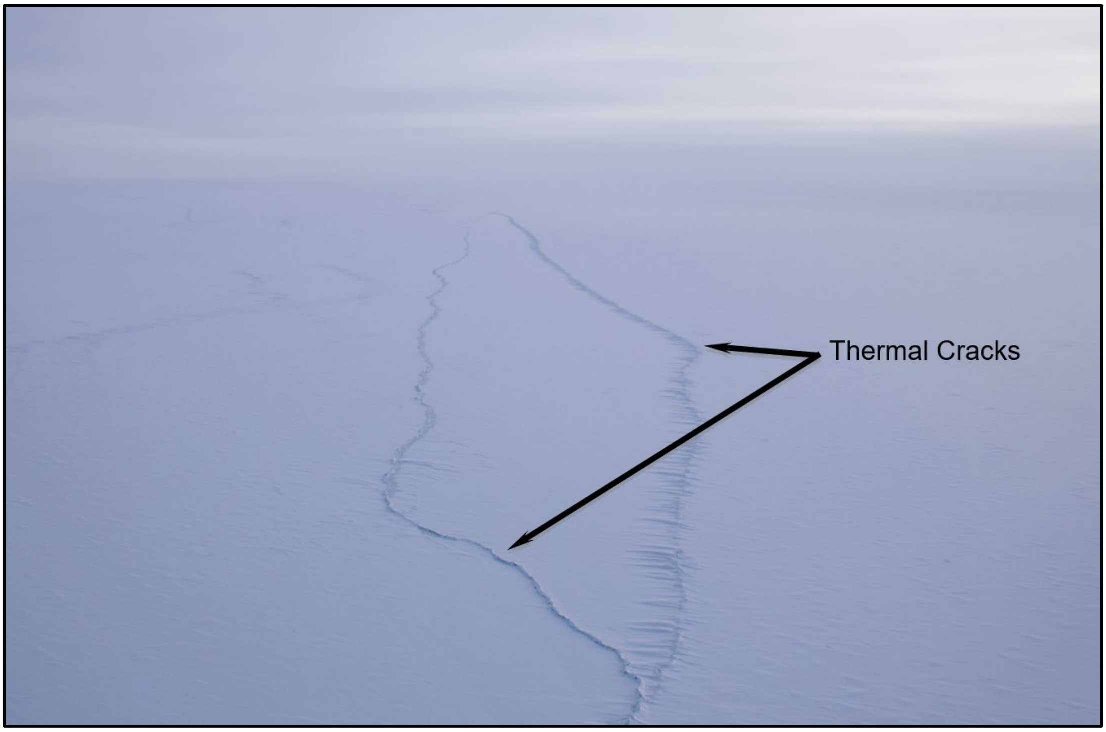

Plate 5-1. Flat First-Year Ice and Two Thermal Cracks near Prospective Liberty Pipeline Route in Stefansson Sound (looking southeast on February 22, 2020)

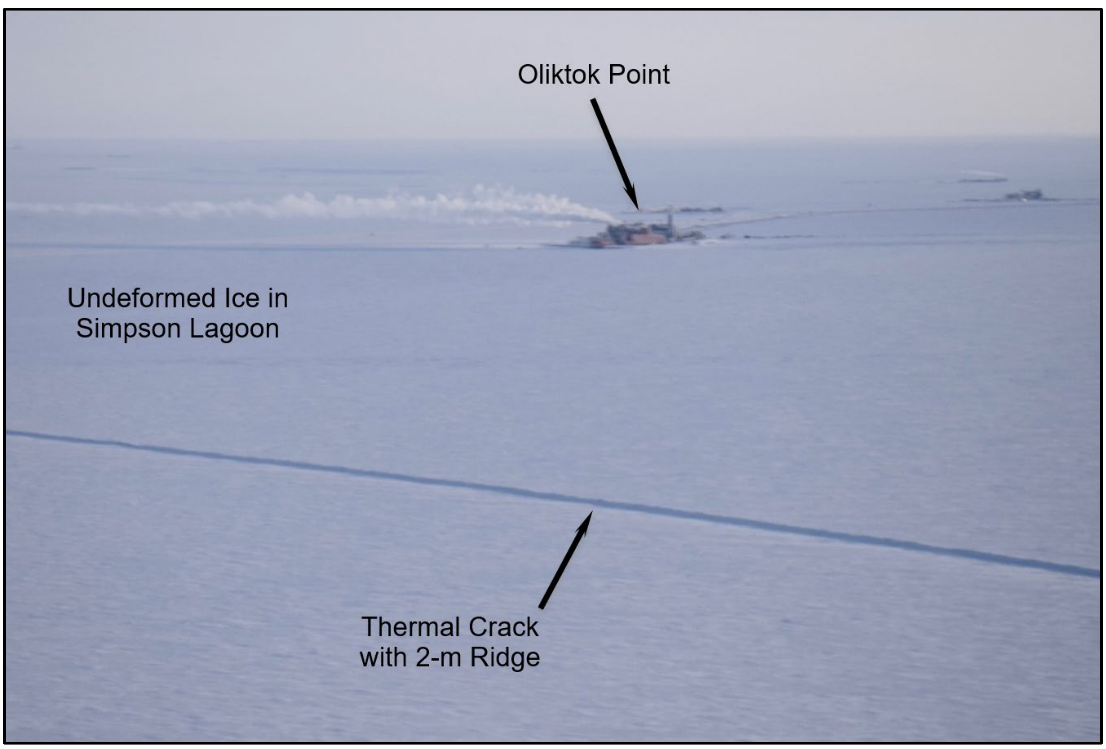

Plate 5-2. Flat First-Year Ice and Thermal Crack with 2-m Ridge off Oliktok Point (looking southeast on February 23, 2020)

5.5.2 Landfast Ice and Shear Zone

In keeping with the predominance of westerly winds and paucity of easterly storms that characterized the 2019-20 freeze-up season, the landfast ice zone was found to be narrow and poorly-developed at the time of the flights. Deformation in the shear zone (where the pack ice grinds against the seaward edge of the landfast ice) was small by historical standards, with ridge and rubble heights typically ranging from 1 to 2 m and peaking at 4 m to the east of Prudhoe Bay. To the west of Prudhoe Bay, the heights tended to range from 2 to 3 m with maximum values of 8 m between Admiralty Bay and Point Barrow, and 7 m north of Long Island and also on Weller Bank (Plate 5-3). As illustrated in Plate 5-4, shear lines in the landfast ice zone were poorly defined, with low ridge heights and meandering orientations.

Despite localized deviations, the landfast ice edge observed during the flights bore a close resemblance to that derived from the post-flight RADARSAT-2 image acquired on February 28th (Figure 5-27). This finding indicates that the ice edge to the east of Weller Bank retreated between February 21st, when the pre-flight image was obtained, and the 22nd, when the first flight took place, in apparent response to the westerly winds that began on the 20th (Figure 5-26). Although the ice remained grounded on Weller Bank (Plate 5-3) during the wind shift, an open lead 6 nm (11 km) to the southwest of Stamukhi Shoal (Plate 5-5) provided clear evidence that it had broken loose from this customary anchor point (Plate 5-6).

5.5.3 Offshore Ice

Outside the landfast ice zone, flat first-year floes with diameters ranging from several hundred meters to several kilometers predominated. The diameters tended to be larger in the Central Beaufort, and to decrease in the general vicinity of Point Barrow. Deformation of the first-year ice was modest, with ridge and rubble heights typically ranging from 1 to 3 m. Relatively small multi-year ice floes with diameters to 200 m were observed at scattered locations.

5.5.4 Leads

Numerous leads, most of which were in various stages of refreezing, were observed outside the landfast ice zone. They tended to be narrow, with widths less than 500 m, and oriented parallel to the coast (Plate 5-7). The largest, with a width that typically ranged from 1 to 3 km, was a flaw lead marking the landfast ice edge between Pitt Point and Point Barrow (Figure 5-29; Plate 5-4). The leads were caused by the westerly winds that began on February 20th (Figure 5-26).

Plate 5-3. Grounded Rubble with Heights to 7 m on East Side of Weller Bank (looking east on February 23, 2020)

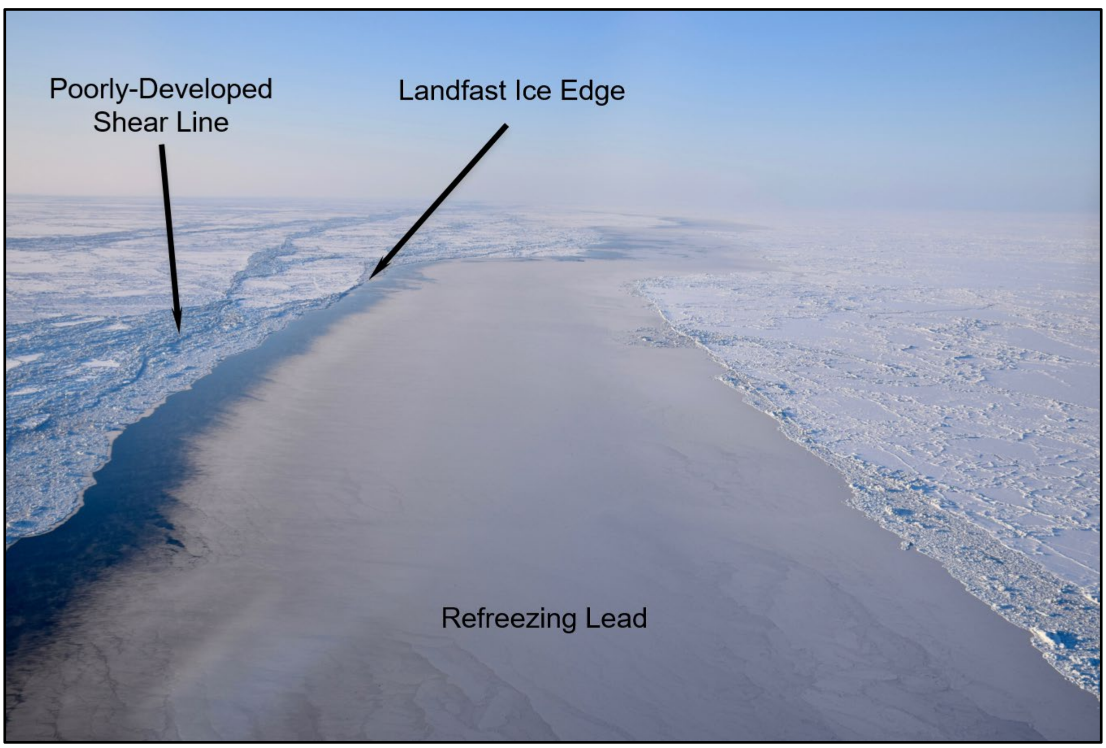

Plate 5-4. Landfast Ice Edge with Poorly-Developed Shear Line 16 nm Northeast of Admiralty Bay (looking northwest on February 23, 2020)

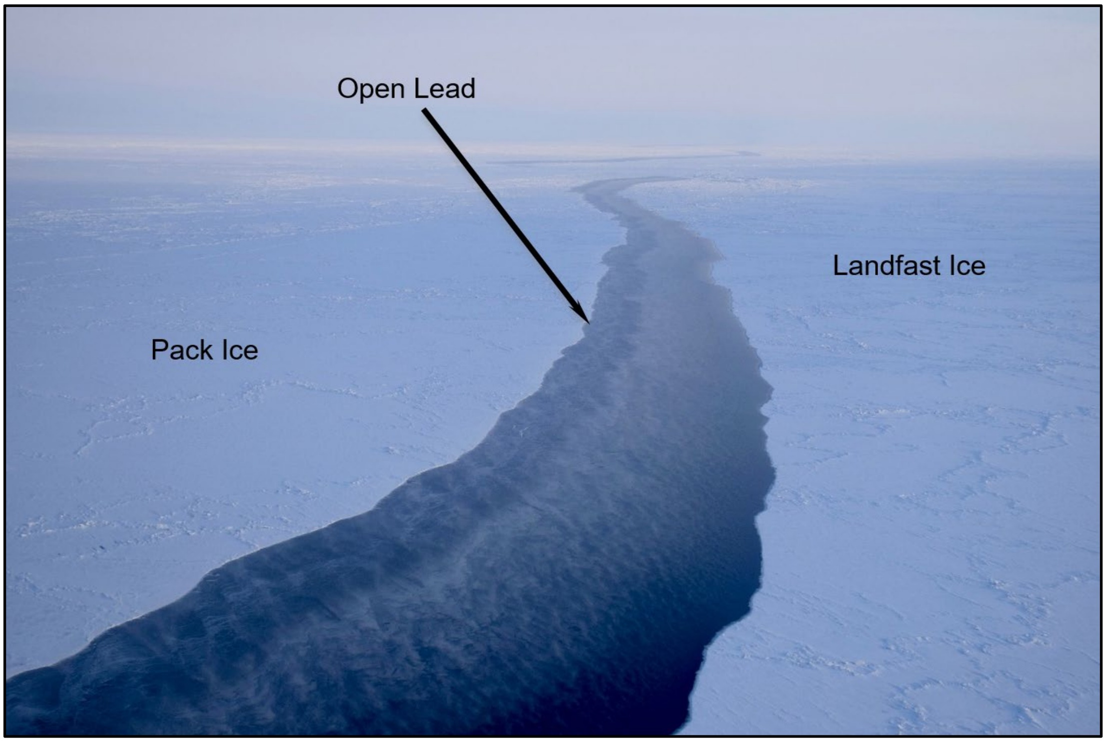

Plate 5-5. Landfast Ice Edge Defined by Open Lead 6 nm Southwest of Stamukhi Shoal (looking east on February 23, 2020)

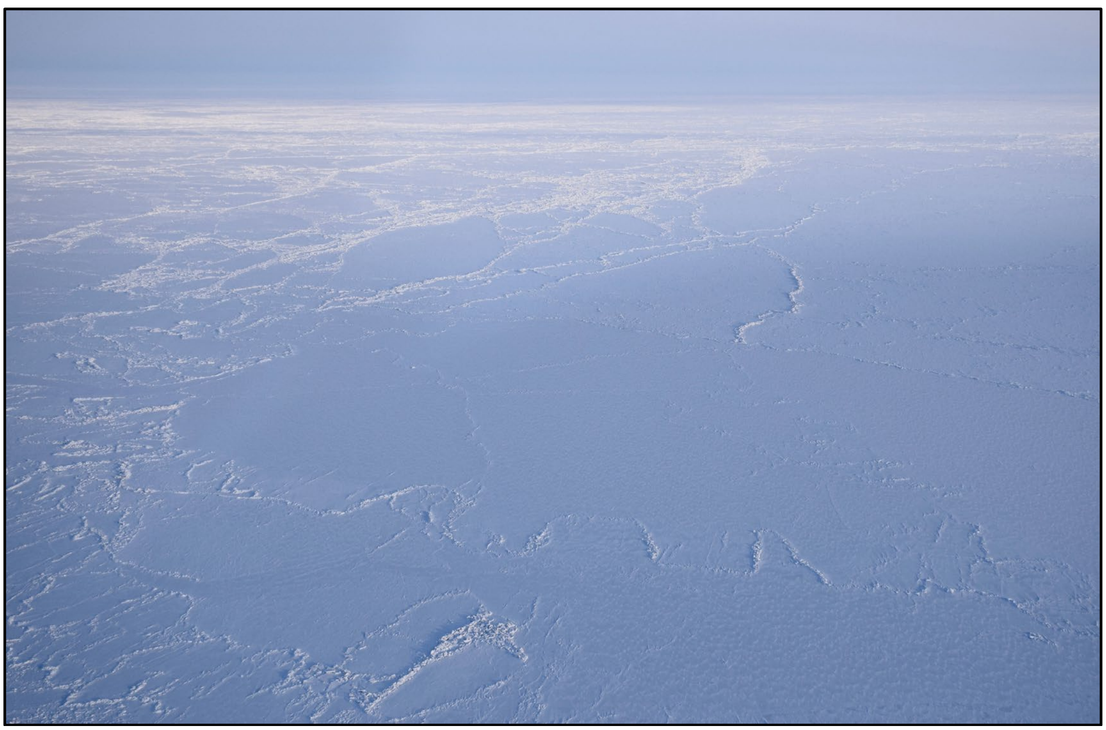

Plate 5-6. Absence of Grounded Rubble on Stamukhi Shoal (looking east on February 23, 2020)

Plate 5-7. Small, Recently-Formed Lead in Pack Ice 16 nm North of Pingok Island (looking east on February 23, 2020)

5.5.5 Ice Pile-Ups

Thirty-two ice pile-ups were discovered in the central portion of the Alaskan Beaufort Sea during the two reconnaissance flights. As discussed in Section 5.1, nine of these are believed to have formed between October 25th and 30th while the remaining 23 are believed to have formed between November 23rd and December 9th. In both cases, the ice canopy was subjected to strong winds that changed direction, resulting in a loss of confinement. The characteristics of these features are presented in Table 5–5, with representative examples provided in Plates 5-8 and 5-9.

5.5.6 Multi-Year Ice

The ability of the field crew to identify multi-year ice was hampered by recent snowfall, which tended to obscure its characteristic gray, leathery surface. Notwithstanding this impediment, fragments and small floes were observed intermittently in the region between Camden and Harrison Bays. The highest concentrations, which peaked at 90% in localized areas, were found in the southern portion of Camden Bay (Plate 5-10), while the largest floes, with horizontal dimensions to 300 m, were found outside the barrier islands to the northwest of Prudhoe Bay (Plate 5-11). Although much larger multi-floes are evident in the RADARSAT-2 images obtained on February 21st and 28th (Figures 5-28 and 5-29, respectively), they were located well north of the flight paths.

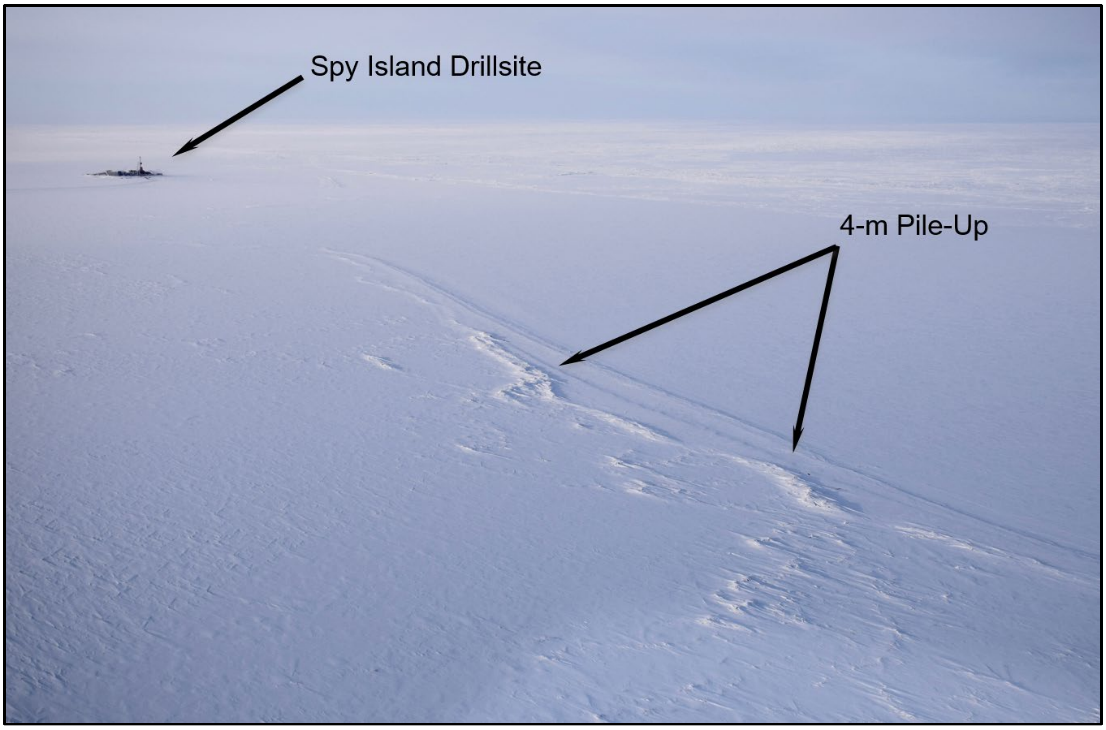

Plate 5-8. 4-m Pile-up that Encroached 5 m onto Spy Island from Southwest (looking northwest on February 23, 2020)

Plate 5-9. 4-m Pile-Up with 10-m Encroachment and 5-m Pile-Up with No Encroachment on Northstar Production Is. (looking east on February 23, 2020)

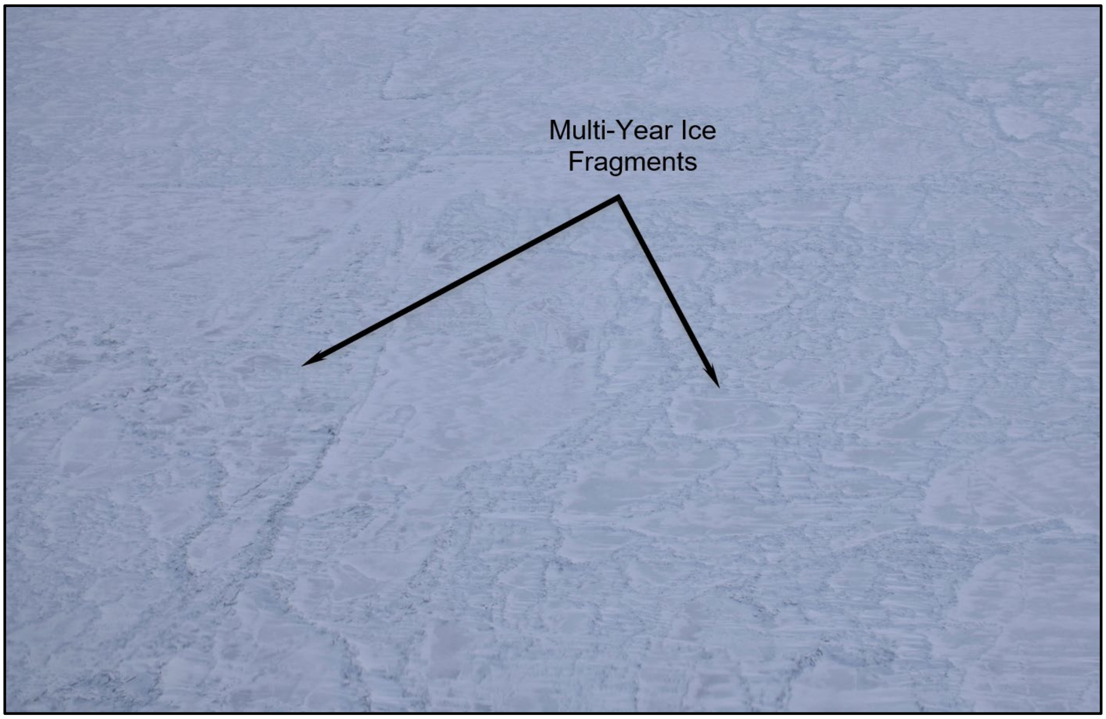

Plate 5-10. 80% Concentration of Multi-Year Ice Fragments in South Camden Bay (looking east on February 22, 2020)

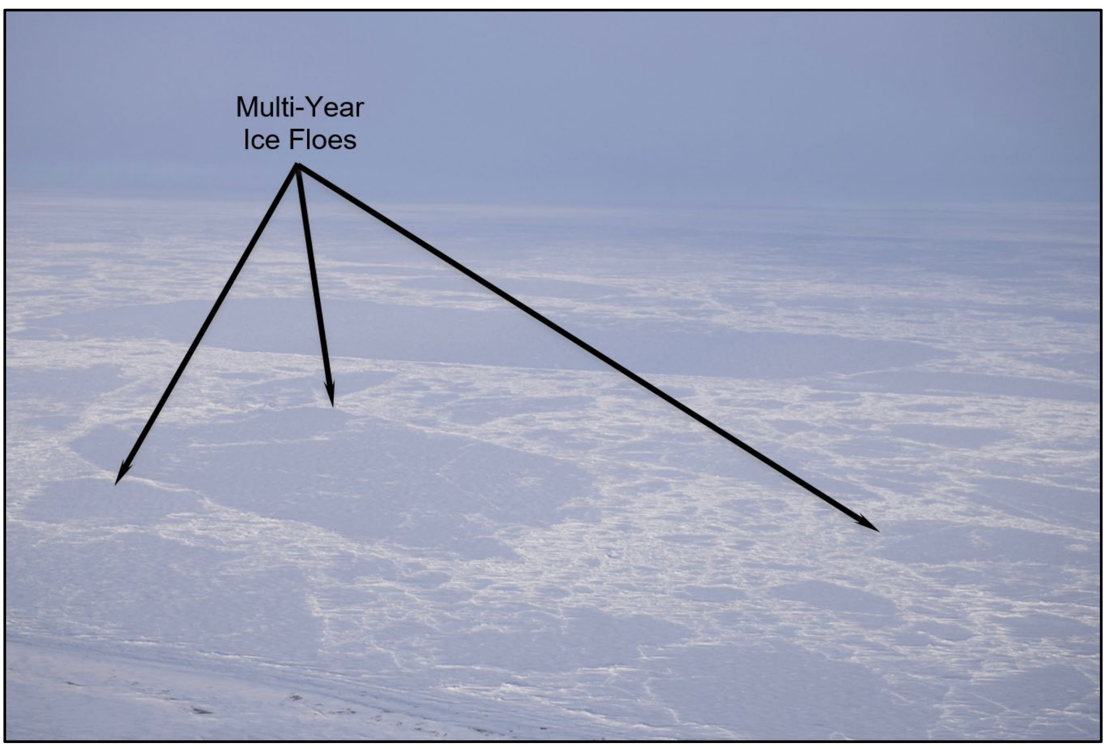

Plate 5-11. Multi-Year Ice Floes with Diameters to 300 m 10 nm Northwest of Prudhoe Bay (looking northwest on February 23, 2020)

5.5.7 Ice Conditions in Camden Bay Prospects

The ice conditions in the Camden Bay Prospects were found to be relatively uniform, with patches of undeformed first-year ice interspersed with occasional ridges and rubble. Within the landfast ice zone, which occupied the southernmost 3 to 5 nm (6 to 9 km) of the Prospects, the ridges and rubble heights typically were limited to 1 m. Farther offshore, in the pack ice, heights of 1 to 2 m predominated (Plate 5-12). The pack ice also contained numerous small, refreezing leads. Although multi-year ice was not observed in the Prospects, grounded fragments with diameters to 10 m were detected to the south in Mary Sachs entrance.

The landfast ice edge, which was located approximately 10 nm (19 km) north of Mary Sachs Entrance, was marked by an inconspicuous 2-m ridge (Plate 5-13). The ridge was found to coincide with location of the ice edge derived from the February 28th RADARSAT-2 image (Figure 5-27).

5.5.8 Ice Conditions in Harrison Bay Prospects

As in the case of the Camden Bay Prospects, the ice canopy in the Harrison Bay Prospects consisted of areas of undeformed first-year ice interspersed with ridges and rubble (Plate 5-6 and Plate 5-14). The ridges and rubble were more extensive, however, and attained heights to 3 m. Multi-year ice was observed at one location in the northeast portion of the Prospects, where the concentration was less than 10% and the maximum floe diameter was estimated at 200 m.

The only lead noted in the Prospects, located 6 nm (11 km) south of Stamukhi Shoal and oriented in a northwesterly-southeasterly direction, marked the edge of the landfast ice zone (Section 5.5.2; Plate 5-5). The landfast ice on the southwest side of the lead occupied approximately 60% of the Prospects, while the pack ice on the northeast side, including that in the vicinity of Stamukhi Shoal (Plate 5-6), occupied the remaining 40%.

5.5.9 Ice Conditions in Liberty Prospect

With the exception of several thermal cracks in the general vicinity (Plate 5-1), the ice at the site of the prospective Liberty Drilling and Production Island and on the pipeline route to shore was found to be flat and featureless.

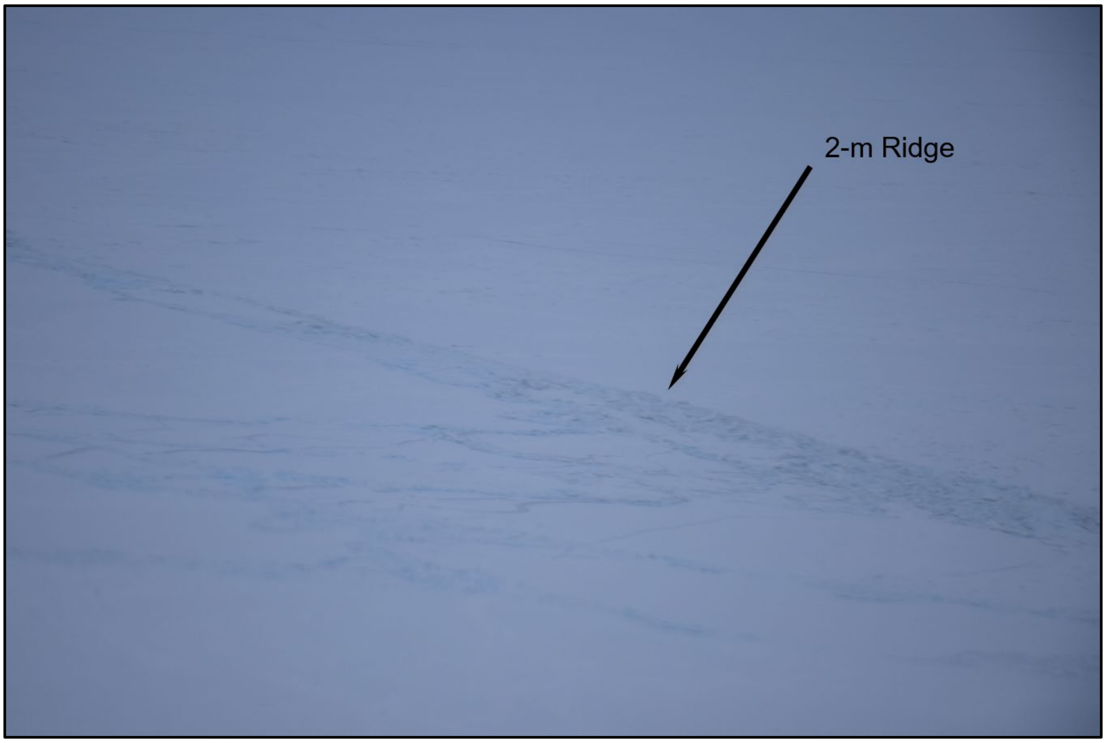

Plate 5-12. Undeformed First-Year ice with 2-m Ridge in Camden Bay Prospects 23 nm North of Mary Sachs Entrance (looking north on February 22, 2020)

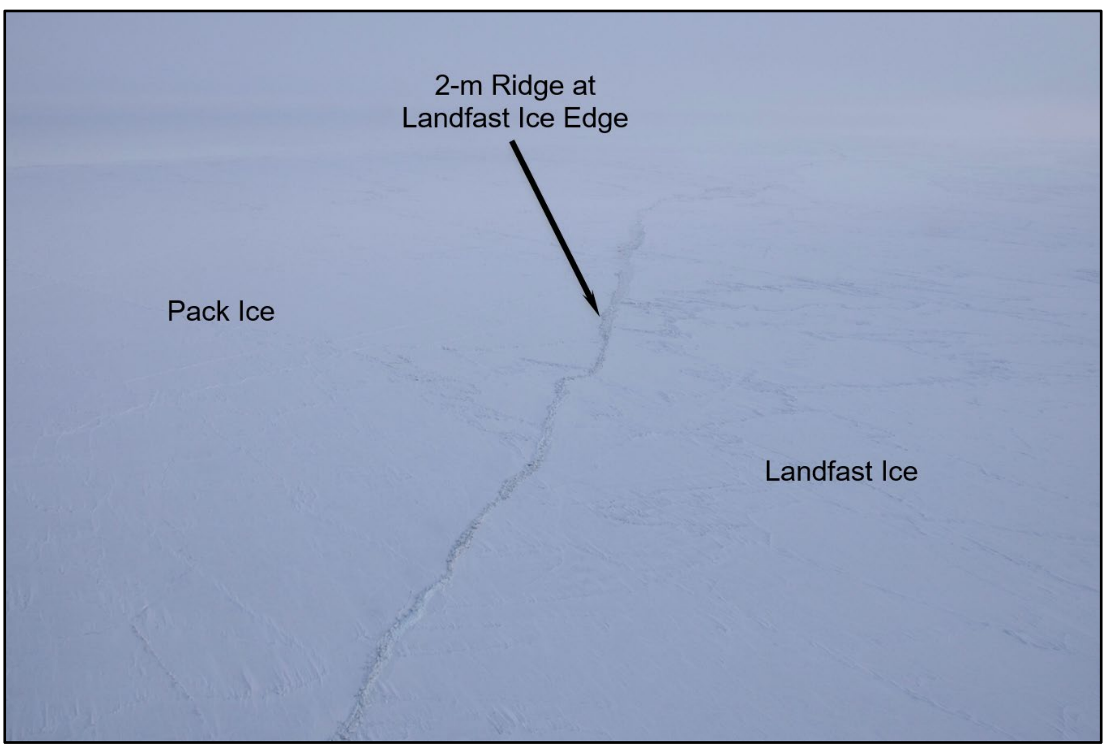

Plate 5-13. 2-m Ridge at Landfast Ice Edge in Camden Bay Prospects (looking east on February 23, 2020)

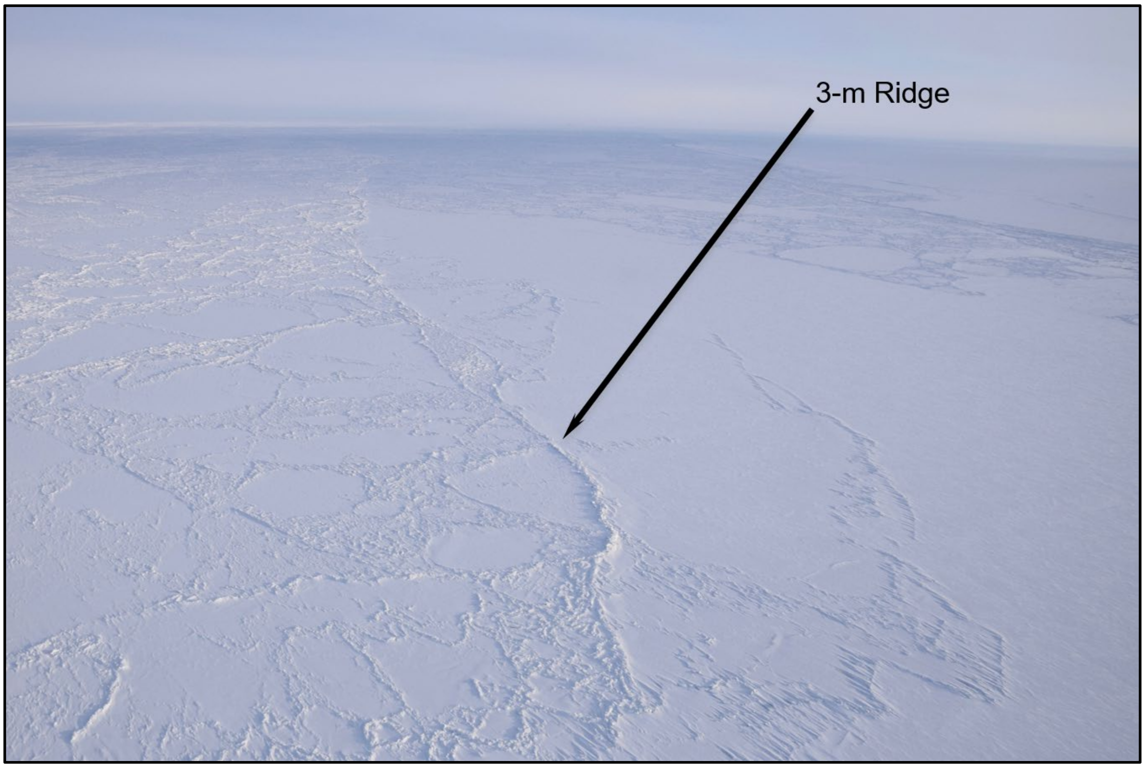

Plate 5-14. Undeformed First-Year Ice Flanked by 3-m Ridge and 2-m Rubble in Southeastern Portion of Harrison Bay Prospects (looking east on February 23, 2020)

6. CHUKCHI SEA FREEZE-UP

Section 6.1 presents a concise overview of the 2019-20 freeze-up season in the northeast Chukchi Sea. As in the case of Section 5.1, emphasis is placed on summary tables. A detailed analysis of the conditions that prevailed from October 2019 through February 2020 follows in Sections 6.2 through 6.4.

6.1 Overview

Air Temperatures: The air temperatures recorded at Utqiagvik Airport followed a pattern similar to that at Deadhorse (Section 5.1), with a warm phase during the early portion of the freeze-up study period and a cold phase at the end. The primary difference was the occurrence of a transition phase in which the values tended to remain close to the normal range. The characteristics of each phase are summarized below:

- *Warm Phase (October 1st - December 17th)*: The daily average air temperatures exceeded the normal range on 75 of the 78 days while never falling below;
- *Transition Phase (December 18th - January 23rd)*: The daily average air temperatures exceeded the normal range on ten of the 37 days and fell below on seven;
- *Cold Phase (January 24th - February 29th)*: The daily average air temperatures exceeded the normal range on one of the 37 days and fell below on 29.

During the cold phase, the daily average temperature was less than or equal to -30°F (-34°C) on 16 occasions. The minimum value, -39°F (-39°C), occurred on February 27th. Over the entire study period (October through February), the temperatures exceeded the normal range on 86 days (57% frequency) and dropped below the normal range on 36 days (24% frequency).

Winds: The wind conditions during the 2019-20 freeze-up season are summarized in Table 6-1, which is based on the daily average speeds and directions recorded at Utqiagvik Airport. Easterlies outnumbered westerlies in November, December, and January, while westerlies prevailed in October and February. Over the entire five-month study period, easterlies occurred 55% of the time versus 45% for westerlies. This distribution differed markedly from that at Deadhorse, where westerlies occurred with a frequency of 64%. The monthly average speeds at Utqiagvik declined over the course of the five-month study period, with values of 13 kt (7 m/s) in both October and November, 11 kt (6 m/s) in December, 9 kt (5 m/s) in January, and 7 kt (4 m/s) in February.

Table 6-1. Chukchi Sea Wind Characteristics, October 2019–February 2020

Month	Easterly Wind Predominance (days)	Westerly Wind Predominance (days)	Average Speed (kt)
October	14	17	13
November	18	12	13
December	24	7	11
January	17	14	9
February	11	18	7
Total Days	**84**	**68**	n/a
Frequency (%)	**55**	**45**	n/a

Note: Table 6-1 is based on the daily average values recorded at Utqiagvik Airport.

Storms: The characteristics of all storm events with daily average sustained wind speeds that exceeded 15 kt (8 m/s) at Utqiagvik Airport are presented in Table 6-2. Of the 13 storms that occurred during the study period, nine were easterlies and four were westerlies. The storm population was mild in terms of both intensity and duration. The maximum wind speed of 24 kt (12 m/s) occurred during a westerly event at the end of October, while the maximum duration of 4 days was associated with an easterly storm in early December.

Ice Cover: Ice began to form in Kasegaluk Lagoon, the Kuk River Inlet, and Peard Bay in mid-October, but freeze-up proceeded slowly in the weeks that followed due to a combination of warm air temperatures, exceptionally warm sea surface temperatures, and a series of storms that occurred in rapid succession (Table 6-2). Complete coverage of these three semi-enclosed basins did not take place until the last week in November.

Although ice appeared in the exposed waters adjacent to the coast during the first week in November, it failed to coalesce into a near-continuous strip spanning the entire length of the study area until the end of the month. Farther offshore, first-year pack ice began to stream west past Point Barrow during the second week of November but stalled in response to periods of westerly winds. As a result, most of the Chukchi Sea remained ice-free at month-end.

Air temperatures remained below the freezing point of seawater (29°F; -2°C) after November 10th. However, a strong predominance of easterly (offshore) winds in December that included three easterly storms delayed the attainment of complete ice cover adjacent to the coast until December 26th. On that date, one day after the winds had shifted from easterly to westerly, nearshore freeze-up and complete freeze-up of the Chukchi Sea basin occurred simultaneously.

Table 6-2. Chukchi Sea Storm Characteristics, October 2019–February 2020[1]

Month[2]	Day	Duration (days)	Maximum Easterly Wind Speed[3] (kt)	Maximum Westerly Wind Speed[3] (kt)
October	11	1	-	19
October	16-18	3	19	-
October	27-28	2	20	-
October	29-31	3	-	24
November	8	1	17	-
November	21-22	2	17	-
November	26	1	22	-
November	28-29	2	-	20
December	1	1	21	-
December	7-10	4	21	-
December	17	1	20	-
January	11	1	17	-
January	14	1	-	23
Total Duration	n/a	**23**	n/a	n/a
Total Number of Events	n/a	n/a	**9**	**4**

Notes:

1 Table 6-2 includes all storm events with a daily average sustained wind speed exceeding 15 kt (8 m/s) at Utqiagvik Airport.

2 No storms occurred in February 2020.

3 "Maximum Wind Speed" refers to highest daily average sustained wind speed that occurred during each storm event.

Ice Thickness: The thickness of undeformed first-year ice at the end of each month was estimated using the relationship of Lebedev (Bilello, 1960) in concert with the accumulated FDD at Utqiagvik Airport shown in Table 4-1. The method of calculation is identical to that presented for the Beaufort Sea in Section 5.1. The results are provided in Table 6-3, which indicates that undisturbed first-year ice attained a maximum thickness of 148 cm on May 21st.

Landfast Ice: The development of landfast ice along the Chukchi Sea coast was delayed by the same factors that retarded the occurrence of freeze-up: warm air temperatures,

Table 6-3. Chukchi Sea Computed Ice Thickness, October 2019 – May 2020[1]

Date	Accumulated FDD	Ice Thickness[2] (cm)
30 September 2019	0	0
31 October 2019	48	9
30 November 2019	406	31
31 December 2019	1,318	61
31 January 2020	2,621	90
29 February 2020	4,224	119
31 March 2020	5,284	136
30 April 2020	5,907	145
21 May 2020	6,122	148

Notes:
[1] Table 6-3 is based on the daily average air temperature data recorded at Utqiagvik Airport.
[2] Ice thickness is computed from accumulated FDD using method of Lebedev (Bilello, 1960).

warm sea surface temperatures, and a series of easterly storms. The predominance of easterly winds that began in November also played a role. The first traces of landfast ice appeared in Kasegaluk Lagoon, the Kuk River Inlet, and Peard Bay in mid-November, with complete coverage of each basin following two weeks later at month-end.

Although several small patches of landfast ice formed in the exposed waters adjacent to the coast during the first half of December, a continuous strip encompassing the entire length of the study area between Point Barrow and Point Lay did not develop until the occurrence of westerly winds at month-end. The maximum width, 18 nm (33 km), was located off Skull Cliff.

Most of the newly-formed landfast ice was lost during the first half of January, a period in which winds with a significant offshore component prevailed. A partial rebound occurred during the second half of the month, when westerly winds resulted in the re-establishment of a continuous strip. The maximum width, 9 nm (17 km), was realized at two locations: off Skull Cliff and off the northern end of Kasegaluk Lagoon.

The predominance of westerly winds that began during the second half of January persisted throughout February, causing additional expansion of the landfast ice zone. The ice reached Blossom Shoals, its customary anchor point off Icy Cape, by mid-month. Modest growth thereafter produced a width that ranged from less than 1 nm (2 km) off South Kasegaluk Lagoon and Point Belcher to 21 nm (39 km) off North Kasegaluk Lagoon.

Ice Pile-Ups: Fifty-seven ice pile-ups occurred on the shoreline between Utqiagvik and Point Lay during the 2019-20 freeze-up season (Table 6-4). Thirty-seven were located on the seaward side of the barrier islands fronting Kasegaluk Lagoon while one was located on the landward side. The remaining 19 were located between North Kasegaluk Lagoon and Utqiagvik. The dimensions were large by historical standards, with heights ranging from 1 to 20 m, encroachment distances from negligible to 30 m, and alongshore lengths from 50 m to 8 km. The tallest pile-up (20 m) was located on Icy Cape; the largest encroachment (30 m) occurred 14 nm (26 km) southwest of Utqiagvik. The block thicknesses were estimated to vary from 30 to 60 cm.

The sole pile-up in South Kasegaluk Lagoon probably resulted from an easterly storm on November 26th followed closely by a westerly storm on the 28th and 29th (Table 6-2). After attaining a maximum one-hour sustained speed of 30 kt (15 m/s) during the first storm, the winds backed from east through south to west and freshened to an identical speed of 30 kt (15 m/s) during the second storm. The calculated thickness of first-year ice was 30 cm at this time, suggesting that the ice remained susceptible to displacement despite the confinement afforded by the lagoon. Outside the barrier islands, insufficient ice was present in the nearshore region to produce pile-ups of consequence.

In the absence of strong westerly winds capable of driving the ice ashore in December, the remaining 56 pile-ups are believed to have been caused by a storm sequence in mid-January similar to that in late November. In this case, an easterly storm with a maximum one-hour sustained wind speed of 20 kt (10 m/s) on the 11th preceded a westerly storm with a maximum one-hour speed of 29 kt (15 m/s) on the 14th (Table 6-2).

Coastal Flaw Lead: From December 2019 through February 2020, the flaw lead that forms off the Chukchi Sea coast in response to offshore winds opened on seven separate occasions. The frequency of occurrence, which averaged 54% for the entire three-month period, was only 23% in December due to the paucity of landfast ice (a prerequisite for the formation of a flaw lead) during the first two thirds of the month. The frequency increased to 65% in January and 76% in February, as illustrated in Figure 6-1. The maximum width, 75 nm (139 km) occurred in January, while the maximum length, 250 nm (463 km), occurred in both January and February. The lead persisted for periods that ranged from one to 20 days.

Table 6-4. Ice Pile-Ups on Chukchi Sea Coast during 2019-20 Freeze-Up Season

No.	Location	Formation Date	Arrived From	Length[1] (m)	Height[2] (m)	Encroachment[3] (m)
1	South of Icy Cape	Jan 11 - 14	W	1,950	10	8
2	South of Icy Cape	Jan 11 - 14	W	1,650	5	5
3	South of Icy Cape	Jan 11 - 14	W	1,450	7	7
4	South of Icy Cape	Jan 11 - 14	W	200	4	3
5	South of Icy Cape	Jan 11 - 14	W	50	3	5
6	South of Icy Cape	Jan 11 - 14	W	200	4	6
7	South of Icy Cape	Jan 11 - 14	W	1,950	10	10
8	South of Icy Cape	Jan 11 - 14	W	100	2	3
9	South of Icy Cape	Jan 11 - 14	W	450	3	5
10	South of Icy Cape	Jan 11 - 14	W	1,850	3	3
11	South of Icy Cape	Jan 11 - 14	W	2,100	4	5
12	South of Icy Cape	Jan 11 - 14	W	1,000	3	8
13	South of Icy Cape	Jan 11 - 14	W	1,050	2	4
14	South of Icy Cape	Jan 11 - 14	W	100	2	8
15	South of Icy Cape	Jan 11 - 14	W	1,000	2	8
16	South of Icy Cape	Jan 11 - 14	W	1,450	1	4
17	South of Icy Cape	Jan 11 - 14	W	1,050	2	5
18	South of Icy Cape	Jan 11 - 14	W	1,900	1	4
19	South of Icy Cape	Jan 11 - 14	W	500	1	3
20	South of Icy Cape	Jan 11 - 14	W	350	5	7
21	South of Icy Cape	Jan 11 - 14	W	600	2	10
22	South of Icy Cape	Jan 11 - 14	W	500	3	0
23	South of Icy Cape	Jan 11 - 14	W	1,300	5	10
24	South of Icy Cape	Jan 11 - 14	W	3,200	20	20
25	South Kasegaluk Lag.	Nov 26 - 29	S	150	2	8
26	East of Icy Cape	Jan 11 - 14	N	500	5	20
27	East of Icy Cape	Jan 11 - 14	N	3,650	1	3
28	East of Icy Cape	Jan 11 - 14	N	2,000	3	3
29	East of Icy Cape	Jan 11 - 14	N	500	2	3

(continued)

Table 6-4. Ice Pile-Ups on Chukchi Sea Coast during 2019-20 Freeze-Up Season (continued)

No.	Location	Formation Date	Arrived From	Length[1] (m)	Height[2] (m)	Encroachment[3] (m)
30	East of Icy Cape	Jan 11 - 14	N	150	3	5
31	East of Icy Cape	Jan 11 - 14	N	1250	2	5
32	East of Icy Cape	Jan 11 - 14	NW	100	4	6
33	East of Icy Cape	Jan 11 - 14	NW	5,100	8	10
34	East of Icy Cape	Jan 11 - 14	NW	100	2	5
35	East of Icy Cape	Jan 11 - 14	NW	7,950	8	10
36	East of Icy Cape	Jan 11 - 14	NW	1,300	4	12
37	East of Icy Cape	Jan 11 - 14	NW	400	2	5
38	East of Icy Cape	Jan 11 - 14	NW	7,250	10	15
39	Kasegaluk Lag.-Kuk R.	Jan 11 - 14	NW	6,650	20	15
40	Kasegaluk Lag.-Kuk R.	Jan 11 - 14	NW	1,950	5	8
41	Kasegaluk Lag.-Kuk R.	Jan 11 - 14	NW	1,400	3	10
42	Kasegaluk Lag.-Kuk R.	Jan 11 - 14	NW	750	2	3
43	Kuk River-Pt. Belcher	Jan 11 - 14	NW	50	2	3
44	Kuk River-Pt. Belcher	Jan 11 - 14	NW	500	2	4
45	Kuk River-Pt. Belcher	Jan 11 - 14	NW	2,050	2	7
46	Kuk River-Pt. Belcher	Jan 11 - 14	NW	2,150	3	10
47	Kuk River-Pt. Belcher	Jan 11 - 14	NW	750	5	10
48	Pt. Belcher-Utqiagvik	Jan 11 - 14	N	850	3	5
49	Pt. Belcher-Utqiagvik	Jan 11 - 14	N	400	2	0
50	Pt. Belcher-Utqiagvik	Jan 11 - 14	N	400	3	5
51	Pt. Belcher-Utqiagvik	Jan 11 - 14	W	3,200	5	8
52	Pt. Belcher-Utqiagvik	Jan 11 - 14	W	1,750	15	25
53	Pt. Belcher-Utqiagvik	Jan 11 - 14	W	450	5	30
54	Pt. Belcher-Utqiagvik	Jan 11 - 14	W	100	7	8
55	Pt. Belcher-Utqiagvik	Jan 11 - 14	W	1,650	5	8
56	Pt. Belcher-Utqiagvik	Jan 11 - 14	W	200	2	3
57	Pt. Belcher-Utqiagvik	Jan 11 - 14	W	1,250	4	6

Notes:
[1] "Length" indicates alongshore extent of pile-up.
[2] "Height" indicates maximum height of pile-up relative to MSL.
[3] "Encroachment" indicates distance ice advanced onto subaerial beach.

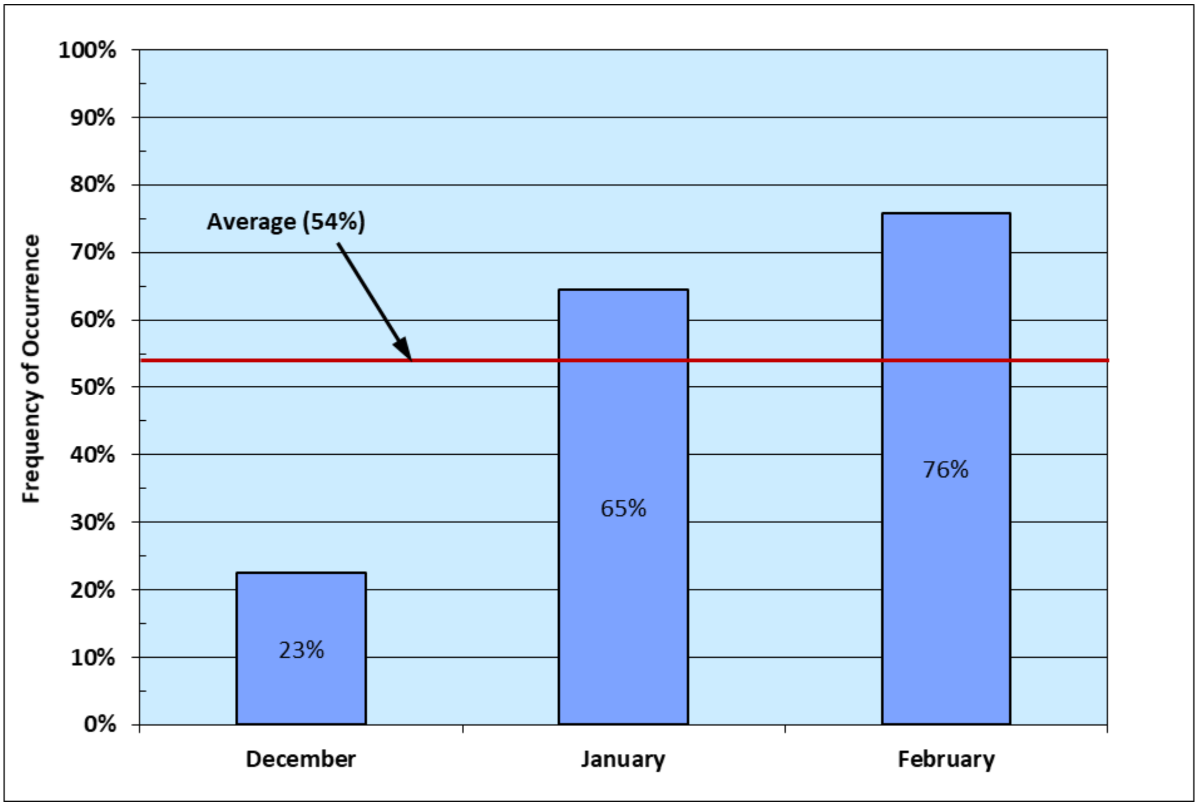

Figure 6-1. Frequency of Occurrence of Chukchi Sea Flaw Lead, December 2019 – February 2020

Multi-Year Ice: Multi-year ice drifting west in the Alaskan Beaufort Sea reached the vicinity of Point Barrow at the end of November (Section 5.4.1). It remained stalled at that location until mid-December, when multi-year floes began to move into the region northwest of the Point. On December 23rd, the ice drifted south of the Point after entering the first flaw lead of the freeze-up season. A larger flaw lead appeared at the end of December, allowing the ice to move within 2 nm (4 km) of Icy Cape by early January. Farther offshore, the multi-year ice edge trended toward the northwest, passing through the 168ºW meridian in the vicinity of 72º40'N.

The ice continued to advance to the south and west of Point Barrow during the remainder of January, reaching the Hanna Shoal and Burger Prospects in mid-month and the vicinity of Point Lay at month-end. Changes in the ice edge were minimal in February, with the western boundary tending to follow the 163ºW meridian between the 70ºN and 72ºN parallels.

Ice Drift: As in the case of the Beaufort, ice drift in the Chukchi was investigated using multi-year floes that appeared in successive RADARSAT-2 images. Seven of the 11 floes tracked in the Beaufort (Section 5) moved into the Chukchi over the course of the study period. These were monitored along with two additional floes identified for the first time in the Chukchi. The results are presented in Table 6-5.

All nine floes moved toward the west, with the net displacements varying from southwest to northwest. The average monthly speeds, which were computed using the net displacement of each floe in each month in which the tracking period exceeded 15 days, tended to be lower than in the Beaufort. The maximum value, 8.0 nm/day (14.8 km/day) occurred in December when easterly winds reinforced the Beaufort Gyre (Figure 1-1) and the nascent pack ice provided minimal confinement. The minimum, a meager 0.4 nm/day (0.7 km/day), occurred in February when westerly winds predominated. The mean value of the average monthly speeds over the three-month period-of-record (December through February) was 3.0 nm/day (5.6 km/day).

Table 6-5. Multi-Year Ice Floe Average Monthly Speeds in Chukchi Sea, December 2019 - February 2020

Month	No. of Floes	Maximum Speed (nm/day)	Minimum Speed (nm/day)	Average Speed (nm/day)
December	4	8.0	5.2	6.7
January	6	2.3	0.4	1.1
February	7	1.8	0.7	1.2
Average	n/a	n/a	n/a	**3.0**

Note: Average monthly speeds were derived from the net displacements that occurred over periods ranging from 17 to 31 days (depending on the availability of RADARSAT-2 images).

6.2 Early Freeze-Up

6.2.1 October 2019

Meteorological Conditions: The daily values of average and maximum sustained wind speed, average wind direction, and average air temperature at Utqiagvik Airport are shown in Figure 6-2. As in Section 5, the red and blue color bands in this and all subsequent meteorological plots denote the ranges of parameters defined in Table 5-7. Unless indicated otherwise, the wind speeds discussed in the text refer to the daily average values rather than the daily maximum values or hourly average values.

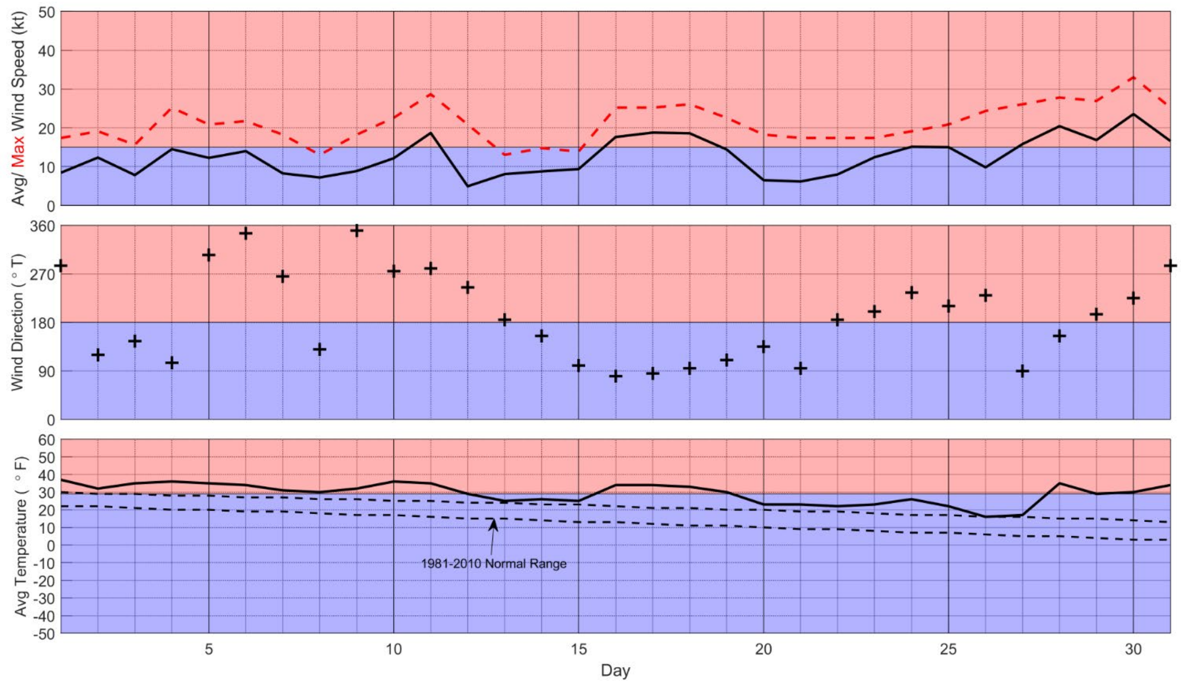

Figure 6-2. Meteorological Conditions at Utqiagvik Airport in October 2019

The daily average air temperatures in October 2019 were exceptionally warm, exceeding the normal range on 30 of the 31 days. They averaged 29°F (-2°C, which is the freezing point of sea water) and dropped below that value on only 11 occasions.

Westerly winds prevailed by a narrow margin, occurring on 17 days versus 14 for easterlies. The average wind speed, 13 kt (7 m/s), matched that in November as the highest recorded during the study period. The storm population consisted of two easterly and two westerly events:

- October 11th: one-day westerly with maximum speed of 19 kt (10 m/s);
- October 16th-18th: three-day easterly with maximum speed of 19 kt (10 m/s);
- October 27th-28th: two-day easterly with maximum speed of 20 kt (10 m/s);
- October 29th-31st: three-day westerly with maximum speed of 24 kt (12 m/s).

Ice Cover: Ice began to form in Kasegaluk Lagoon, the Kuk River Inlet, and Peard Bay during the third week in October, approximately one week after FDD began to accumulate at Utqiagvik Airport (Figure 6-3). Freeze-up proceeded slowly in the weeks that followed, reflecting warm air temperatures (Figure 6-2), exceptionally warm sea surface temperatures (Figures 5-5 and 5-6), and frequent storms (Table 6-2). As shown in Figure 6-4, the ice coverage was incomplete in the lagoon areas and totally lacking in the remainder of the Chukchi Sea study area at month-end.

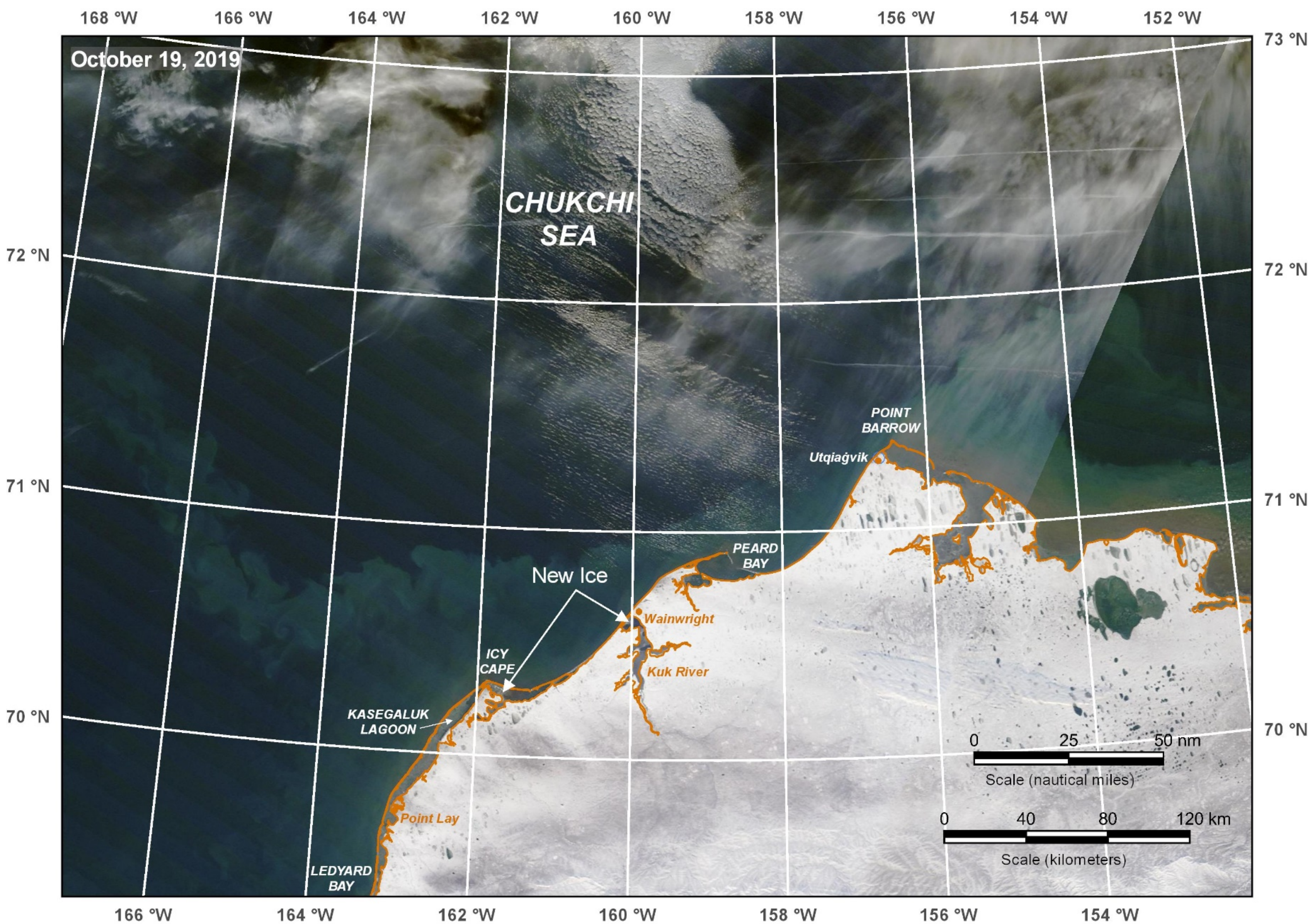

After: NASA, 2019

Figure 6-3. MODIS Image of Chukchi Sea Acquired on October 15, 2019

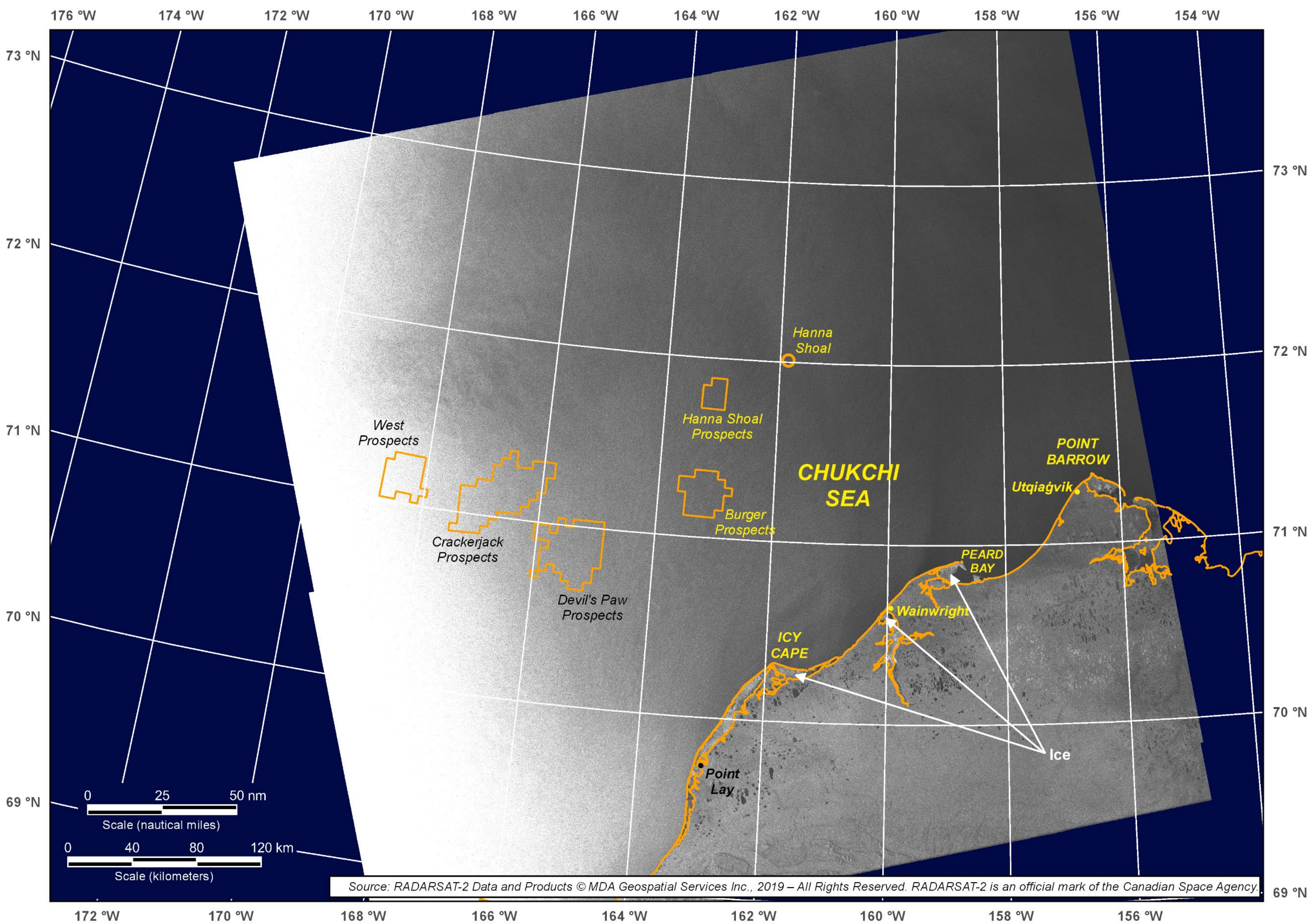

Figure 6-4. RADARSAT-2 Image of Chukchi Sea Acquired on October 29, 2019

Ice Thickness: The thickness of undisturbed first-year ice at the end of October was computed to be 9 cm (Table 6-3).

6.2.2 November 2019

Meteorological Conditions: The wind and temperature data acquired at Utqiagvik Airport are shown in Figure 6-5. The unseasonably warm air temperatures that prevailed in October continued throughout November. Over the course of the month, the daily average readings topped the normal range on 29 days and never dropped below. The average for the month was 17°F (-8°C).

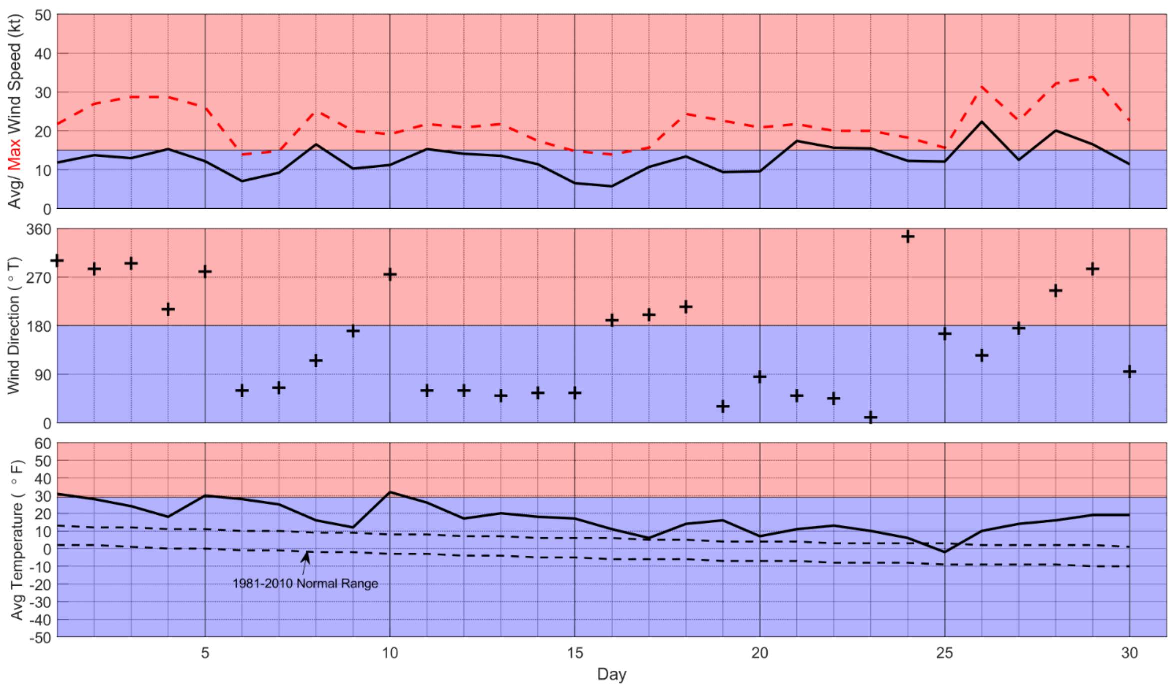

Figure 6-5. Meteorological Conditions at Utqiagvik Airport in November 2019

In contrast to October, when westerly winds predominated, easterlies prevailed on 18 of the 30 days in November. The average speed was 13 kt (7 m/s). Four storms took place over the course of the month, three of which were concentrated in the nine-day period that began on the 21st and ended on the 29th:

- November 8th: one-day easterly with maximum speed of 17 kt (9 m/s);
- November 21st-22nd: two-day easterly with maximum speed of 17 kt (9 m/s);
- November 26th: one-day easterly with maximum speed of 22 kt (11 m/s);
- November 28th -29th: two-day westerly with maximum speed of 20 kt (10 m/s).

Ice Cover: As in October, the formation of first-year ice was slowed by a combination of warm air temperatures (Figure 6-5), warm sea surface temperatures (Figures 6-6 and 6-7) and frequent storms (Table 6-2). Although the ice concentrations in the lagoons increased markedly during the first week of the month, complete coverage of these areas did not occur until the last week. In similar fashion, ice appeared in the exposed waters adjacent to the coast during the first week but failed to coalesce into a near-continuous strip spanning the entire length of the study area until the end of the month.

First-year pack ice began to stream west past Point Barrow during the second week of November (Figure 6-8) but then stalled in response to periods of westerly winds that culminated in a westerly storm on the 28th and 29th. As a result, most of the Chukchi Sea remained ice-free at month-end (Figure 6-9).

Ice Thickness: The calculated thickness of undisturbed first-year ice increased from 9 cm at the beginning of the month to 31 cm at the end (Table 6-3).

Landfast Ice: The development of landfast ice in November was delayed by the same factors that slowed the progress of freeze-up: warm air temperatures, warm sea surface temperatures, and a series of easterly storms. A predominance of easterly winds also inhibited landfast ice growth. The first traces appeared in Kasegaluk Lagoon, the Kuk River Inlet, and Peard Bay in mid-November, with complete coverage of each basin following two weeks later at month-end (Figure 6-10). The exposed waters along the coast remained bereft of landfast ice throughout the month.

Ice Pile-Ups: During the ice reconnaissance flight conducted on February 25th, a single pile-up was observed on the lagoon side of one of the barrier islands fronting South Kasegaluk Lagoon. As discussed in Section 6.1, this feature probably resulted from an easterly storm on November 26th followed by a westerly storm on the 28th and 29th. The height was estimated to be 2 m, the encroachment onto the subaerial beach to be 8 m, and the alongshore length to be 150 m (Table 6-4).

6.3 Late Freeze-Up

6.3.1 December 2019

Meteorological Conditions: The wind and temperature data recorded at Utqiagvik Airport in December 2019 are provided in Figure 6-11. The unseasonably warm air temperatures that occurred in October and November continued through December 17th, producing 16 days on which the average value exceeded the normal range. Commencing on the 18th, distinctly cooler temperatures prevailed, with the daily average values lying within

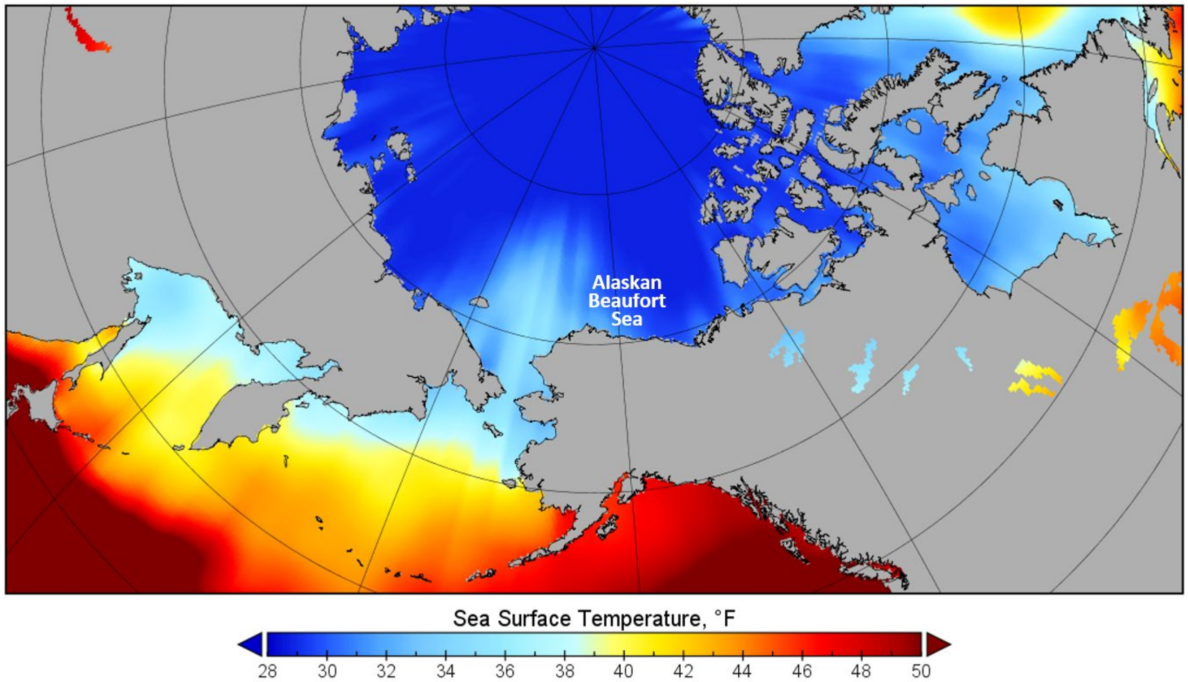

Data Source: NOAA, 2020b

Figure 6-6. Mean Sea Surface Temperature in November 2019

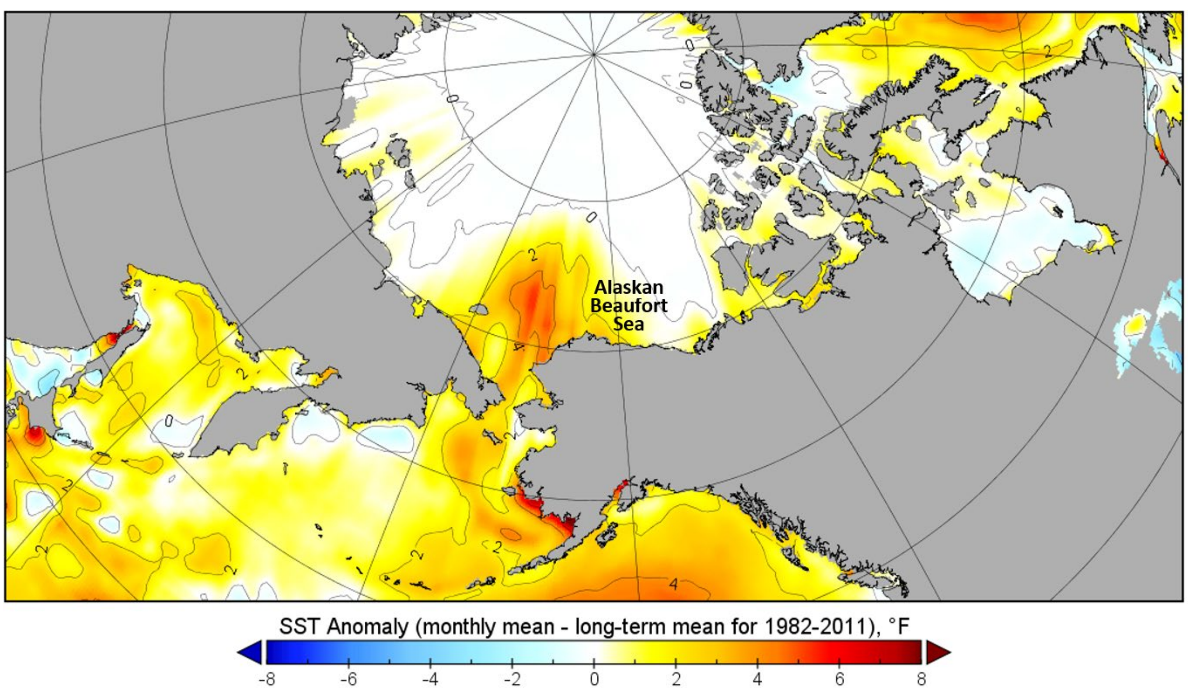

Data Source: NOAA, 2020b

Figure 6-7. Mean Sea Surface Temperature Anomaly in November 2019

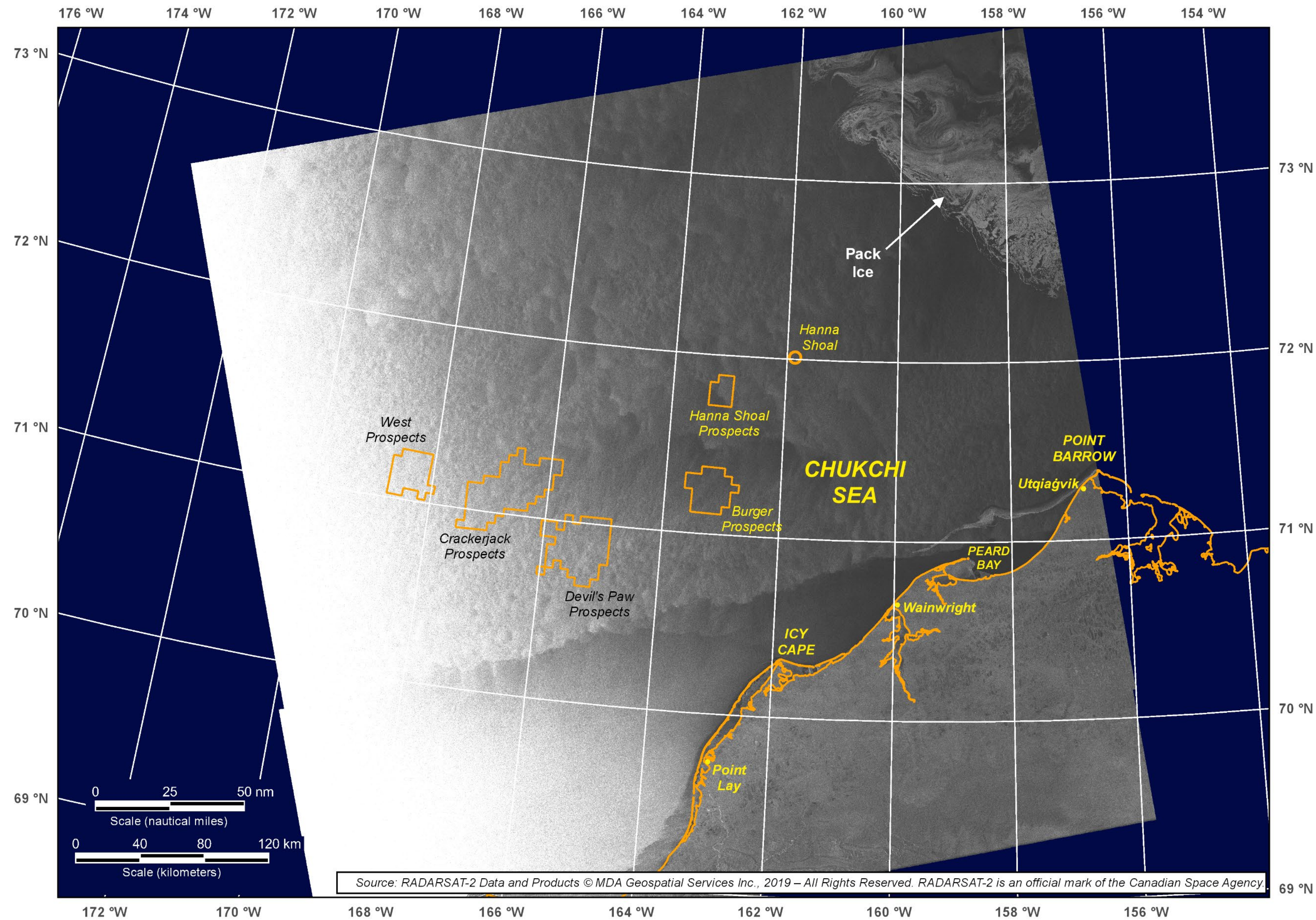

Figure 6-8. RADARSAT-2 Image of Chukchi Sea Acquired on November 15, 2019

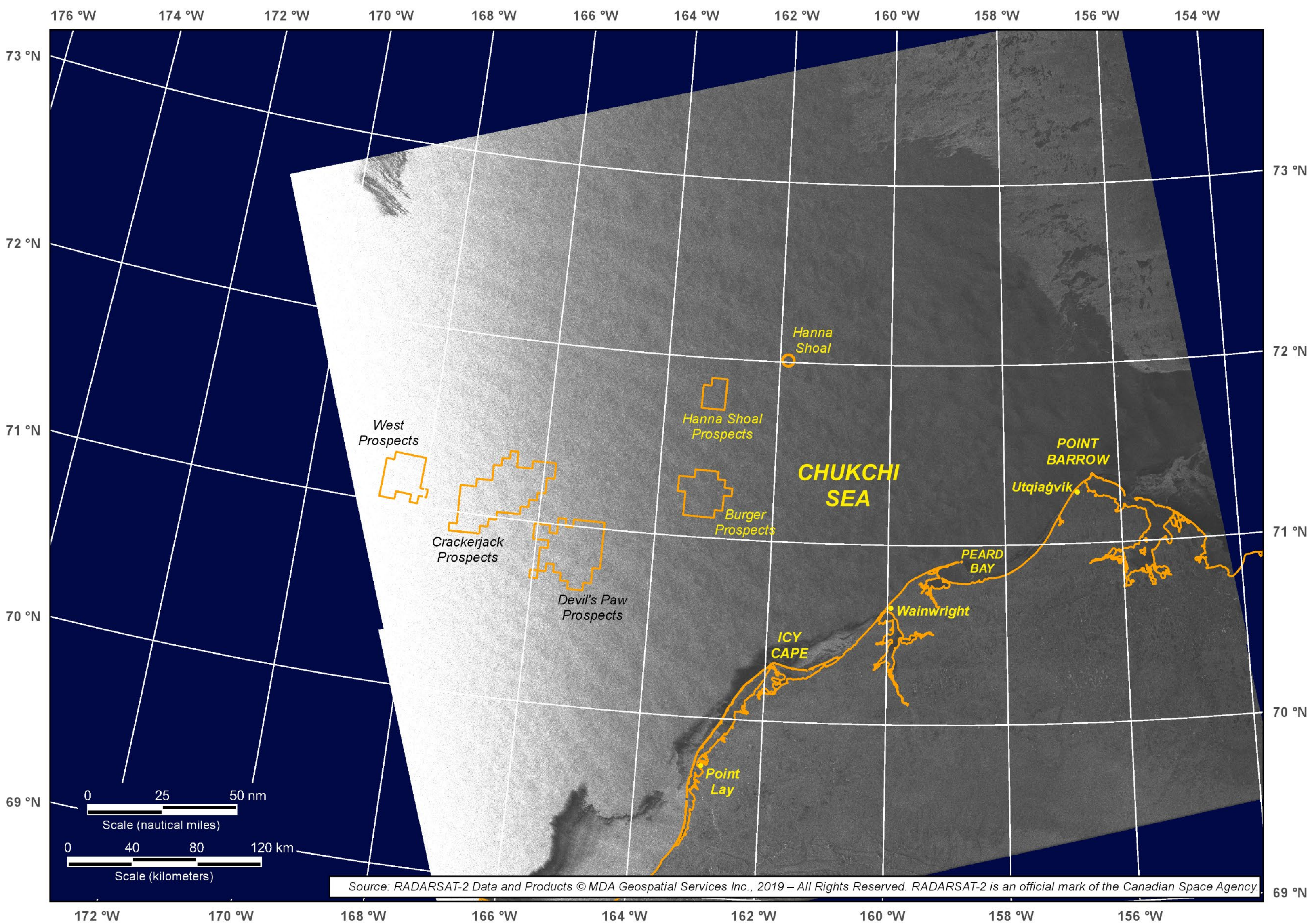

Figure 6-9. RADARSAT-2 Image of Chukchi Sea Acquired on November 29, 2019

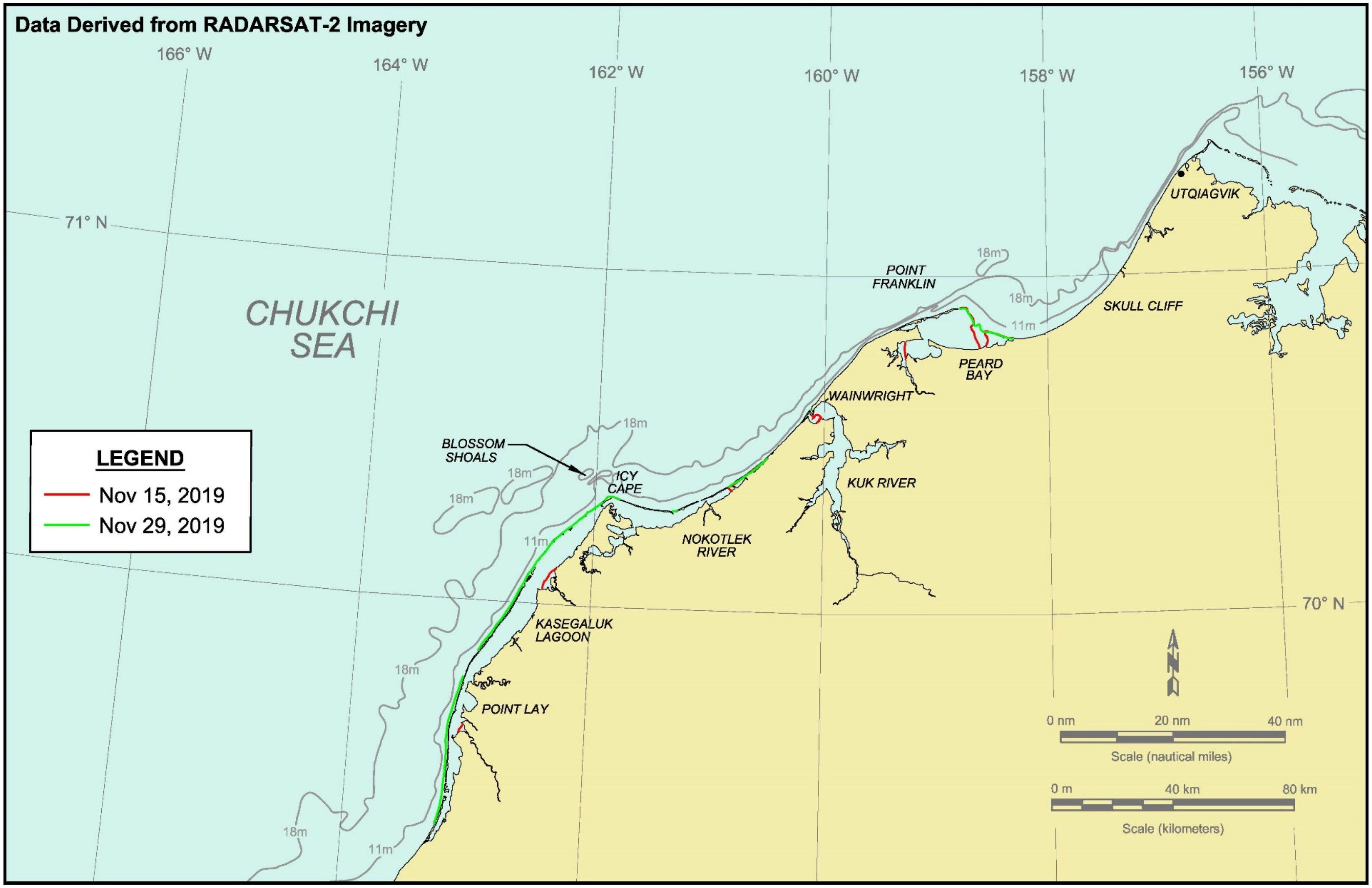

Figure 6-10. Chukchi Sea Landfast Ice Edge in November 2019

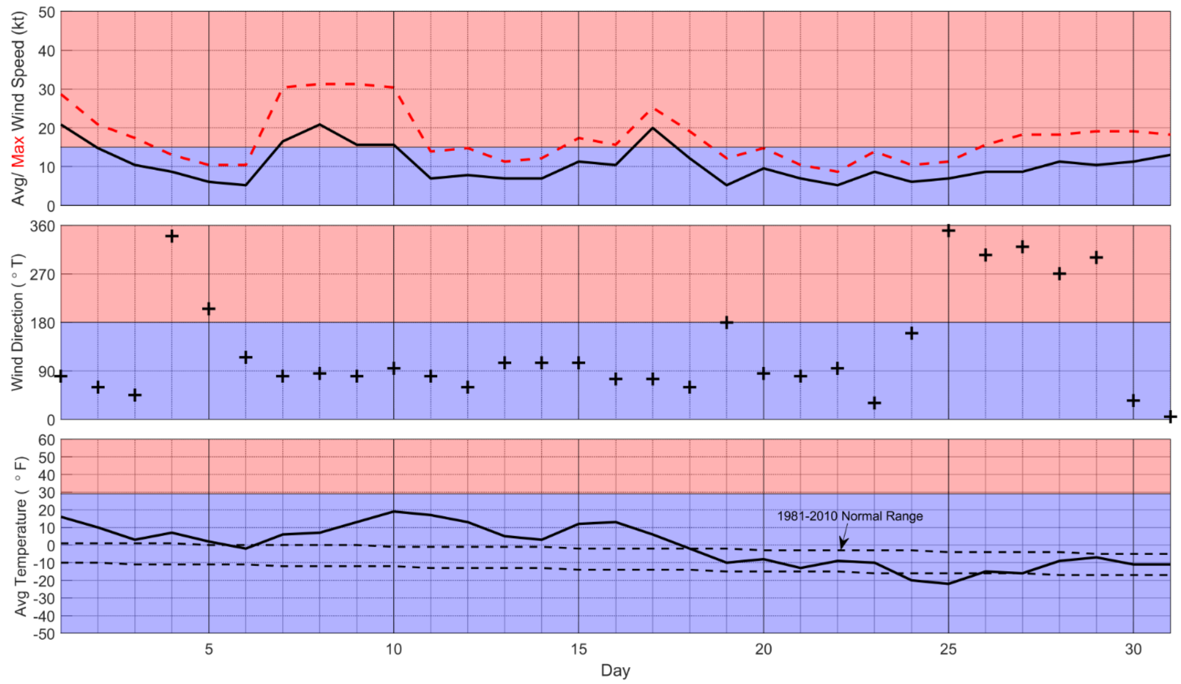

Figure 6-11. Meteorological Conditions at Utqiagvik Airport in December 2019

the normal range on twelve occasions and falling below on two. The average temperature for the month was 0°F (-18°C).

Easterly winds outnumbered westerlies by a wide margin in December: 24 days with easterlies versus only seven with westerlies. The average speed was 11 kt (6 m/s). Three storms occurred over the course of the month, all of which were easterly:

- December 1st: one-day easterly with maximum speed of 21 kt (11 m/s);
- December 7th-10th: four-day easterly with maximum speed of 21 kt (11 m/s);
- December 17th: one-day easterly with maximum speed of 20 kt (10 m/s).

Ice Cover: As is readily apparent from a comparison of Figure 6-9 and Figure 6-12, the ice concentration in the Chukchi Sea increased substantially during the first half of December due to a combination of ice entering from the Alaskan Beaufort Sea and *in situ* freezing. Easterly winds punctuated by easterly storms drove the ice away from the coast, however, preventing the occurrence of freeze-up until December 26th. On that date, one day after the wind direction shifted from easterly (offshore) to westerly (onshore), nearshore freeze-up and complete freeze-up of the Chukchi Sea basin occurred simultaneously (Figure 6-13). One thousand, one hundred and nineteen FDD had accumulated at Utqiagvik Airport at that time.

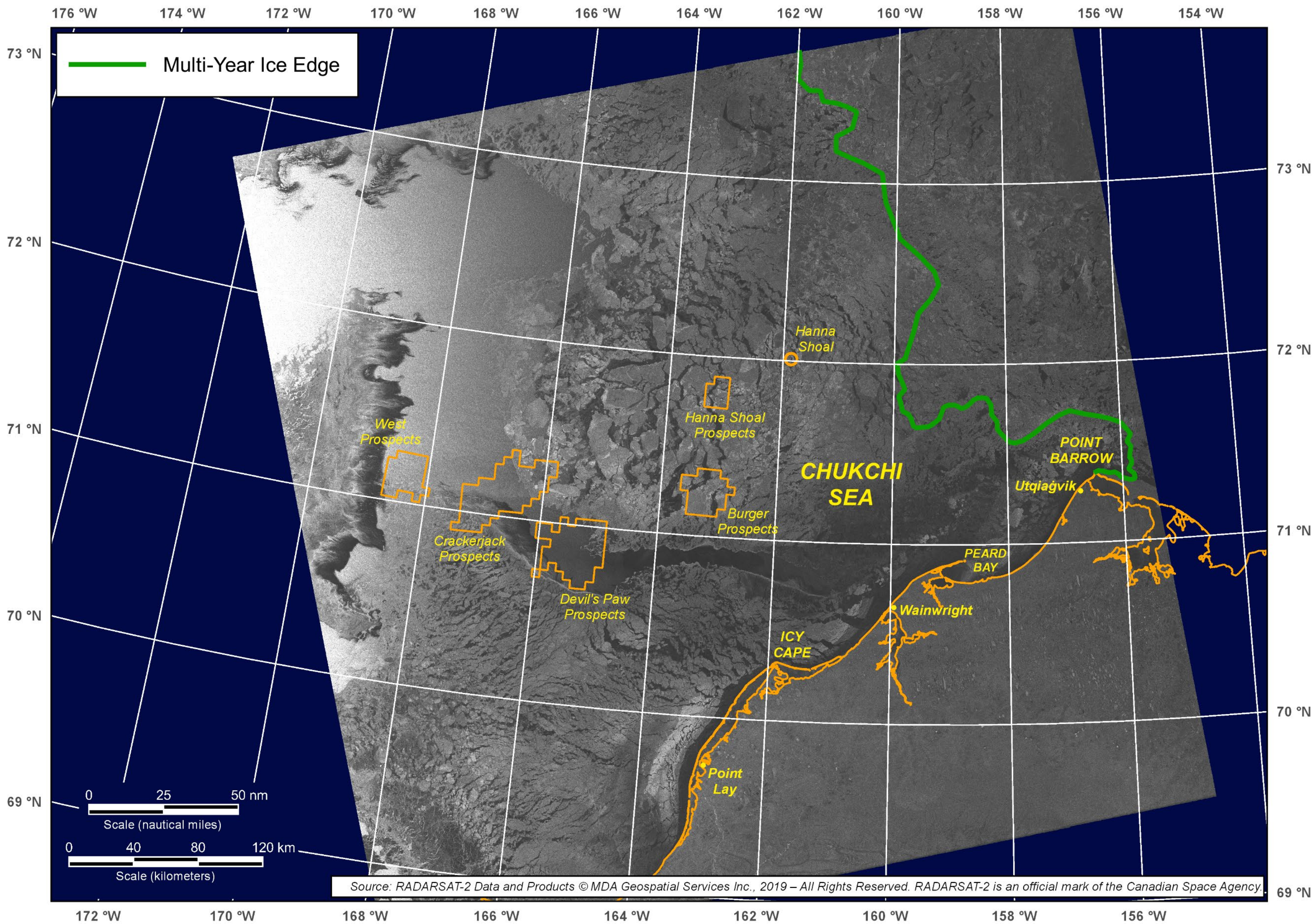

Figure 6-12. RADARSAT-2 Image of Chukchi Sea Acquired on December 16, 2019

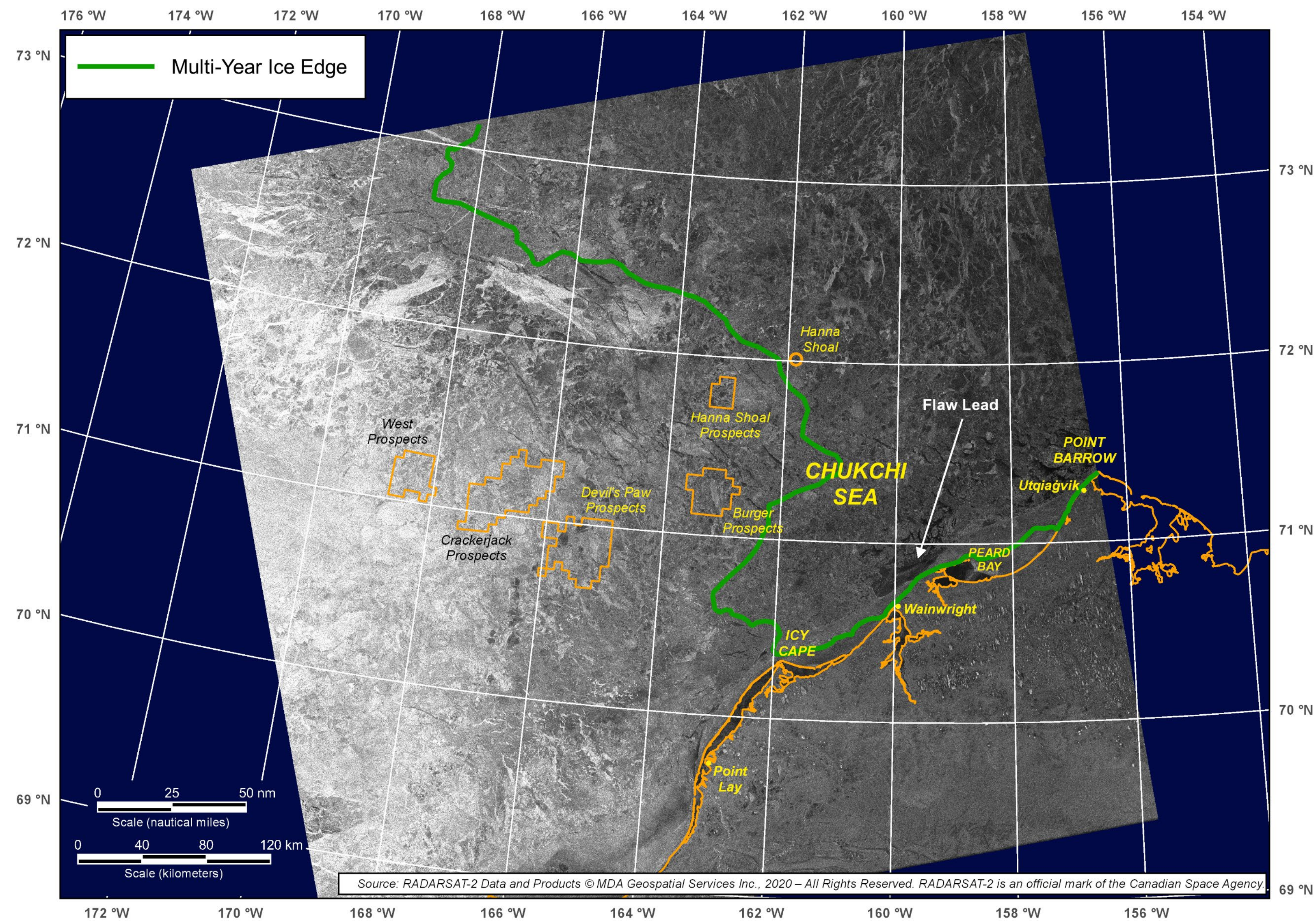

Figure 6-13. RADARSAT-2 Image of Chukchi Sea Acquired on January 2, 2020

To provide a quantitative understanding of freeze-up in the Chukchi Sea lease areas, the percentage of ice coverage was assessed in five representative prospects (Hanna Shoal, Burger, Crackerjack, West, and Devil's Paw) using RADARSAT-2 and VIIRS imagery (Section 4). As shown in Table 6-6, pack ice entered the Hanna Shoal Prospects during the first week in December, the Burger Prospects during the second, and the Crackerjack, West, and Devil's Paw Prospects during the third. Complete coverage of all five prospects occurred by January 2nd (Figure 6-13).

Table 6-6. Ice Cover in Chukchi Sea Prospects during Freeze-Up

Date	Ice Cover at Hanna Shoal	Ice Cover at Burger	Ice Cover at Crackerjack	Ice Cover at West	Ice Cover at Devil's Paw
November 29[1]	0%	0%	0%	0%	0%
December 4[2]	80%	0%	0%	0%	0%
December 12[2]	80%	80%	0%	0%	0%
December 16[1]	80%	80%	50%	Trace	20%
December 19[2]	100%	90%	80%	70%	60%
December 26[2]	100%	90%	100%	100%	100%
January 2[1]	100%	100%	100%	100%	100%
January 9[2]	100%	100%	100%	100%	90%
January 16[1]	100%	100%	100%	100%	90%
February 2[1]	100%	100%	100%	100%	100%
February 19[1]	100%	100%	100%	100%	100%
February 26[1]	100%	100%	100%	100%	100%

Notes:
[1] Ice cover estimated using RADARSAT-2 imagery.
[2] Ice cover estimated using VIIRS imagery.

Ice Thickness: The calculated thickness of undisturbed first-year ice increased by 30 cm in December, from 31 to 61 cm.

Landfast Ice: The successive locations of the landfast ice edge were estimated from RADARSAT-2 images obtained on November 29th, December 16th, and January 2nd (Figure 6-14). During the first interval, expansion of the landfast ice zone was precluded by a strong predominance of easterly (offshore) winds and two easterly storms. As a result, the landfast ice at mid-month was confined to the semi-protected lagoon areas along with several small patches in the exposed waters adjacent to the coast.

The situation changed abruptly in late December, when westerly winds, cold air temperatures, and an absence of easterly storms produced a continuous strip of landfast ice that encompassed the entire length of the study area. The maximum width, 18 nm (33 km), occurred off Skull Cliff.

Ice Pile-Ups: None of the ice pile-ups observed during the aerial reconnaissance flight on February 25th are believed to have occurred in December.

Coastal Flaw Lead: Based on analysis of daily VIIRS imagery (RAMMB, 2020; GINA, 2020) and one RADARSAT-2 image, the coastal flaw lead opened from December 20th through 24th and again on December 30th. In both cases, the feature developed in response to moderate easterly winds. Prior to December 20th, the existence of a flaw lead was precluded by the near-absence of landfast ice.

The lead remained small between the 20th and 24th, with a maximum width of 10 nm (19 km) and length of 30 nm (56 km). The lead that appeared on the 30th expanded rapidly, attaining a width of 35 nm (65 km) and length of 80 nm (149 km) on the 31st. It persisted for 14 days and attained its maximum dimensions - 75 nm (139 km) wide and 250 nm (463 km long) - in January. The seven days that the flaw lead existed in December represented a frequency of occurrence of 23%.

Multi-Year Ice: As discussed in Section 5.4.1, multi-year ice drifting west in the Alaskan Beaufort Sea reached the vicinity of Point Barrow at the end of November. It remained stalled at that location until mid-December, when multi-year floes began to move into the region northwest of the Point. On December 23rd, the ice drifted south of the Point into the first flaw lead of the freeze-up season. The larger flaw lead that followed at the end of the month allowed the ice to move within 2 nm (4 km) of Icy Cape by early January (Figure 6-13). Farther offshore, the multi-year ice edge trended toward the northwest, passing through the 168ºW meridian in the vicinity of 72º40'N.

Ice Drift: Ice movement rates in the northern Chukchi Sea were derived from the successive positions of four multi-year floes: Floes A, H, I, which had been tracked previously

"THIS INFORMATION IS DISTRIBUTED SOLELY FOR THE PURPOSE OF PRE-DISSEMINATION PEER REVIEW UNDER APPLICABLE INFORMATION QUALITY GUIDELINES. IT HAS NOT BEEN FORMALLY DISSEMINATED BY BSEE. IT DOES NOT REPRESENT AND SHOULD NOT BE CONSTRUED TO REPRESENT ANY BSEE DETERMINATION OR POLICY."

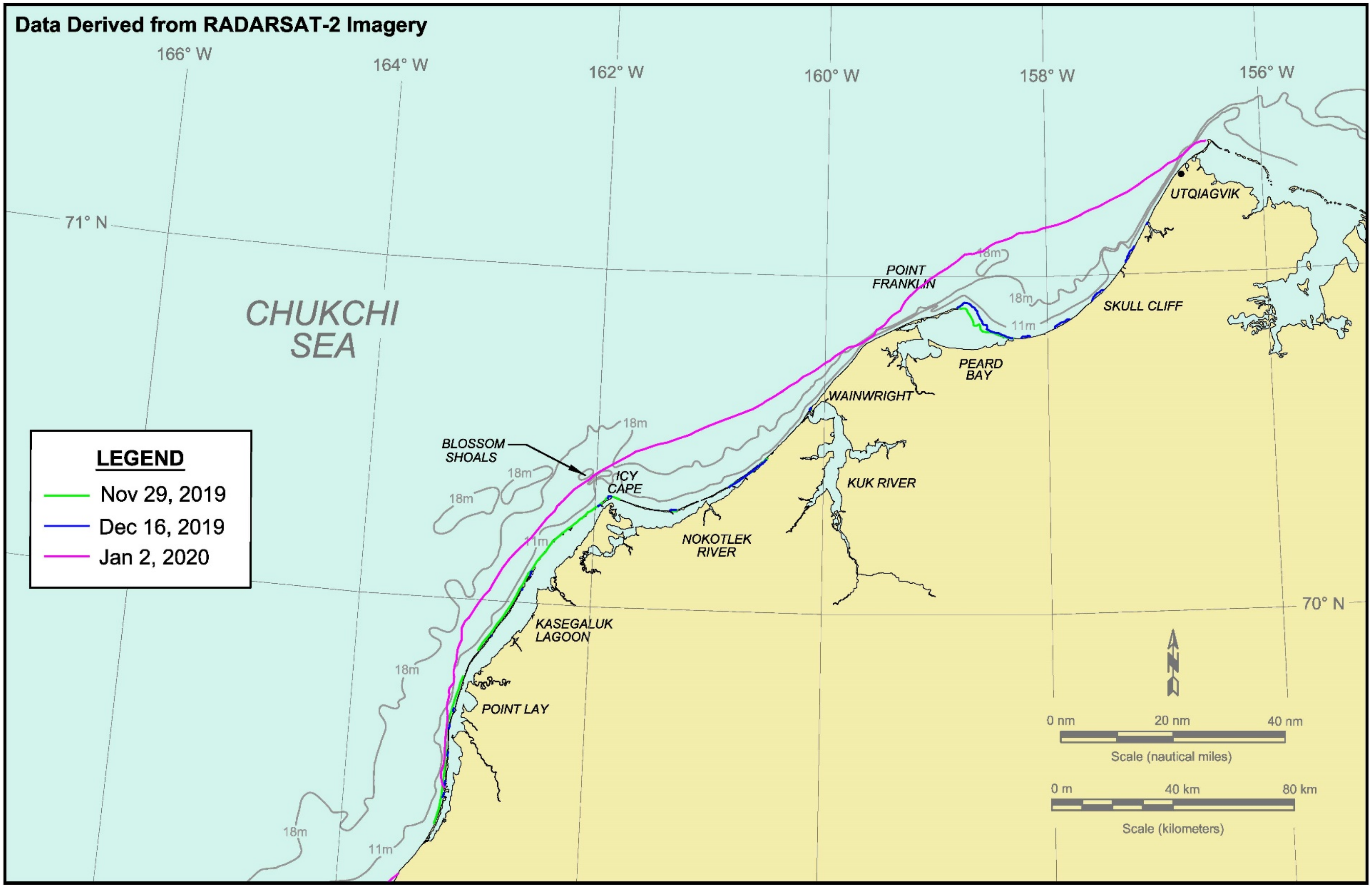

Figure 6-14. Chukchi Sea Landfast Ice Edge in December 2019

in the Beaufort, and Floe K, with an average diameter of 8 km, which was identified for the first time in the Chukchi. The floes were tracked during the 17-day period between December 16th and January 2nd using RADARSAT-2 images obtained on those dates. Their trajectories are shown in Figure 6-15.

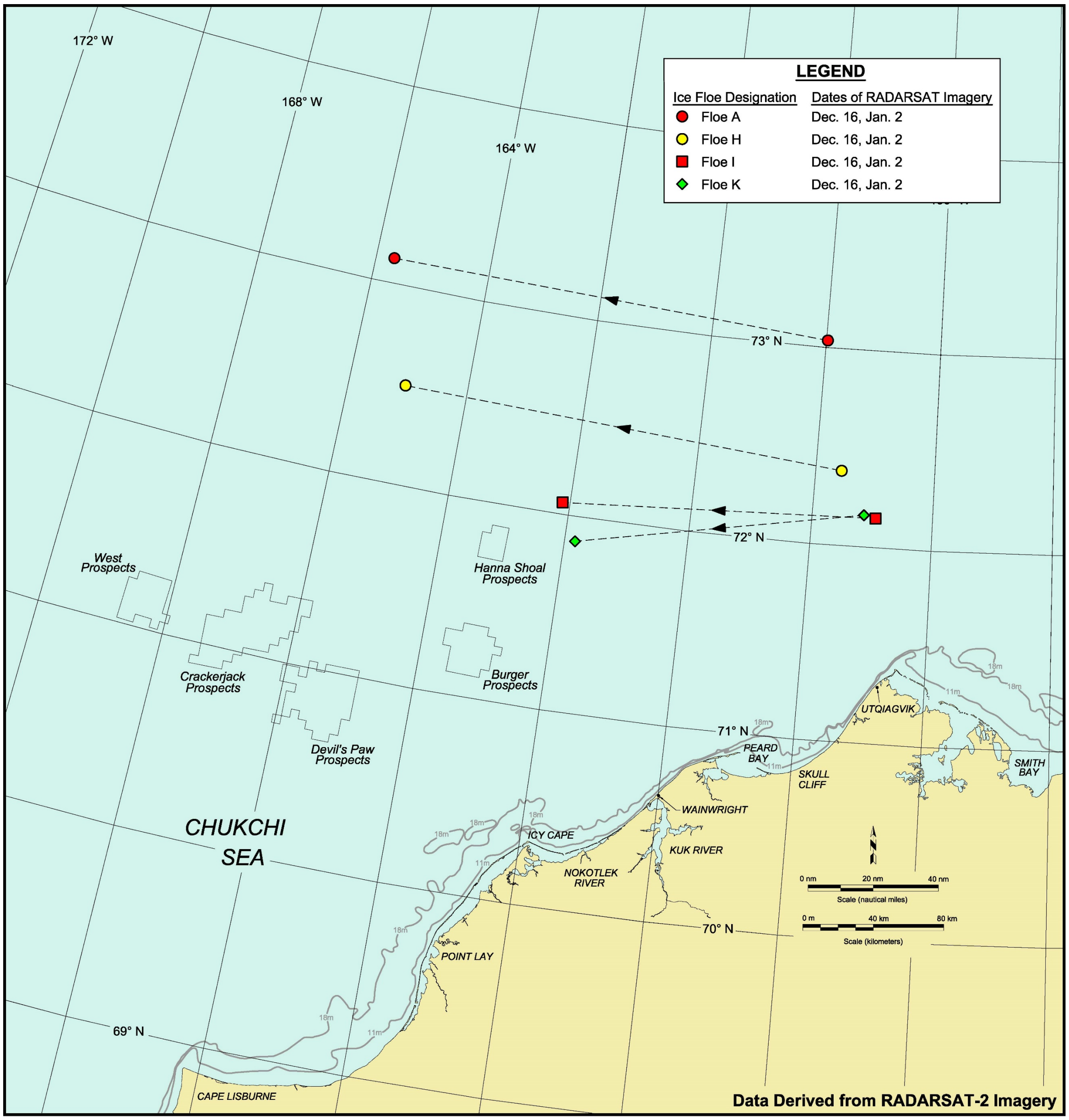

Figure 6-15. Chukchi Sea Multi-Year Ice Floe Displacements in December 2019

In keeping with the predominance of easterly winds during this period, all four floes experienced significant displacements to the west. The speeds were the highest recorded in the Chukchi during the freeze-up study period, an outcome produced by the easterly winds reinforcing the Beaufort Gyre in concert with the minimal confinement provided by the nascent pack ice. The average speeds ranged from 5.2 nm/day (9.6 km/day) to 8.0 nm/day (14.8 km/day) with a mean value of 6.7 nm/day (12.4 km/day).

Additional data on ice drift were derived from the daily positions of IABP Buoy X (Section 4.4), which moved from the Beaufort into the Chukchi on December 23rd. During the ensuing eight days, a period dominated by moderate westerly winds, the floe experienced a net displacement of 34 nm (63 km) to the southwest (Figure 6-16). The average speed computed on the basis of this displacement was a sluggish 4.3 nm/day (8.0 km/day). The peak speed between successive daily positions was 7.3 nm/day (13.5 km/day). It occurred on December 30th after the wind had shifted from northwesterly to northeasterly (Figure 6-17).

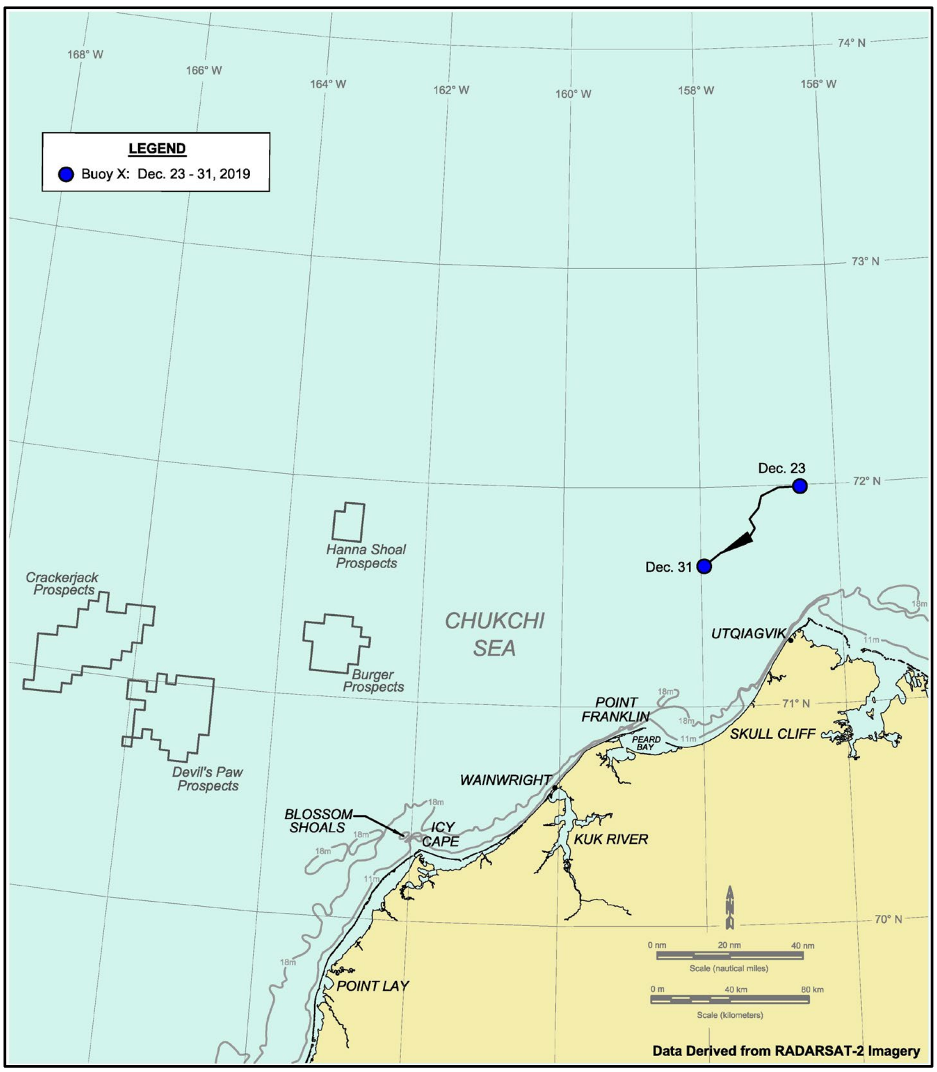

Figure 6-16. Chukchi Sea Drift Buoy Track in December 2019

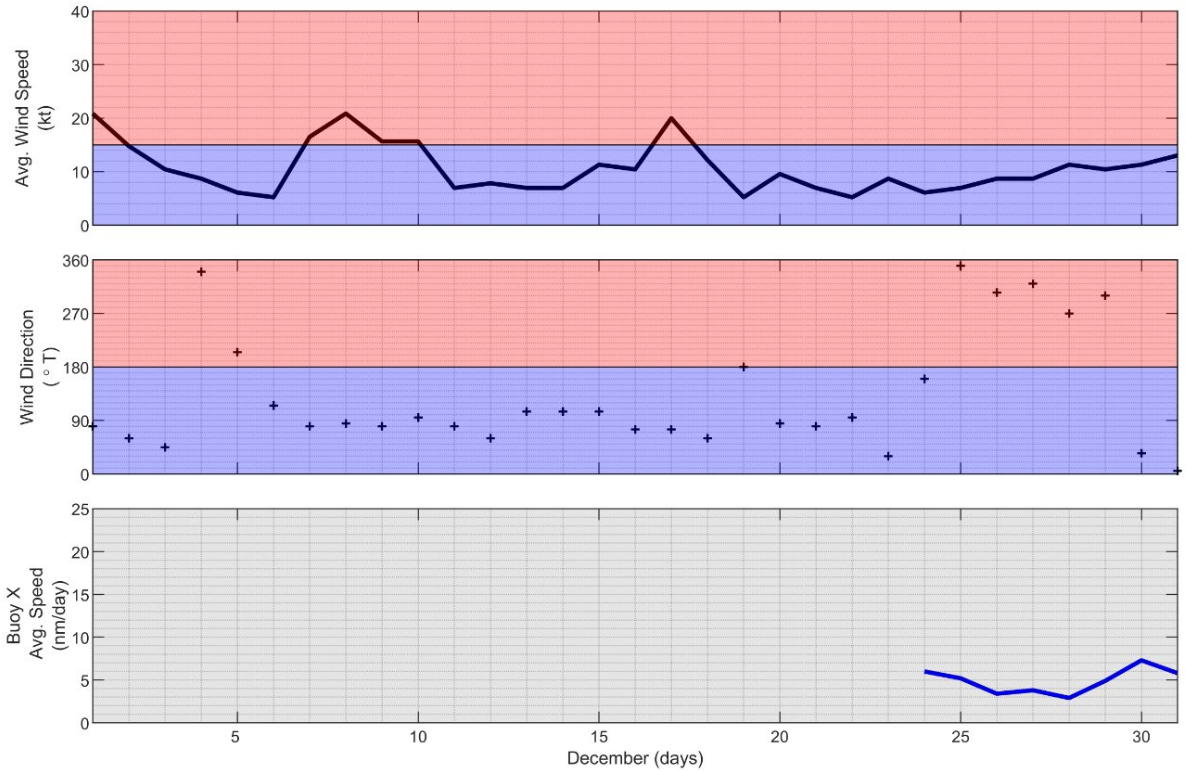

Figure 6-17. Chukchi Sea Drift Buoy Daily Average Speed in December 2019

6.3.2 January 2020

Meteorological Conditions: Figure 6-18 presents the wind and temperature data recorded at Utqiagvik Airport in January 2020. During the first 12 days of the month, the air temperatures tended to fall within or slightly below the normal range. A brief stretch of unseasonably warm weather ensued, with the daily average temperature peaking at 10°F (-12°C) on the 14th. Ten days later, on the 24th, the temperature dropped below normal in what marked the beginning of a cold spell that persisted for the remainder of the freeze-up study period. Over the course of the entire month, the temperatures exceeded the normal range on ten days and dropped below on 13. The mean value was -13°F (-25°C).

As in November and December, easterly winds outnumbered westerlies. The margin was small, however, with easterlies occurring on 17 days that were concentrated in the first half of the month, and westerlies on 14 days that were concentrated in the second half. The average speed was 9 kt (5 m/s). Storm activity was muted, consisting of one brief storm from each direction:

- January 11th: one-day easterly with maximum speed of 17 kt (9 m/s);
- January 14th: one-day westerly with maximum speed of 23 kt (12 m/s).

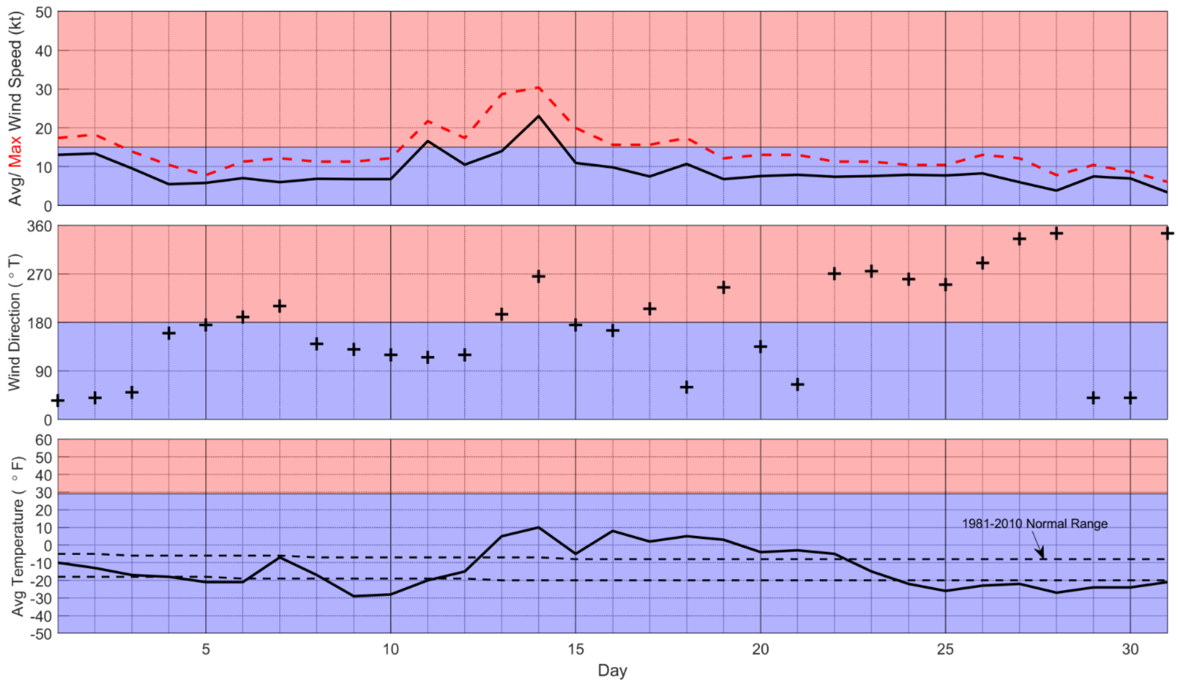

Figure 6-18. Meteorological Conditions at Utqiagvik Airport in January 2020

Ice Thickness: The calculated ice thickness increased from 61 cm at the beginning of the month to 90 cm at the end (Table 6-3).

Landfast Ice: Figure 6-19 illustrates the locations of the landfast ice edge derived from RADARSAT-2 images obtained on January 2nd, January 16th, and February 2nd. Most of the landfast ice that formed in late December was lost during the first half of January in response to winds with a significant southerly (offshore) component (Figure 6-18). As a result, the extent of the landfast ice zone in mid-January bore a close resemblance to that in mid-December (Figure 6-14).

A partial rebound occurred during the second half of January, when westerly winds resulted in the re-establishment of a continuous strip of landfast ice. The maximum width, 9 nm (17 km), was realized off Skull Cliff and also off the northern end of Kasegaluk Lagoon. Conversely, the width approached zero both in the vicinity of Point Belcher and to the south of Point Lay.

Ice Pile-Ups: Of the 57 ice pile-ups observed during the aerial reconnaissance flight on February 25th, all but one are believed to have formed in mid-January. As detailed in Section 6.1, they probably resulted from an easterly storm on the 11th that was followed by a westerly storm on the 14th.

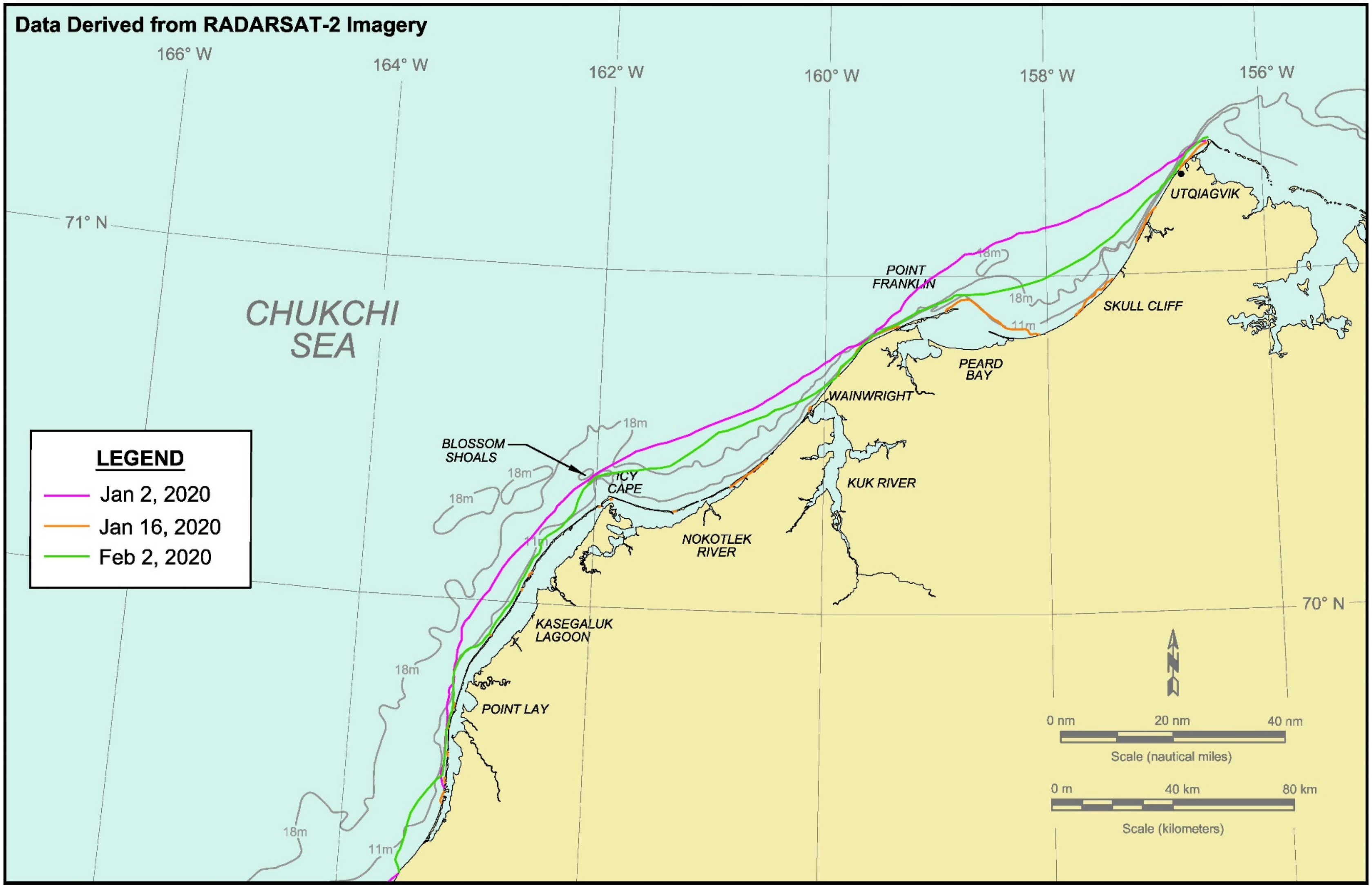

Figure 6-19. Chukchi Sea Landfast Ice Edge in January 2020

Although the number of pile-ups was consistent with those recorded in prior freeze-up studies, the dimensions were relatively large. The heights ranged from 1 to 20 m, the encroachment distances from negligible to 30 m, and the alongshore lengths from 50 m to 8 km (Table 6-4). The pile-ups were composed of ice blocks ranging from 30 to 60 cm thick.

Coastal Flaw Lead: The coastal flaw lead that appeared on December 30th (Section 6.3.1) remained open through January 13th, a period dominated by easterly winds. After closing in response to the westerly storm that occurred on the 14th, it reopened from the 18th through 20th and again on the 22nd. In both cases, its appearance was prompted by the advent of easterly winds. The fourth and final opening in January took place on the 29th, again in response to easterly winds. The lead remained open through February 1st.

The aggregate persistence of the lead in January was 20 days, representing a 65% frequency of occurrence. The maximum dimensions for the month, a length of 250 nm (463 nm) and width of 75 nm (139 km), occurred during the first opening (December 30th through January 13th). The three openings that followed produced more modest dimensions, with maximum widths of 10, 5, and 20 nm (19, 9, and 10 km), respectively.

Multi-Year Ice: The multi-year ice floes that began to move around Point Barrow in late December continued to advance to the southwest in January. As shown in Figure 6-20, the ice moved past Icy Cape and entered the Hanna Shoal and Burger Prospects by mid-month, aided by the presence of the coastal flaw lead. Changes in the ice edge were muted in the weeks that followed, but a narrow tongue extended south to the vicinity of Point Lay at month-end (Figure 6-21).

Ice Drift: Ice movement rates were investigated using six multi-year floes. Two had been tracked in the Chukchi in December (Floes I and K), one arrived from the Beaufort in January (Floe G), and three were identified in the Chukchi for the first time in January (Floes J, L, and M, with average diameters ranging from 6 to 10 km). The successive positions of the floes were derived from RADARSAT-2 images obtained on January 2nd, January 16th, and February 2nd.

The floe trajectories are displayed in Figure 6-22. Whereas the southernmost four floes experienced net displacements to the northwest during the first interval between images and to the east during the second, the northernmost two floes moved to the north during both intervals. This disparity appears to reflect differing degrees of confinement, in that the southernmost floes were located in the region influenced by the flaw lead while the northernmost floes were more constrained by the pack ice. As a result, the southernmost floes

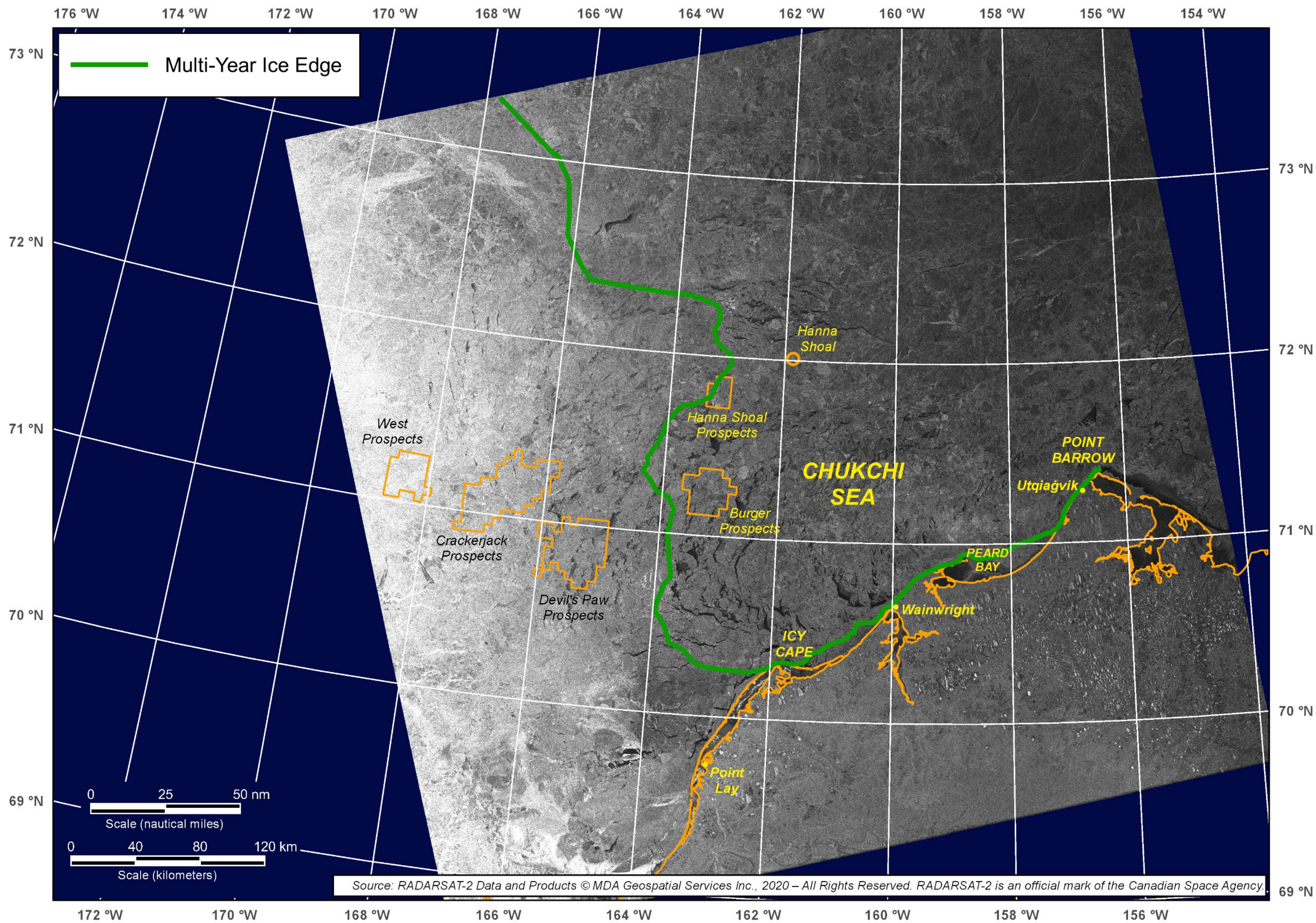

Figure 6-20. RADARSAT-2 Image of Chukchi Sea Acquired on January 16, 2020

“THIS INFORMATION IS DISTRIBUTED SOLELY FOR THE PURPOSE OF PRE-DISSEMINATION PEER REVIEW UNDER APPLICABLE INFORMATION QUALITY GUIDELINES. IT HAS NOT BEEN FORMALLY DISSEMINATED BY BSEE. IT DOES NOT REPRESENT AND SHOULD NOT BE CONSTRUED TO REPRESENT ANY BSEE DETERMINATION OR POLICY.”

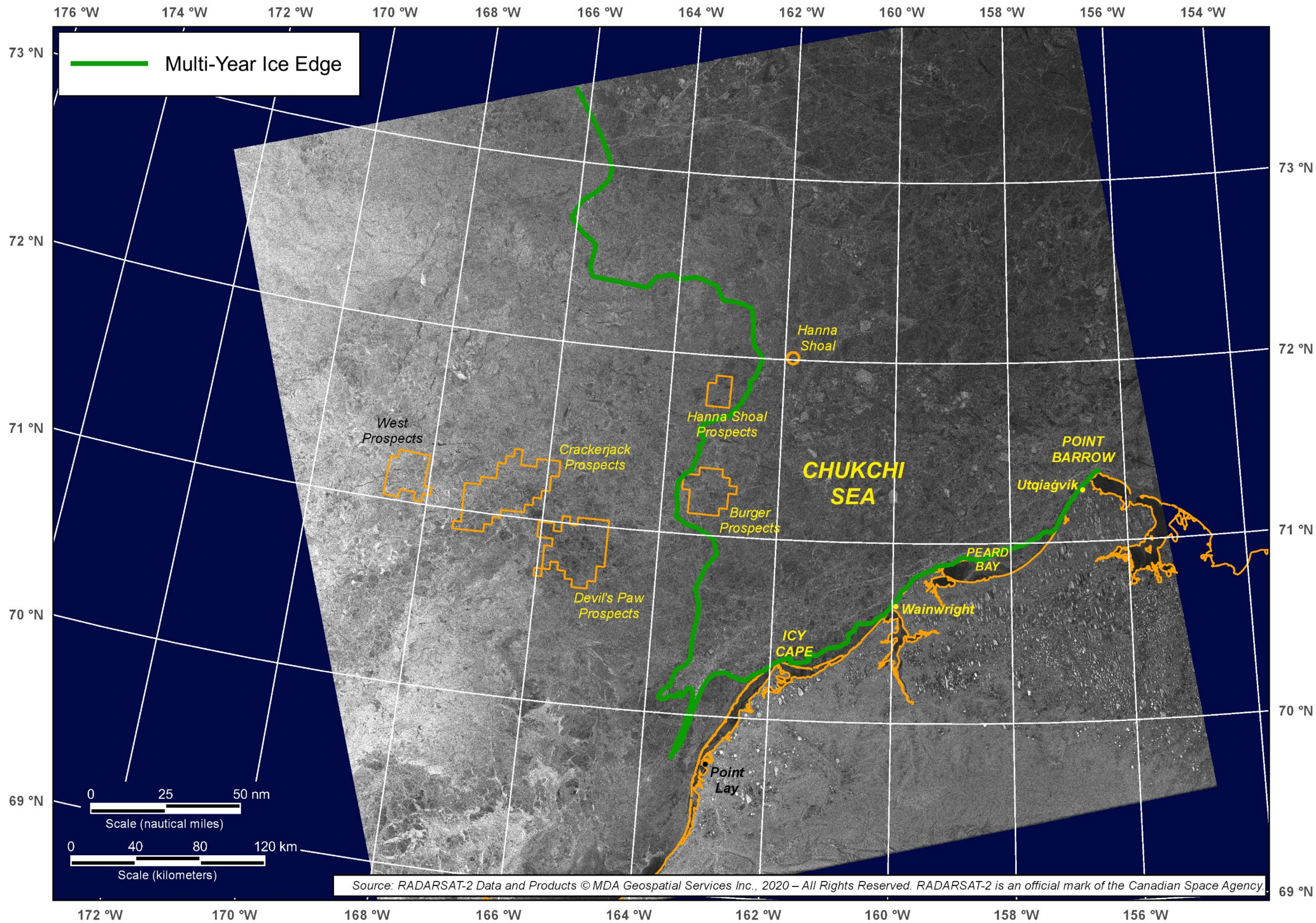

Figure 6-21. RADARSAT-2 Image of Chukchi Sea Acquired on February 2, 2020

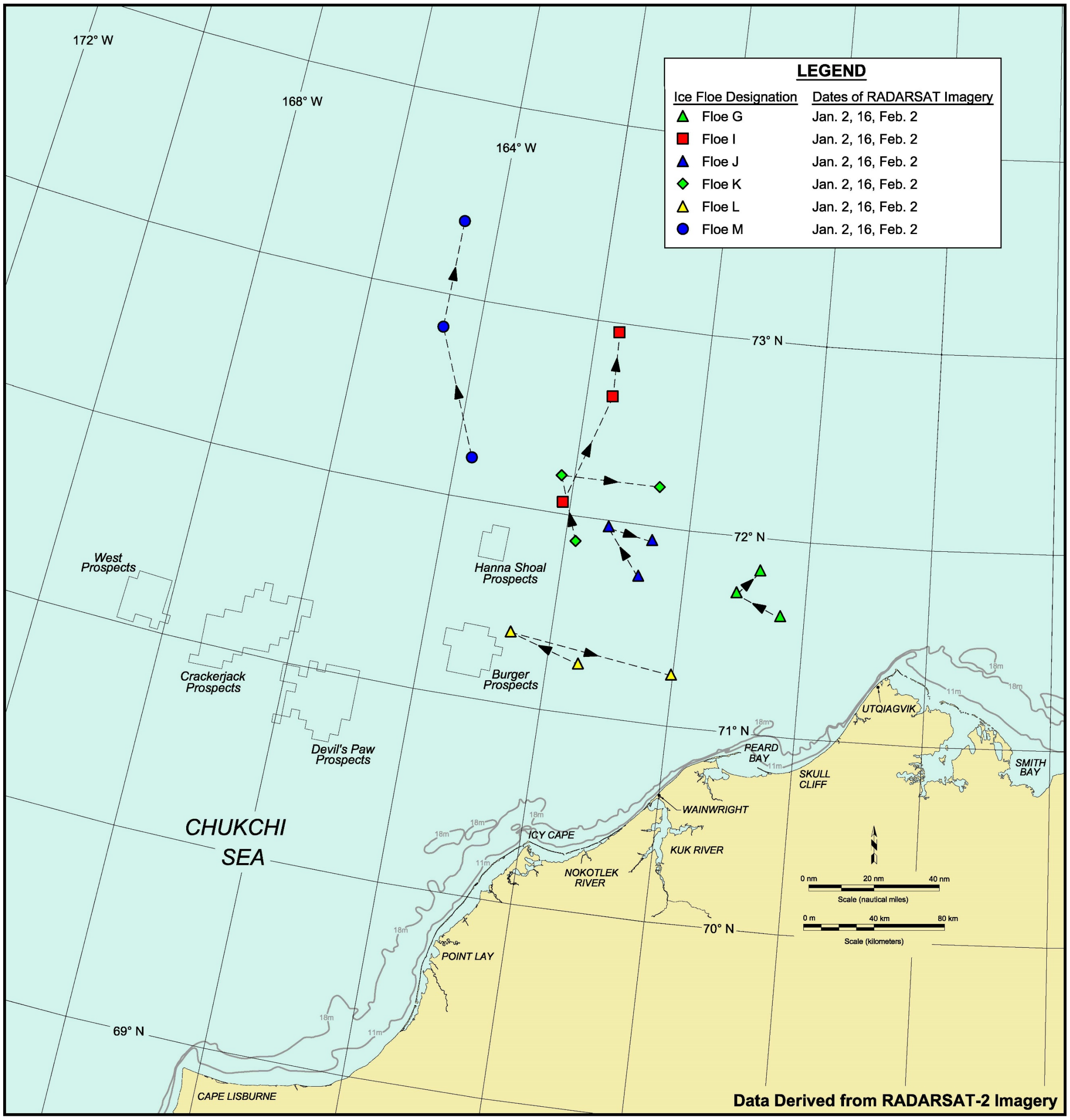

Figure 6-22. Chukchi Sea Multi-Year Ice Floe Displacements in January 2020

were able to respond to the easterly winds that prevailed during the first half of the month and the westerlies that prevailed during second. Farther offshore, the northernmost floes appear to have responded to the strong southerly component of the winds (both easterly and westerly) that prevailed until the last week of the month (Figure 6-18). Alternatively, the movement of these floes may have been governed by wind conditions that differed substantially from those at Utqiagvik.

The floe speeds were substantially lower than those recorded in December, with along-track values ranging from 1.1 to 2.9 nm/day (2.0 to 5.4 km/day) between January 2nd and 16th, and from 0.6 to 3.0 nm/day (1.1 to 5.6 km/day) between January 16th and February 2nd. The average monthly speeds, computed on the basis of the net displacements that occurred between January 2nd and February 2nd, varied from 0.4 to 2.3 nm/day (0.7 to 4.3 km/day) while averaging 1.1 nm/day (2.0 km/day).

The trajectory of IABP Buoy X is displayed in Figure 6-23, while its daily average speed is plotted in Figure 6-24. Its track resembled that of Floe K, with a net displacement to the northwest followed by a net displacement to the east. Like Floe K, which was located in close proximity, Buoy X was able to respond to changes in the wind direction due to the minimal confinement afforded by the flaw lead.

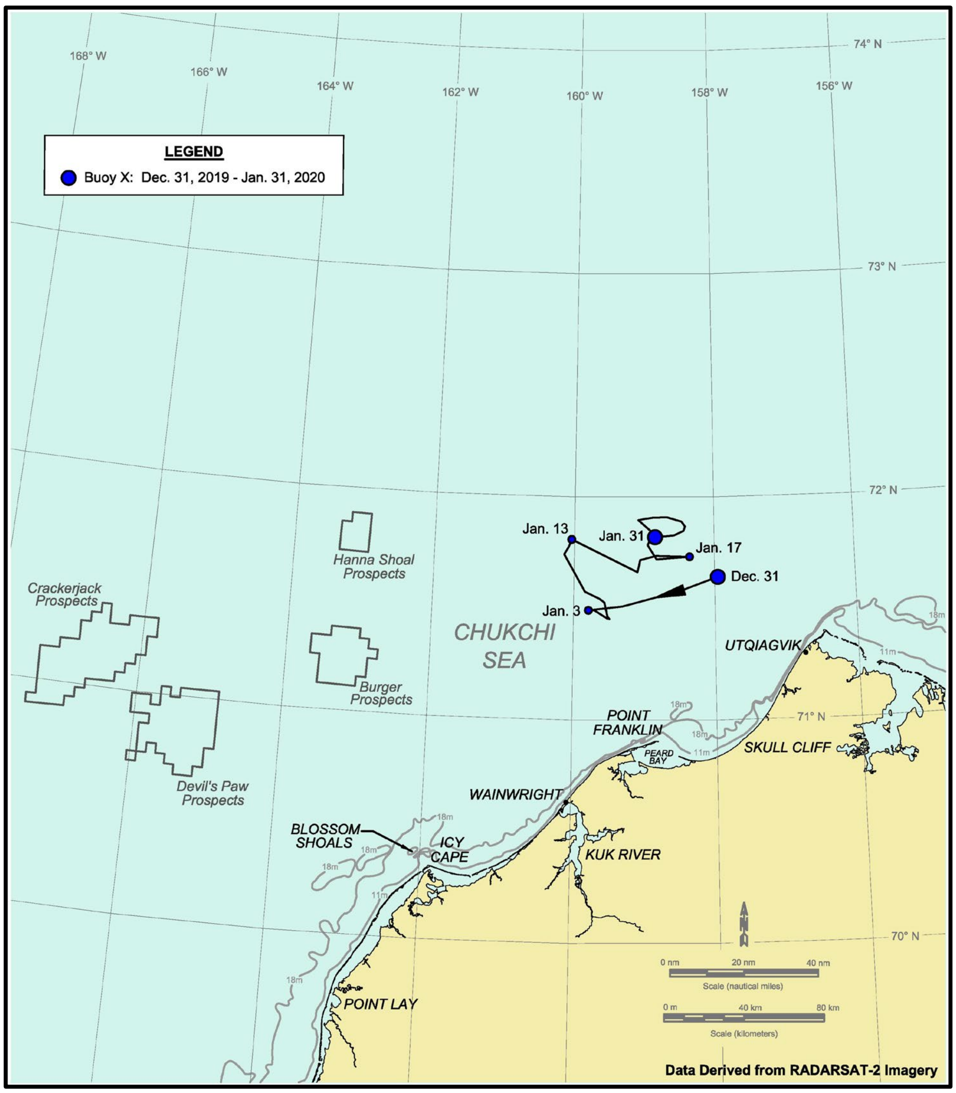

Figure 6-23. Chukchi Sea Drift Buoy Track in January 2020

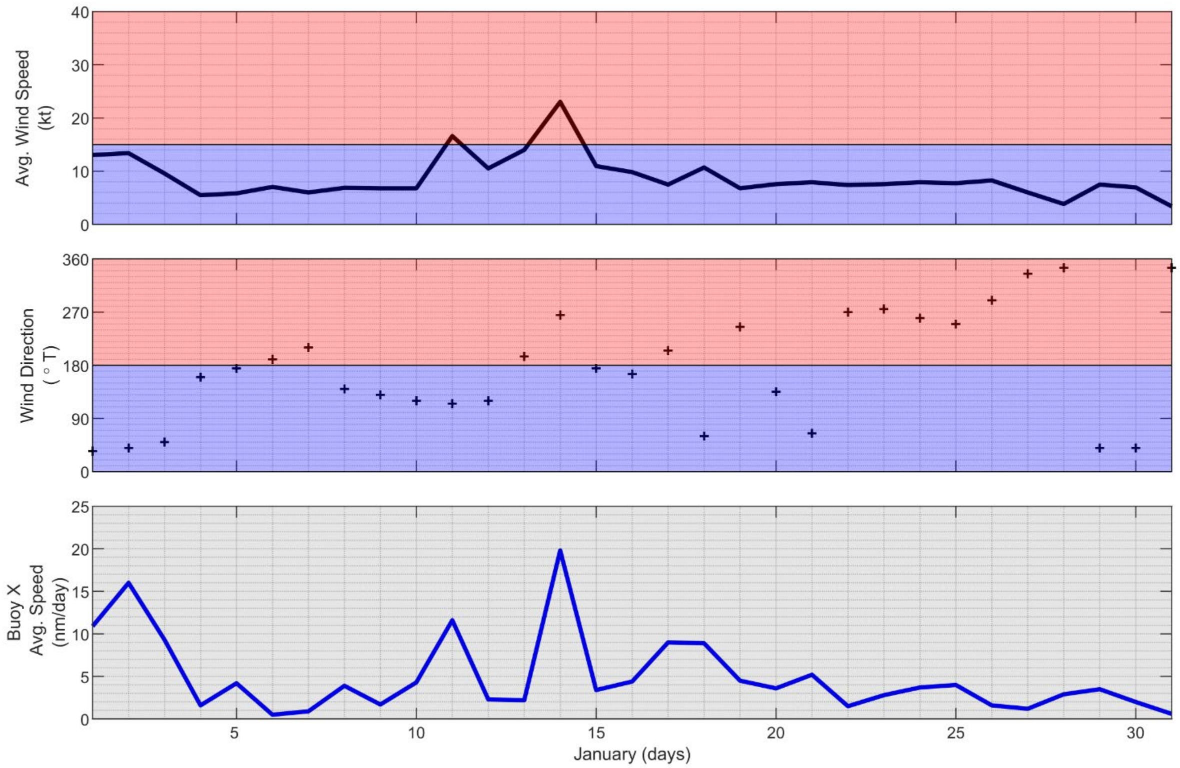

Figure 6-24. Chukchi Sea Drift Buoy Daily Average Speed in January 2020

The average speed of Buoy X computed on the basis of the net displacement over the course of the month was 0.6 nm/day (1.1 km/day). The peak speed between successive daily positions, 19.8 nm day (36.7 km/day), occurred on January 14th during a one-day westerly storm. The daily average wind speed during this event was 23 kt (12 m/s; Figure 6-24), resulting in a wind factor of 3.6%.

6.3.3 February 2020

Meteorological Conditions: The wind and temperature data acquired at Utqiagvik Airport in February 2020 are presented in Figure 6-25. The cold spell that began on January 24th persisted throughout the month of February, producing daily average air temperatures that exceeded the normal range on only one occasion while falling below on 21.

In contrast to November, December, and January, westerly winds predominated in February, occurring on 18 of the 29 days. The average speed for the month, 7 kt (4 m/s), was the lowest recorded during the five-month study period, and there were no storms.

Ice Thickness: The calculated ice thickness at the end of the month was 119 cm, representing 29 cm more than at the beginning.

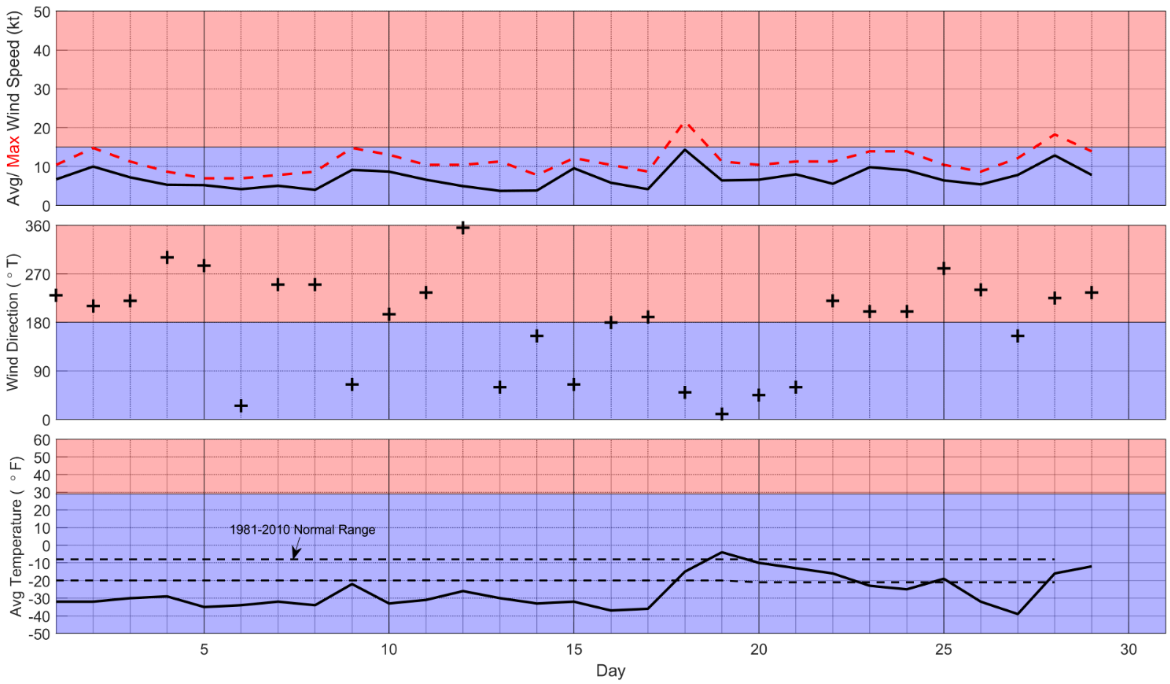

Figure 6-25. Meteorological Conditions at Utqiagvik Airport in February 2020

Landfast Ice: Figure 6-26 presents the locations of the landfast ice edge derived from RADARSAT-2 images acquired on February 2nd, 19th, and 26th. During the first interval, between the 2nd and 19th, light westerly winds caused the landfast ice zone to expand by amounts that ranged from negligible to as much as 7 nm (4 km) off North Kasegaluk Lagoon and in the vicinity of Point Lay. Of particular note was the fact that the ice became solidly grounded on Blossom Shoals, a customary anchor point, for the first time in the 2019-20 freeze-up season.

During the second interval, between February 9th and 26th, the continued dominance of light westerly winds coupled with an absence of easterly storms fostered additional expansion of the landfast ice in the vicinity of Icy Cape. At the end of this period, the width of the landfast ice zone was 3 nm (6 km) off Utqiagvik, 13 nm (24 km) off Skull Cliff, 21 nm (39 km) off North Kasegaluk Lagoon, and 4 nm (7 km) off Point Lay.

Coastal Flaw Lead: As discussed in Section 6.3.2, the flaw lead that formed on January 29th persisted through February 1st. The lead reopened for one day on February 6th in response to easterly winds, and again on February 10th following another short burst of easterlies on the day prior. It remained open from the 10th through month-end despite a

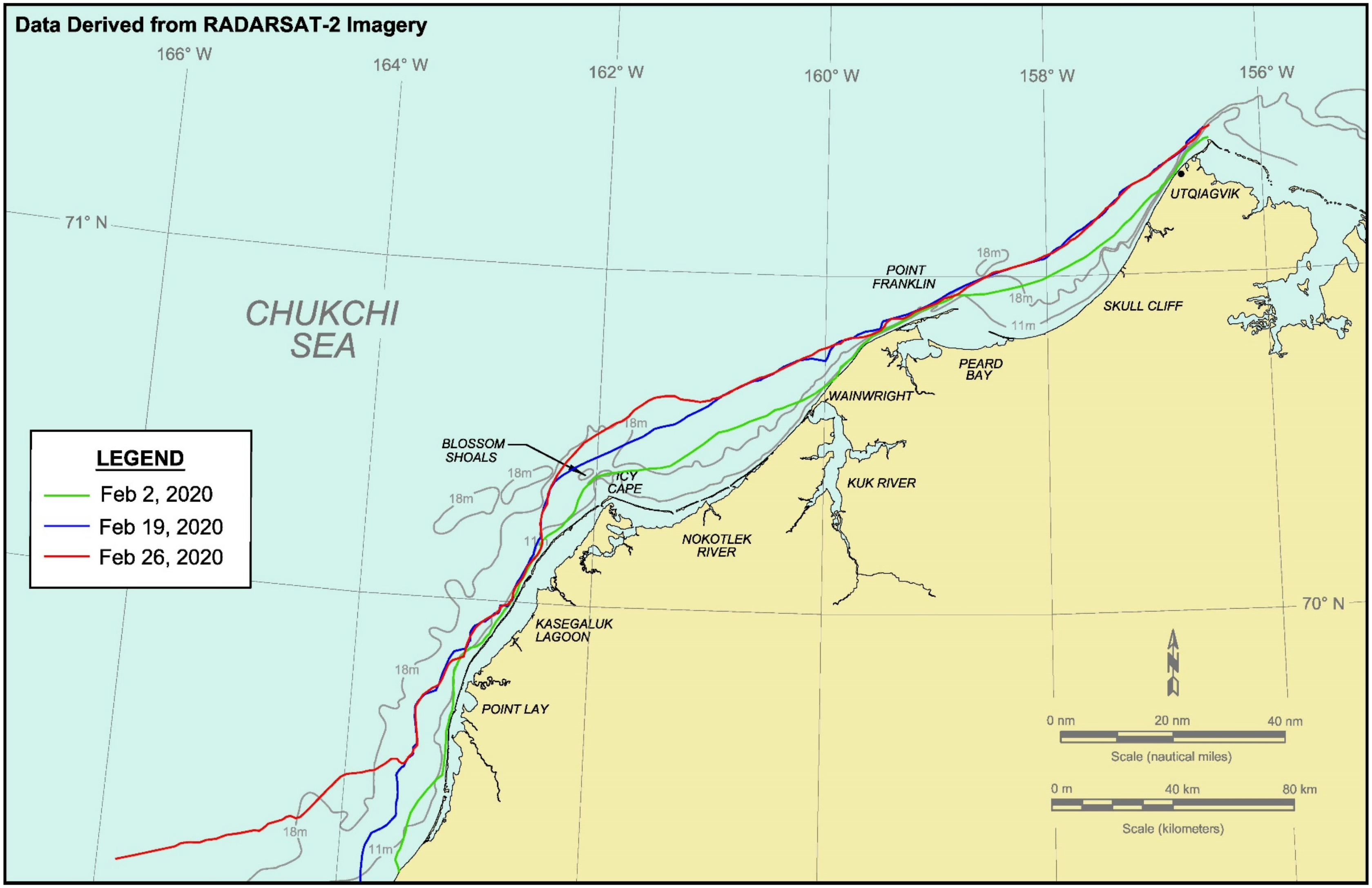

Figure 6-26. Chukchi Sea Landfast Ice Edge in February 2020

mixture of easterlies and westerlies during this 20-day period (Figure 6-27). The apparent contradiction of the lead persisting in the face of westerly (onshore) winds appears to have resulted from the low wind speeds associated with the westerlies (Figure 6-25).

Over the course of the month, the lead was present on 22 days, representing a 76% frequency of occurrence. The maximum length of 250 nm (463 km) and width of 45 nm (83 km) both occurred during the prolonged opening that began on the 10th.

Multi-Year Ice: As is evident from a comparison of Figures 6-21, 6-27, and 6-28, the advance of multi-year ice into the Chukchi Sea stalled in February, and the western edge of the ice remained relatively static. The most significant change was an expansion of the tongue of ice that first appeared off Point Lay in late January (Figure 6-21). The lack of additional penetration is consistent with the existence of a relatively compact, stable ice canopy that resulted from light westerly winds and an absence of easterly storms. In the region containing multi-year ice, the concentrations ranged from negligible to an estimated 20%.

Ice Drift: Ice movement rates were investigated using seven multi-year floes, consisting of six that had been tracked in the Chukchi in January (Floes G, I, J, K, L, and M), and one that moved from the Beaufort to the Chukchi at the beginning of February (Floe F). The successive positions of the floes shown in Figure 6-29 were derived from RADARSAT-2 images acquired on February 2nd (all except Floe F), 4th (Floe F), 19th (all floes) and 26th (all floes).

All seven floes described similar tracks that produced modest displacements to the southwest. This outcome is consistent with the predominance of westerly winds (which reduced the westerly set of the Beaufort Gyre), absence of easterly storms, and compact ice canopy that were cited above as factors contributing to the absence of additional multi-year ice penetration into the Chukchi.

The floe speeds were the lowest recorded during the freeze-up study period, with along-track values ranging from 1.0 to 2.2 nm/day (1.9 to 4.1 km/day) in early February followed by 0.8 to 2.0 nm/day (1.5 to 3.7 km/day) in late February. The slightly higher speeds that prevailed during the first part of the month mirror the slightly higher frequency of easterly winds that occurred in this period.

The average monthly speeds, computed on the basis of the net displacements that occurred between the first and last RADRSAT-2 images, varied from 0.7 to 1.8 nm/day (1.3 to 3.3 km/day). The average was 1.2 nm/day (2.2 km/day).

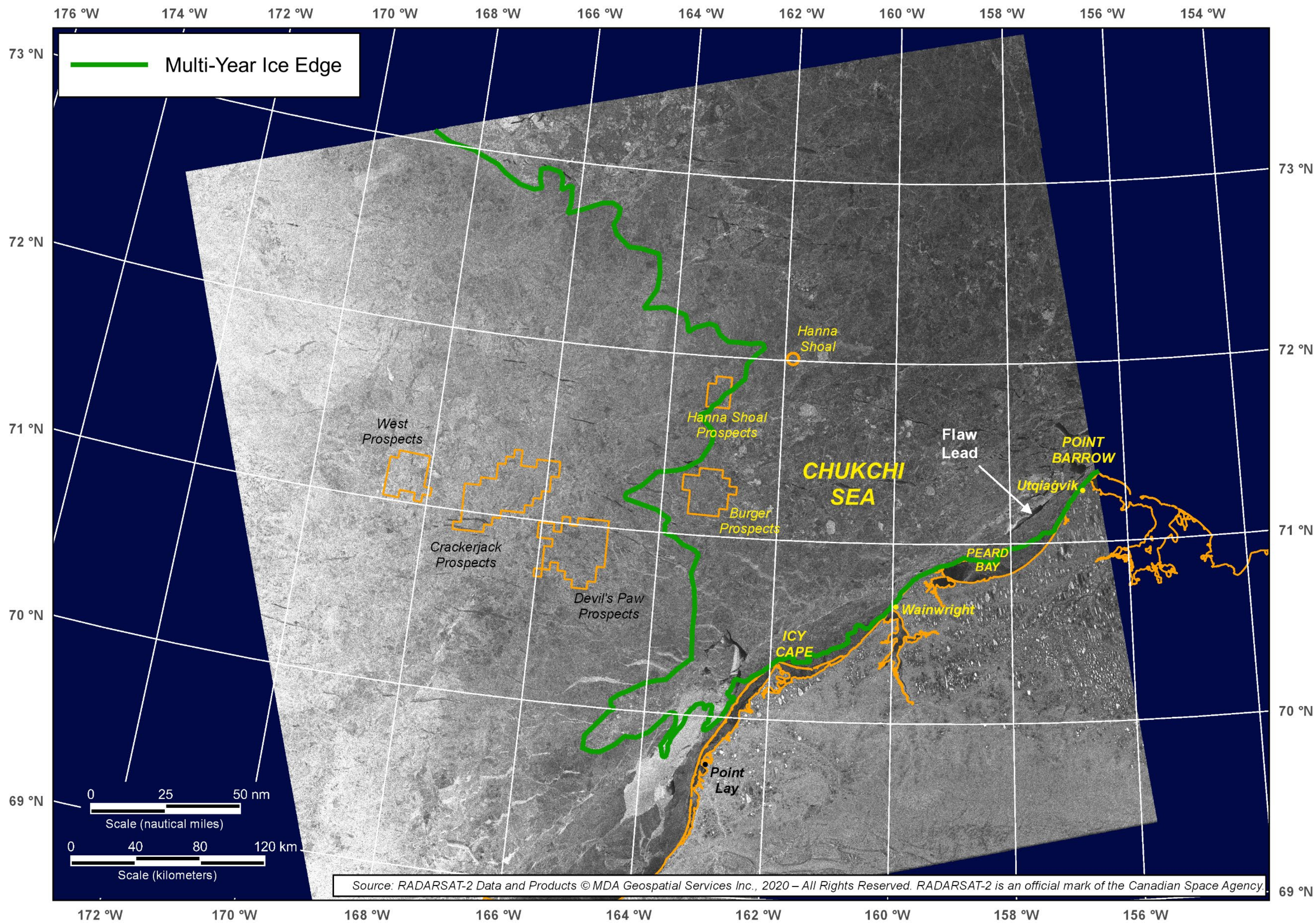

Figure 6-27. RADARSAT-2 Image of Chukchi Sea Acquired on February 19, 2020

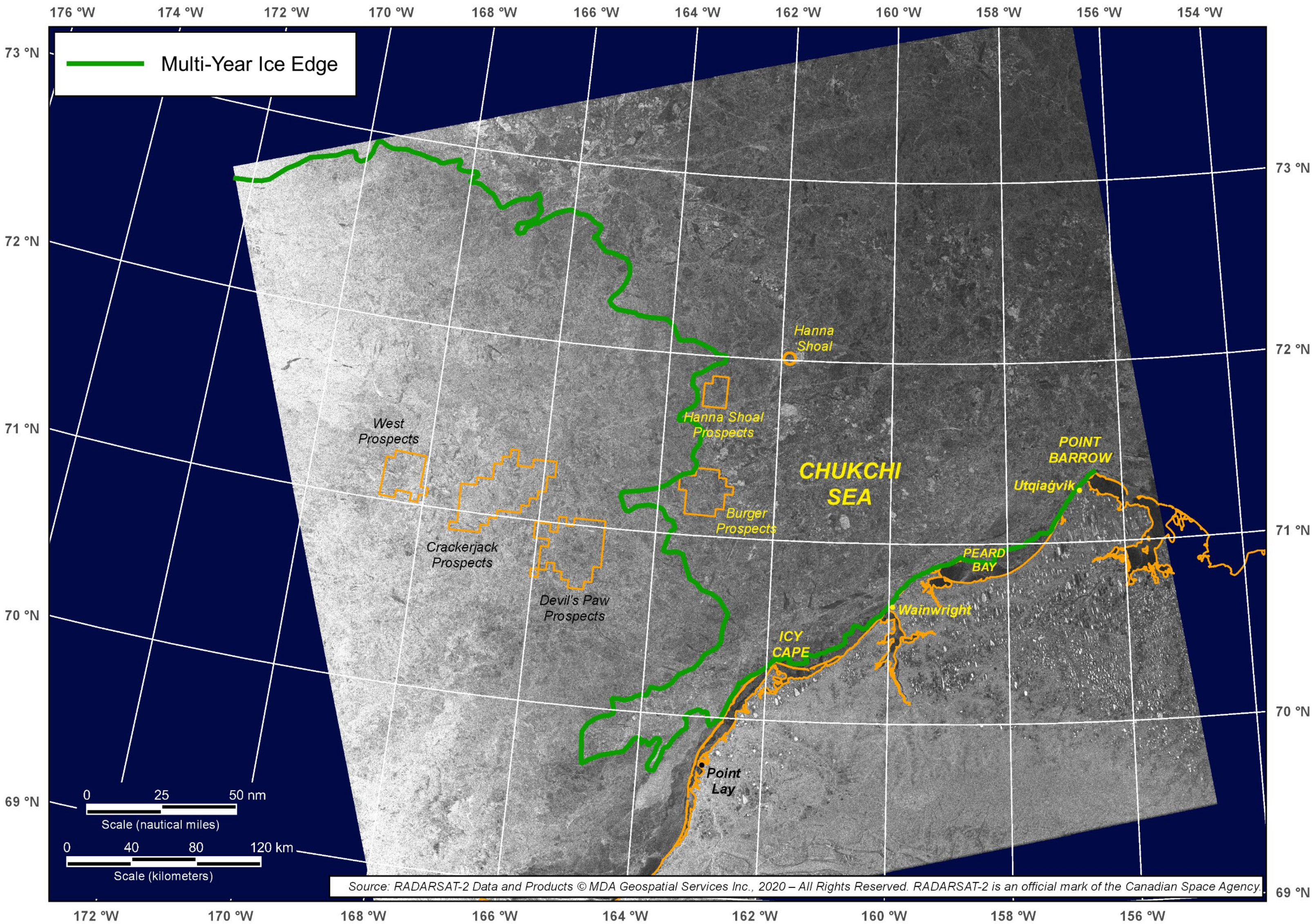

Figure 6-28. RADARSAT-2 Image of Chukchi Sea Acquired on February 26, 2020

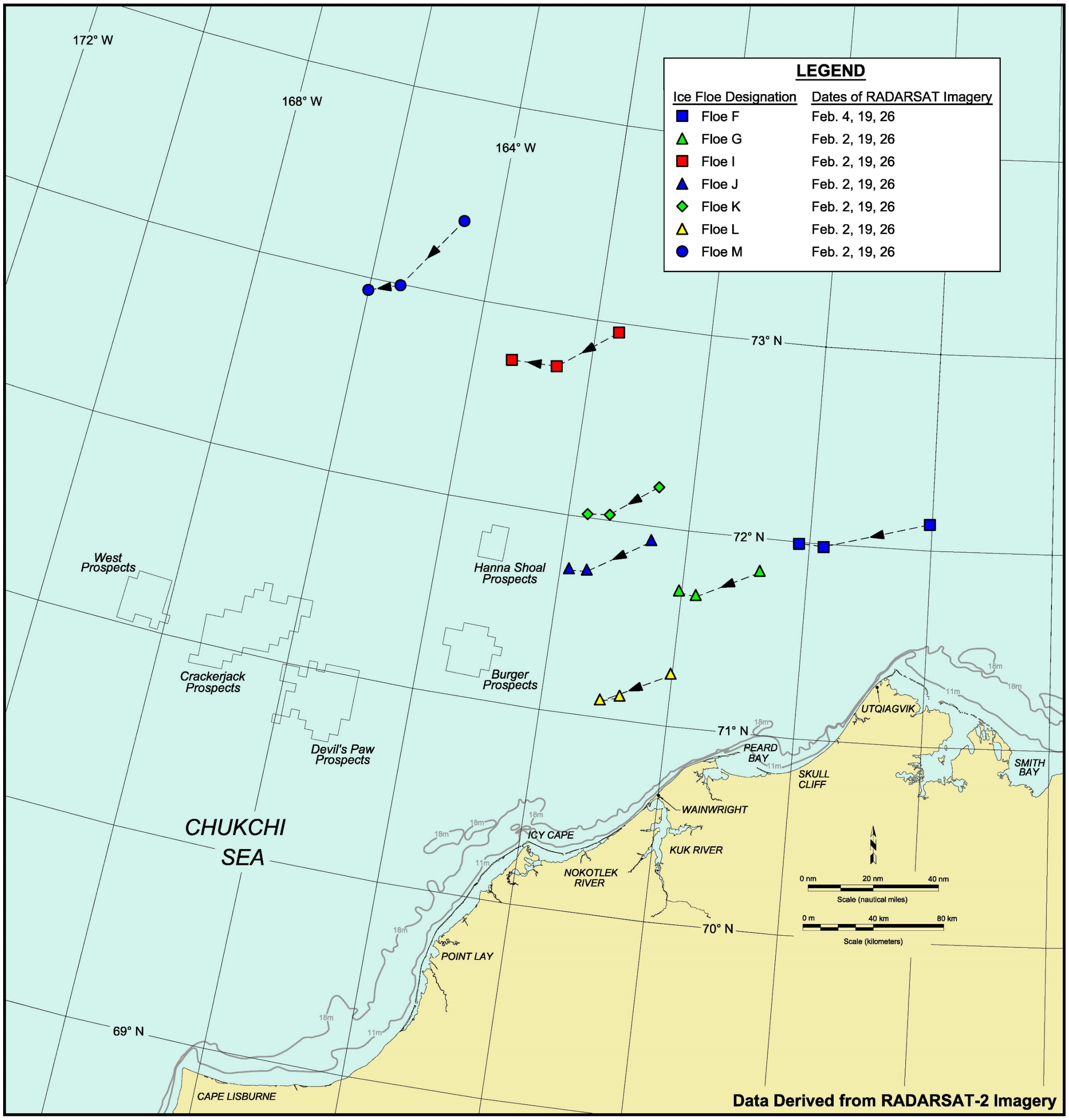

Figure 6-29. Chukchi Sea Multi-Year Ice Floe Displacements in February 2020

As shown in Figure 6-30, IABP Buoy X traveled to the east on February 1st and 2nd, to the west-southwest between the 2nd and 21st, and then back to the east-northeast between the 21st and 29th. Although the tracking period was longer and the intervals between successive positions much shorter, the linear trajectory and small net displacement of the buoy resemble those of the multi-year floes whose tracks are displayed in Figure 6-29.

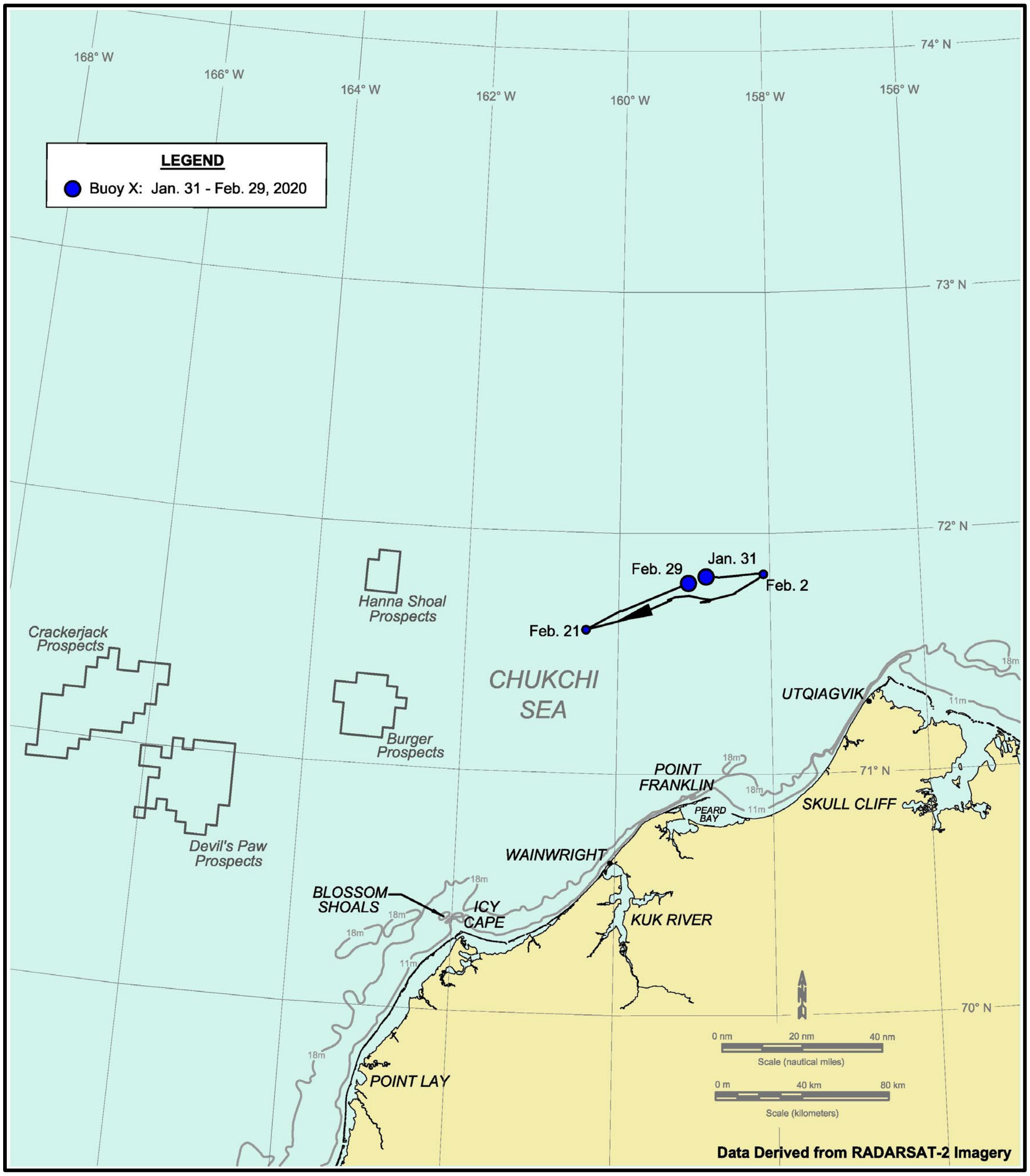

Figure 6-30. Chukchi Sea Drift Buoy Track in February 2020

The net displacement over the course of the month was a miniscule 5 nm (9 km) to the west-southwest, yielding an average speed of 0.2 nm/day (0.4 km/day). The peak speed between successive daily positions, 11.9 nm/day (22.1 km/day), occurred on February 28th (Figure 6-31). The daily average wind speed at Utqiagvik Airport was 13 kt (7 m/s) on this date, and the associated wind factor was 3.8%.

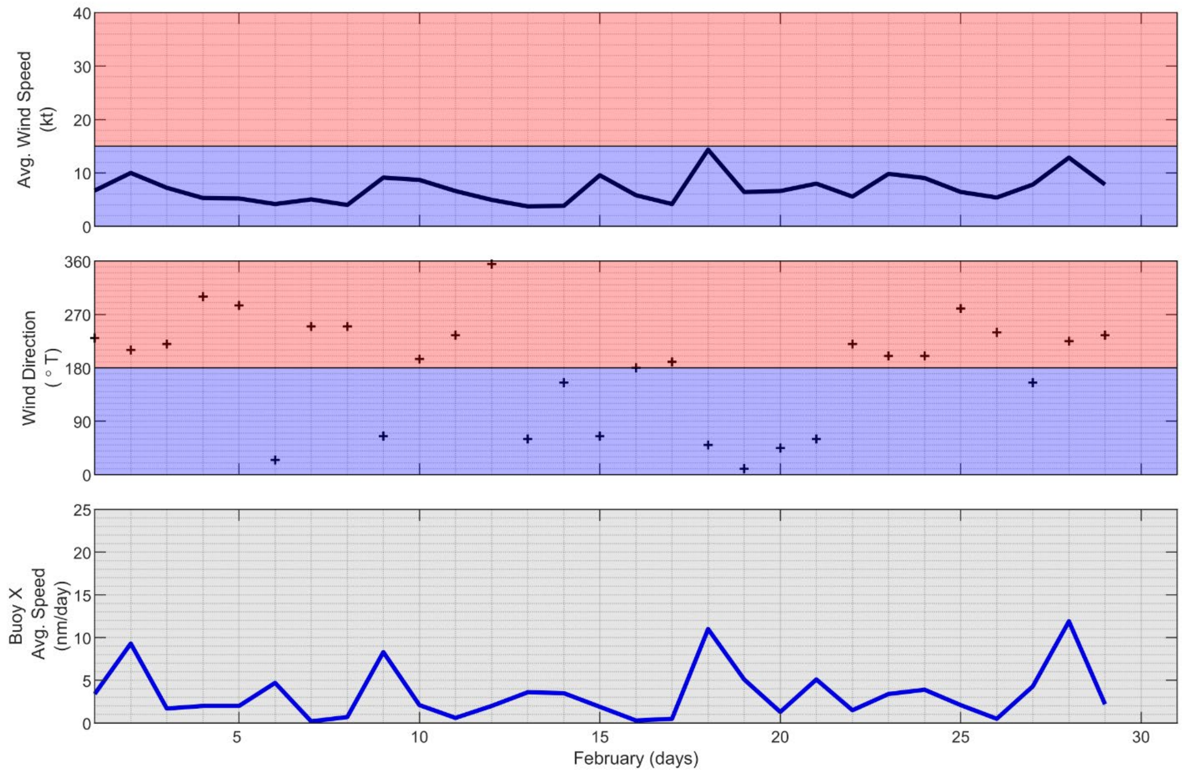

Figure 6-31. Chukchi Sea Drift Buoy Daily Average Speed in February 2020

6.4 Reconnaissance Flights

Aerial reconnaissance missions were undertaken in the Chukchi Sea on February 24th and 25th, at the end of the freeze-up study period. Chukchi Sea Flight No. 1 (Flight "C1" on Drawing CFC-1070-01-003) focused on the offshore region to the northwest and west of Utqiagvik, including Hanna Shoal and the Hanna Shoal and Burger Prospects. It should be noted that the Hanna Shoal Prospects are centered approximately 25 nm (46 km) to the southwest of Hanna Shoal itself (Figure 1-4). Chukchi Sea Flight No. 2 (Flight "C2" on the same drawing) was used to observe the coastal and nearshore region between Utqiagvik and Point Lay. A MODIS image obtained on the 24th is provided in Figure 6-32, while the RADARSAT-2 image acquired on February 26th appears in Figure 6-28.

6.4.1 Lagoon Ice

Most of the ice in the protected waters of Kasegaluk Lagoon, the Kuk River Inlet, and Peard Bay was found to be flat and featureless. Widely-scattered patches of 0.5-m rubble were observed in both Kasegaluk Lagoon and Peard Bay, however. The ice conditions in Peard Bay are shown in Plate 6-1, while those in South Kasegaluk Lagoon are shown in Plate 6-2.

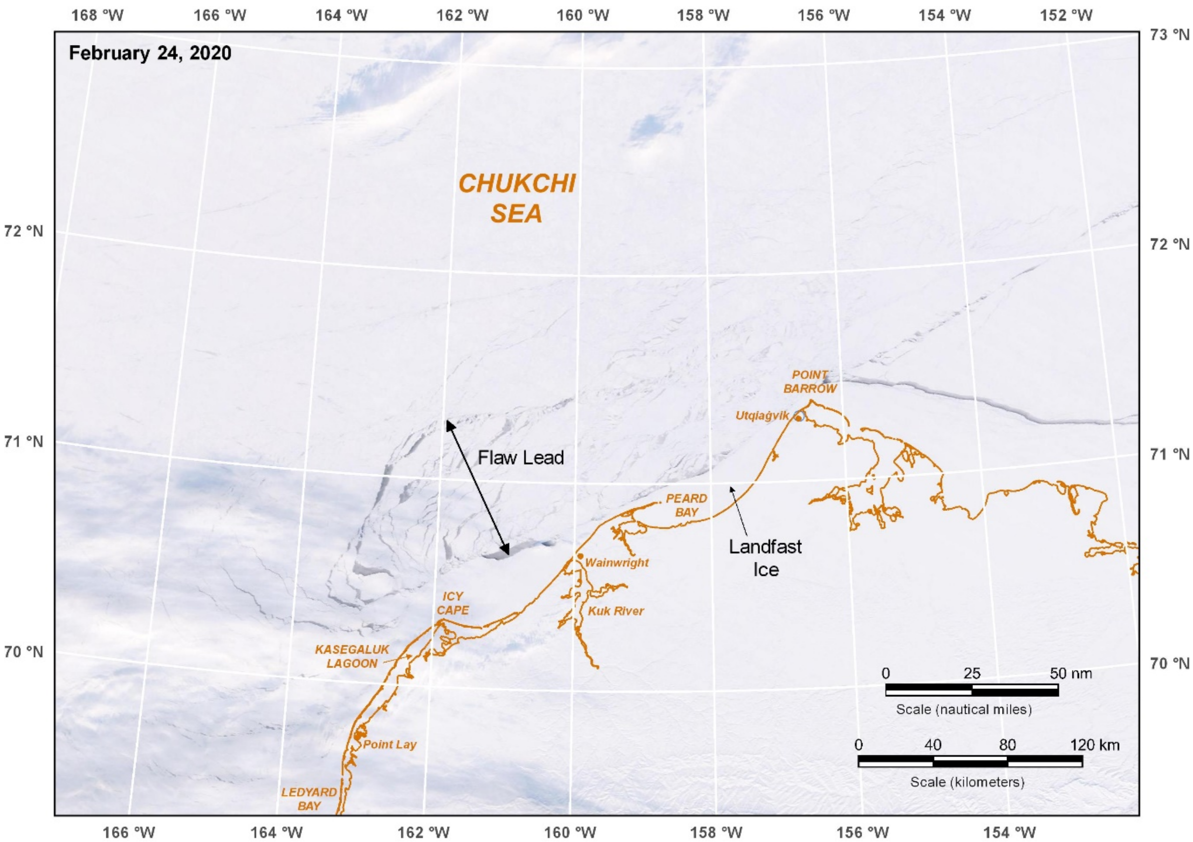

Figure 6-32. MODIS Image of Chukchi Sea Acquired on February 24, 2020

6.4.2 Landfast Ice

The landfast ice edge observed during the flights was consistent with that derived from the RADARSAT-2 image acquired on February 26th and shown in Figure 6-28. In keeping with the predominance of westerly winds and absence of easterly storms in the weeks preceding the flights, the width of the landfast ice zone was greater than that observed during many of the reconnaissance missions conducted in support of prior freeze-up studies (*e.g.*, Coastal Frontiers and Vaudrey, 2015; 2016; 2017).

The ice was anchored by grounded ridges and rubble piles with heights that typically ranged from 2 to 5 m and occasionally reached 7 m (Plate 6-2). At Blossom Shoals, anchoring was provided by a massive rubble pile that extended 25 m above the surrounding sea ice (Plate 6-3).

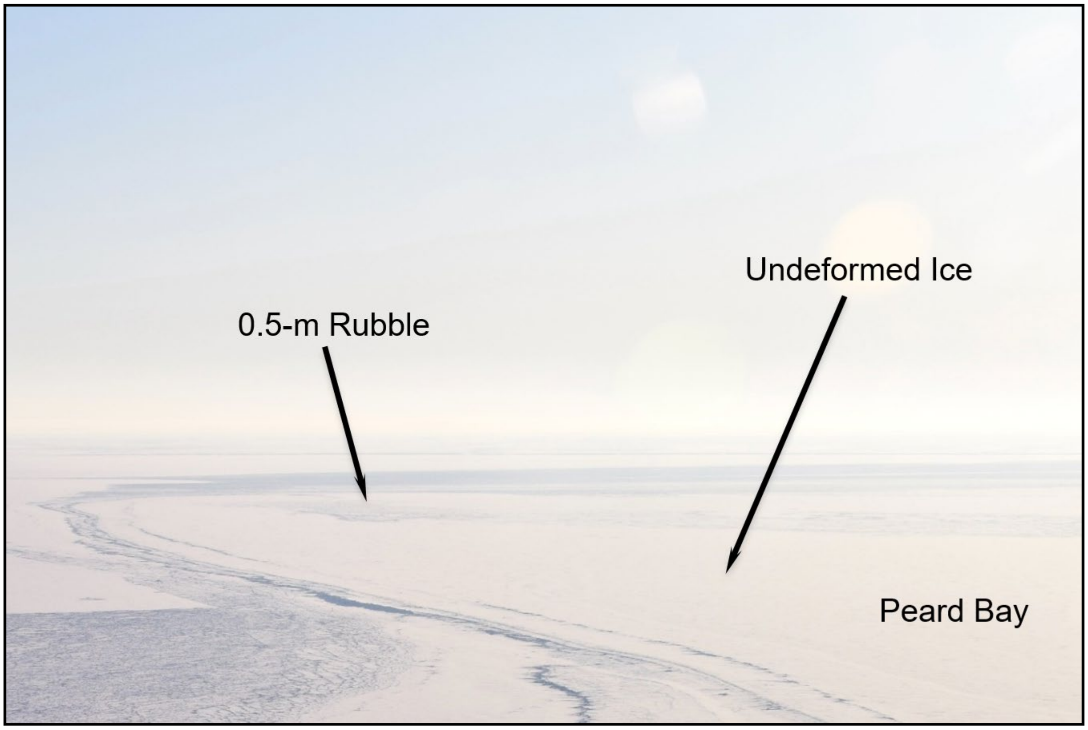

Plate 6-1. Undeformed Ice with Patch of 0.5-m Rubble in Peard Bay (looking south on February 25, 2020)

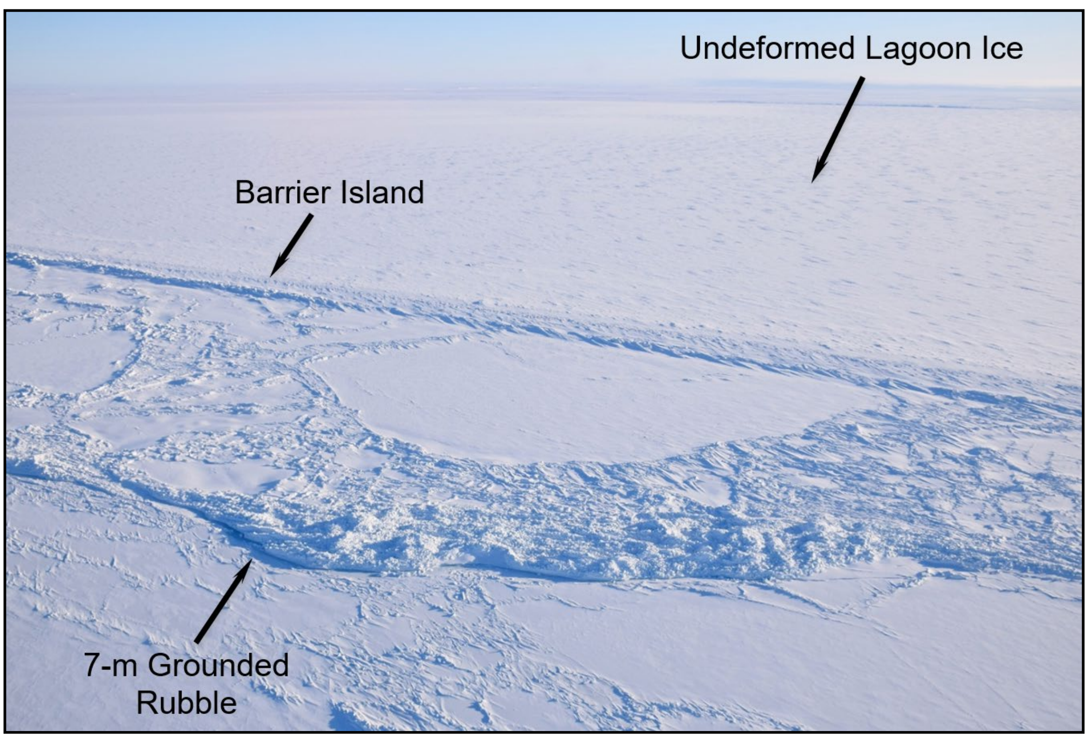

Plate 6-2. Undeformed Ice in South Kasegaluk Lagoon; 7-m Rubble Anchoring Landfast Ice (looking east on February 25, 2020)

Y BSEE DETERMINATION OR POLICY.”

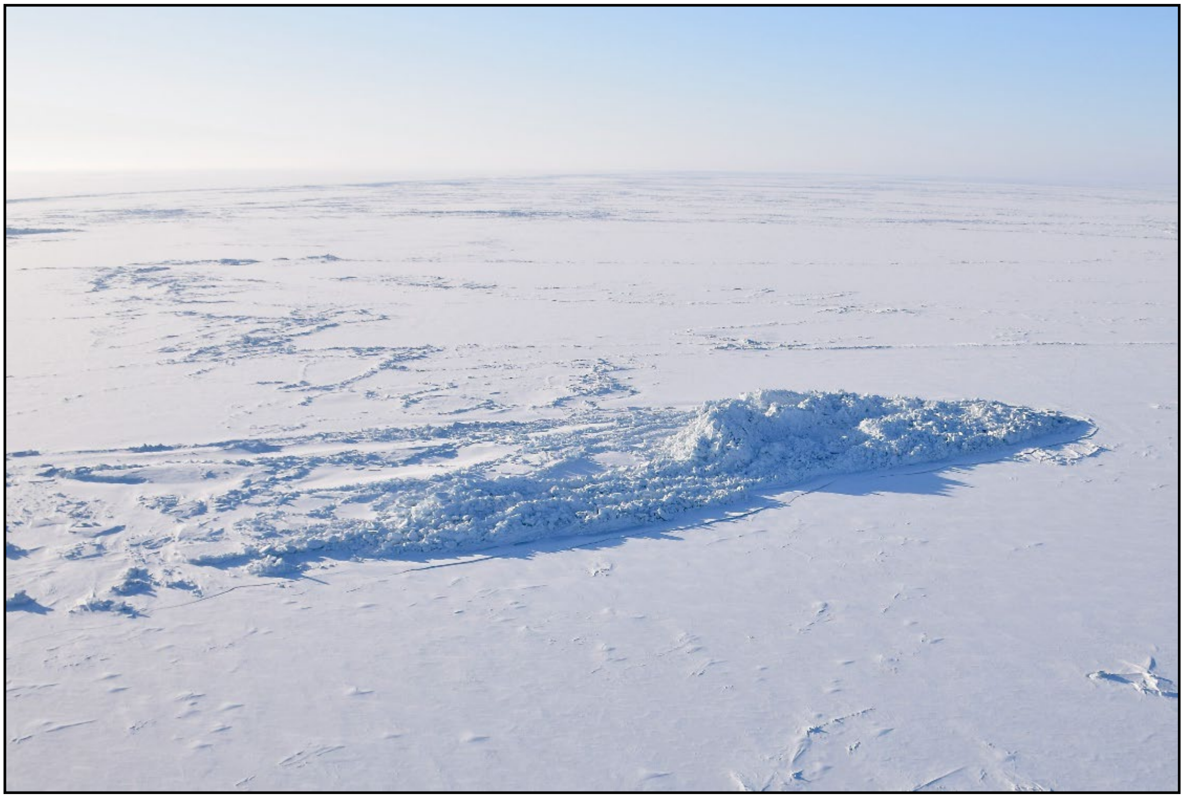

Plate 6-3. 25-m Rubble Pile on Blossom Shoals
(looking southwest on February 25, 2020)

6.4.3 Leads

Although the Chukchi Sea flaw lead typically develops in response to easterly winds, the moderate south-southwesterlies that prevailed from February 22nd through 24th contained an offshore component that was sufficient to maintain a narrow, refreezing lead adjacent to the landfast ice at the time of the flights (Plate 6-4). Numerous secondary leads emanating from this feature increased the width of the flaw lead to as much as 45 nm (83 km) (Figure 6-32). Farther offshore, the pack ice contained small leads, both open and refreezing, the density of which tended to decrease with distance to the south. A representative example from the Hanna Shoal Prospects is provided in Plate 6-5.

6.4.4 Pack Ice

The pack ice consisted primarily of first-year floes with diameters typically ranging from less than 500 m to 1 km and occasionally reaching 3 km (Plate 6-6). Deformation was moderate. Ridge and rubble heights of 2 to 3 m were common but heights to 5 m were observed in some areas, particularly in the vicinity of the flaw lead.

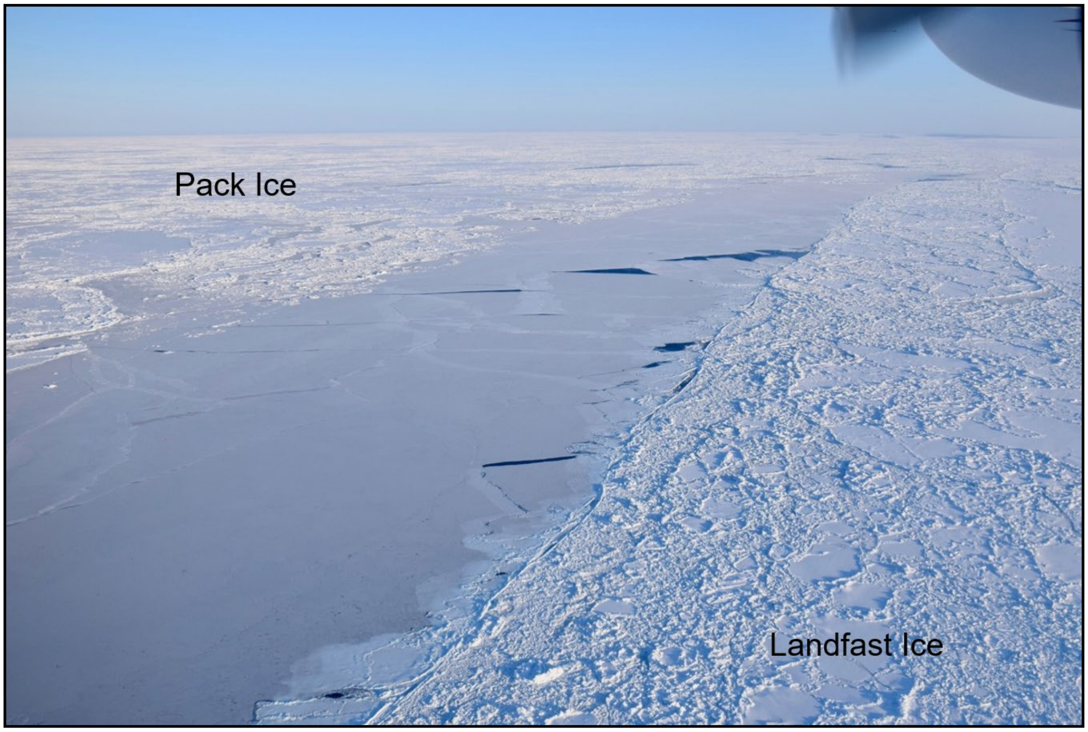

Plate 6-4. Refreezing Flaw Lead off Utqiagvik (looking northeast on February 25, 2020)

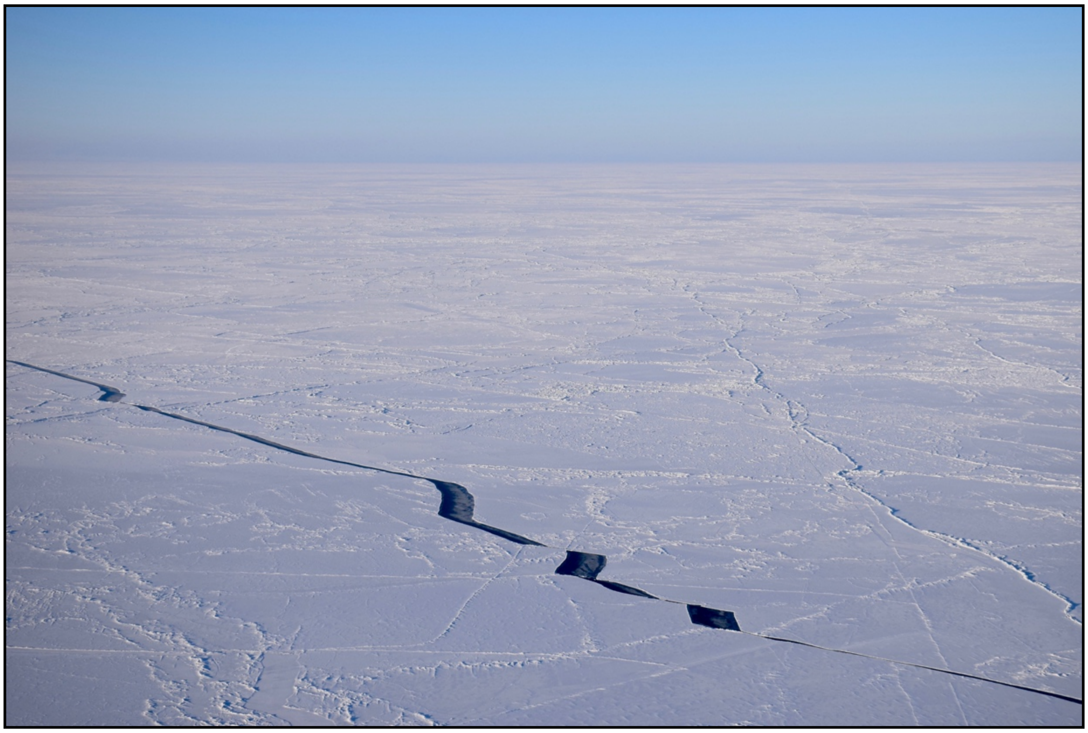

Plate 6-5. Narrow Lead and First-Year Ice in Hanna Shoal Prospects (looking west on February 24, 2020)

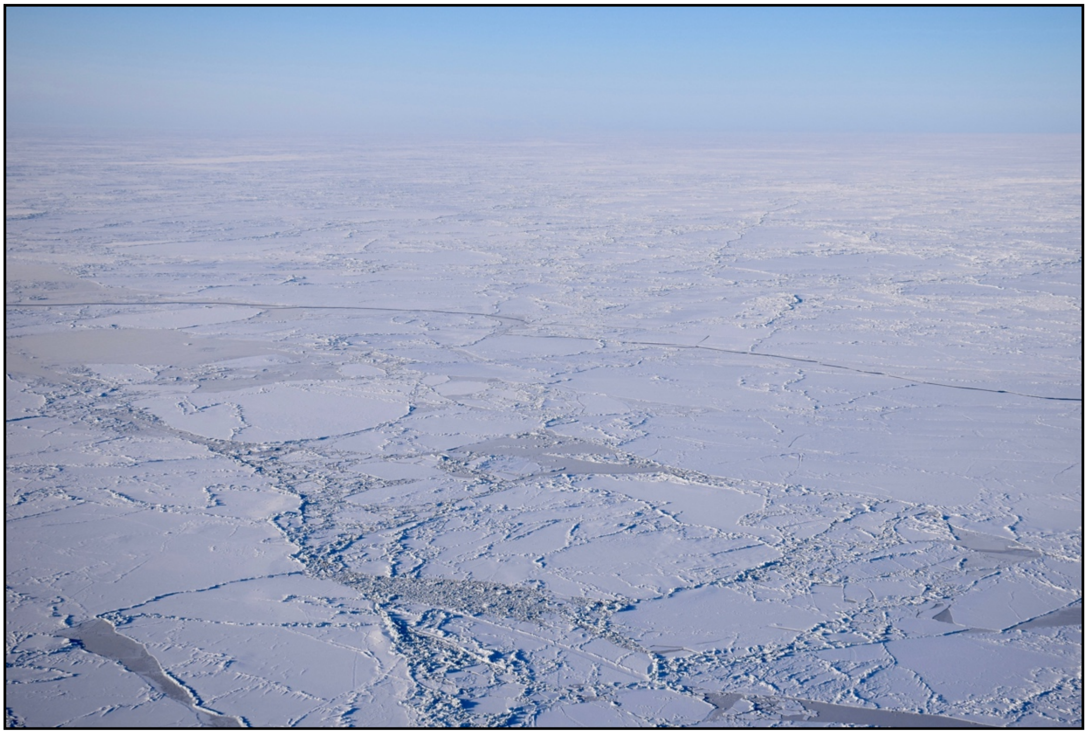

Plate 6-6. First Year Floes with Ridge and Rubble Heights to 4 m in Burger Prospects (looking west on February 24, 2020)

6.4.5 Ice Pile-Ups

Fifty-seven ice pile-ups were observed during the flight conducted on February 25th. As discussed in Section 6.1, the sole pile-up in South Kasegaluk Lagoon probably resulted from an easterly storm on November 26th that was followed by a westerly storm on the 28th and 29th. The remaining 56 pile-ups are believed to have formed in response to a similar easterly-westerly storm sequence that occurred from January 11th through 14th. The characteristics of all 57 pile-ups are summarized in Table 6-4, with representative examples shown in Plates 6-7 and 6-8.

6.4.6 Multi-Year Ice

Numerous multi-year ice floes were observed during both reconnaissance flights. The concentrations ranged from negligible to 30% in the offshore region, and from negligible to 20% in the nearshore region. The floes contained ridge heights to 5 m.

Although the maximum horizontal dimensions typically ranged from tens to hundreds of meters, substantially larger floes were noted in the offshore region to the west and northwest of Utqiagvik. The largest, an elliptical feature approximately 9 km long and 5 km wide with a maximum ridge height of 3 m, was located 80 nm (148 km) due west of

Plate 6-7. Massive, 20-m Pile-Up that Encroached 20 m onto Icy Cape (looking east on February 25, 2020)

Plate 6-8. 15-m Pile-Up that Encroached 25 m Onshore and Overtopped Skull Cliff (looking northeast on February 25, 2020)

Utqiagvik. Plate 6-9 displays a multi-year ice floe with an estimated diameter of 250 m and ridge height of 5 m that was located 10 nm (19 km) northwest of Utqiagvik.

Relatively small multi-year floes, with maximum horizontal dimensions typically less than 100 m but occasionally reaching 300 m, were embedded in the landfast ice zone at concentrations ranging from negligible to 20%. A representative example is shown in Plate 6-10.

6.4.7 Ice Conditions in Chukchi Sea Prospects

The ice canopy was relatively uniform in the Hanna Shoal Prospects, consisting of flat, first-year floes with maximum horizontal dimensions to 1 km, intermittent ridges and rubble with heights of 2 to 5 m, and multiple small leads, both open and refreezing (Plate 6-5). No multi-year ice was evident.

Similar conditions prevailed in the Burger Prospects. Flat, first-year floes predominated, with maximum horizontal dimensions to 1 km and ridge and rubble heights to 4 m (Plate 6-6). Multiple small leads, both open and refreezing, were present. The primary difference from the Hanna Shoal Prospects was the presence of multi-year ice floes in the northern half of the Burger Prospects. The concentration was less than 10%, and the maximum horizontal dimensions were small, ranging from tens of meters to 300 m. The ridge heights on these floes peaked at 4 m.

6.4.8 Katie's Floeberg

Katie's Floeberg forms each winter when ice rubble accumulates on Hanna Shoal, which lies 110 nm (204 km) northwest of Utqiagvik at 72°N, 162°W (Drawing CFC-1070-01-003). The shallowest water depth on the shoal is about 12 m, while the surrounding depths exceed 30 m.

The floeberg was identified as early as 1966 using Nimbus satellite imagery (Kovacs, *et al*., 1976). Its formation and growth have been described by a number of prior investigators, including Stringer and Barrett (1975), Kovacs, *et al*. (1976), Toimil and Grantz (1976), Barrett and Stringer (1978), and Vaudrey and Thomas (1981). In April 1980, the feature existed as a large oval of grounded first-year and multi-year rubble measuring 9 km long, 4.6 km wide, and up to 18 m above sea level (Vaudrey and Thomas, 1981). The long axis was oriented northeast-southwest, and the shallowest water depth was located at the southwest tip.

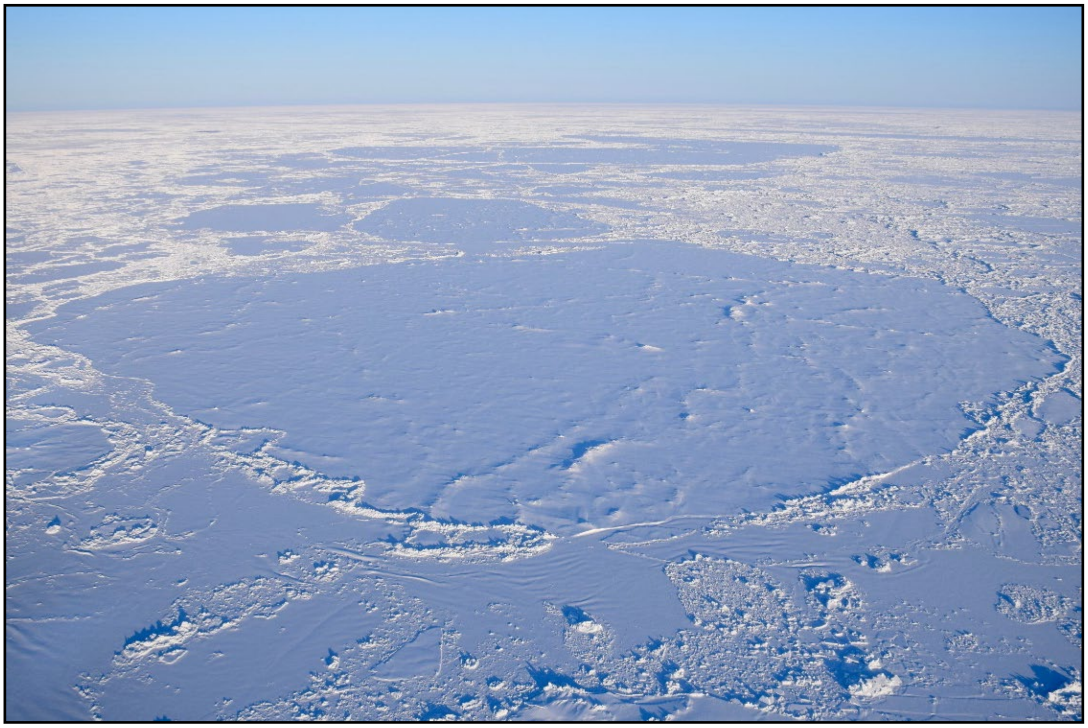

Plate 6-9. Multi-Year Ice Floe with Diameter of 250 m and Ridge Height of 5 m Located 10 nm Northwest of Utqiagvik (looking north on February 24, 2020)

Plate 6-10. Small Multi-Year Ice Floe Embedded in Landfast Ice 11 nm Southwest of Utqiagvik (looking west on February 25, 2020)

During the eight freeze-up studies conducted from 2009-10 through 2016-17, the floeberg was observed on five occasions: February 2011, February 2012, March 2014, February 2015, and February 2016 (Coastal Frontiers and Vaudrey, 2011; 2012a; 2014; 2015; 2016). The dimensions varied substantially, with lengths ranging from 2.8 to 10.0 km, widths from 1.2 to 5.0 km and maximum rubble heights from 8 to 12 m above sea level.

In February 2020, as in 2010, 2013, and 2017 (Coastal Frontiers and Vaudrey, 2010; 2013; 2017), Katie's Floeberg had not developed prior to the offshore reconnaissance flight. Instead, an agglomeration of multi-year ice floes with a combined diameter of 6.5 km had become grounded on Hanna Shoal (Plate 6-11). Ridges with heights to 5 m were present in the interior of the feature, along with rubble with an identical height of 5 m on its southwest side.

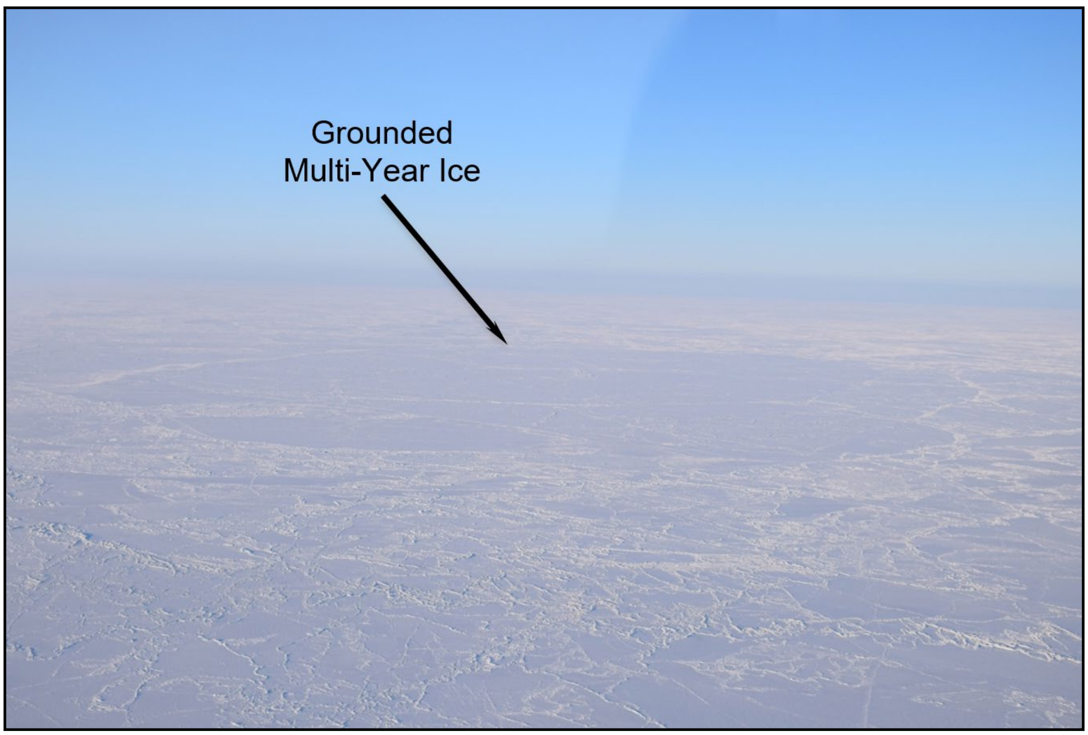

Plate 6-11. Agglomeration of Multi-Year Ice Floes Grounded on Hanna Shoal (looking northwest on February 24, 2020)

7. TRENDS

The primary objectives of this section are to characterize present-day freeze-up processes and recent trends using the data acquired during nine of the past eleven freeze-up seasons (2009-10 through 2016-17, and 2019-20), and to identify long-term trends by comparing the present-day processes with those in the 1980s.

Two of the most important influences on freeze-up are the air temperatures and wind conditions. Accordingly, the temperature and wind data from Utqiagvik Airport are analyzed to investigate perceived trends toward warmer conditions and higher storm frequencies. Both of these trends may make the sea ice more dynamic during freeze-up (Walsh and Eicken, 2007). Utqiagvik was selected over Deadhorse due to its longer period of record for meteorological data.

Following the analysis of air temperatures and winds, seven key aspects of ice behavior are evaluated: the timing of freeze-up, the duration of freeze-up, first-year ice growth, landfast ice development and stability, the Chukchi Sea flaw lead, multi-year ice invasions, and ice drift. Comparisons between the recently acquired data and those from the 1980s are used to assess long-term trends in ice behavior during freeze-up.

7.1. Air Temperatures

As discussed in Section 4.1, freezing-degree days (FDD) were computed as the difference between the freezing point of seawater (29°F; -2°C) and the daily average air temperature, and then accumulated by month. Negative FDD that resulted from air temperatures exceeding 29°F after freeze-up had begun were subtracted from the total.

Table 7-1 presents the accumulated FDD at Utqiagvik Airport for each winter season from 1970-71 through 2019-20. The table is divided into two parts, with the top portion showing the 25-year period from 1970-71 through 1994-95 and the bottom portion the subsequent 25-year period from 1995-96 through 2019-20. The column on the right side displays the rank of each winter over the 50-year period of record, with the highest ranking (No. 1) assigned to the warmest winter (fewest FDD at the end of the winter season) and the lowest ranking (No. 50) to the coldest (most FDD at the end of the winter season). The ten warmest winter seasons (50-yr rank of 1 through 10) are shown in red type.

Despite the cold temperatures that prevailed from late January through the end of February (Section 6.1), the winter of 2019-20 was the sixth warmest in the 50-year period of record, with 6,122 FDD. The warmest winter, with 4,764 FDD, occurred in 2017-18, while

Table 7-1. Accumulated Freezing-Degree Days (<29°F) at Utqiagvik, 1970-71 through 2019-20

Year	Sep	Oct	Nov	Dec	Jan	Feb	Mar	Apr	May	50-yr Rank
1970-71	129	1,013	2,009	3,224	4,727	6,270	7,734	8,738	9,098	49
1971-72	7	466	1,351	2,603	4,004	5,402	6,912	7,914	8,252	45
1972-73	30	275	1,103	2,092	3,410	4,591	6,135	7,086	7,393	29
1973-74	9	307	958	2,024	3,255	4,859	6,381	7,488	7,826	40
1974-75	18	725	1,823	3,546	5,263	6,453	7,579	8,584	8,891	48
1975-76	155	893	2,102	3,677	5,162	6,667	8,043	8,976	9,342	50
1976-77	12	486	1,281	2,689	3,836	5,107	6,694	7,756	8,066	43
1977-78	0	272	1,309	2,444	3,529	4,738	5,963	6,785	7,176	22
1978-79	17	696	1,404	2,734	3,710	5,082	6,496	7,393	7,684	34
1979-80	0	310	895	2,166	3,496	4,636	5,891	6,875	7,247	23
1980-81	117	566	1,586	2,969	3,896	5,148	6,384	7,221	7,389	28
1981-82	105	564	1,452	2,602	3,845	4,839	6,122	7,022	7,407	30
1982-83	32	723	1,896	3,084	4,578	5,821	7,136	7,925	8,300	46
1983-84	153	835	1,666	2,546	3,919	5,717	7,128	8,316	8,700	47
1984-85	0	366	1,479	2,799	3,925	5,218	6,517	7,585	7,780	37
1985-86	60	635	1,424	2,537	3,901	4,959	6,407	7,508	7,784	38
1986-87	13	404	1,262	2,359	3,661	5,033	6,295	7,306	7,579	33
1987-88	51	240	1,272	2,447	3,672	4,931	6,224	7,052	7,337	26
1988-89	49	886	2,164	3,351	4,994	5,546	6,637	7,327	7,687	35
1989-90	0	363	1,611	2,805	4,417	5,878	7,131	7,776	7,903	42
1990-91	25	400	1,477	2,863	4,177	5,499	6,947	7,718	7,748	36
1991-92	27	384	1,494	2,883	4,358	5,788	6,972	7,818	8,076	44
1992-93	154	666	1,569	2,737	4,027	5,150	6,439	7,114	7,300	25
1993-94	27	210	924	2,074	3,252	4,313	5,776	6,649	6,972	18
1994-95	60	699	1,827	3,222	4,493	5,758	7,175	7,817	7,898	41
Average	**50**	**535**	**1,494**	**2,739**	**4,060**	**5,336**	**6,685**	**7,590**	**7,873**	
Std. Dev.	**53**	**231**	**345**	**444**	**563**	**597**	**582**	**600**	**611**	
Year	**Sep**	**Oct**	**Nov**	**Dec**	**Jan**	**Feb**	**Mar**	**Apr**	**May**	**50-yr Rank**
1995-96	0	326	1,076	2,343	3,463	4,776	5,849	6,719	6,830	17
1996-97	87	816	1,431	2,469	3,911	5,120	6,425	7,184	7,473	31
1997-98	5	293	830	2,089	3,441	4,661	5,644	6,178	6,339	9
1998-99	0	132	1,023	2,275	3,681	4,860	6,243	7,179	7,375	27
1999-00	18	371	1,251	2,657	3,979	5,263	6,493	7,337	7,792	39
2000-01	31	392	1,251	2,300	3,510	4,388	5,764	6,584	7,137	21
2001-02	39	638	1,507	2,654	4,070	5,371	6,315	7,127	7,273	24
2002-03	0	175	849	1,811	3,028	4,269	5,483	6,104	6,329	8
2003-04	0	167	945	2,061	3,210	4,703	6,063	6,897	7,065	20
2004-05	9	243	1,045	2,205	3,341	4,501	5,636	6,436	6,648	14
2005-06	8	237	1,143	2,156	3,421	4,475	5,930	6,908	7,059	19
2006-07	0	102	790	1,769	3,160	4,258	5,615	6,232	6,599	12
2007-08	0	170	616	1,525	2,922	4,387	5,792	6,428	6,648	14
2008-09	3	195	933	1,809	3,109	4,103	5,492	6,297	6,438	11
2009-10	6	125	981	1,988	3,391	4,479	5,687	6,312	6,608	13
2010-11	7	199	739	1,925	3,121	4,113	5,216	6,117	6,388	10
2011-12	3	183	1,059	2,264	3,814	5,013	6,588	7,319	7,556	32
2012-13	0	76	765	1,959	3,131	4,463	5,598	6,451	6,676	16
2013-14	34	161	799	1,786	2,889	3,897	4,945	5,696	5,775	4
2014-15	0	235	809	1,926	3,150	4,149	5,398	6,066	6,174	7
2015-16	9	260	1,058	2,292	3,198	4,159	5,290	5,847	5,911	5
2016-17	0	32	495	1,383	2,283	3,263	4,385	5,047	5,194	3
2017-18	0	169	510	1,223	2,258	2,951	3,867	4,539	4,764	1
2018-19	0	134	752	1,833	3,006	3,682	4,387	5,034	5,114	2
2019-20	0	48	406	1,318	2,621	4,224	5,284	5,907	6,122	6
Average	**10**	**235**	**923**	**2,001**	**3,244**	**4,381**	**5,576**	**6,318**	**6,531**	
Std. Dev.	**20**	**175**	**275**	**381**	**460**	**564**	**665**	**723**	**768**	

the second warmest, with 5,114 FDD, occurred in 2018-19. It is noteworthy that the past seven winters, beginning in 2013-14, constitute the seven warmest on record. The coldest winter, with 9,342 FDD, occurred in 1975-76.

The accumulated FDD at the end of each winter season are plotted as a time series in Figure 7-1. The long-term warming trend implied by the recent air temperatures is readily apparent, with the number of FDD decreasing at an average rate of 54 per year since 1970-71. In addition, the rate of warming appears to be increasing: whereas the accumulated FDD trended lower at an average rate of 34 per year from 1970-71 through 1994-95, the rate nearly doubled to 62 per year from 1995-96 through 2019-20.

Acceleration in the rate of warming also is evident on a decadal time scale. Based on the data presented in Table 7-1, the average annual accumulated FDD declined by 3.8% from the 1970s to the 1980s, 5.2% from the 1980s to the 1990s, 8.1% from the 1990s to the 2000s, and 12.0% during the past ten winters. The total decline from the 1970s to the most recent decade is 26.3%. Melling and Riedel (2005) reported a more gradual warming trend in the air temperatures at Tuktoyaktuk, Canada. For the 30-year period from 1975 through 2004, they found that the average annual accumulated FDD decreased at a rate of 3.3% per decade.

Substantial deviations from the long-term warming trend, with durations of one to six years, are clearly evident in Figure 7-1. The relative magnitude of these deviations has increased; as shown in Table 7-1, the standard deviation in FDD at the end of the winter season amounted to 7.8% of the mean value from 1970-71 through 1994-95, versus 11.8% from 1995-96 through 2019-20.

Additional information on the increase in air temperatures that has occurred since the 1970s is provided in Figure 7-2, which compares the monthly average values at Utqiagvik over the past eleven winters (2009-10 through 2019-20) with those from 1971-72 through 1999-2000. The differences between the monthly values in 2019-20 alone and the long-term monthly averages also are shown. Over the past eleven years, the monthly average value has exceeded the long-term value by at least 3.9°F (2.2°C) in every month from September through May. The largest increases occurred in October (10.2°F; 5.7°C), November (9.4°F; 5.2°C) and February (8.0°F; 4.4°C). Seasonally, the greatest rise took place during early freeze-up, averaging: 7.8°F (4.3°C) from September through November. Subsequently, from December through May, the average monthly increase was 5.8°F (3.2°C). Over the entire nine-month period from September through May, the average temperature exceeded the

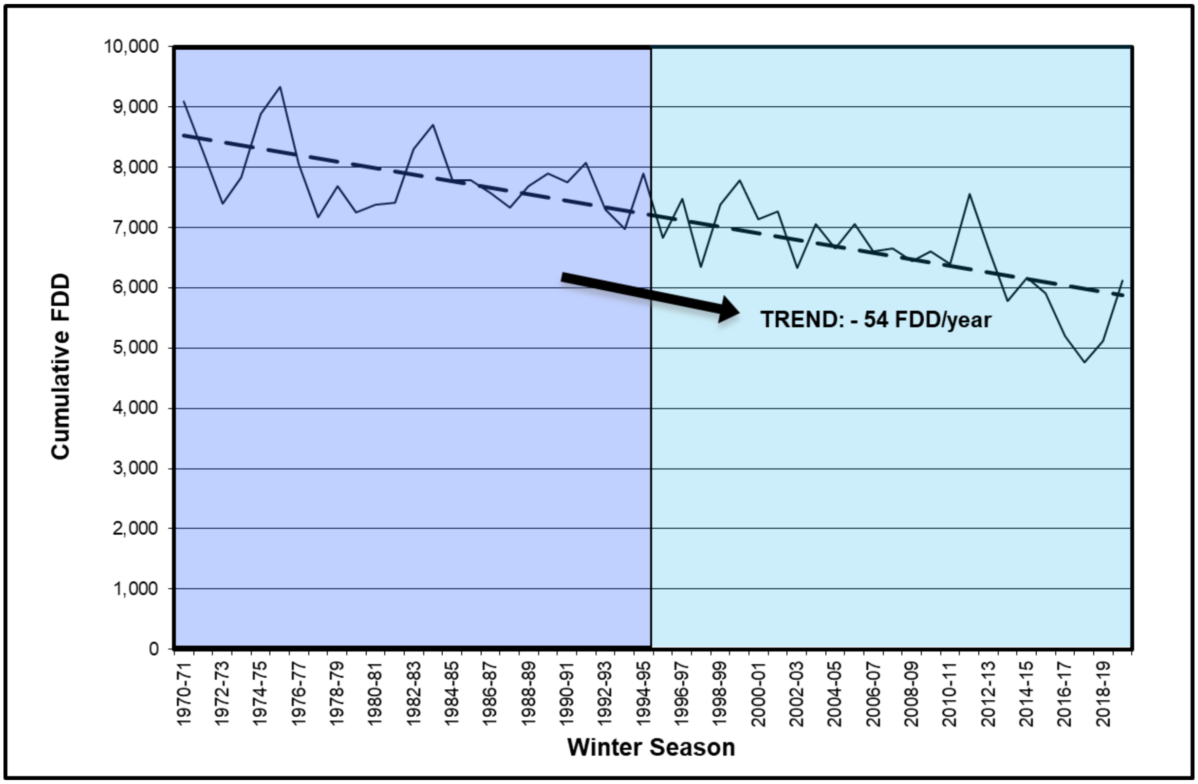

Figure 7-1. Accumulated FDD (<29°F) at Utqiagvik, 1970-71 through 2019-20

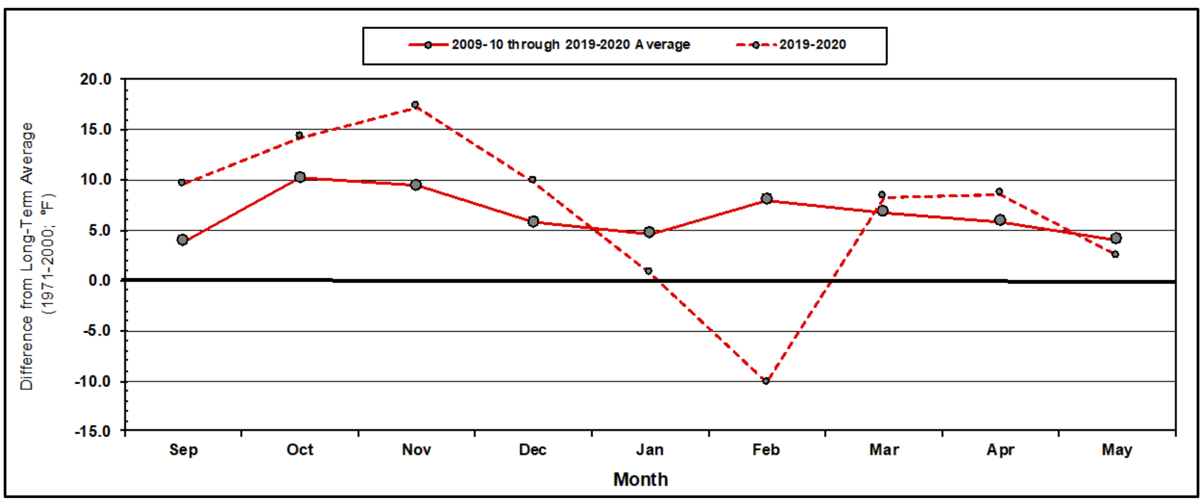

Figure 7-2. Differences between Recent Monthly Air Temperatures and Long-Term Average Values at Utqiagvik

long-term average value by 6.5°F (3.6°C). Lindsay and Zhang (2005) reported a similar pattern of pronounced increases in surface air temperatures over the Arctic Ocean during the fall and winter months.

As shown in Figure 7-2, the differences between the monthly average temperatures in 2019-20 and the long-term monthly averages varied substantially. The values ranged from 17.3°F (9.6°C) above the long-term average in November 2019 to 10.2°F (5.7°C) below in February 2020. The average superelevation over the nine-month period from September through May was 6.7°F (3.7°C).

Trends: Since the 1970s, progressively warmer winter seasons have caused the number of accumulated freezing-degree days at Utqiagvik to decline at an average rate of 54 per year. The rate of warming has accelerated, with the greatest increase in temperature taking place during the early portion of freeze-up.

7.2. Winds

The wind directions that prevailed at Deadhorse and Utqiagvik Airports from October through February from 2009-10 through 2016-17 and in 2019-20 are provided in Tables 7-2 and 7-3. The data are displayed graphically in Figure 7-3, which shows the frequency of occurrence of easterly winds at each site.

When compared with the eight freeze-up seasons from 2009-10 through 2016-17, 2019-20 was marked by exceptionally low percentages of easterly winds. In the Beaufort, easterlies prevailed only 36% of the time, which tied 2016-17 for the minimum frequency recorded in recent freeze-up studies. By comparison, westerlies and easterlies occurred with equal frequencies (50%) when the data from 2009-10 through 2016-17 are aggregated.

In the Chukchi, easterlies prevailed by a margin of 55% to 45%, but the frequency was substantially lower than the prior minimum of 61% recorded in both 2013-14 and 2016-17. During the eight freeze-up seasons from 2009-10 through 2016-17, easterlies occurred with an average frequency of 69% while westerlies occurred with a frequency of 31%.

The storms that occurred at Deadhorse and Utqiagvik Airports in recent freeze-up seasons are summarized in Tables 7-4 and 7-5. Both the number of discrete storm events and the total number of days with storm conditions (“storm-days”) are shown. As in the case of Sections 5 and 6, a storm is defined as an event during which the daily average sustained wind speed exceeds 15 kt (8 m/s).

Storm frequency, particularly with respect to easterly events, was low by recent standards. In the Beaufort, where nine easterly and seven westerly storms occurred on average during the freeze-up seasons from 2009-10 and 2016-17, only four easterlies and five westerlies were recorded in 2019-20. The numbers of easterly storms (4), easterly storm

Table 7-2. Beaufort Sea Wind Directions, 2009-10 through 2016-17 and 2019-20

Season	2009-10 East	2009-10 West	2010-11 East	2010-11 West	2011-12 East	2011-12 West	2012-13 East	2012-13 West	2013-14 East	2013-14 West	2014-15 East	2014-15 West	2015-16 East	2015-16 West	2016-17 East	2016-17 West	2009-10 through 2016-17 Average East	2009-10 through 2016-17 Average West	2019-20 East	2019-20 West
October	20	11	25	6	23	8	6	25	15	16	18	13	22	9	20	11	19	12	**12**	**19**
November	19	11	15	15	7	23	4	26	10	20	23	7	19	11	10	20	13	17	**12**	**18**
December	15	16	13	18	15	16	14	17	13	18	20	11	16	15	11	20	15	16	**14**	**17**
January	7	24	16	15	3	28	18	13	18	13	14	17	21	10	7	24	13	18	**10**	**21**
February	16	12	8	20	19	10	21	7	11	17	12	16	28	1	7	21	15	13	**6**	**23**
Total Days	77	74	77	74	67	85	63	88	67	84	87	64	106	46	55	96	75	76	**54**	**98**
Frequency	**51%**	**49%**	**51%**	**49%**	**44%**	**56%**	**42%**	**58%**	**44%**	**56%**	**58%**	**42%**	**70%**	**30%**	**36%**	**64%**	**50%**	**50%**	**36%**	**64%**

Note: Table 7-2 is based on the average daily wind directions recorded at Deadhorse Airport.

Table 7-3. Chukchi Sea Wind Directions, 2009-10 through 2016-17 and 2019-20

Season	2009-10 East	2009-10 West	2010-11 East	2010-11 West	2011-12 East	2011-12 West	2012-13 East	2012-13 West	2013-14 East	2013-14 West	2014-15 East	2014-15 West	2015-16 East	2015-16 West	2016-17 East	2016-17 West	2009-10 through 2016-17 Average East	2009-10 through 2016-17 Average West	2019-20 East	2019-20 West
October	23	8	29	2	28	3	10	21	22	9	20	11	27	4	23	8	23	8	**14**	**17**
November	21	9	18	12	16	14	13	17	16	14	26	4	26	4	23	7	20	10	**18**	**12**
December	22	9	22	9	27	4	21	10	17	14	28	3	22	9	18	13	22	9	**24**	**7**
January	13	18	21	10	14	17	29	2	22	9	21	10	29	2	15	16	21	11	**17**	**14**
February	22	6	10	18	23	6	25	3	15	13	15	13	29	0	13	15	19	9	**11**	**18**
Total Days	101	50	100	51	108	44	98	53	92	59	110	41	133	19	92	59	104	47	**84**	**68**
Frequency	**67%**	**33%**	**66%**	**34%**	**71%**	**29%**	**65%**	**35%**	**61%**	**39%**	**73%**	**27%**	**88%**	**12%**	**61%**	**39%**	**69%**	**31%**	**55%**	**45%**

Note: Table 7-3 is based on the average daily wind directions recorded at Utqiagvik Airport.

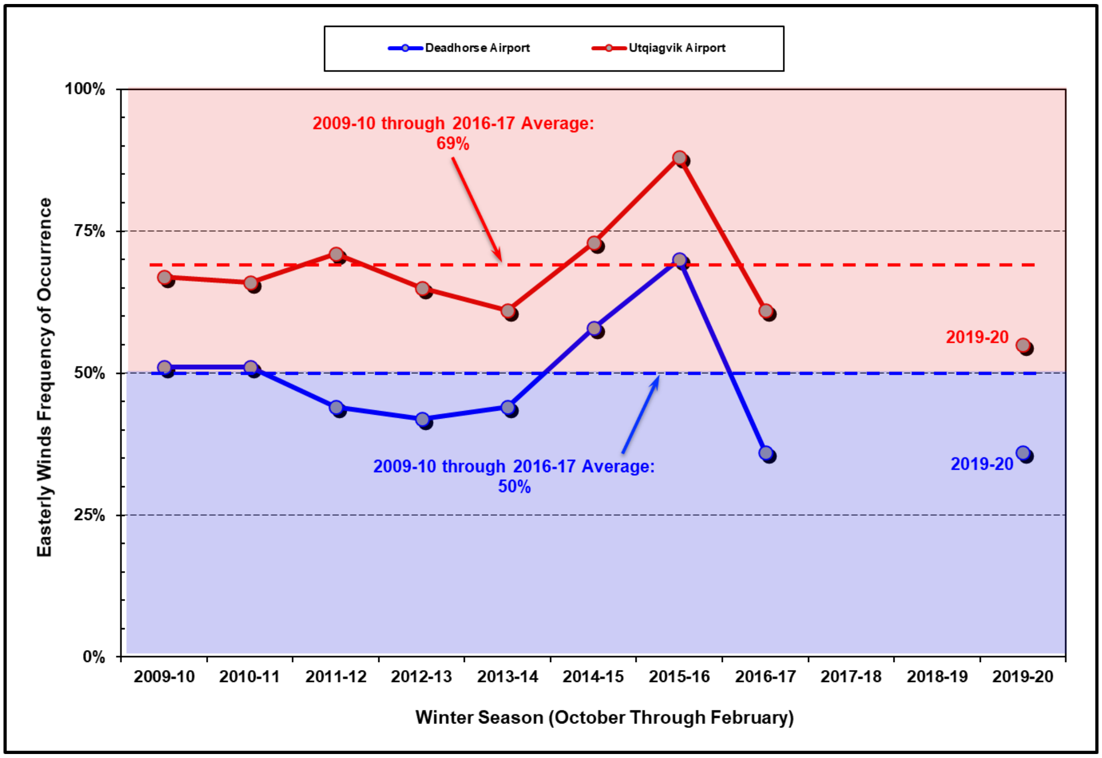

Figure 7-3. Frequency of Occurrence of Easterly Winds at Deadhorse and Utqiagvik

Table 7-4. Beaufort Sea Storms, 2009-10 through 2019-20[1]

Freeze-Up Season[2]	Easterly Storms	Westerly Storms	Total Storms	Easterly Storm-Days	Westerly Storm-Days	Total Storm-Days
2009-10	8	4	12	20	11	31
2010-11	8	10	18	19	21	40
2011-12	7	5	12	15	17	32
2012-13	8	8	16	25	14	39
2013-14	9	11	20	23	20	43
2014-15	10	6	16	26	16	42
2015-16	12	4	16	41	4	45
2016-17	7	6	13	12	19	31
2009-10 through 2016-17 Average	**9**	**7**	**15[3]**	**23**	**15**	**38**
2019-20	**4**	**5**	**9**	**9**	**9**	**18**

Notes:

1 Table 7-4 includes all storm events with a daily average sustained wind speed exceeding 15 kt (8 m/s) at Deadhorse Airport.

2 The period of record extends from October 1st through February 28th/29th.

3 The total no. of storms differs from the sum of easterly and westerly storms due to rounding.

Table 7-5. Chukchi Sea Storms, 2009-10 through 2019-20[1]

Freeze-Up Season[2]	Easterly Storms	Westerly Storms	Total Storms	Easterly Storm-Days	Westerly Storm-Days	Total Storm-Days
2009-10	11	2	13	32	3	35
2010-11	10	8	18	27	13	40
2011-12	8	3	11	21	6	27
2012-13	10	4	14	31	7	38
2013-14	12	7	19	29	13	42
2014-15	13	4	17	33	7	40
2015-16	16	0	16	47	0	47
2016-17	8	6	14	18	19	37
2009-10 through 2016-17 Average	**11**	**4**	**15**	**30**	**8**	**38**
2019-20	**9**	**4**	**13**	**16**	**7**	**23**

Notes:

1 Table 7-5 includes all storm events with a daily average sustained wind speed exceeding 15 kt (8 m/s) at Utqiagvik Airport.

2 The period of record extends from October 1st through February 28th/29th.

days (9), total storms (9), and total storm days (18) in 2019-20 all represented historical minima relative to those from 2009-10 through 2016-17. Storm duration also was low, averaging 2.3 days/event for easterlies and 1.8 days/event for westerlies versus recent averages of 2.6 and 2.1 days/event, respectively.

In the Chukchi, the paucity of storms in 2019-20 was less pronounced than in the Beaufort: nine easterlies and four westerlies versus with recent averages of 11 easterlies and four westerlies. Nevertheless, the numbers of easterly storm days (16) and total storm days (23) represented historical minima, and storm durations were low: 1.8 days/event for both easterlies and westerlies compared with recent averages of 2.7 days/event for easterlies and 2.0 days/event for westerlies.

Notwithstanding the differences between the Beaufort and Chukchi in terms of wind and storm direction, the average numbers of storms and storm-days have been nearly identical for the nine recent freeze-up seasons for which data have been acquired (2009-10 through 2016-17 and 2019-20). Each basin has averaged 15 storms from October through February, with 36 storm-days in the Beaufort and 37 in the Chukchi.

Unfortunately, data pertaining to storm events in the 1980's suitable for direct comparison with those in Tables 7-4 and 7-5 are not readily available. However, an indication of storm conditions in that era was developed by Dickins and Vaudrey (1994), who compiled mid-winter wind data (January through April) at Utqiagvik for the 18-year period from 1977 through 1994. They defined a storm as having a sustained wind speed exceeding 15 kt (8 m/s) for a period exceeding 12 hours. The six winters from 1981 through 1986 were excerpted from this database in order to compare the mid-winter storm frequency in the early 1980s with that which occurred in the recent past.

The results of the comparison are shown in Figure 7-4. Whereas Dickins and Vaudrey computed an average of 8.5 storm events per mid-winter season in the early 1980s, the number has ranged from four (2019-20) to 13 events in recent years. The average, 9.0 storms per winter, represents a *de minimus* increase of less than 6%.

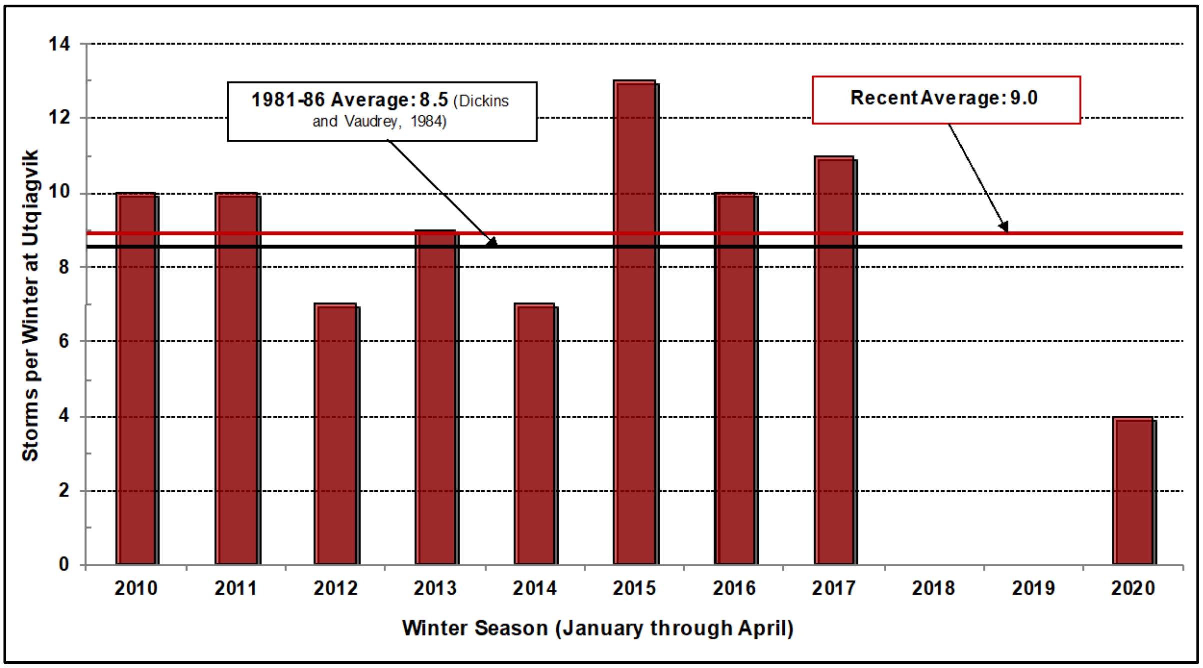

Figure 7-4. Storms per Winter at Utqiagvik Airport, 2010-2019

A cyclical trend in storm frequency is evident in the data compiled by Walsh and Eicken (2007), who tabulated the number of storm events at Utqiagvik during the open-water and freeze-up seasons from 1950 through 2004 (Figure 7-5). The storm count during freeze-up increased from the mid-1950s to early 1960s, declined from the early 1960s to mid-1970s, rose again from the mid-1970s to early 1990s, and remained nearly static from the early 1990s to early 2000s. The criteria used to define storm events are not specified, but the data nevertheless indicate that: (1) the increase in storm frequency that began in the mid-1970s was sustained through the early 2000s and (2) the storm frequency was approximately 50% higher

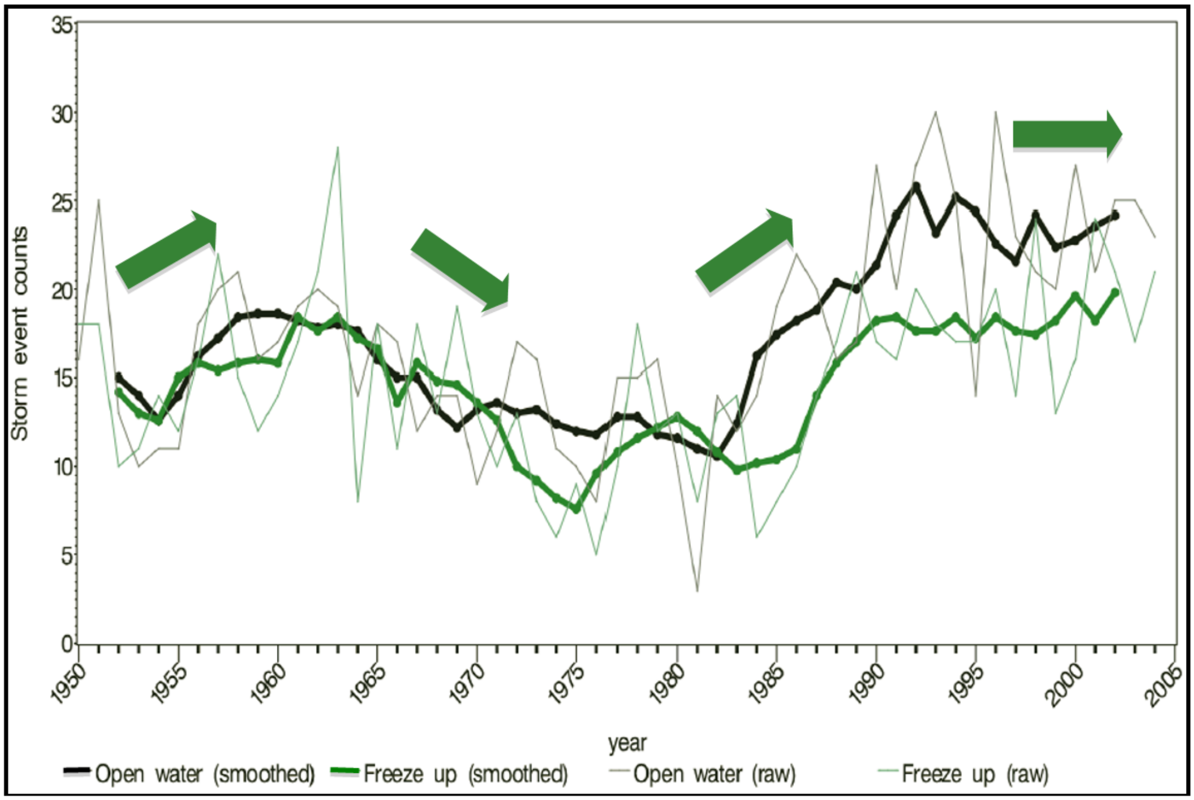

Figure 7-5. Yearly Storm Count at Utqiagvik during Open-Water and Freeze-Up Seasons, 1950-2004 (after Walsh and Eicken, 2007)

in the early 2000s than in the early 1980s. Although other wind characteristics such as direction and duration also influence ice dynamics, the rise in the number of storm events during freeze-up that has occurred since the mid-1970s could be causing an increase in wind-driven ice movement and deformation.

Trends: Since the early 1980s, the frequency of storm events during freeze-up has increased by about 50%. The frequency of mid-winter storms (January through April) appears to have remained stable.

7.3. Timing of Freeze-Up

As discussed in Section 7.1 and illustrated in Figure 7-2, the monthly average air temperatures at Utqiagvik in recent years have exceeded the long-term averages for the period from 1971-72 through 1999-2000 by substantial margins in late summer and early autumn. Based on an analysis conducted by Lindsay and Zhang (2005) using a coupled ice-ocean model, these warmer temperatures in late summer and early autumn have resulted from, and in turn contributed to, a decline in the extent and thickness of the pack ice and an increase in the temperature of the sea surface. This positive feedback loop (Figure 7-6) has caused a

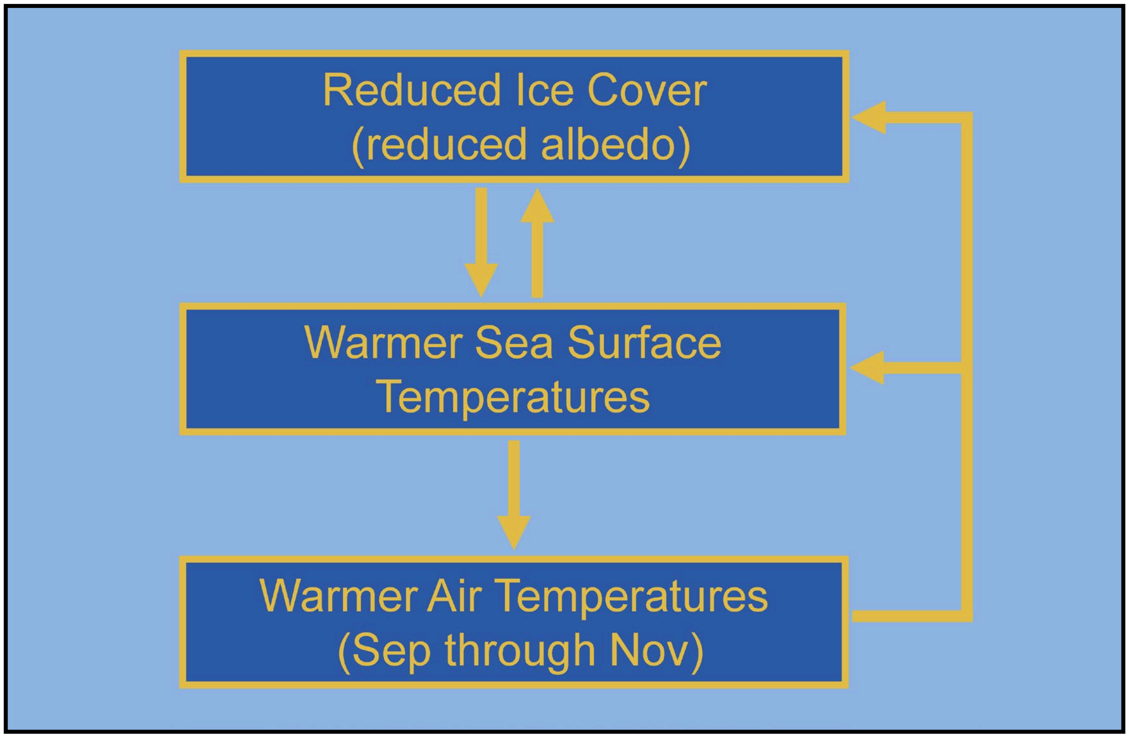

Figure 7-6. Positive Feedback Loop Causing Delay in Onset of Freeze-Up

significant delay in the onset of freeze-up in the Beaufort and Chukchi Seas (National Snow and Ice Date Center, 2020).

Table 7-6 presents the timing of freeze-up in the Alaskan Beaufort Sea from 2009 through 2016 and in 2019. The date of nearshore freeze-up ranged from October 11th to November 11th, with the latter occurring in 2019. The average date, October 28th, is eight days later than the average from 2002 through 2006 (Vaudrey, 2007) and 24 days later than that derived from 11 years of on-site observations and satellite imagery acquired from 1980 through 1985 and 1987 through 1991 (Vaudrey, 1982a; 1983; 1984; 1985a; 1985b; 1986; 1988a; 1989a; 1990; 1991; 1992). The standard deviation in the date of nearshore freeze was nine days in recent years, while the number of accumulated FDD at the time of nearshore freeze-up varied widely, from 80 to 363. The mean value was 204, with a standard deviation of 98.

In the nine years covered by recent freeze-up studies, complete freeze-up in the Alaskan Beaufort Sea took place between October 31st and November 24th. As in the case of nearshore freeze-up, the latest date occurred in 2019. The average date was November 10th, with a standard deviation of ten days. The number of FDD at complete freeze-up varied widely over the period of record, from 201 to 678. The average value was 432, with a standard deviation

Table 7-6. Timing of Freeze-Up in Alaskan Beaufort Sea, 2009-2016 and 2019

Year	Date of First Ice[1]	FDD at Time of First Ice	Date of Nearshore Freeze-Up[1]	FDD at Time of Nearshore Freeze-Up	Date of Complete Freeze-Up[1]	FDD at Time of Complete Freeze-Up
2009	Sep 28	15	Oct 22	106	Nov 9	412
2010	Oct 4	19	Oct 11	80	Nov 2	305
2011	Oct 12	14	Oct 26	102	Nov 1	201
2012	Oct 15	51	Nov 5	363	Nov 12	508
2013	Sep 24	19	Oct 26	197	Nov 20	678
2014	Oct 2	1	Oct 30	193	Nov 5	319
2015	Sep 21	0	Oct 26	219	Oct 31	318
2016	Oct 15	2	Nov 7	280	Nov 23	563
2019	Oct 14	25	Nov 11	300	Nov 24	585
Average	**Oct 5**	**16**	**Oct 28**	**204**	**Nov 10**	**432**
Std. Dev.	**9 days**	**16**	**9 days**	**98**	**10 days**	**159**

Note:
[1] First Ice, Nearshore Freeze-Up, and Complete Freeze-Up are defined in Section 2.

of 159. This outcome confirms the finding of previous freeze-up studies (*e.g.*, Coastal Frontiers and Vaudrey, 2014; 2016) that air temperature alone cannot be used to predict the date of freeze-up, and that other factors such as the sea surface temperature, wind conditions, and salinity must be taken into account.

Recent freeze-up dates in the Chukchi Sea are presented in Table 7-7. Nearshore freeze-up took place between November 4th and December 26th. Once again, the latest freeze-up occurred in 2019. The average was November 26th, with a standard deviation of 15 days. Based on an assessment of landfast ice formation performed by Mahoney, *et al*. (2007), this date is more than one month later than in the mid-1970s. A significant delay in the occurrence of freeze-up also is implied by the research of Rodrigues (2009), who found that the length of the ice-free season off the coast between Point Barrow and Point Lay increased from approximately 30 days in the late 1970s to 125 days in the late 2000s. The number of accumulated FDD at the time of nearshore freeze-up varied widely in recent years, ranging from 265 to 1,271. The average was 715, while the standard deviation was 336.

Complete freeze-up in the Chukchi took place between November 28th and December 27th. The mean value was December 11th, with a standard deviation of 11 days.

Table 7-7. Timing of Freeze-Up in Alaskan Chukchi Sea, 2009-2016 and 2019

Year	Date of First Ice[1]	FDD at Time of First Ice	Date of Nearshore Freeze-Up[1]	FDD at Time of Nearshore Freeze-Up	Date of Complete Freeze-Up[1]	FDD at Time of Complete Freeze-Up
2009	Oct 9	17	Nov 16	535	Nov 29	949
2010	Oct 7	16	Nov 4	265	Dec 7	959
2011	Oct 6	24	Nov 20	601	Nov 30	1,022
2012	Oct 13	4	Nov 15	322	Nov 28	722
2013	Oct 2	39	Nov 26	697	Dec 14	1,104
2014	Oct 7	14	Nov 28	751	Dec 17	1,472
2015	Oct 13	54	Dec 5	1,271	Dec 12	1,576
2016	Oct 15	0	Dec 10	878	Dec 27	1,282
2019	Oct 15	0	Dec 26	1,119	Dec 26	1,119
Average	**Oct 9**	**19**	**Nov 26**	**715**	**Dec 11**	**1,134**
Std. Dev.	**5 days**	**18**	**15 days**	**336**	**11 days**	**269**

Note:
[1] First Ice, Nearshore Freeze-Up, and Complete Freeze-Up are defined in Section 2.

Not surprisingly, the number of accumulated FDD at the time of complete freeze-up spanned a wide range, from 722 to 1,576, with an average value of 1,134 and a standard deviation of 269.

Figure 7-7 compares the timing of nearshore freeze-up in the Alaska Beaufort and Chukchi Seas since 2009. The dates have trended later at exceptionally high rates: 2.3 days per year in the case of the former and 4.6 days per year in the case of the latter. If this pattern continues, nearshore freeze-up will be delayed by one month after only 13 years in the Beaufort and seven years in the Chukchi.

Trend: Freeze-up in the nearshore region of the Alaskan Beaufort Sea currently tends to occur at the end of October, more than three weeks later than in the 1980s. The rate of change has accelerated in recent years, with the date of freeze-up trending later by 2.3 days per year. In the northeastern Chukchi, nearshore freeze-up tends to occur during the fourth week in November, more than a month later than in the 1970s. Once again, the rate of change has accelerated; the date of freeze-up currently is trending later by 4.6 days per year. These high rates of change imply that the length of the open-water season will increase substantially in the years ahead.

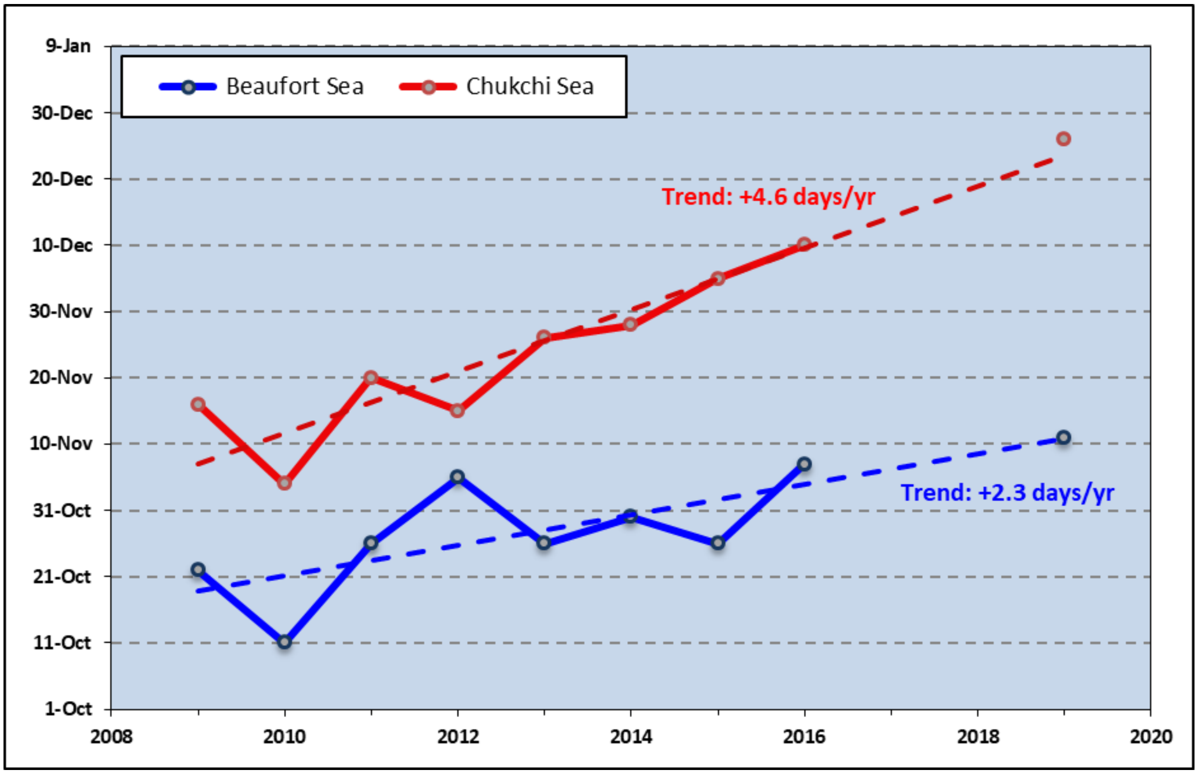

Figure 7-7. Timing of Nearshore Freeze-Up in Alaskan Beaufort and Chukchi Seas, 2009-2019

7.4. Duration of Freeze-Up

Table 7-8 chronicles the progression of freeze-up from first ice to complete cover in the Alaskan Beaufort Sea from 2009 through 2016 and in 2019. The period from the first appearance of ice along the coast to nearshore freeze-up averaged 24 days, while that from nearshore freeze-up to complete freeze-up averaged 13 days. Combining these two phases yields an average of duration of 37 days from first ice to complete freeze-up, with a standard deviation of 11 days.

Table 7-9 presents comparable information for the Chukchi Sea. The period from first ice to nearshore freeze-up averaged 48 days, while that from nearshore freeze-up to complete freeze-up averaged 15 days. These values produce an average duration of 63 days from first ice to complete freeze-up, with a standard deviation of ten days.

The duration of freeze-up in the two basins is compared in Figure 7-8, which illustrates the total time from first ice to complete freeze-up. Notwithstanding significant interannual variations, the data indicate that the duration of freeze-up is not only considerably longer in the Chukchi, but also increasing at nearly twice the rate as in the Beaufort: 1.9 days per year in the former versus 1.0 days per year in the latter.

Table 7-8. Duration of Freeze-Up in Alaskan Beaufort Sea, 2009-2019 and 2019

Year	Days from First Ice to Nearshore Freeze-Up[1]	Days from Nearshore to Complete Freeze-Up[1]	Days from First Ice to Complete Freeze-Up[1]
2009	24	18	42
2010	7	22	29
2011	14	6	20
2012	21	7	28
2013	32	25	57
2014	28	6	34
2015	35	5	40
2016	23	16	39
2019	28	13	41
Average	**24**	**13**	**37**
Std. Dev.	**9**	**8**	**11**

Note:
[1] First Ice, Nearshore Freeze-Up, and Complete Freeze-Up are defined in Section 2.

Table 7-9. Duration of Freeze-Up in Alaskan Chukchi Sea, 2009-2019 and 2019

Year	Days from First Ice to Nearshore Freeze-Up[1]	Days from Nearshore to Complete Freeze-Up[1]	Days from First Ice to Complete Freeze-Up[1]
2009	38	18	56
2010	28	33	61
2011	45	10	55
2012	33	13	46
2013	55	18	73
2014	52	19	71
2015	53	7	60
2016	56	17	73
2019	72	0	72
Average	**48**	**15**	**63**
Std. Dev.	**14**	**9**	**10**

Note:
[1] First Ice, Nearshore Freeze-Up, and Complete Freeze-Up are defined in Section 2.

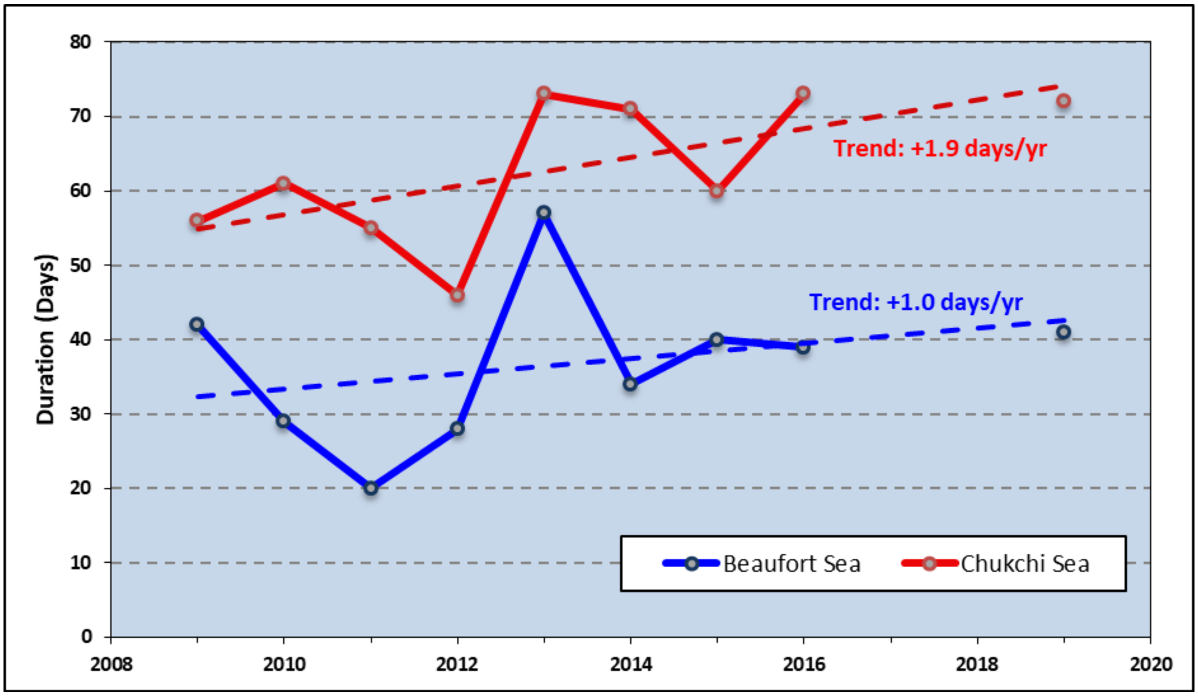

Figure 7-8. Duration of Freeze-Up in Alaskan Beaufort and Chukchi Seas, 2009-2019

Trend: The duration of freeze-up in the Alaskan Beaufort Sea, from first ice to complete freeze-up, currently averages 37 days with a standard deviation of 11 days. In the Chukchi, the duration is substantially longer, averaging 63 days with a standard deviation of ten days. The duration in the Beaufort is increasing at a rate of 1.0 days per year, while that in the Chukchi is increasing at 1.9 days per year.

7.5. First-Year Ice Growth

As discussed in Section 5.1, the growth of undeformed first-year ice can be estimated on the basis of FDD using the relationship of Lebedev (Bilello, 1960). Table 7-10 presents the computed ice thickness on a monthly basis for each winter season from 1970-71 through 2019-20. The results were obtained using the FDD data for Utqiagvik Airport compiled in Table 7-1 and are presented in a comparable format with the highest ranking (50-yr rank of 1) assigned to the lowest predicted ice thickness and lowest ranking (50-yr rank of 50) assigned to the highest ice thickness.

The computed thickness of first-year ice in the Chukchi Sea was 148 cm at the end of the 2019-20 winter season, tied with 2014-15 as the sixth lowest in the 50-year period of record. In keeping with the air temperatures discussed in Section 7.1, the past seven winters (2013-14 through 2019-20) have produced the seven lowest ice thicknesses during this period. The average thickness during the past 11winters (the period encompassed by the recent

Table 7-10. Computed Ice Thickness (cm) at Utqiagvik, 1970-71 through 2019-20

Year	Sep	Oct	Nov	Dec	Jan	Feb	Mar	Apr	May	50-yr Rank
1970-71	16	52	77	102	127	150	169	182	186	49
1971-72	3	33	61	90	115	137	158	171	176	45
1972-73	7	24	55	79	105	125	148	161	165	27
1973-74	3	26	50	78	102	129	151	166	170	37
1974-75	5	43	73	108	135	152	167	180	183	48
1975-76	18	48	79	110	134	155	173	184	189	50
1976-77	4	34	60	92	113	133	156	169	173	43
1977-78	0	24	60	87	107	127	145	157	162	22
1978-79	5	42	63	93	110	133	153	165	169	34
1979-80	0	26	48	81	107	126	144	158	163	23
1980-81	15	37	67	97	114	134	151	163	165	27
1981-82	14	37	64	90	113	129	148	160	165	27
1982-83	7	43	75	99	125	143	161	172	176	45
1983-84	17	47	69	89	114	142	161	176	181	47
1984-85	0	29	65	94	114	135	153	167	170	37
1985-86	10	40	63	89	114	131	152	166	170	37
1986-87	4	31	59	85	110	132	150	164	167	32
1987-88	9	23	59	87	110	130	149	160	164	25
1988-89	9	48	81	104	131	139	155	164	169	34
1989-90	0	29	68	94	122	144	161	170	171	41
1990-91	6	30	65	95	118	139	159	169	169	34
1991-92	6	30	65	95	121	143	159	170	173	43
1992-93	17	41	67	93	116	134	152	161	164	25
1993-94	6	21	49	79	102	121	143	155	159	18
1994-95	10	42	73	102	123	143	162	170	171	41
Average	**8**	**35**	**65**	**92**	**116**	**136**	**155**	**167**	**171**	
Std. Dev.	**6**	**9**	**9**	**9**	**9**	**9**	**7**	**7**	**7**	
Year	**Sep**	**Oct**	**Nov**	**Dec**	**Jan**	**Feb**	**Mar**	**Apr**	**May**	**50-yr Rank**
1995-96	0	27	54	85	106	128	144	156	157	17
1996-97	13	46	64	87	114	133	152	162	166	31
1997-98	2	25	46	79	106	126	141	149	151	8
1998-99	0	16	52	83	110	129	149	162	165	27
1999-00	5	29	59	91	115	135	153	164	170	37
2000-01	7	30	59	84	107	122	143	154	161	20
2001-02	8	40	66	91	117	137	150	161	163	23
2002-03	0	19	47	73	98	120	139	147	151	8
2003-04	0	18	50	79	102	127	147	158	161	20
2004-05	3	23	53	82	104	124	141	152	155	14
2005-06	3	22	56	81	105	123	145	158	160	19
2006-07	0	14	45	72	101	120	140	149	154	12
2007-08	0	18	39	66	96	122	143	152	155	14
2008-09	2	20	50	73	100	117	139	150	152	11
2009-10	3	15	51	77	105	123	142	150	154	12
2010-11	3	20	43	76	100	117	135	148	151	8
2011-12	2	19	53	83	112	132	154	164	167	32
2012-13	0	12	44	76	100	123	140	152	155	14
2013-14	7	18	45	72	96	114	131	142	143	4
2014-15	0	22	46	76	100	118	137	147	148	6
2015-16	3	24	53	84	101	118	136	144	145	5
2016-17	0	7	34	62	83	103	122	132	134	3
2017-18	0	18	35	58	83	97	113	124	128	1
2018-19	0	16	44	73	98	110	122	132	133	2
2019-20	0	9	31	61	90	119	136	145	148	6
Average	**2**	**21**	**49**	**77**	**102**	**121**	**140**	**150**	**153**	
Std. Dev.	**3**	**9**	**9**	**9**	**9**	**9**	**10**	**10**	**11**	

Note: Ice thicknesses were calculated using the corresponding FDD values in Table 7-1.

freeze-up studies) was 146 cm, which is 25 cm less than that computed for the six-year period from 1980-81 through 1985-86.

Additional perspective on the diminished growth of first-year ice is provided by Figure 7-9, which compares the computed thickness of undeformed first-year ice at the end of each month in each of the past eleven winter seasons with the corresponding average value for the period from 1970-71 through 1989-90. Even in 2011-12, the coldest winter in the recent past, the ice failed to attain the average thickness that prevailed in the 1970s and 1980s. During the most recent winter, the ice thickness tended to remain in the lower half of the envelope defined by recent values despite the occurrence of exceptionally cold temperatures in late January and February (Section 5.1).

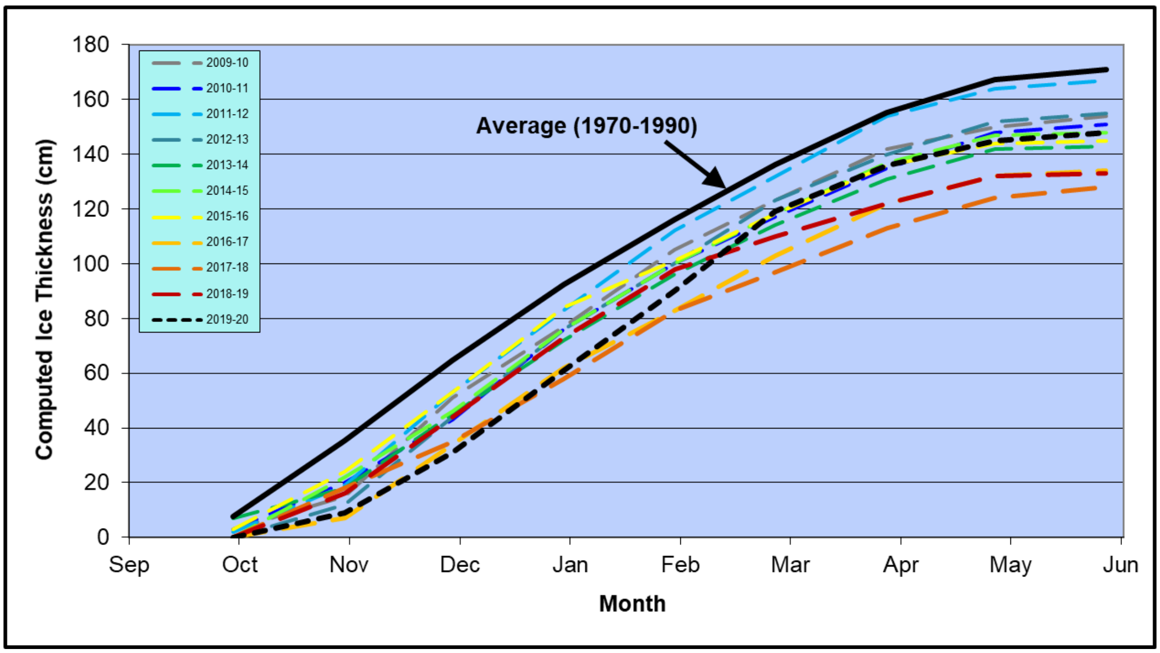

Figure 7-9. Computed Thickness of First-Year Ice: Recent Winters vs. 1970s and 1980s

The reduction in ice thickness attributable to warmer air temperatures may be exacerbated by an increase in the depth of the snow cover. To quantify the relative importance of these and other factors, Brown and Cote (1992) investigated the interannual variability in the maximum ice thickness at four sites in the Canadian High Arctic between 1950 and 1989 using a one-dimensional model of ice growth based on heat transfer. The depth of the snow cover was found to be the most important factor, explaining 30% to 60% of the variance in the maximum first-year ice thickness due to its insulating effect. Density fluctuations in the snow cover were estimated to account for an additional 15% to 30% of the variance. In contrast, annual variations in air temperature accounted for less than 4% of the variance in the maximum thickness attained by first-year ice.

As shown in Figure 7-10, the average snowfall at Utqiagvik during the five-month period from October through February increased dramatically in the 1990s and 2000s. From 30 cm in the 1980s, it increased to 57 cm in the 1990s and 88 cm in the 2000s. More recently, from 2010-11 through 2018-19, the average value of 89 cm was nearly unchanged from that in the 2000s, but nevertheless nearly three times greater than that in the 1980s. Over the entire 49-year period of record (1970-71 through 2018-19), snowfall during the freeze-up season increased at an average rate of 1.6 cm/yr.

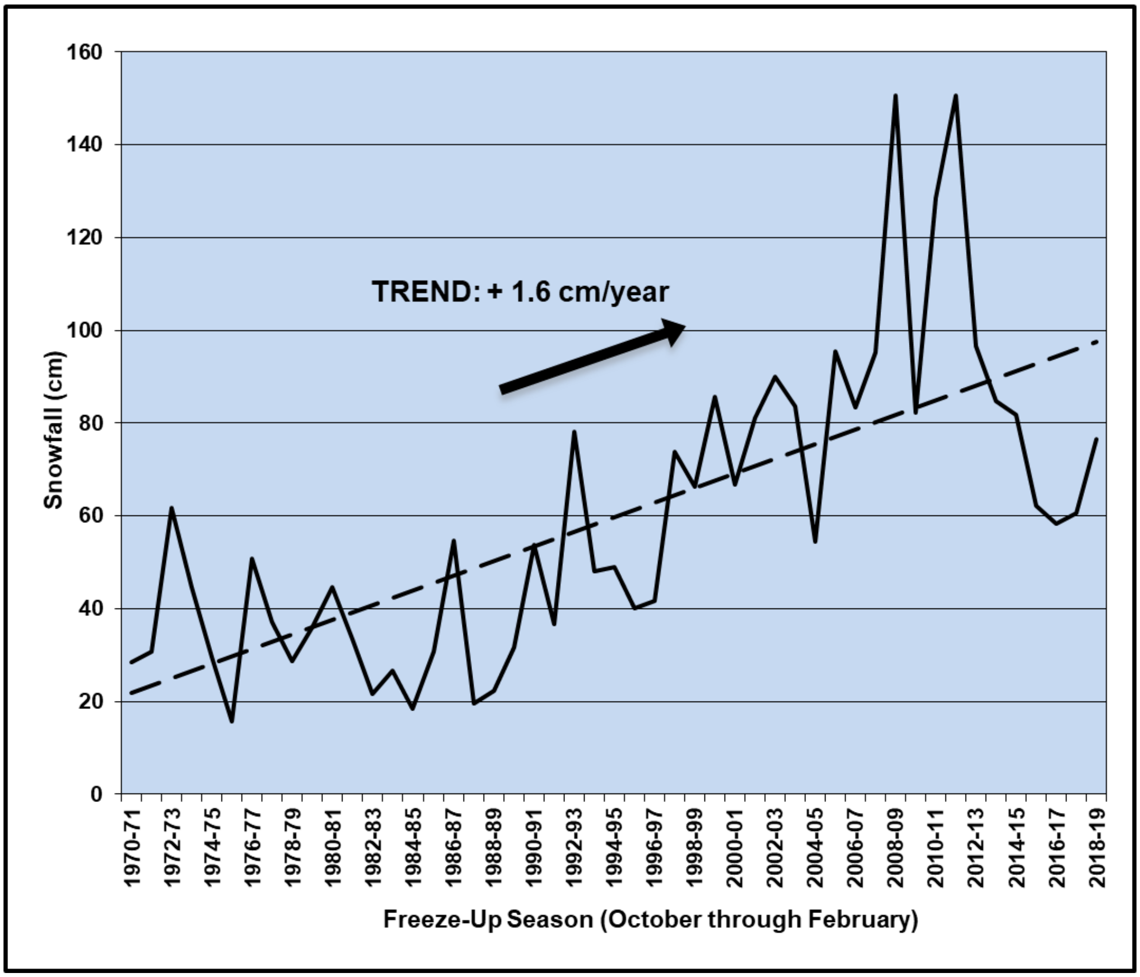

Data Source: National Weather Service, 2019

Figure 7-10. Annual Snowfall at Utqiagvik from October through February, 1970-71 through 2018-19

In addition to reducing ice thickness, higher air temperatures tend to prolong the existence of leads and retard the production of new ice in those leads. Furthermore, higher temperatures and the insulating effect of heavier snowfall tend to decrease the degree of consolidation that occurs in ridges and rubble fields, and to reduce the overall strength of the ice canopy.

Trend: Based on air temperature alone, the thickness of undeformed first-year ice attained during an average winter has decreased by 25 cm (15%) since the early 1980s. However, a significant increase in snowfall may be causing an even greater reduction in the ice thickness due to its insulating effect. Other temperature-related factors, including reduced ice production in leads, decreased consolidation of ridges and rubble fields, and reduced ice strength, serve to amplify the impact of reduced thickness on ice dynamics.

7.6. Landfast Ice

Data presented by investigators that include Barry, *et al*. (1979), Eicken, *et al*. (2006), and Mahoney, *et al*. (2012), as well as those acquired during the freeze-up studies that began in 2009-10 (Coastal Frontiers and Vaudrey, 2010; 2011; 2012a; 2013; 2014; 2015; 2016; 2017), indicate that characteristic patterns and features of the ice cover tend to recur on an annual basis. Such patterns include the evolution of the landfast ice zone and the distribution of leads and polynyas over the course of the winter. Factors that contribute to these recurring patterns include the seasonal cycles of meteorological and oceanographic conditions, the orientation of the shoreline and bathymetric contours, and the presence or absence of islands and shoals.

Beaufort Sea: The wind, which tends to be coast-parallel in the Alaskan Beaufort Sea, constitutes the dominant driving force for ice movement. Easterlies produce westerly ice movement with an onshore component, creating a stable landfast ice zone that ultimately extends to the vicinity of the 20-m isobath (Mahoney, *et al*., 2012). The western Beaufort between Point Barrow and Prudhoe Bay contains numerous shoals that are located up to 25 nm (46 km) offshore. The most prominent are Weller Bank, which lies off Harrison Bay, and Stamukhi Shoal, which lies off Pingok Island (Figure 1-3). As discussed in Section 5, the large, grounded rubble piles that typically form on these shoals serve as anchor points for a relatively wide expanse of landfast ice. In contrast, to the east of Prudhoe Bay, water depths increase more rapidly off the barrier islands from Cross to Flaxman, and off the coast in the vicinity of Barter Island. In these areas, the landfast ice zone typically remains less than 5 nm (9 km) wide. An exception occurs in Camden Bay, where landfast ice can extend more than 10 nm (19 km) offshore.

In the early 1980s, a well-grounded shear zone tended to form in the region west of Prudhoe Bay by mid-November. In recent years, however, this process has been delayed by the warm air temperatures that have prevailed in September, October, and November (Section 7.1). The landfast ice has tended to remain poorly-grounded and subject to breakout events until much later in the freeze-up season, with the attainment of stability ranging from early December in 2015-16 (Coastal Frontiers and Vaudrey, 2016) to late February in 2016-17

(Coastal Frontiers and Vaudrey, 2017), and early March in 2014-15 (Coastal Frontiers and Vaudrey, 2015). Even greater departures from the 1980s occurred in 2010-11 and 2019-20. In both cases, the formation of a securely-grounded shear zone was inhibited by a paucity of sustained easterly winds and energetic easterly storms. As a result, the ice failed to remain grounded on Stamukhi Shoal and the landfast ice zone remained narrow and unstable throughout freeze-up (Coastal Frontiers and Vaudrey, 2011; Section 5.1).

To the east of Prudhoe Bay, the contrast between the 1980s and recent years has encompassed not only the timing but also the extent of landfast ice development. A well-established, firmly-grounded shear zone formed off the barrier islands during five of the six freeze-up periods monitored in the 1980s. In six of the nine years covered by recent freeze-up studies, however, including 2019-20, the ice in part or all of this region remained poorly-grounded and mobile throughout freeze-up.

Chukchi Sea: As discussed in Section 6, easterly (offshore) winds and relatively steep slopes in the nearshore area limit the extent of the landfast ice in the Chukchi Sea to a narrow strip along the shoreline. The seaward edge typically lies within 5 to 10 nm (9 to 19 km) of the coast but can retreat to the coast itself during breakout events triggered by offshore winds. Such an event occurred off Skull Cliff in February 2016 (Coastal Frontiers and Vaudrey, 2016), and again in January 2020 (Section 6.3.2). Exceptions to this behavior are most likely to occur in the semi-protected embayments to the east of Icy Cape and Point Franklin, where the landfast ice tends to be wider and more stable.

Due to its dynamic nature, particularly with respect to breakout events, the landfast ice zone in the Chukchi fails to exhibit the progressive expansion over the course of the freeze-up season typically seen in the Beaufort. As a result, its maximum seaward extent is poorly correlated with water depth (Mahoney, *et al*., 2012). In addition, the dynamic nature of the landfast ice zone increases the potential for ridge and rubble formation in the nearshore region, and for pile-ups at the shoreline.

A narrow, ephemeral landfast ice zone was observed in the northeast Chukchi Sea during a significant portion of each of the nine freeze-up seasons studied since 2009-10. Instability was particularly prevalent in 2010-11, 2012-13, and 2015-16; in each instance, a continuous strip of landfast ice failed to materialize throughout freeze-up (Coastal Frontiers and Vaudrey, 2011; 2013; 2016).

Trend: In the Alaskan Beaufort Sea, the extent of the landfast ice zone to the west of Prudhoe Bay is similar to that observed in the 1980s but the landfast ice develops more slowly. To the east of Prudhoe Bay, a stable, well-grounded shear zone is less likely to form during freeze-up and develops more slowly in those years when it does occur. In the Chukchi, the narrow, ephemeral nature of the landfast ice zone noted in the 1980s continues to prevail today.

7.7. Coastal Flaw Lead

Seaward of the landfast ice zone in the northeast Chukchi Sea, the ice is driven offshore during periods of easterly and, on some occasions, southerly winds. The resulting flaw lead separates the mobile pack ice from the stationary landfast ice and generates new ice throughout the winter as it experiences repeated cycles of opening, expanding, and either closing or refreezing. A recent study by Hirano, *et al.* (2016) suggests that upwelling of relatively warm, dense water from Barrow Canyon also contributes to the formation and maintenance of the lead. Once again, offshore winds serve as the driving force. The width of the lead can vary substantially depending on the duration, direction, and intensity of the winds.

Based on the trends identified in the preceding subsections, including warmer air temperatures, increased storminess, and slower ice growth during freeze-up, it was hypothesized that the ice canopy might be more prone to displacement, and therefore that the flaw lead might occur more frequently, than in the 1980s (Coastal Frontiers and Vaudrey, 2013). However, an assessment of the period from December through April for the 21 winters from 1993-94 through 2013-14 found that the frequency of occurrence had not changed appreciably (Ward, *et al*., 2015). Specifically, the flaw lead was present 51% of the time during the first ten winters and 49% during the next 11. The frequency with which the lead extended to the northeast of Point Barrow also appeared to have remained constant; an extended flaw lead was present 35% of the time during first ten winters and 37% during the next 11.

Trend: Notwithstanding trends toward warmer air temperatures, increased storminess, and slower ice growth during freeze-up, the frequencies with which the flaw lead and extended flaw lead occur off the Chukchi Sea coast have remained unchanged since the 1990s.

7.8. Multi-Year Ice

Two types of multi-year ice can occur in the Beaufort and Chukchi Seas: (1) true multi-year floes from the permanent polar pack in the Arctic Ocean ("pack floes"), and (2) second-year floes that develop when grounded fragments of thick first-year features survive the summer months due to factors that may include cold air temperatures and mild winds. The first-year features consist of ridges and rubble fields formed off the coast of the Beaufort Sea and in the Canadian Arctic Archipelago. When they become second-year floes, they can be distinguished from pack floes by their more jagged appearance, with many embedded ridges, and greater thickness (6 to 9 m for second-year floes versus 3 to 5 m for pack floes). Henceforth, the term "multi-year ice floes" will be used to refer to both pack floes and second-year floes.

Beaufort Sea: When the initial round of freeze-up studies was conducted in the 1980s, large multi-year ice floes were present in the nearshore region of the Alaskan Beaufort Sea during three of the six freeze-up seasons: 1980-81, 1983-84, and 1985-86 (Vaudrey, 1981a; 1981b; 1982a; 1983; 1984; 1985a; 1986). Grounded multi-year fragments with diameters as large as 120 m were observed during the other three seasons (1981-82, 1982-83, and 1984-85).

In the nine years that preceded the resumption of freeze-up studies in 2009-10, large multi-year floes invaded the nearshore region on only one occasion: 2001-02, when a low concentration approached the coast in the western Beaufort during the initial stages of freeze-up. The next invasion occurred in 2009-10, when a high concentration of massive floes with embedded ridges moved from Canada into the nearshore region of the Alaskan Beaufort, proceeded west to Point Barrow, and split into northern and southern branches in the Chukchi (Coastal Frontiers and Vaudrey, 2010). Although small, grounded fragments of second-year ice were observed adjacent to the barrier islands in 2010-11 and 2015-16 (Coastal Frontiers and Vaudrey, 2011; 2016), and two small patches of second-year ice drifted away from Point Barrow in October 2016 (Section 4.3.1), large multi-year floes remained absent from the southern portion of the Alaskan Beaufort Sea from 2010-11 through 2017-18. Back-to-back invasions followed in 2018-19 and 2019-20 (Section 5). Hence, during the past 20 years, such floes have entered the nearshore region on only four occasions.

Chukchi Sea: Multi-year ice was present in the Chukchi Sea during each of the three freeze-up seasons from 1983-84 through 1985-86 (Vaudrey, 1984; 1985a; 1986) and also during the midwinter season of 1987 (Vaudrey, 1987a). The invasions were characterized by concentrations as high as 70%, and southerly limits between 71°N and 70°30'N.

In ten of the 20 winters from 2000-01 through 2019-20, an extended flaw lead channeled large multi-year floes into the region south and west of Point Barrow: 2000-01, 2001-02, 2003-2004, 2005-06, 2008-09, 2009-10, 2011-12, 2013-14, 2015-16, and 2019-20 (Ward, *et al.*, 2015; Section 6). The invasions all followed a similar pattern, which involves four phases:

- ***Flaw Lead:*** a flaw lead develops off the northeast coast of the Chukchi Sea in response to sustained offshore winds.

- ***Extended Flaw Lead:*** an extended flaw lead results when the flaw lead stretches to the north and east of Point Barrow. As discussed by Eicken, *et al*. (2006), this northward extension (the "Barrow Arch") is caused by westward movement of the Beaufort Sea pack ice, which in turn is caused by easterly winds.
- ***Multi-Year Ice in Extended Flaw Lead:*** multi-year floes can enter the extended flaw lead if it extends sufficiently far north to intersect the southern boundary of this ice. Because the floes lose confinement in the lead, they can travel to the southwest at relatively high speeds.
- ***Multi-Year Gateway:*** a "Multi-Year Gateway" forms when multi-year floes that have entered the extended flaw lead move into the region south and west of Point Barrow. A representative example of the Gateway that occurred in March 2001 is provided in Figure 7-11.

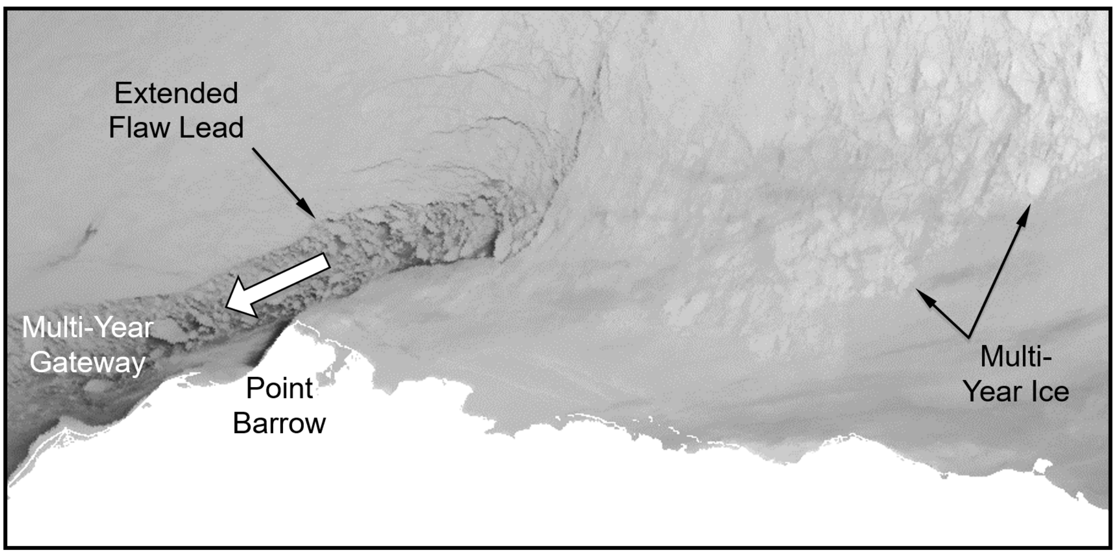

After Eicken, *et al*., 2006

Figure 7-11. AVHRR Image Acquired on March 12, 2001 Illustrating Multi-Year Gateway

While the Multi-Year Gateway represents the primary means by which multi-year ice enters the Chukchi Sea, an alternate mechanism ("Early-Season Entry") has been noted on four occasions: November 2010 (Ward, *et al*., 2015), November 2014 (Coastal Frontiers and Vaudrey, 2015), November 2015 (Coastal Frontiers and Vaudrey, 2016), and November 2018. In each case, the floes began to move into the region south and west of Point Barrow when the ice canopy was in an early stage of development. The Early-Season Entry that occurred in 2015 is illustrated in Figure 7-12, which shows multi-year ice adjoining open water in the region between the Hanna Shoal and Burger Prospects. Although the Multi-Year Gateway and Early-Season Entry are distinctly different phenomena, they share a key characteristic: a lack of confinement that allows multi-year ice floes to move to the southwest at relatively high speeds.

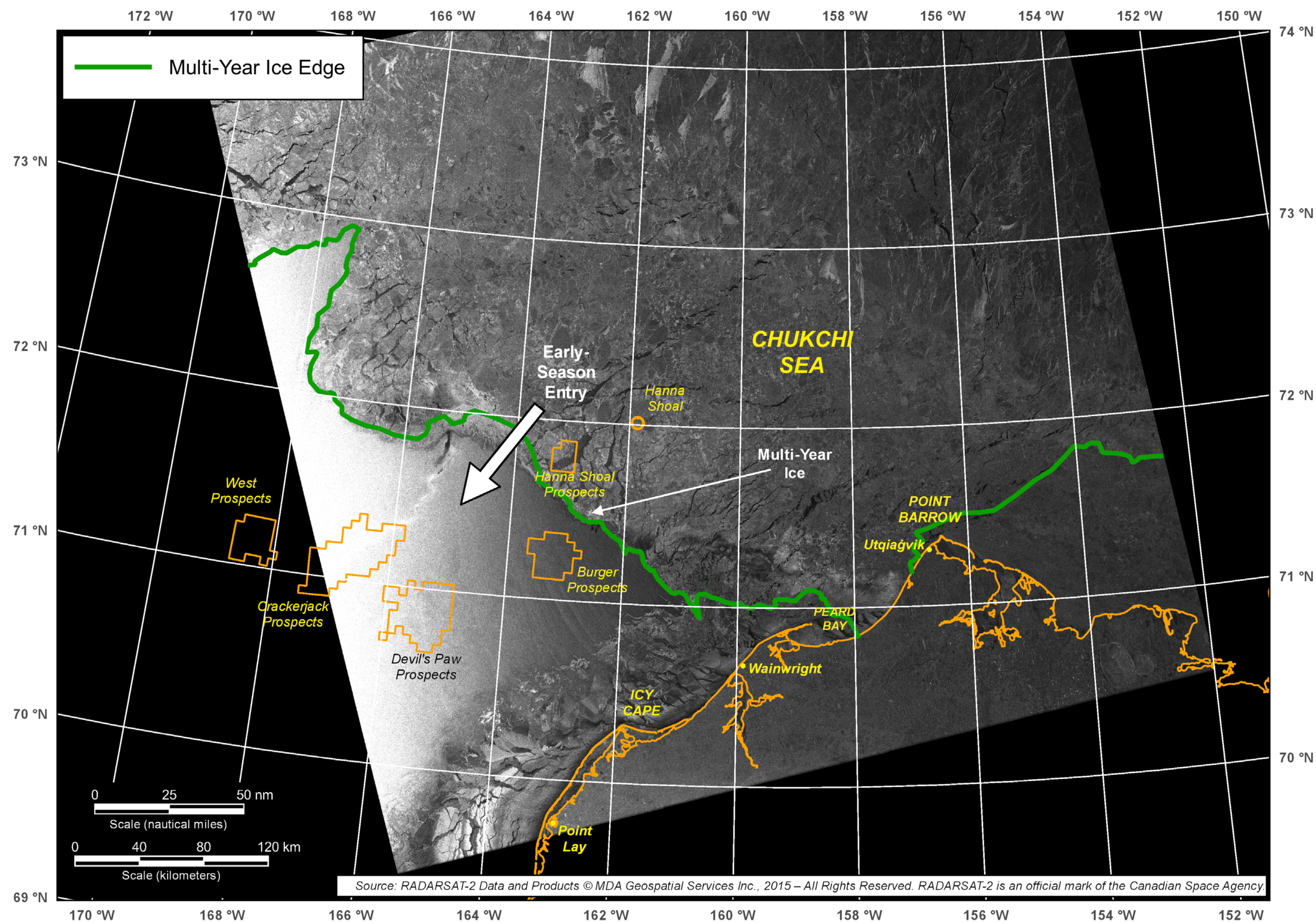

Figure 7-12. RADARSAT-2 Image Acquired on November 16, 2015 Illustrating Early-Season Entry

Together, the Multi-Year Gateway and Early-Season Entry have caused multi-year ice to invade the region south and west of Point Barrow in 13 of the past 20 freeze-up seasons. The invasions resulted from the Multi-Year Gateway alone in nine seasons, Early Season Entry alone in three seasons, and both phenomena in 2015-16.

Trend: The probability of large multi-year ice floes invading the nearshore region of the Alaskan Beaufort Sea in any given year is substantially less than in the 1980s. This change may be explained in part by a reduction in the amount of multi-year ice comprising the permanent polar pack (Perovich, *et al.*, 2013) and in part by an increase in the northerly retreat of the ice edge during the summer months, both of which have reduced the opportunities for pack floes to enter the nearshore area. In addition, warmer air temperatures, longer open-water seasons, and increased storminess have decreased the likelihood that first-year ridges and rubble will survive the summer melt season to become second-year floes of any consequence. Nevertheless, as demonstrated in both 2018-19 and 2019-20, the possibility of multi-year ice encounters cannot be ruled out in the nearshore region of the Alaskan Beaufort Sea. Furthermore, small fragments of second-year ice analogous to those observed in 2010-11 and 2015-16 can be present even if large multi-year floes remain well offshore.

The probability of multi-year ice entering the Chukchi Sea to the south and west of Utqiagvik also has decreased since the 1980s, but to a lesser extent than in the Beaufort. Although the factors that have reduced the probability of invasions in the Beaufort apply to the Chukchi as well, their impact has been mitigated by the ability of the Multi-Year Gateway and Early-Season Entry to divert multi-year floes to the southwest.

7.9. Ice Drift

Pack ice movement in the Beaufort and northern Chukchi Seas consists of two components: (1) long-term, steady-state movement caused by the rotation of the Beaufort Gyre (Figure 1-1), and (2) short-term, transient movement caused by local winds. As the latter varies greatly depending on the wind conditions and degree of ice confinement, insufficient data exist to compare the short-term motions observed in recent years with those in the 1980s. It is worth noting, however, that a multi-year ice floe tracking study conducted in the Alaskan Beaufort Sea during the 1984 open-water season led to the following conclusions: (1) the wind factor is not constant for floes in the nearshore area, but varies as a function of wind speed, wind direction, water depth, and keel depth; (2) although the data exhibit considerable scatter, wind factors of 4% to 6% are common during periods of strong winds (Tekmarine, *et al.,* 1985).

Long-term pack ice motion, often referred to as "ice flux" or "ice drift", plays a key role in the design of fixed structures in that it governs the number of encounters with design ice features (such as multi-year floes) over a specified period (such as the design life). Detailed analyses of ice movement were omitted from the freeze-up studies conducted from 1980-81 through 1985-86, but median ice drift values were derived from several ice buoy programs conducted in the mid- to late 1980s (Vaudrey, 1987b; 1988b; 1989b; 1989c) and from the successive positions of two large multi-year ice floes identified in AVHRR images in Fall 1988 (Vaudrey, 1989a). The speeds in the months of November and December ranged from 4.9 to 6.3 nm/day (9.1 to 11.7 km/day; Vaudrey, 2007).

In the current round of freeze-up studies, monthly drift rates were derived for multi-year ice floes in November and December using RADARSAT-2 images acquired in 2010, 2011, 2013, 2014, 2015, and 2019. The data from the Alaskan Beaufort Sea, where the floes are exposed to the westward set of the Beaufort Gyre, are summarized in Table 7-11. The drift rates ranged from 1.2 to 10.4 nm/day (2.2 to 18.5 km/day), with an average value of 5.8 nm/day (10.8 km/day).

Table 7-11. Beaufort Sea Ice Drift in November and December

Year	Maximum Monthly Drift Rate (nm/day)	Minimum Monthly Drift Rate (nm/day)	Average Monthly Drift Rate (nm/day)
2010	7.8	5.5	7.1
2011	8.3	4.9	6.3
2013	3.4	1.2	1.9
2014	10.0	5.1	6.8
2015	8.8	4.7	6.8
2019	10.4	2.3	5.7
Average	n/a	n/a	**5.8**

Note: Monthly drift rates were derived from RADARSAT-2 images for periods that exceeded 14 days.

Although the data obtained from the recent studies are not suitable for direct comparison with those from the 1980s due to differences in the methods of acquisition and analysis, they nevertheless suggest that drift rates during the early stages of freeze-up have not changed appreciably. This finding runs counter to the hypothesis of Walsh and Eicken (2007), who suggested that reduced ice thickness and increased storminess may lead to increased rates of ice movement.

Trend: Based on the limited data acquired in recent years, the drift rate for pack ice in the Alaskan Beaufort Sea during the early stages of freeze-up averages about 6 nm/day (11 km/day). This value is comparable to that which prevailed in the 1980s.

8. SUMMARY AND CONCLUSIONS

8.1. Milestones

Freeze-up in 2019-20 was distinguished by exceptionally warm air temperatures during the early months followed by cold temperatures during the later months. Additional distinguishing characteristics included a high frequency of westerly winds, a paucity of storms, particularly in January and February, and nearshore invasions of large, multi-year ice floes in both the Beaufort and Chukchi Seas. Phenomena that exceeded the ranges established during the eight prior freeze-up studies conducted from October through February in 2009-2010 through 2016-17 are summarized below:

Beaufort Sea

- Highest frequency of westerly winds (64%, tied with 2016-17);
- Lowest number of easterly storms (4) and easterly storm-days (9);
- Lowest number of total storms (9) and total storm days (18);
- Latest occurrence of nearshore freeze-up (November 11th) and complete freeze-up (November 24th);
- First occasion in two decades when large, multi-year ice floes invaded the nearshore region in two consecutive years (2018-19 and 2019-20).

Chukchi Sea

- Highest average air temperature in the month of September (40.8°F or 4.9°C);
- Lowest average air temperature in the month of February (-26.1°F or -32.3°C);
- Largest negative deviation from the long-term average air temperature in a single month (-10.2°F or -5.7°C in February);
- Highest frequency of westerly winds (45%);
- Lowest number of easterly storm-days (16);
- Lowest number of total storm days (23);
- Latest occurrence of first ice (October 15th, tied with 2016) and nearshore freeze-up (December 26th);
- First occasion on which nearshore freeze-up and complete freeze-up occurred simultaneously (December 26th).

8.2. Detailed Findings

Entire Study Area

1. ***Air Temperatures:*** The air temperatures during the 2019-20 winter season were warm by historical standards, but unexceptional compared to those in the recent past. Specifically, the temperatures at Utqiagvik Airport were the sixth warmest in past 50 winters, but also the sixth warmest in the 11 winters from 2009-11 through 2019-20. Those at Deadhorse Airport were the ninth warmest in this 11-winter period.

2. ***First-Year Ice Growth:*** The computed thickness of undeformed first-year ice at the end of the 2019-20 winter season was 162 cm in the Alaskan Beaufort Sea and 148 cm in the Chukchi Sea, based on accumulations of 7,143 and 6,122 FDD at Deadhorse and Utqiagvik Airports, respectively. The thickness in the Beaufort was the third highest in the past 11 winters, while that in the Chukchi was tied with that in 2014-15 as the sixth highest. The highest values in recent years, 176 cm in the Beaufort and 167 cm in the Chukchi, occurred in 2011-12.

Beaufort Sea

1. ***Late Summer:*** The ice cover in the Alaskan Beaufort Sea diminished rapidly in July and early August, reflecting the prevalence of warm air temperatures and clear skies. Subsequently, from mid-August through mid-September, the rate of loss slowed. The minimum ice extent, which occurred on September 18th, tied those in 2007 and 2016 as the second lowest since the acquisition of satellite-based data began in 1979.

2. ***Timing of Freeze-Up:*** Freeze-up began in mid-October with the formation of ice along the coast between Admiralty Bay and Point Brownlow. Nearshore freeze-up occurred on November 11th, followed by complete freeze-up on November 24th. During the nine years covered by recent freeze-up studies (2009-11 through 2016-17 and 2019-20), the average date for the occurrence of nearshore freeze-up was October 28th with a standard deviation of nine days. The average date for the occurrence of complete freeze-up was November 10th with a standard deviation of ten days.

3. ***Duration of Freeze-Up:*** The duration of freeze-up was 41 days, consisting of 28 days from first ice to nearshore freeze-up and an additional 13 days from nearshore freeze-up to complete freeze-up. During the nine years covered by recent freeze-up studies, the duration averaged 37 days with a standard deviation of 11 days.

4. ***Wind Regime:*** Based on the daily average wind directions recorded at Deadhorse Airport, westerlies predominated in each of the five months from October through February. The frequencies of occurrence ranged from 55% in December to 79% in February. Over the entire five-month study period, westerlies outnumbered easterlies by

a margin of 64% to 36%. The average monthly speeds were tightly clustered and relatively low by historical standards, with values of 11 kt (6 m/s) recorded in October, November, and December, and 9 kt (5 m/s) in January and February.

5. ***Storm Events:*** Storm events with daily average wind speeds exceeding 15 kt (8 m/s) occurred on only nine occasions encompassing 18 days. Four of the events were easterlies, while five were westerlies. The numbers of easterly storms (4), easterly storm days (9), total storms (9), and total storm days (18) all represented historical minima relative to 2009-10 through 2016-17. Storm duration was low, averaging 2.3 days/event for easterlies and 1.8 days/event for westerlies.

6. ***Landfast Ice:*** Landfast ice began to develop in early November, with growth occurring first in the western portion of the study area and subsequently in the eastern portion. The ice continued to expand offshore through the first half of December, but the advance stalled during the second half of the month. Substantial expansion followed in January, causing the landfast ice edge to reach one of its customary anchor points, Weller Bank, by mid-month and a second, Stamukhi Shoal, by early February. A reversal occurred at the end of February when a brief westerly storm caused the ice edge to retreat by distances up to 20 nm (37 km). Although the ice remained grounded on Weller Bank, it was displaced from Stamukhi Shoal - a development that underscored the absence of a well-developed, firmly-grounded shear zone during the 2019-20 freeze-up season.

7. ***Ice Pile-Ups:*** Thirty-two ice pile-ups formed in the central portion of the Alaskan Beaufort Sea during the 2019-20 freeze-up season. Two were located on the Endicott Project's Endeavor Island, two on Northstar Production Island, one on the Oooguruk Offshore Drillsite (ODS), one on the Spy Island Drillsite (SID), and 26 on natural barrier islands and shoals. The dimensions of the pile-ups were unexceptional by historical standards, with heights ranging from 1 to 7 m above sea level, encroachment distances from negligible to 20 m onto the subaerial beach, and lengths from 50 m to 2 km alongshore. The thicknesses of the ice blocks comprising the piles ranged from 20 to 50 cm.

8. ***Multi-Year Ice:*** Multi-year ice began to drift west into the Alaskan Beaufort Sea study area during the second week in October. In the absence of a well-developed first-year ice canopy, the multi-year floes advanced rapidly to the west in November. Some of the ice at the southern boundary was incorporated into the landfast ice zone in late November and early December, and remained there through the end of the freeze-up study period in February. The concentrations typically were less than 10%. Farther offshore, where the multi-year floes tended to be larger, the concentrations ranged from less than 10% to 50% in December, less than 10% to 60% in January, and less than 10% to 70% in February. The only region lacking multi-year ice for an extended period of time was a

tongue of first-year ice that developed between the U.S.-Canadian border and Harrison Bay in mid-December, and persisted through February just offshore of the landfast ice zone.

Chukchi Sea

1. ***Timing of Freeze-Up:*** Ice began to form in Kasegaluk Lagoon, the Kuk River Inlet, and Peard Bay in mid-October, but freeze-up proceeded slowly in the weeks that followed. Complete coverage of these semi-enclosed basins did not take place until the last week in November. Although ice appeared in the exposed waters adjacent to the coast during the first week in November, it failed to coalesce into a near-continuous strip spanning the entire length of the study area until the end of the month. Farther offshore, first-year pack ice began to stream west past Point Barrow during the second week of November but stalled in response to periods of westerly winds. As a result, most of the Chukchi Sea remained ice-free at the end of November. A strong predominance of easterly winds in December delayed the attainment of complete ice cover adjacent to the coast until December 26th. On that date, nearshore freeze-up and complete freeze-up occurred simultaneously. During the nine years covered by recent freeze-up studies (2009-11 through 2016-17 and 2019-20), the average date for the occurrence of nearshore freeze-up was November 26th with a standard deviation of 15 days. The average date for the occurrence of complete freeze-up was December 11th with a standard deviation of 11 days.

2. ***Duration of Freeze-Up:*** Nearshore freeze-up and complete freeze-up both occurred 72 days after first ice. During the nine years covered by recent freeze-up studies, the duration of freeze-up (from first ice to complete freeze-up) averaged 63 days with a standard deviation of ten days.

3. ***Wind Regime:*** Easterlies outnumbered westerlies in November, December, and January, while westerlies prevailed in October and February. Over the entire five-month study period, easterlies outpaced westerlies by a margin of 55% to 45%. The monthly average speeds declined over the course of freeze-up, decreasing from 13 kt (7 m/s) in October and November to 11 kt (6 m/s) in December, 9 kt (5 m/s) in January, and 7 kt (4 m/s) in February.

4. ***Storm Events:*** Thirteen storm events took place from October through February, consisting of nine easterlies and four westerlies. The easterlies produced 16 storm-days while the westerlies produced 7 storm-days. The numbers of easterly storm-days (16) and total storm days (23) represented historical minima relative to 2009-10 through 2016-17. As in the case of the Beaufort, storm duration was low, averaging 1.8 days/event for both easterlies and westerlies.

"THIS INFORMATION IS DISTRIBUTED SOLELY FOR THE PURPOSE OF PRE-DISSEMINATION PEER REVIEW UNDER APPLICABLE INFORMATION QUALITY GUIDELINES. IT HAS NOT BEEN FORMALLY DISSEMINATED BY BSEE. IT DOES NOT REPRESENT AND SHOULD NOT BE CONSTRUED TO REPRESENT ANY BSEE DETERMINATION OR POLICY."

5. ***Landfast Ice:*** The first traces of landfast ice appeared in Kasegaluk Lagoon, the Kuk River Inlet, and Peard Bay in mid-November. Although several small patches of landfast ice formed in the exposed waters adjacent to the coast during the first half of December, a continuous strip encompassing the entire length of the study area between Point Barrow and Point Lay did not develop until month-end. Most of the newly-formed landfast ice was lost during the first half of January, a period in which winds with a significant offshore component prevailed. A partial rebound occurred during the second half of January, when westerly winds resulted in the re-establishment of a continuous strip. Additional expansion followed in February, causing the landfast ice to reach Blossom Shoals, its customary anchor point, by mid-month. At the end of the month, the width of the landfast ice zone ranged from less than 1 nm (2 km) off South Kasegaluk Lagoon and Point Belcher to 21 nm (39 km) off North Kasegaluk Lagoon.

6. ***Coastal Flaw Lead:*** From December 2019 through February 2020, the distinctive flaw lead that forms off the Chukchi Sea coast in response to offshore winds opened on seven different occasions. The frequency of occurrence, which averaged 54% over the three-month period, increased from 23% in December to 65% in January and 76% in February. The maximum width, 75 nm (139 km) occurred in January, while the maximum length, 250 nm (463 km), occurred in both January and February. The lead persisted for periods that ranged from one to 20 days.

7. ***Pack Ice:*** When a reconnaissance flight was performed at the end of February, the pack ice on the west side of the flaw lead consisted primarily of first-year floes with diameters typically ranging from less than 500 m to 1 km and occasionally reaching 3 km. Deformation was moderate. Ridge and rubble heights of 2 to 3 m were common but heights to 5 m were observed in some areas, particularly in the vicinity of the flaw lead.

8. ***Ice Pile-Ups:*** Fifty-seven ice pile-ups occurred on the shoreline between Utqiagvik and Point Lay during the 2019-20 freeze-up season. Thirty-seven were located on the seaward side of the barrier islands fronting Kasegaluk Lagoon while one was located on the landward side. The remaining 19 were located between North Kasegaluk Lagoon and Utqiagvik. The dimensions were large by historical standards, with heights ranging from 1 to 20 m, encroachment distances from negligible to 30 m, and alongshore lengths from 50 m to 8 km. The block thicknesses varied from 30 to 60 cm.

9. ***Multi-Year Ice:*** Multi-year ice drifting west in the Alaskan Beaufort Sea reached the vicinity of Point Barrow at the end of November. It remained stalled at that location until mid-December, when multi-year floes began to move into the region northwest of the Point. On December 23rd, the ice drifted south of the Point after entering the first flaw lead of the freeze-up season. A larger flaw lead appeared at the end of December, allowing the ice to move within 2 nm (4 km) of Icy Cape by early January. The ice

continued to advance to the south and west of Point Barrow during the remainder of January, reaching the Hanna Shoal and Burger Prospects in mid-month and the vicinity of Point Lay at month-end. Changes in the ice edge were minimal in February, with the western boundary tending to follow the 163ºW meridian between the 70ºN and 72ºN parallels.

Trends

1. ***Air Temperatures:*** Since the 1970s, progressively warmer winter seasons have caused the number of accumulated freezing-degree days at Utqiagvik to decline at an average rate of 54 per year. The rate of warming has accelerated, with the greatest increase in temperature occurring during the early portion of freeze-up.

2. ***Winds:*** Since the early 1980s, the frequency of storm events during freeze-up has increased by about 50%. The frequency of mid-winter storms (January through April) appears to have remained stable.

3. ***Timing of Freeze-Up:*** Nearshore freeze-up currently tends to occur at the end of October in the Alaskan Beaufort Sea and during the fourth week in November in the northeastern Chukchi Sea. The former is more than three weeks later than in the 1980s, while the latter is more than one month later than in the 1970s. The rate of change has accelerated in recent years, with the date of freeze-up currently trending later by 2.3 days per year in the Beaufort and 4.6 days per year in the Chukchi. These high rates of change imply that the length of the open-water season will increase substantially in the years ahead.

4. ***Duration of Freeze-Up:*** The duration of freeze-up in the Alaskan Beaufort Sea, from first ice to complete freeze-up, currently averages 37 days with a standard deviation of 11 days. In the Chukchi, the duration is substantially longer, averaging 63 days with a standard deviation of ten days. The duration in the Beaufort is increasing at a rate of 1.0 days per year, while that in the Chukchi is increasing at 1.9 days per year.

5. ***First-Year Ice Growth:*** Based on air temperature alone, the thickness of undeformed first-year ice attained during an average winter has decreased by 25 cm (15%) since the early 1980s. However, a significant increase in snowfall may be causing an even greater reduction in the ice thickness due to its insulating effect. Other temperature-related factors, including reduced ice production in leads, decreased consolidation of ridges and rubble fields, and reduced ice strength, serve to amplify the impact of reduced thickness on ice dynamics.

6. ***Landfast Ice Development and Stability*:** In the Alaskan Beaufort Sea, the extent of the landfast ice zone to the west of Prudhoe Bay is similar to that observed in the 1980s but the landfast ice develops more slowly. To the east of Prudhoe Bay, a stable, well-

grounded shear zone is less likely to develop during freeze-up and develops more slowly in those years when it does occur. In the Chukchi, the narrow, ephemeral nature of the landfast ice zone noted in the 1980s continues to prevail today.

7. ***Coastal Flaw Lead:*** Notwithstanding trends toward warmer air temperatures, increased storminess, and slower ice growth during freeze-up, the frequencies with which the flaw lead and extended flaw lead occur off the Chukchi Sea coast have remained unchanged since the 1990s.

8. ***Multi-Year Ice in the Alaskan Beaufort Sea:*** The probability of large multi-year ice floes invading the nearshore portion of the Alaskan Beaufort Sea during freeze-up is substantially less than in the 1980s. This change has resulted in part from a reduction in the amount of multi-year ice comprising the permanent polar pack and in part from an increase in the northerly retreat of the ice edge during the summer months, both of which have reduced the opportunities for pack floes to enter the nearshore area. In addition, warmer air temperatures, longer open-water seasons, and increased storminess have decreased the likelihood that first-year ridges and rubble will survive the summer melt season to become second-year floes of any consequence. Nevertheless, as demonstrated in both 2018-19 and 2019-20, the possibility of multi-year ice invasions cannot be ruled out in the nearshore region of the Alaskan Beaufort Sea. The probability of an invasion in any given freeze-up season currently is about 20%, based on four such occurrences in the past 20 years.

9. ***Multi-Year Ice in the Chukchi Sea:*** The probability of multi-year ice entering the Chukchi Sea to the south and west of Point Barrow also has decreased since the 1980s, but to a lesser extent than in the Beaufort. Although the factors that have reduced the probability of invasions in the Beaufort apply to the Chukchi as well, their impact has been mitigated by the ability of the Multi-Year Gateway and Early-Season Entry to divert multi-year ice floes to the southwest. The probability of an invasion in any given freeze-up season currently is about 65%, based on 13 invasions in the past 20 years.

10. ***Ice Drift:*** The limited data acquired in recent years indicate that the drift rate for pack ice in the Alaskan Beaufort Sea averages about 6 nm/day (11 km/day) during the early stages of freeze-up. This value is comparable to that which prevailed in the 1980s.

9. REFERENCES

Arguez, A., I. Durre, S. Applequist, M. Squires, R. Vose, X. Yin, and R. Bilotta, 2010, “NOAA's U.S. Climate Normals (1981-2010)”, NOAA National Climatic Data Center, 2015, http://www.ncdc.noaa.gov/cdo-web/datatools/normals.

Barrett, S.A. and W.J. Stringer, 1978, “Growth Mechanisms of Katie’s Floeberg”, *Arctic and Alpine Research*, Vol. 10, No. 4, pp.775-783.

Barry, R.G., R.E. Moritz, and J.C. Rogers, 1979, “The Fast Ice Regimes of the Beaufort and Chukchi Sea Coasts”, *Cold Regions Science and Technology*, Vol. 1, pp. 129-152.

Bilello, M., 1960, “Formation, Growth, and Decay of Sea Ice in the Canadian Arctic Archipelago”, SIPRE Research Report 65, Hanover, New Hampshire.

Brown, R. and P. Cote, 1992, “Interannual Variability of Landfast Ice Thickness in the Canadian High Arctic 1950-89”, *Arctic*, Vol. 45, No. 3, pp. 273-284.

Canadian Ice Service, 2019 and 2020, Ice Forecast and Observations, https://www.canada.ca/en/environment-climate-change/services/ice-forecasts-observations.html.

Coastal Frontiers Corporation, 2015, “Northstar Development 2014 Pipeline Route Monitoring Program”, report prepared for BP Exploration (Alaska) Inc., Moorpark, California, 64 pp. + appen.

Coastal Frontiers Corporation and Vaudrey and Associates, Inc., 2010, “2009-10 Freeze-Up Study of the Alaskan Beaufort and Chukchi Seas”, Joint Industry Project performed for Shell International Exploration and Production, Inc., and the U.S. Minerals Management Service, Chatsworth, California, 100 pp. + appen.

Coastal Frontiers Corporation and Vaudrey and Associates, Inc., 2011, “2010-11 Freeze-Up Study of the Alaskan Beaufort and Chukchi Seas”, Joint Industry Project performed for Shell Offshore, Inc., and Bureau of Ocean Energy Management, Regulation, and Enforcement, U.S. Dept. of the Interior, Chatsworth, California, 149 pp. + appen.

Coastal Frontiers Corporation and Vaudrey and Associates, Inc., 2012a, “2011-12 Freeze-Up Study of the Alaskan Beaufort and Chukchi Seas”, Joint Industry Project performed for Shell International Exploration and Production, Inc., and Bureau of Safety and Environmental Enforcement, U.S. Dept. of the Interior, Chatsworth, California, 182 pp. + appen.

Coastal Frontiers Corporation and Vaudrey and Associates, Inc., 2012b, "Ice Encroachment in the Alaskan Beaufort and Chukchi Seas", Joint Industry Project performed for Shell Exploration and Production Company, and Bureau of Safety and Environmental Enforcement, U.S. Dept. of the Interior, Chatsworth, California, 78 pp. + appen.

Coastal Frontiers Corporation and Vaudrey and Associates, Inc., 2013 (revised January 2014), "2012-13 Freeze-Up Study of the Alaskan Beaufort and Chukchi Seas", Joint Industry Project performed for Shell Gulf of Mexico Inc. and Shell Offshore Inc., Statoil Petroleum AS, and Bureau of Safety and Environmental Enforcement, U.S. Dept. of the Interior, Moorpark, California, 175 pp. + appen.

Coastal Frontiers Corporation and Vaudrey and Associates, Inc., 2014, "2013-14 Freeze-Up Study of the Alaskan Beaufort and Chukchi Seas", Joint Industry Project performed for Shell Gulf of Mexico Inc. and Shell Offshore Inc., and Bureau of Safety and Environmental Enforcement, U.S. Dept. of the Interior, Moorpark, California, 185 pp. + appen.

Coastal Frontiers Corporation and Vaudrey and Associates, Inc., 2015, "2014-15 Freeze-Up Study of the Alaskan Beaufort and Chukchi Seas", Joint Industry Project performed for Shell Offshore Inc. and Bureau of Safety and Environmental Enforcement, U.S. Dept. of the Interior, Moorpark, California, 200 pp. + appen.

Coastal Frontiers Corporation and Vaudrey and Associates, Inc., 2016, "2015-16 Freeze-Up Study of the Alaskan Beaufort and Chukchi Seas", Joint Industry Project performed for Shell Offshore Inc. and Bureau of Safety and Environmental Enforcement, U.S. Dept. of the Interior, Moorpark, California, 203 pp. + appen.

Coastal Frontiers Corporation and Vaudrey and Associates, Inc., 2017, "2016-17 Freeze-Up Study of the Alaskan Beaufort and Chukchi Seas", prepared for Bureau of Safety and Environmental Enforcement, U.S. Dept. of the Interior, Moorpark, California, 180 pp. + appen.

Csanady, G.T., 1982, *Circulation in the Coastal Ocean*, D. Reidel Publishing Co., Boston, Massachusetts, 279 pp.

Dickins, D. and K. Vaudrey, 1994, "Phase III Ice Conditions, ANS Gas Commercialization Study: Marine Export Facilities", prepared for Arco Alaska Inc., BP Exploration (Alaska) Inc., and Exxon Company, USA, prepared by DF Dickins Associates Ltd., Salt Spring Island, British Columbia, and Vaudrey & Associates Inc., San Luis Obispo, California.

Eicken, H., L. Shapiro, A. Gaylord, A. Mahoney, and P. Cotter, 2006, "Mapping and Characteristics of Recurring Spring Leads and Landfast Ice in the Beaufort and Chukchi Seas", OCS Study MMS 2005-068, U.S. Department of the Interior, Mineral Management Service, Alaska Outer Continental Shelf Region, Anchorage, Alaska.

GINA, 2019 and 2020, GINA Alaska Direct Broadcast Satellite Data Portal, feeder.gina.alaska.edu.

Hirano, D., Y. Fukamaci, E. Watanabe, K. Ohshima, K. Iwamoto, A.R. Mahoney, H. Eicken, D. Simizu, and T. Tamura, 2016, "A Wind-Driven, Hybrid Latent and Sensible Heat Coastal Polynya off Barrow, Alaska", *Journal of Geophysical Research: Oceans*, 121, doi:10.1002/2015JC011318, 18 pp.

Kovacs, A., A. Gow, and W. Dehn, 1976, "Islands of Grounded Sea Ice", CRREL Report 76-4, Hanover, New Hampshire.

Lindsay, R.W. and J. Zhang, 2005, "The Thinning of Arctic Sea Ice, 1988-2003: Have We Passed a Tipping Point?", *Journal of Climate*, Vol. 18, November 15, 2005, pp. 4879-4894.

MacDonald, Dettwiler and Associates, Ltd., 2020, https://mdacorporation.com/docs/default-source/brochures/isg/surveillance-and-intelligence/space-missions/radar/radarsat-2-information-products.pdf?sfvrsn=6.

Mahoney, A., H. Eicken, A. Gaylord, and L. Shapiro, 2007, "Alaska Landfast Sea Ice: Links with Bathymetry and Atmospheric Circulation", *Journal of Geophysical Research*, Vol. 112, C02001.

Mahoney, A., H. Eicken, L. Shapiro, R. Gens, T. Heinrichs, F. Meyer, and A. Graves, 2012, "Mapping and Characterization of Recurring Spring Leads and Landfast Ice in the Beaufort and Chukchi Seas", Final Report, OCS Study BOEM 2012-067, University of Alaska Fairbanks, Fairbanks, Alaska, 154 pp.

MDA Geospatial Services, Inc., 2019, "RADARSAT-2 Single User License", LI-11525-34 V1.11, Richmond, B.C., Canada, 3 pp.

Melling, H. and D. Riedel, 2005, "Trends in the Draft and Extent of Seasonal Pack Ice, Canadian Beaufort Sea", *Geophysical Research Letters*, Vol. 32, L24501.

NASA, 2019 and 2020, Worldview Snapshots, https://wvs.earthdata.nasa.gov.

National Ice Center, 2019 and 2020, https://www.natice.noaa.gov/Main_Products.htm.

National Ocean Service, 2020, http://tidesandcurrents.noaa.gov.

National Snow and Ice Data Center, 2019a, "Beware the Ides of July", Arctic Sea Ice News and Analysis, July 16, 2019, http://nsidc.org/arcticseaicenews/2019/07.

National Snow and Ice Data Center, 2019b, "Dead heat", Arctic Sea Ice News and Analysis, August 15, 2019, http://nsidc.org/arcticseaicenews/2019/08//.

National Snow and Ice Data Center, 2019c, "Arctic sea ice reaches second lowest minimum in satellite record", Arctic Sea Ice News and Analysis, September 23, 2019, http://nsidc.org/arcticseaicenews/2019/09/.

National Snow and Ice Data Center, 2019d, "Falling up", Arctic Sea Ice News and Analysis, October 3, 2019, http://nsidc.org/arcticseaicenews/2019/10/falling-up/.

National Snow and Ice Data Center, 2020, "Environment: Climate", All About Sea Ice, April 3, 2020, https://nsidc.org/cryosphere/seaice/environment/global_climate.html.

National Weather Service, 2019, Forecast Office Fairbanks, AK, https://www.weather.gov/afg/.

National Weather Service, 2020, Alaska Region Headquarters, https://www.weather.gov/afc/ice.

NOAA, 2020a, NOAA's Local Climatological Data, https://www.ncdc.noaa.gov/cdo-web/datatools/lcd.

NOAA, 2020b, NOAA's Optimum Interpolation Sea Surface Temperature dataset (OISST v2), monthly series as compiled by NOAA's Physical Science Laboratory (PSL), https://psl.noaa.gov/data/gridded/data.noaa.oisst.v2.html.

Perovich, D., S. Gerland, S. Hendricks, W. Meier, M. Nicolaus, J. Richter-Menge, and M. Tschudi, 2013, "Arctic Report Card, Update for 2013", Sea Ice, NOAA, http://www.arctic.noaa.gov/reportcard/sea_ice.html.

RAMMB, 2019 and 2020, NOAA's Regional and Mesoscale Meteorology Branch, rammb.cira.colostate.edu.

Reece, A.M., 2009, personal communication, Shell International Exploration and Production, Inc., Houston, Texas.

Rigor, I. G., 2020 (compiled by Polar Science Center), *IABP Drifting Buoy Pressure, Temperature, Position, and Interpolated Ice Velocity, Version 1*. Boulder, Colorado, doi: http://dx.doi.org/10.7265/N53X84K7.

Rodrigues, J., 2009, "The Increase in the Length of the Ice-Free Season in the Arctic", *Cold Regions Science and Technology*, Vol. 59, pp. 78-101.

Stringer, W. and S. Barrett, 1975, "Ice Motion in the Vicinity of a Grounded Floeberg", *Proceedings POAC-75*, Fairbanks, Alaska.

Tekmarine, Inc., Polar Alpine, Inc., and Offshore and Coastal Technologies, Inc., 1985, "1984 Beaufort Sea Multiyear Ice Floe Tracking Study", AOGA Project No. 280, Sierra Madre, California, 233 pp. + appen.

Toimil, L. and A. Grantz, 1976, "Origin of a Bergfield in the Northeastern Chukchi Sea and its Influence on the Sedimentary Environment", *AIDJEX Bulletin 34*, December 1976.

Vaudrey, K.D., 1981a, "1980 Freezeup Study of the Barrier Island Chain and Harrison Bay", AOGA Project No. 129, Vaudrey & Associates, Inc., Missouri City, Texas, 32 pp. + appen.

Vaudrey, K. D., 1981b, "Beaufort Sea Multiyear Ice Features Survey, Volume I: Field Study", AOGA Project No. 139, Vaudrey & Associates, Inc., Missouri City, Texas, 36 pp. + appen.

Vaudrey, K.D., 1982a, "1981 Freezeup Study of the Barrier Island Chain and Harrison Bay", AOGA Project No. 160, Vaudrey & Associates, Inc., Missouri City, Texas, 30 pp. + appen.

Vaudrey, K.D., 1982b, "Ice Cracking in Stefansson Sound during the Winter of 1981-82", Memorandum prepared for ARCO Alaska and Shell Oil Company, San Luis Obispo, California.

Vaudrey, K.D., 1983, "1982 Freezeup Study of the Barrier Island Chain and Harrison Bay Region", AOGA Project No. 200, Vaudrey & Associates, Inc., San Luis Obispo, California, 32 pp. + appen.

Vaudrey, K.D., 1984, "1983 Freezeup Study of the Beaufort and Upper Chukchi Seas", AOGA Project No. 246, Vaudrey & Associates, Inc., San Luis Obispo, California, 48 pp. + appen.

Vaudrey, K.D., 1985a, "1984 Freezeup Study of the Beaufort and Upper Chukchi Seas", AOGA Project No. 282, Vaudrey & Associates, Inc., San Luis Obispo, California, 44 pp. + appen.

Vaudrey, K.D., 1985b, "Historical Summary of the 1980-82 Freezeup Seasons and 1981-83 Breakup Seasons (Volume 1 of 2)", AOGA Project No. 275, Vaudrey & Associates, Inc., San Luis Obispo, California, 79 pp.

Vaudrey, K.D., 1986, "1985 Freezeup Study of the Beaufort and Upper Chukchi Seas", AOGA Project No. 327, Vaudrey & Associates, Inc., San Luis Obispo, California, 49 pp + appen.

Vaudrey, K.D., 1987a, "1986-87 Chukchi Sea Ice Conditions", AOGA Project No. 346, Vaudrey & Associates, Inc., San Luis Obispo, California, 68 pp + appen.

Vaudrey, K.D., 1987b, "1985-86 Ice Motion Measurements in Camden Bay", AOGA Project No. 328a, Vaudrey & Associates, Inc., San Luis Obispo, California, 2 Volumes, 70 pp + appen.

Vaudrey, K., 1988a, "1987 Summer and Freeze-Up Ice Conditions in the Beaufort and Chukchi Seas Developed from Satellite Imagery", AOGA Project No. 360, Vaudrey & Associates, Inc., San Luis Obispo, California.

Vaudrey, K.D., 1988b, "1987 Ice Motion Measurements in the Eastern Beaufort Sea", prepared for Amoco Production Company and Unocal Corporation, prepared by Vaudrey & Associates, Inc., San Luis Obispo, California.

Vaudrey, K., 1989a, "1988 Summer and Freeze-Up Ice Conditions in the Beaufort and Chukchi Seas Developed from Satellite Imagery", AOGA Project No. 370, Vaudrey & Associates, Inc., San Luis Obispo, California.

Vaudrey, K.D., 1989b, "1988-89 Ice Motion Measurements in the Dease Inlet – Smith Bay Region Using ARGOS Buoys", prepared for Mobil Research and Development Corporation, prepared by Vaudrey & Associates, Inc., San Luis Obispo, California.

Vaudrey, K. D., 1989c, "Statistical Analysis of Ice Movement in the Beaufort and Chukchi Seas using 1979-87 ARGOS Buoy Data", prepared for Unocal Science and Technology Division, prepared by Vaudrey & Associates, Inc., San Luis Obispo, California.

Vaudrey, K., 1990, "1989 Summer and Freeze-Up Ice Conditions in the Beaufort and Chukchi Seas Developed from Satellite Imagery", AOGA Project No. 372, Vaudrey & Associates, Inc., San Luis Obispo, California.

Vaudrey, K., 1991, "1990 Summer and Freeze-Up Ice Conditions in the Beaufort and Chukchi Seas Developed from Satellite Imagery", AOGA Project No. 381, Vaudrey & Associates, Inc., San Luis Obispo, California.

Vaudrey, K., 1992, "1991 Summer and Freeze-Up Ice Conditions in the Beaufort and Chukchi Seas Developed from Satellite Imagery", AOGA Project No. 386, Vaudrey & Associates, Inc., San Luis Obispo, California.

Vaudrey, K., 2007, "Effects of Recent Climate Change on Sea Ice Conditions in the Alaskan Beaufort and Chukchi Seas", prepared for Shell International Exploration and Production, Inc., prepared by Vaudrey & Associates, Inc., San Luis Obispo, California.

Vaudrey, K. and B. Thomas, 1981, "Katie's Floeberg – 1980", report prepared for the Kopanoar Partners by Gulf Research and Development Company, Houston, Texas.

Vinas, M-J, 2019: "2019 Arctic Sea Minimum Tied for Second Lowest on Record", NASA, https://www.nasa.gov/feature/goddard/2019-arctic-sea-ice-extent-fourth-lowest-on-record.

Walsh, J. and H. Eicken, 2007, "Sea Ice Changes Affecting Alaska: Offshore Transportation, Coastal Communities, Marine Ecosystems", presented at Symposium on the Impact of an Ice-Diminishing Arctic on Naval and Maritime Operations, sponsored by National Ice Center and U.S. Arctic Research Commission, 10-12 July 2007, Washington, D.C.

Ward, E.G., C. Leidersdorf, J. Coogan, and K. Vaudrey, 2015, "Multi-Year Ice Incursions into the Chukchi Sea", OTC 25476, *Proc.* 2015 *Arctic Technology Conference*, Copenhagen, Denmark, 13 pp.

World Meteorological Organization, 2014, "Sea Ice Nomenclature", WMO publication No. 259 by the Joint Technical Commission for Oceanography and Marine Meteorology (JCOMM). Initially published in 1970.